

Politecnico di Torino

Master's Degree in Energy and Nuclear Engineering
Graduation session October 2022

Master's Thesis

Technical-economic feasibility analysis of green hydrogen production in Patagonia and transport to Italy for the decarbonisation of the steel industry



Supervisors

Prof. Ing. Massimo Santarelli
Prof. Ing. Gabriel Correa Perelmuter
Ing. Paolo Marocco

Candidate

Luca Spelozzi

Abstract

The work carried out in this thesis aims to evaluate the technical and economic feasibility of producing low-cost green hydrogen in Patagonia Argentina, exploiting wind energy, and ocean shipping to Italy to satisfy the demand of the national steel industry. Two production scenarios have been evaluated, related to the hydrogen demand needed to decarbonise the Direct Reduced Iron production process. The first scenario assumes the replacement of 30 % of natural gas with pure hydrogen. The annual hydrogen demand is 143,144 tonnes. In the second scenario is assumed the total replacement of natural gas with pure hydrogen, to completely abate CO₂ emissions. The annual hydrogen demand rises to 355,702 tonnes.

Two carriers for storage and transport have been studied and compared; ammonia, synthesised via the Haber-Bosch process and liquefied at a temperature of -33 °C, and liquid hydrogen, which requires a temperature of -253 °C to be liquefied. Maritime transport is carried out by dedicated ships, designed to keep the carriers in cryogenic conditions.

For both carriers, the Levelized Cost of Hydrogen (LCOH) has been calculated, which considers the costs of production, storage, transport and, in the case of ammonia, also reconversion into hydrogen. For the design and economic calculations related to the production phase, four configurations have been considered, the first involves the production of hydrogen in an off-grid alkaline plant, the second involves grid integrated alkaline electrolyser. The third and fourth configurations involve the production of hydrogen by means of a PEM electrolyser, in the third case off-grid, while in the fourth case it is fed by a grid-wind mix providing a 100 % capacity factor.

The results obtained show that the value chain of LH₂ provides a lower LCOH than NH₃, although the ammonia is characterised by more competitive storage and transport costs. The biggest drawback of ammonia is the high cost and inefficiency of cracking and purification, in addition to a more complicated production process compared to liquid hydrogen, which arrives at the destination terminal as end product. None of the two carriers provides a competitive final hydrogen cost [\$/kgH₂].

Ammonia is an attractive carrier that provides competitive storage and transport costs for applications requiring NH₃ as final product. The LCOA has also been calculated.

Sensitivity analysis has been performed for each scenario analysed, studying the variation of the LCOH in relation to the most relevant parameters influencing the cost of hydrogen.

Acknowledgements

Questa tesi è dedicata a tutte le persone che mi hanno accompagnato durante il percorso universitario, che è stato pieno di emozioni e momenti che rimarranno sempre nel mio cuore. Un ringraziamento speciale va ai miei genitori, Rita e Costantino, che non hanno mai smesso di aiutarmi e supportarmi in tutte le scelte che ho fatto, ed hanno saputo crescermi, insegnandomi quali fossero i veri valori della vita.

Ringrazio la mia famiglia a Torino, che mi ha accolto nel migliore dei modi quando sono arrivato e mi ha sempre aiutato durante tutto il percorso universitario.

Ringrazio Pia, di cui mi sono innamorato proprio all'università, che è sempre stata al mio fianco aiutandomi nei momenti più difficili, che mi ha sempre fatto sentire amato e con cui ho condiviso e continuo a condividere i momenti più belli della mia vita.

Ringrazio tutti i miei amici, partendo da quelli di una vita, che ogni volta che sono tornato a Marina mi hanno sempre fatto sentire a casa, e tutti gli amici che ho conosciuto a Torino, con cui ho condiviso tanti momenti ricchi di spensieratezza di felicità.

Infine, ringrazio tutte le persone che ho conosciuto nei due indimenticabili viaggi che ho intrapreso durante lo studio, soprattutto i compagni di avventura con cui ho condiviso parte della mia esperienza, anche solamente un'escursione, una chiacchiera o una risata.

Luca Spelorzi

Contents

<i>Abstract</i>	iii
<i>Acknowledgements</i>	v
<i>Contents</i>	vi
<i>List of figures</i>	x
<i>List of Tables</i>	xiv
<i>List of acronyms</i>	xvii
1 Literature review	19
1.1 <i>Background</i>	19
1.2 <i>Argentina energetic scenario</i>	20
1.2.1 <i>Assessment of the potential for green production in Argentina</i>	21
1.3 <i>Italian energetic scenario</i>	22
1.3.1 <i>Assessment for the potential of renewables in Italy</i>	24
1.4 <i>The role of the hydrogen in the global decarbonisation scenario</i>	25
1.5 <i>State-of-the-art steel production</i>	29
1.6 <i>Decarbonisation alternatives for the steel industry</i>	33
1.7 <i>State of the art hydrogen production</i>	38
1.7.1 <i>Green hydrogen production</i>	39
1.8 <i>Hydrogen transportation and energy carriers</i>	44
1.9 <i>Conventional ammonia production process</i>	50
1.10 <i>Green ammonia production and transport</i>	52
1.10.1 <i>Desalinator</i>	52
1.10.2 <i>Air separation units</i>	56
1.10.3 <i>Hydrogen storage</i>	59
1.10.4 <i>Ammonia synthesis unit</i>	63
1.10.5 <i>Ammonia storage</i>	64
1.10.6 <i>Ammonia cracking</i>	66
<i>References Chapter 1</i>	68
2 Supply chain design	75
2.1 <i>Purpose of the work</i>	75
2.2 <i>Hydrogen Demand</i>	75
2.3 <i>Ammonia production supply chain</i>	79
2.3.1 <i>Electricity</i>	83

2.3.2	<i>Balance of the process</i>	83
2.3.3	<i>Electrolyser</i>	85
2.3.4	<i>Desalinator</i>	89
2.3.5	<i>Hydrogen compressor</i>	91
2.3.6	<i>Hydrogen storage buffer</i>	94
2.3.7	<i>Cryogenic air separation unit</i>	96
2.3.8	<i>Nitrogen compressor</i>	97
2.3.9	<i>Ammonia synthesis plant</i>	98
2.3.10	<i>Ammonia liquefaction and storage</i>	101
2.4	<i>Ammonia transportation and cracking</i>	103
2.4.1	<i>Loading terminal</i>	105
2.4.2	<i>Oceanic transport</i>	106
2.4.3	<i>Unloading Terminal</i>	115
2.4.4	<i>Cracking and purification plants</i>	116
2.5	<i>CO₂ saved and emitted during production and transportation phases</i>	120
2.6	<i>Liquid hydrogen production supply chain</i>	122
2.6.1	<i>Balance of the process</i>	124
2.6.2	<i>Electrolyser</i>	125
2.6.3	<i>Desalinator</i>	128
2.6.4	<i>Liquefaction plant</i>	130
2.6.5	<i>Liquid hydrogen storage</i>	132
2.6.6	<i>Loading terminal</i>	134
2.6.7	<i>Oceanic transport</i>	136
2.6.8	<i>Unloading terminal</i>	140
2.7	<i>CO₂ saved and emitted during production and transportation phases</i>	141
<i>References Chapter 2</i>		144
3 Economic analysis		149
3.1	<i>Description of used parameters</i>	149
3.2	<i>Ammonia supply chain</i>	150
3.2.1	<i>Electrolyser</i>	151
3.2.2	<i>Desalinator</i>	154
3.2.3	<i>Levelized cost of produced hydrogen</i>	155
3.2.4	<i>Hydrogen compressor</i>	156
3.2.5	<i>Hydrogen storage buffer</i>	158
3.2.6	<i>Air separation unit</i>	159

3.2.7	<i>Nitrogen compressor</i>	161
3.2.8	<i>Haber-Bosch plant</i>	162
3.2.9	<i>Levelized cost of ammonia production process</i>	163
3.2.10	<i>Liquid ammonia storage and loading terminal facility</i>	166
3.2.11	<i>Maritime transport</i>	168
3.2.12	<i>Liquid ammonia storage and unloading terminal facility</i>	170
3.2.13	<i>Ammonia cracking and hydrogen purification plant</i>	171
3.2.14	<i>Civil works and other costs</i>	173
3.3	<i>Levelized cost of ammonia carrier supply chain</i>	175
3.4	<i>LCOA evaluation considering ammonia as final product</i>	179
3.5	<i>Liquid hydrogen supply chain</i>	181
3.5.1	<i>Electrolyser</i>	181
3.5.2	<i>Desalinator</i>	182
3.5.3	<i>Hydrogen liquefaction plant</i>	183
3.5.4	<i>Liquid hydrogen storage and loading terminal</i>	185
3.5.5	<i>Maritime transport</i>	186
3.5.6	<i>Liquid hydrogen storage and unloading terminal</i>	187
3.5.7	<i>Civil works and other costs</i>	189
3.6	<i>Final levelized cost of liquid hydrogen carrier supply chain</i>	190
<i>References Chapter 3</i>		193
4 Sensitivity analysis		197
4.1	<i>Permitted use of the electricity grid for hydrogen production</i>	197
4.2	<i>Sensitivity analysis considering only one variable</i>	201
4.2.1	<i>Wind capacity factor</i>	201
4.2.2	<i>Electrolyser consumption</i>	206
4.2.3	<i>Electrolyser CAPEX</i>	210
4.2.4	<i>Wind electricity cost</i>	213
4.3	<i>Sensitivity analysis considering two variables</i>	218
4.3.1	<i>Capacity factor and electrolyser consumption</i>	219
4.3.2	<i>Capacity factor and wind energy cost</i>	222
4.3.3	<i>Capacity factor and electrolyser CAPEX</i>	224
4.3.4	<i>Electrolyser CAPEX and wind energy cost</i>	227
4.3.5	<i>Electrolyser CAPEX and electrolyser consumption</i>	229
4.3.6	<i>Wind energy cost and electrolyser consumption</i>	232
4.4	<i>Best feasible scenario by varying all parameters</i>	235

4.5	<i>Sensitivity analysis for ammonia as final product</i>	236
4.5.1	<i>Capacity factor and electrolyser consumption</i>	237
4.5.2	<i>Capacity factor and wind energy cost</i>	238
4.5.3	<i>Capacity factor and electrolyser CAPEX</i>	239
4.5.4	<i>Wind energy cost and electrolyser CAPEX</i>	240
4.5.5	<i>Electrolyser consumption and electrolyser CAPEX</i>	241
4.5.6	<i>Electrolyser consumption and wind energy cost</i>	242
4.6	<i>Best feasible scenario by varying all parameters</i>	243
	<i>References Chapter 4</i>	244
5	<i>Conclusions</i>	245
	<i>Appendix A</i>	249

List of figures

Figure 1.1: Argentina energy production mix 2018 (the Author)	21
Figure 1.2a; 1.2b: Wind speed [m/s] at 50 m above ground level map (Sigal et al., 2014); annual average solar radiation [kWh/m ² /day]	22
Figure 1.3: Italy energy production mix 2021 (the Author)	23
Figure 1.4a, 1.4b: Annual average solar radiation [kWh/m ² /day] (Energoclub, n.d.); wind speed [m/s] at 75 m above ground level map (Consulente Energia, n.d.).....	25
Figure 1.5: Hydrogen application fields (IRENA, 2022)	27
Figure 1.6: BF-BOF crude steel production route (Berger, 2020)	31
Figure 1.7: EAF steel production route (Berger, 2020)	33
Figure 1.8: Carbon capture and storage technology (Berger, 2020).....	34
Figure 1.9: MIDREX direct reduced iron production plant (Chevrier, 2020).....	37
Figure 1.10: Grey, blue and green hydrogen production differences (POSCO Newsroom, 2020)	39
Figure 1.11: General scheme and operation of an alkaline electrolysis cell (Rodríguez & Amores, 2020)	41
Figure 1.12: General scheme and operation of an PEM electrolysis cell (Rashid et al., 2015) ..	42
Figure 1.13: General scheme and operation of an SOEC electrolysis cell (Ursúa et al., 2012) ..	43
Figure 1.14: Liquid organic hydrogen carrier supply chain (International Renewable Energy Agency (IRENA), 2022a)	48
Figure 1.15: Haber-Bosch conventional process (Process, n.d.)	51
Figure 1.16: Green ammonia production and storage process (Alternative Green and Cost- Effective Processes for Ammonia Production – Green Ammonia, n.d.)	52
Figure 1.17: Multi flash stage desalination process (Curto et al., 2021).....	54
Figure 1.18: Reverse osmosis process (SOURCE)	55
Figure 1.19: Simplified flowsheet of cryogenic air separation unit (Morgan, 2013)	57
Figure 1.20: Pressure swing adsorption plant (Seshan, 1989)	58
Figure 1.21: Hydrogen liquefaction process based on joule brayton refrigeration cycle and solar adsorption chilling (Asadnia & Mehrpooya, 2018).....	61
Figure 1.22: Ammonia synthesis loop scheme (Cheema & Krewer, 2018)	63
Figure 1.23: Liquid ammonia liquefaction and storage process (the Author)	66
Figure 1.24: Ammonia cracking and hydrogen purification process (Crystec et al.)	67
Figure 2.1: Ammonia production process - Option 1 (the Author).....	80
Figure 2.2: Ammonia production process - Option 2 (the Author).....	81
Figure 2.3: Ammonia production process - Option 3 (the Author).....	82
Figure 2.4: Compressed hydrogen storage tank (Hyfindr)	94

Figure 2.5: Ammonia refrigeration cycle and cryogenic storage (the Author)	101
Figure 2.6: NH ₃ storage, transport, and reconversion supply chain (the Author)	104
Figure 2.7: Ammonia cracking and hydrogen purification process (the Author).....	117
Figure 2.8: LH ₂ supply chain (the Author)	123
Figure 2.9: Hydrogen liquefaction process (the Author).....	131
Figure 2.10: LH ₂ loading terminal facilities (Eria, 2020)	135
Figure 3.1: Levelized cost of hydrogen production, (NH ₃ supply chain).....	155
Figure 3.2: CAPEX composition of ammonia production processes for cheapest configuration	164
Figure 3.3: CAPEX composition of ammonia production processes for most expensive configuration	164
Figure 3.4: Levelized cost of final hydrogen related to ammonia production process, scenario 1	165
Figure 3.5: Levelized cost of final hydrogen related to ammonia production process, scenario 2	166
Figure 3.6: Levelized cost of ammonia supply chain, scenario 1 and 2	176
Figure 3.7: Final levelized cost of hydrogen, scenario 1 (NH ₃ supply chain).....	177
Figure 3.8: Final levelized cost of hydrogen, scenario 2 (NH ₃ supply chain).....	178
Figure 3.9: Final levelized cost of ammonia, scenario 1.....	179
Figure 3.10: Final levelized cost of ammonia, scenario 2.....	180
Figure 3.11: Levelized cost of hydrogen, liquid hydrogen supply chain, scenario 1.....	190
Figure 3.12: Levelized cost of hydrogen, liquid hydrogen supply chain, scenario 2.....	191
Figure 4.1: Specific emissions of hydrogen production trend for alkaline and PEM electrolyzers	199
Figure 4.2: Indirect emissions limit for completely grid integration in electrolysis process ...	200
Figure 4.3: Hydrogen cost production trend respect wind capacity factor, alkaline – scenario 1	201
Figure 4.4: Hydrogen cost production trend respect wind capacity factor, PEM – scenario 1202	
Figure 4.5: Hydrogen cost production trend respect wind capacity factor, alkaline – scenario 2	203
Figure 4.6: Hydrogen cost production trend respect wind capacity factor, PEM – scenario 2203	
Figure 4.7: Final LCOH with respect wind capacity factor variation, scenario 1	204
Figure 4.8: Final LCOH with respect wind capacity factor variation, scenario 2	205
Figure 4.9: Hydrogen cost production trend respect electrolyser consumption, alkaline – scenario 1	206
Figure 4.10: Hydrogen cost production trend respect electrolyser consumption, PEM – scenario 1	207
Figure 4.11: Final LCOH with respect electrolyser consumption variation, scenario 1	209

Figure 4.12: Final LCOH with respect electrolyser consumption variation, scenario 2	210
Figure 4.13: Hydrogen cost production trend respect electrolyser CAPEX, alkaline	211
Figure 4.14: Hydrogen cost production trend respect electrolyser CAPEX, PEM	211
Figure 4.15: Final LCOH with respect electrolyser CAPEX.....	213
Figure 4.16: Hydrogen cost production trend respect wind energy cost, alkaline, scenario 12	214
Figure 4.17: Hydrogen cost production trend respect wind energy cost, PEM, scenario 1	215
Figure 4.18: Final LCOH with respect wind electricity cost, scenario 1	216
Figure 4.19: Final LCOH with respect wind electricity cost, scenario 2	217
Figure 4.20: Levelized cost of hydrogen production with respect capacity factor and electrolyser consumption.....	219
Figure 4.21: Final levelized cost of hydrogen for NH ₃ supply chain with respect capacity factor and electrolyser consumption.....	220
Figure 4.22: Final levelized cost of hydrogen for LH ₂ supply chain with respect capacity factor and electrolyser consumption.....	221
Figure 4.23: Levelized cost of hydrogen production with respect capacity factor and wind electricity cost	222
Figure 4.24: Final levelized cost of hydrogen for NH ₃ supply chain with respect capacity factor and wind energy cost	223
Figure 4.25: Final levelized cost of hydrogen for LH ₂ supply chain with respect capacity factor and wind energy cost	224
Figure 4.26: Levelized cost of hydrogen production with respect capacity factor and electrolyser CAPEX.....	225
Figure 4.27: Final levelized cost of hydrogen for NH ₃ supply chain with respect capacity factor and electrolyser CAPEX	226
Figure 4.28: Final levelized cost of hydrogen for LH ₂ supply chain with respect capacity factor and electrolyser CAPEX	226
Figure 4.29: Levelized cost of hydrogen production with respect wind electricity cost and electrolyser CAPEX.....	227
Figure 4.30: Final levelized cost of hydrogen for NH ₃ supply chain with respect wind electricity cost and electrolyser CAPEX.....	228
Figure 4.31: Final levelized cost of hydrogen for LH ₂ supply chain with respect wind electricity cost and electrolyser CAPEX.....	229
Figure 4.32: Levelized cost of hydrogen production with respect electrolyser power consumption and CAPEX	230
Figure 4.33: Final levelized cost of hydrogen for NH ₃ supply chain with respect electrolyser power consumption and CAPEX.....	231
Figure 4.34: Final levelized cost of hydrogen for LH ₂ supply chain with respect electrolyser power consumption and CAPEX.....	232
Figure 4.35: Levelized cost of hydrogen production with respect electrolyser power consumption and wind energy cost	233

Figure 4.36: Final levelized cost of hydrogen for NH ₃ supply chain respect electrolyser consumption and wind energy cost	234
Figure 4.37: Final levelized cost of hydrogen for LH ₂ supply chain respect electrolyser consumption and wind energy cost	235
Figure 4.38: LCOH of hydrogen production and delivery both for NH ₃ and LH ₂ carriers, varying all the parameters	236
Figure 4.39: Final levelized cost of ammonia with respect electrolyser power consumption and capacity factor	237
Figure 4.40: Final levelized cost of ammonia with respect wind electricity cost and capacity factor	238
Figure 4.41: Final levelized cost of ammonia with respect electrolyser CAPEX and capacity factor	239
Figure 4.42: Final levelized cost of ammonia with respect electrolyser CAPEX and wind energy cost	240
Figure 4.43: Final levelized cost of ammonia with respect electrolyser CAPEX and power consumption.....	241
Figure 4.44: Final levelized cost of ammonia with respect electrolyser consumption and wind energy cost	242
Figure 4.45: LCOA considering hydrogen production, ammonia synthesis, storage and transport.....	243

List of Tables

Table 2.1: Annual demand of HBI for use in the blast furnace	76
Table 2.2: Annual demand of reduced iron for use in electric arc furnace	76
Table 2.3: NG-H ₂ mixing scenarios for reducing gas	77
Table 2.4: Quantity of hydrogen needed to provide thermal energy for processes	78
Table 2.5: Total demand of hydrogen in the two analysed scenarios	78
Table 2.6: Mass balance of hydrogen and ammonia for the entire supply chain, scenario 1 ...	84
Table 2.7: Mass balance of hydrogen and ammonia for the entire supply chain, scenario 2 ...	85
Table 2.8: Technical specifications alkaline electrolyser	86
Table 2.9: Technical specifications PEM electrolyser	87
Table 2.10: Electrolyser plant power and capacities for different scenarios, (NH ₃ supply chain)	89
Table 2.11: Desalinator plant power and capacities for different scenarios, (NH ₃ supply chain)	91
Table 2.12: Specific compression work, electricity consumption and compressor power for different scenarios.....	93
Table 2.13: Hours of storage and tank size based on capacity factors	95
Table 2.14: Plant capacity, annual electricity consumption and plant power for both scenarios	97
Table 2.15: Compressor capacity, electricity consumption and power, for both scenarios	98
Table 2.16: Technical data of Haber-Bosch synthesis plant for both scenarios	100
Table 2.17: Technical and energetic results for storage and refrigeration cycle, scenarios 1 and 2	103
Table 2.18: Vessel ship duration, number of trips per year and required number of vessels needed, for small, medium, and big ship size	108
Table 2.19: Ship power, NH ₃ consumption, fuel tank size, HFO pilot fuel consumption, for small, medium and large size vessels	111
Table 2.20: Total vessel length, NH ₃ evaporation rate, NH ₃ evaporated annually, for all the vessel size	113
Table 2.21: Fuel consumption and CO ₂ emission for HFO ship transportation, for all size vessels.....	114
Table 2.22: Storage Boil-Off, NH ₃ evaporated and energy consumption in unloading terminal, scenarios 1 and 2	116
Table 2.23: Process mass balance, thermal and electrical energy consumption	119
Table 2.24: Processes specific emissions, annual CO ₂ emissions and emissions saved for scenario 1	121

Table 2.25: Processes specific emissions, annual CO ₂ emissions and emissions saved for scenario 2	121
Table 2.26: mass balance of liquid hydrogen supply chain, scenarios 1 and 2 (LH ₂ supply chain)	125
Table 2.27: Electrolyser plant power and capacities for different scenarios, (LH ₂ supply chain)	127
Table 2.28: Desalinator plant power and capacities for different scenarios, (LH ₂ supply chain)	129
Table 2.29: Hydrogen liquefaction plant capacity, total energy consumption and plant power, Scenarios 1 and 2.....	132
Table 2.30: Liquid hydrogen storage tank, days of storage ensured, Boil-Off rate and annual H ₂ evaporated, scenarios 1 and 2	133
Table 2.31: LH ₂ transport duration, annual vessel capacity transported, number of vessels required, scenarios 1 and 2	137
Table 2.32: Vessel power, transportation fuel consumption, fuel tank capacity, annual fuel consumption, scenarios 1 and 2.....	138
Table 2.33: Boil-Off hydrogen during transport.....	139
Table 2.34: Fuel consumption and CO ₂ emission for HFO ship transport.....	140
Table 2.35: Unloading storage terminal tanks, Boil-Off rate and electricity consumed.....	141
Table 2.36: Processes specific emissions, annual CO ₂ emissions and emissions saved for scenario 1	142
Table 2.37: Processes specific emissions, annual CO ₂ emissions and emissions saved for scenario 2	143
Table 3.1: CAPEX and OPEX considered for alkaline and PEM electrolysers	151
Table 3.2: Electrolyser cost analysis, scenario 1 (NH ₃ supply chain).....	152
Table 3.3: Electrolyser LCOH composition, scenario 1 (NH ₃ supply chain)	153
Table 3.4: Electrolyser LCOH composition, scenario 2 (NH ₃ supply chain)	153
Table 3.5: Desalinator cost analysis, scenario 1 (NH ₃ supply chain)	154
Table 3.6: Compressor CAPEX equation's parameter	157
Table 3.7: H ₂ Compressor cost analysis, scenario 1	157
Table 3.8: Economic analysis of compressed hydrogen storage tank	159
Table 3.9: ASU cost analysis, scenario 1 and 2	160
Table 3.10: Nitrogen compressor cost analysis, scenario 1 and 2	162
Table 3.11: Ammonia synthesis plant economic analysis, scenarios 1 and 2	163
Table 3.12: Loading storage ammonia terminal plant economic analysis, scenarios 1 and 2	168
Table 3.13: Maritime transportation economic analysis, scenario 1 (NH ₃ supply chain).....	169
Table 3.14: Unloading storage ammonia terminal plant economic analysis, scenarios 1 and 2	171

Table 3.15: Ammonia cracking and hydrogen purification plant economic analysis, scenarios 1 and 2	173
Table 3.16: Specific area for NH ₃ process plants, base and additional cost indexes	174
Table 3.17: Areas of the plants involved in the NH ₃ production process, CAPEX civil works and other costs, LCOH for scenario 1 (NH ₃ supply chain)	175
Table 3.18: Electrolyser cost analysis, scenario 1, (LH ₂ supply chain)	182
Table 3.19: Desalinator cost analysis, scenario 1, (LH ₂ supply chain)	183
Table 3.20: Economic calculations hydrogen liquefaction plant, scenarios 1 and 2	184
Table 3.21: Economic calculation LH ₂ storage tank and loading terminal infrastructures, scenarios 1 and 2	186
Table 3.22: Maritime transportation economic analysis, scenarios 1 and 2 (LH ₂ supply chain)	187
Table 3.23: Economic calculation LH ₂ storage tank and unloading terminal infrastructures, scenarios 1 and 2	188
Table 3.24: Areas of the plants involved in the NH ₃ production process, CAPEX civil works and other costs, LCOH for scenario 1	189
Table 4.1: Grid integration limits related to CO ₂ emissions thresholds, for alkaline and PEM electrolyzers	199
Table 4.2: Final LCOH with respect wind capacity factor variation, scenario 1	204
Table 4.3: Final LCOH with respect wind capacity factor variation, scenario 2	205
Table 4.4: Final LCOH with respect electrolyser consumption variation, scenario 1	208
Table 4.5: Final LCOH with respect electrolyser consumption variation, scenario 2	209
Table 4.6: Final LCOH with respect electrolyser CAPEX	212
Table 4.7: Final LCOH with respect wind electricity cost, scenario 1	216
Table 4.8: Final LCOH with respect wind electricity cost, scenario 2	217
Table A1: LCOH final hydrogen NH ₃ supply chain, scenario 1	249
Table A2: LCOH final hydrogen NH ₃ supply chain, scenario 2	250
Table A3: LCOH final hydrogen LH ₂ supply chain, scenario 1	251
Table A4: LCOH final hydrogen LH ₂ supply chain, scenario 2	252
Table A5: LCOA final ammonia NH ₃ supply chain, scenario 1	253
Table A6: LCOA final ammonia NH ₃ supply chain, scenario 2	254

List of acronyms

DRI	Direct Reduced Iron
HBI	Hot Briquetted Iron
EAFF	Electric Arc Furnace
HM	Hot Metal
BF	Blast Furnace
BOF	Basic Oxygen Furnace
SMR	Steam Methane Reforming
CCS	Carbon Capture (and) Storage
NG	Natural Gas
GHG	Greenhouse Gas
RO	Reverse Osmosis
MFS	Multi Flash Stage
MED	Multiple Effect Distillation
SEC	Specific Energy Consumption
SFC	Specific Fuel Consumption
FC	Fuel Consumption
PEM	Proton Exchange Membrane
SOEC	Solid Oxide Electrolyser
AEM	Anion Exchange Membrane
HFO	Heavy Fuel Oil
BOG	Boil Off Gas
ASU	Air Separation Unit
PSA	Pressure Swing Adsorption
LH ₂	Liquefied Hydrogen
LCOH	Levelized Cost Of Hydrogen
LCOA	Levelized Cost Of Ammonia
LCOW	Levelized Cost Of Water
LOHC	Liquid Organic Hydrogen Carriers
MCH	Methylcyclohexane
IEA	International Energy Agency
IRENA	International Renewable Energy Agency
O&M	Operation and Maintenance
CAPEX	Capital Expenditure
OPEX	Operational Expenditure

Chapter 1

Literature review

1.1 Background

Nowadays, anthropogenic activities are responsible for the emissions of 51 billion tons of greenhouse gases, most of which are carbon dioxide, but also include methane, nitrous oxide and fluorinated gases. In 2019, the total carbon emitted by the energy sector was about 33 Gt of CO₂. The increase in the concentration of greenhouse gases in the atmosphere causes the greenhouse effect that impedes the sun's rays from leaving the atmosphere, resulting in global warming, which is affecting our planet's delicate climate balance, and causing droughts and extreme natural phenomena, such as hurricanes and bushfires.

Several international agreements have been established for the development of common strategies to arrest the Global Warming problem, through common political actions and huge investments on research of all technologies that promise to reduce emissions. The most famous is the Paris Agreement, which took place in 2015. The stated goal is the containment of the average temperature by 1,5 °C compared to pre-industrial age values. The countries of the European Union have pledged to reduce emissions by 2030 by 55 % compared to 1990 emissions, including a 32 % share of renewables in the energy mix, and then increasing it, with the goal of becoming the first climate-neutral economy and society by 2050 (Paris, 2016). Italy has developed the 'Piano Nazionale Integrato per l'Energia e il Clima' in 2018, to achieve its decarbonization goals, which sets binding targets to 2030 on energy efficiency, renewables, and CO₂ emissions reduction. Specifically, this plan includes five areas of focus, which are decarbonization, efficiency, energy security, development of the internal energy market and research, innovation, and competitiveness. The goal is the 56% decrease in emissions in the heavy industry sector, and a 35 % decrease in the tertiary and transport sectors (Ministero dello Sviluppo Economico, 2019).

The stated target of limiting global average temperature increase to no more than 1,5 °C above pre-industrial levels implies decarbonizing all sectors of the economy by 2050. This will be a massive challenge, especially because of the lack of the proper technologies in important industrial sectors. Renewable energies, complemented by other technologies, can play a key

role in these sectors, although they have not currently been exploited to their full potential (IRENA, 2020). As part of the process of transition to a low-carbon economy and society, the energy sector has the responsibility to contribute through the development of high-performance technologies with low environmental impact. The sustainability of the energy system must be addressed through a multidisciplinary approach based on the interaction of technical aspects, economic, environmental, and social factors. The role of energy technologies is crucial in mitigating impacts on climate, ecosystems and health; their deployment and development can lead to positive impacts also in the economic and social context (ENEA, 2020). To achieve the climate's objectives IRENA has assumed scenarios based on a combination of 'five reduction measures', consisting of energy demand reduction and energy efficiency to minimize energy waste. The second point of interest is the direct use of electricity generated from renewable sources to electrifying some industrial processes that are currently powered by renewable sources. The use of green hydrogen and derived molecules as energy carriers that can store and transport energy is the fourth point, finally there is the implementation of CO₂ reduction measures such as Carbon Capture and Storage (IRENA, 2020).

1.2 Argentina energetic scenario

Argentina is a developing country with an expanding economy. Most of the production chain is in the centre of the country, where the largest urban areas are concentrated, such as the capital Buenos Aires, where about one third of the population lives, and the other two cities of Cordoba and Rosario.

National energy demand has grown steadily in recent years, reaching a record level in 2021, with 133,8 TWh, 5,2 % more than the previous year. The industrial sector has seen an annual increase of 12,3 % in its demand. In the residential sector, the increase was 2 % and in the commercial sector 3,7 %.

The Argentina's energy mix has a strong dependence from hydrocarbons, particularly natural gas, as shown in graphic 1.1. In 2018, 87 % of the total national energy supply came from fossil fuels, in particular natural gas covered the 58 % of national energy production, oil 28 % and 1 % from coal, with a low relative weight of other sources such as hydropower and nuclear energy. In 2018, renewable energy accounted for only 5 % of national energy production (Mastronardi et al., 2019).

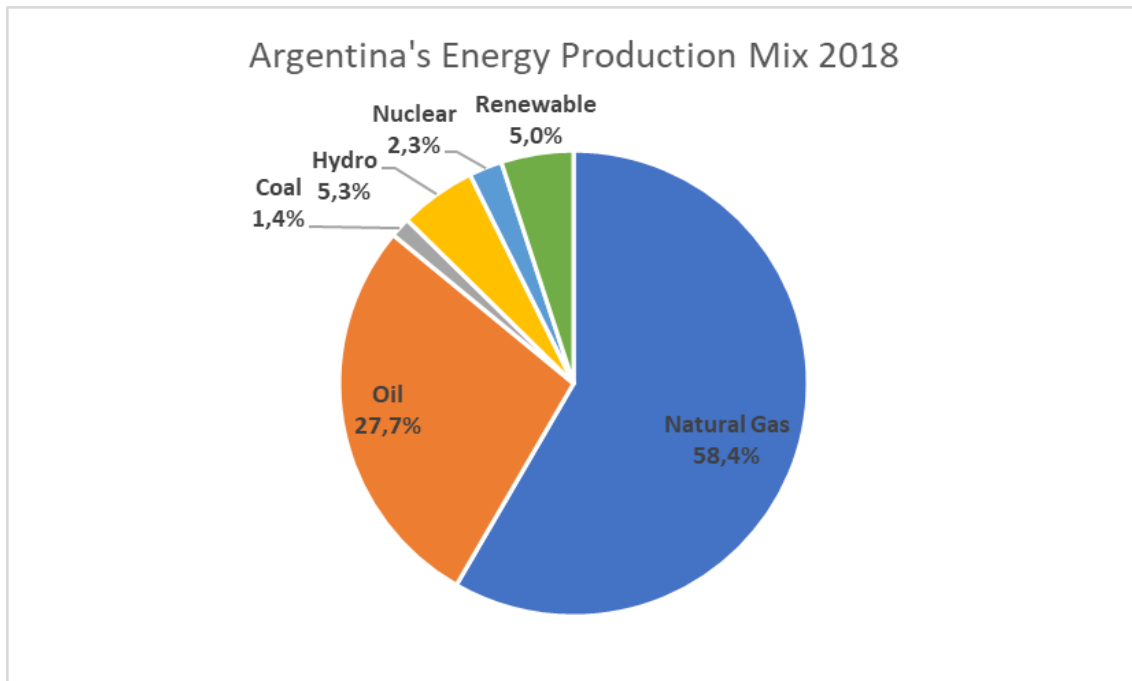


Figure 1.1: Argentina energy production mix 2018 (the Author)

The production of renewables has increased significantly in recent years, achieving 13 % of the country's electricity demand in 2021, respect 10 % in 2020. The improvement was largely due to the incorporation of 1005 MW of installed capacity, representing an increase of 24 % from 2020. The technology that contributed most to production during the year was wind power (74 %), followed by solar PV (13 %), small hydro (7 %) and bioenergy (6 %). Similarly, of the new projects inaugurated in 2021, 42,3 % correspond to wind technology, 30,8 % to bioenergy, 15,4 % to solar photovoltaics and 11,5 % to small hydropower projects. Argentina currently has 187 renewable energy projects in operation, adding more than 5182 MW of power to the national energy matrix (UNCUYO, 2022).

The national energy target for the year 2030 is to achieve 30% renewable energies, mainly by developing onshore wind power, reaching 10.000 MW of power installed.

1.2.1 Assessment of the potential for green production in Argentina

Argentina is characterised by enormous solar and wind potential. Almost the entire southern part has huge wind power potential, estimated to be more than 2000 GW, and is characterised by average wind speeds above 10 m/s in large areas and potential capacity factors often exceeding 60 %. The north-western part of the country, near the Andes Mountains, is arid and has a high solar irradiation of more than 5,5 kWh/m² per day (Armijo & Philibert, 2020).

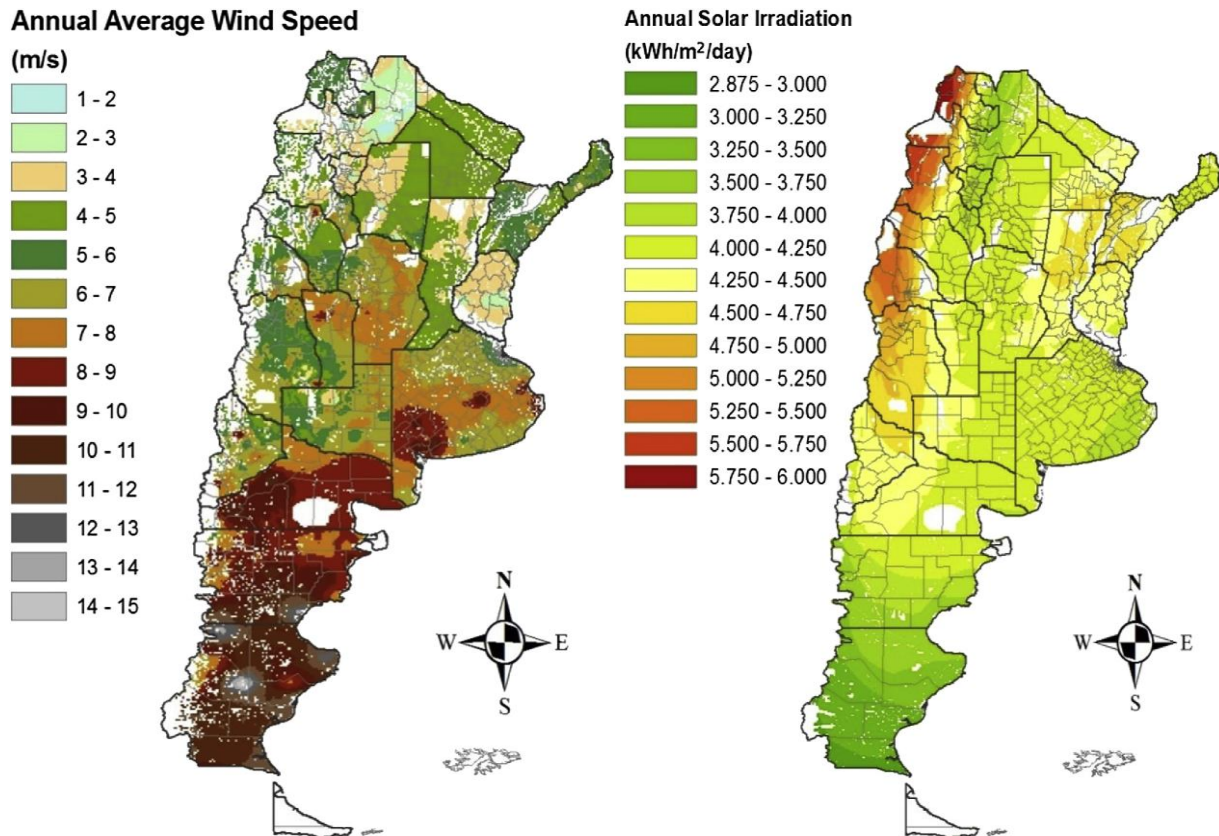


Figure 1.2 a; 1.2b: Wind speed [m/s] at 50 m above ground level map (Sigal et al., 2014); annual average solar radiation [kWh/m²/day]

According to the study carried out by (Sigal et al., 2014), it can be observed that the region of Patagonia, and some regions in the centre of the country, have the highest hydrogen production potential, with values exceeding 200 tons/km² per year. In the south of the province of Chubut, near the city Comodoro Rivadavia, there is one of the highest potentials, estimated at 464 tons/km²/year. The country's solar potential is very high in all the departments of the Andes, from the province of Mendoza up to the north, is over 180 tons/km²/year. In addition, the central provinces of Entre Rios, Chaco and Corrientes, which are located in the north-east of the state, have a solar potential of between 180 and 200 tons/km²/year.

1.3 Italian energetic scenario

In 2021, the Italian economy registered intensive growth, the overall added value of the production sectors increased in volume by 6,5 %, while the energy sector showed a growth of 4,9 %. During the same year, final energy consumption increased by a total of 11,4 % compared to 2020. The increase includes all sectors, in particular transport (+22,4 %), residential (+8,2 %)

and industry (+6,7 %). Primary energy demand stood at 153.024 ktoe, that correspond to an annual increase of 6,2 %.

Italy has a strong energy dependence on foreign countries, as shown by graphic 1.3. In 2021, the national production of energy sources decreased by 3,4 % overall, while net energy imports increased by 8,3 %. The need for electricity was met 86,5 % from domestic production, which amounted to 274,8 TWh and the remaining 13,5 % from net imports from abroad, amounting to 42,8 TWh.

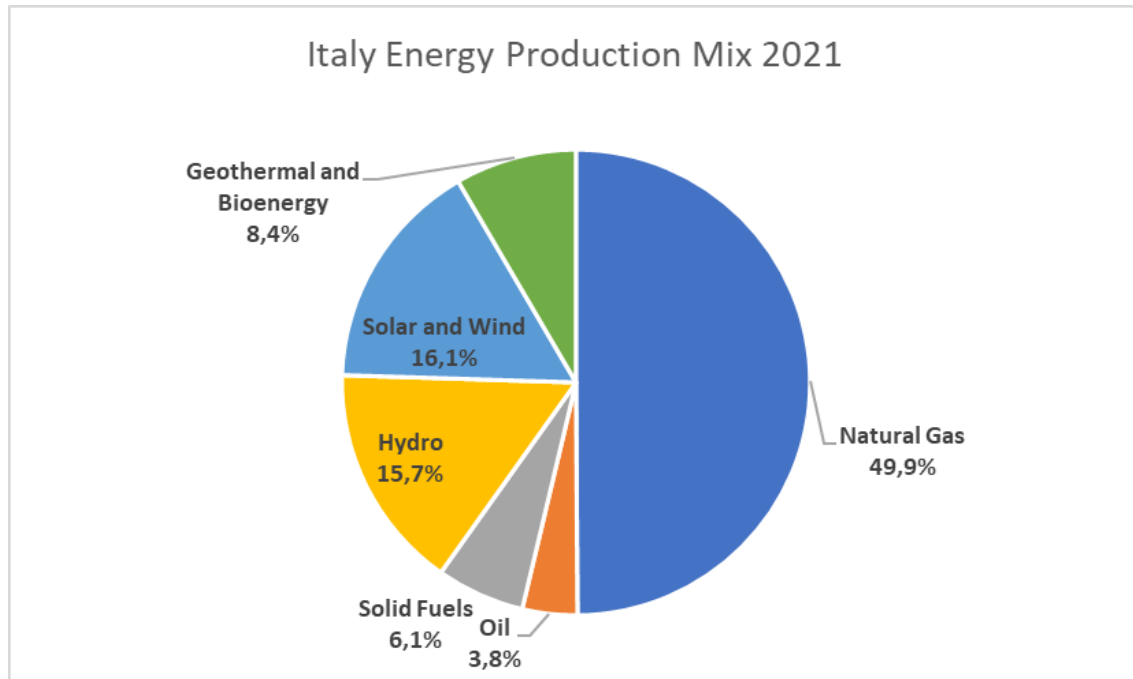


Figure 1.3: Italy energy production mix 2021 (the Author)

Non-renewable thermoelectric power accounted for 59,7 %, with 6,1 % coming from plants fuelled with solid fuels, 3,8 % from oil products and other fuels, and 49,9 % from plants fuelled with natural gas. Regarding renewable energy sources, in 2021 these were widely used in Italy both to produce electricity and heat, and in the form of biofuels. Overall, the share of renewables in gross final consumption is estimated at around 19 %. In the electricity sector, hydroelectric power contributed 15,7 % of total production. There was an increase in wind power production of 10,8 % with respect the previous year, which together with photovoltaics contributed 16,1 % of gross production. The remaining 8,5 % is generated by geothermal and bioenergy. In the thermal sector energy consumption from renewables increased by about 5 % compared to 2020, mainly due to the increased use of solid biomass, such as the wood. Finally, in the transport sector, there was a 15 % increase in the release of biofuels for

consumption compared to the previous year (Ministero della Transizione Ecologica & Dipartimento per l'Energia ed il Clima, 2021).

By the end of 2021, the total number of renewable electricity generation plants reached 1 million, with a capacity of about 38 GW, ensuring a production of 65 TWh of fossil free energy. Italy's decarbonisation targets include an acceleration in the development of wind and photovoltaics, ensuring an installation of at least 3800 MW by 2030. The current national target is to achieve renewables share of more than 30 % in the national energy production mix for the year 2030.

One of the strategies for sustainable development is energy communities, through which an estimated 17 GW of renewable capacity will be installed, for a total investment of €13,4 billion in the current decade.

1.3.1 Assessment for the potential of renewables in Italy

Italy has great potential for photovoltaic energy, and good potential for wind and hydroelectric power. According to (Energoclub, n.d.), hydroelectric power is the most exploited, 17 GW of power is installed in Italy, against 22 GW potential, producing 46.000 GWh compared to the 65.000 GWh it could ideally produce annually.

Italy has a wind power potential of 30 GW, but currently has only installed a capacity of 2,6 GW, less than a tenth. The wind power sector could contribute 50.000 GWh annually to energy needs, compared to the 4.000 GWh currently being produced. The offshore potential is estimated to be 3.000 MW, ensuring a potential energy production of 10 TWh per year. The national wind potential is mostly concentrated in the southern regions and the Sicilia and Sardegna islands. The north has a low wind potential and is concentrated in mountainous areas, which are difficult to install.

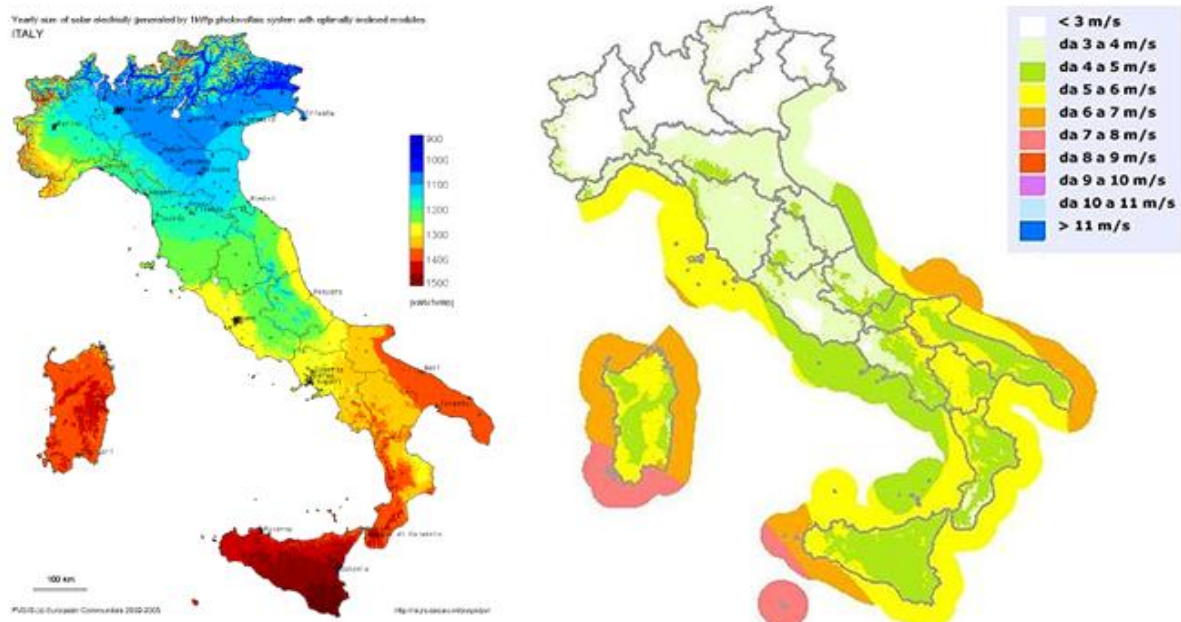


Figure 1.4 a, 1.4b: Annual average solar radiation [kWh/m²/day] (Energoclub, n.d.); wind speed [m/s] at 75 m above ground level map (Consulente Energia, n.d.)

Photovoltaics is the technology with the highest potential in Italy, especially in the south of the country. The theoretical potential installed capacity is 90 GW, for an energy production of 110.000 GWh each year, considering an average productivity of 1.200 MWh/MW/y.

The national average photovoltaic potential varies greatly between the north and south of the country. Under optimal conditions, a 1 kW photovoltaic system has an average output of 1000-1100 kWh/y in northern regions and 1500-1700 kWh/y in southern regions.

1.4 The role of the hydrogen in the global decarbonisation scenario

A new green economy is emerging in which hydrogen will play a significant role with a strong market value in a 100 % renewable future. The expansion of the hydrogen market will have geo-economic and geopolitical implications. Hydrogen will play a key role in the challenge to global change, as it can cut emissions in many energy-intensive sectors without compromising socio-economic development. Currently, green hydrogen has higher production and transport costs than grey hydrogen. Foreseen say that the lowering of costs due to technological maturity will allow green hydrogen to reach a competitive cost in the market by 2030, so this market is expected to explode over the next decade. The green hydrogen market is estimated to have \$11,3 trillion investment opportunities over the next 30 years (IRENA, 2022).

The difficulty of reducing emissions in energy-related sectors is largely due to the global dependence on fossil fuels, which contribute to most CO₂ emissions. One way to decarbonise heavy industries is the electrification of processes using renewables. The main problem with this solution is the volatility of wind and photovoltaic energies, which does not guarantee continuity of operation. In addition, due to the different applications of fossil fuels, many sectors remain difficult to decarbonise with electricity alone. The most important alternative is green hydrogen because it provides flexibility both as a chemical element and as a non-emitting energy carrier (Oliveira et al., 2021).

The hydrogen chain will be very massive and will include all processes of production, transport, conversion, and utilisation of hydrogen, ensuring the connection of energy, heat, and transport sectors. (Energy Agency, 2019) has stipulated key points for the quick development of hydrogen on a global scale. The industrial ports will be the brain centres for scaling up the use of clean hydrogen, providing storage and production bases and improving transport logistics. In addition, the improvement of existing pipelines and the creation of new lines dedicated solely to hydrogen transport will be key to ensuring rapid and continuous land transport. Finally, technological development will be crucial to ensure the penetration of hydrogen in some technological advanced sector, as well as the transport.

To permanently expand the hydrogen market, an important role will be played by the industrial supply chain, which can lead the development of dedicated 'green hydrogen corridors' linking low-cost renewable energy regions with demand centres. Many infrastructures already exist, such as existing natural gas and electricity grids, which can be adapted to hydrogen. Logistics is also very important for the definition and development of international trade routes for hydrogen, which will enable the creation of new production and utilisation facilities. All this will lead to the creation of a global hydrogen market (Renewable Energy Agency, 2020).

The largest consumer and producer of hydrogen is China, which relies on coal. The United States is the second largest consumer and producer of hydrogen in the world, accounting for 13 % of global demand. The European Union has a hydrogen value chain development strategy that must be fully developed and integrated by 2050. By 2024, the EU would like to install an electrolysis capacity of 6 GW, which should increase to 40 GW in the following six years, to ensure an annual hydrogen production of 10 million tonnes. The growth of hydrogen plants will

parallel that of renewable plants, which will grow by about 120 GW of installed capacity (Renewable Energy Agency, 2020).

The figure 1.5 presents all the ‘hard-to-abate’ sectors, characterised by technological, logistical, and economic challenges to be decarbonised, in which hydrogen can be used to achieve this goal.

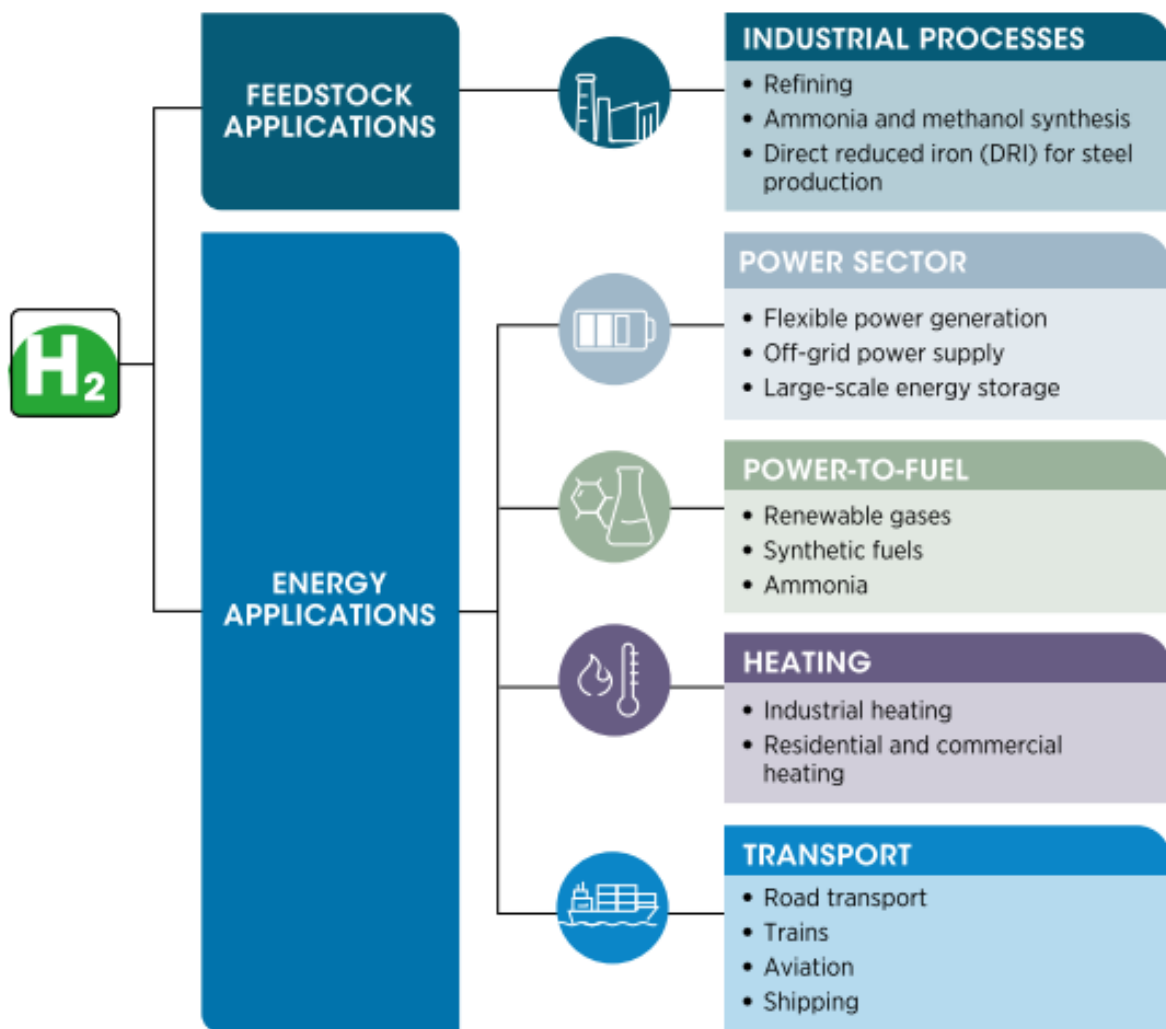


Figure 1.5: Hydrogen application fields (IRENA, 2022)

- Chemical Sector

The chemical industry is in the centre of the modern economy, providing important materials such as fertilisers, synthetic textiles, and drug precursors, supporting the food, pharmaceutical and textile economies. Among many applications, green hydrogen has great potential to be implemented in the chemical synthesis industry, where there is currently a significant demand

for hydrogen globally, 96 % of which is 'grey' hydrogen produced from oil, coal and steam methane reforming. The annual demand of hydrogen for the ammonia synthesis was 30,9 million tonnes in 2020 (International Renewable Energy Agency (IRENA), 2022b).

The most widely used chemical is ammonia, which is used in the production of agricultural fertilisers, in explosives and in cleaning products. Currently, ammonia is produced using fossil fuels, mainly natural gas (Rambhujun et al., 2020).

Another product of the chemical industry is methanol, which is mainly used for the synthesis of other chemicals, such as oil. Methanol is also used in the transport sector, as fuel in internal combustion engines. Green hydrogen can be used to produce methanol to replace the fossil fuels currently in use (International Renewable Energy Agency (IRENA), 2022b).

- Oil Refining Sector

The oil sector is a large consumer of hydrogen, which is used as a reagent for the removal of impurities, such as sulphides, from crude oil in the hydrotreatment process, and is also used for the synthesis of biofuels and oil sands, as well as a feedstock and energy source. Currently, this sector consumes 38 million tonnes of hydrogen annually, which corresponds to one third of world production. According to (Energy Agency, 2019), has been estimated 7 % growth in demand for hydrogen in the oil sector by 2030.

- Transportation, Building and Heating Sectors

Hydrogen can contribute to the decarbonization of transportation, as well as to commercial and residential heating, and meet the thermal energy demands of some industrial processes. In the process of decarbonisation of the transport sector, hydrogen can play a very important role and has potential advantages over conventional fuels. The technologies for using hydrogen are the internal combustion engine, in which hydrogen can be burned, and fuel cells which react hydrogen and oxygen from the air and release water vapour. The combustion of hydrogen in ICEs can produce a small amount of NO_x, while fuel cell electric vehicles are totally environmentally friendly because they only emit water vapour (Sharma & Ghoshal, 2015). The main challenge in using hydrogen as a fuel is its storage, and the supporting infrastructure network, which is currently not adequate for large-scale expansion.

In the residential and commercial heating sector, CO₂ emissions are generated by space and water heating, cooking, and district heating and cooling. By integrating hydrogen into the natural gas network, or by building a pure hydrogen transport network, CO₂ emissions from the heating sector can be reduced.

The heat consumed by industrial processes contributes significantly to CO₂ emissions. Hydrogen combustion would provide the required heat at the temperatures demanded by most industrial processes, such as glass production (1600 °C), blast furnace (1100 °C), steam methane reforming (800 °C), and cement production (1400 °C).

- Power Sector

Renewable Hydrogen will play a key role in the power sector to link energy demand with intermittency production from renewable sources, such as wind and photovoltaic. Hydrogen can provide seasonal energy storage, because, unlike electricity, has the advantage that it can be stored with minimal losses in liquid form, or no losses at all in compressed gas form, for long periods of time (Samsatli & Sheila, 2019). Green hydrogen can be produced by electrolysis when production exceeds demand and stored in underground caverns or reservoirs in the form of compressed gas (Oliveira et al., 2021).

To implement this storage system, it is necessary to invest in new infrastructure for the production, storage, transport and use of green hydrogen.

- Steel Production

The use of hydrogen for crude steel production is highly considered for the reduction of greenhouse gas emissions from the steel industry. This topic is discussed in the next paragraph.

1.5 State-of-the-art steel production

World steel production has increased steadily over the past decades, from 850 to 1878 million tonnes from the begin of the century to 2020. The largest steel manufacturer is China, which alone produces 56,7 % of the world's steel. European countries' steel production in the year 2020 was 139 million tonnes, representing 74 % of world production. Italy ranks 13th in the list of producing countries, with approximately 20 million tonnes of steel produced annually, of which 15,3 % is by the oxygen furnace and 84,7 % by the electric arc furnace, a different statistic

from the European average, where the two production methods are almost equivalent. Italy also produces 3,4 million tonnes of pig iron annually with blast furnaces (Worldsteel, 2021). According to the IEA study, global steel demand is expected to increase by more than one-third until 2050, resulting in higher CO₂ emissions, despite an increase in secondary production and a reduction in energy intensity, reaching 2,7 Gt CO₂ per year by 2050, 7 % more than today. To meet global energy and climate targets, emissions from the steel industry must fall by at least 50 % by 2050 (IEA, 2020).

Conventional steel production is one of the largest CO₂ sources in Europe, being responsible for about 4 % of CO₂ emissions (Berger, 2020). The evolution of alternative steel processes is therefore crucial to contribute to the reduction of carbon dioxide to the atmosphere as evidenced by the European Union's Sustainable Development Strategy, which stated '*The Commission will support cutting-edge technologies for clean steel production in order to achieve zero-emission steel production in 2030 and will assess what part of the funding authorised under the European Coal and Steel Community can be used*' (European Union, 2017).

Several options for decarbonisation are being developed, such as carbon capture and storage (CCS), energy efficiency of current steel production methods, steel recycling and the use of hydrogen (Berger, 2020).

The standard steelmaking processes are the blast furnace with the basic oxygen furnace for primary production, and the electric arc furnace for secondary steel production.

- Blast Furnace and Basic Oxygen Furnace

The BF-BOF route is the leading technology in steel manufacturing, providing 71 % of the world's crude steel production. This system consists in a blast furnace to reduce iron ore to pig iron using coke and then refine it into steel in a basic oxygen furnace (BOF). The BF-BOF route is very polluting, the average emissions from the crude steel production of the top 15 producing countries are 2238 kgCO₂ per tonne of crude steel produced (Fan & Friedmann, 2021).

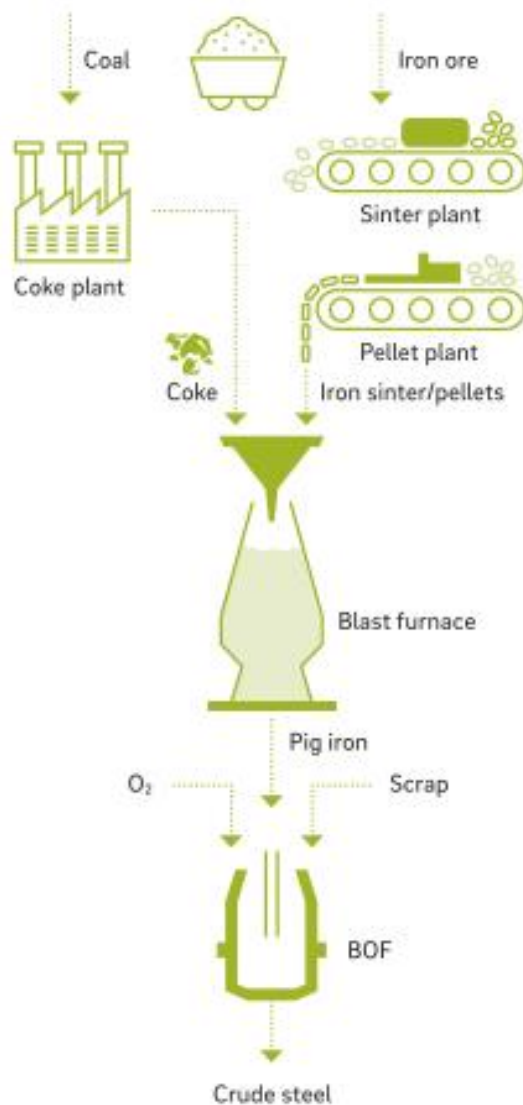


Figure 1.6: BF-BOF crude steel production route (Berger, 2020)

In the reduction process through the blast furnace, the charge inserted consists of coke, limestone material and ground iron ore. The coke has multiple functions, including the development of reducing gas for the reduction of iron oxides according to the following chemical reaction:



Coke also provides the carbon for the steel produced and the heat for the melting process, supports the weight of the material loaded into the top of the blast furnace and acts as a filter for particles and dust. The blast furnace works at high temperatures that are reached by blowing hot air from below (1000 - 1200 °C). The melting is completed in the lowest part of the plant, where the temperature reaches 2000 °C. The cast iron produced is in a liquid state, with a carbon content of around 4-5 %, and then reaches the basic oxygen furnace, into which

oxygen is introduced through a nozzle, to promote the oxidation of certain chemical elements such as carbon and silicon. Varying quantities of scrap can be introduced at this stage (Porta, 2020). The total emissions of the blast furnace-basic oxygen furnace process range between 1,6 and 2 tonnes of CO₂ per tonne of steel produced.

- Electric Arc Furnace

EAF is currently the main technology to produce secondary steel through the recycling of steel scrap. According to (Worldsteel, 2021), EAF contributed 26,3 % of world steel production in the year 2020.

The electric arc furnace melts the scrap by means of an electric arc fired by three consumable cylindrical graphite electrodes. It consists of three parts, the upper chamber that contains the steel scrap to be melted by the electric arc, the cover that allows the passage of the electrodes, the extraction of the flue gases produced by the melting, and the introduction of lime and other materials that react with the impurities and form slag. The lower shaft contains both the molten steel and the slag.

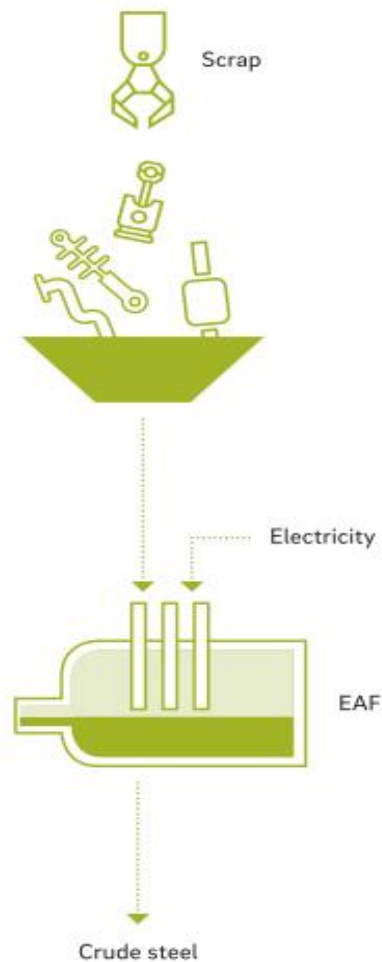


Figure 1.7: EAF steel production route (Berger, 2020)

This process has a lower environmental impact than the BF-BOF process, as the main source of emissions is electricity from the grid, whereas in the primary production process, most emissions are due to the production and use of coke. A significant limitation preventing this technology from expanding further is the limited availability of steel scrap. Electric furnace steel can only be used in certain applications, as it contains higher percentages of impurities, such as sulphur and other residual elements like copper and nickel, than furnace steel (Porta, 2020).

1.6 Decarbonisation alternatives for the steel industry

As explained in the previous section, current steel production methods do not allow for a decarbonisation process in the steel industry for several reasons. Faced with a continuous growth of steel production and decarbonisation targets, radical changes in steel production processes are necessary. The two most important options are the combination of traditional processes with carbon capture and storage facilities, and the use of green hydrogen as a

reducing agent to produce reduced iron, combined with electricity from renewable sources (Vogl et al., 2018).

- Carbon Capture and Storage

Carbon Capture and Storage is a greenhouse gas emission reduction process for many sectors, including thermal plants, refineries, cement production plants and steel mills. Blast furnaces are suitable for the application of CO₂ capture equipment, as emissions are generated in specific areas of the plant, particularly from the combustion of synthesis gas (produced from coke) in the blast furnace, from the iron ore sintering plant, and the coke producing plant (Ding et al., 2020). In recent years, many CO₂ capture techniques have been developed, involving chemical absorption, physical absorption, and separation by cryogenic distillation.

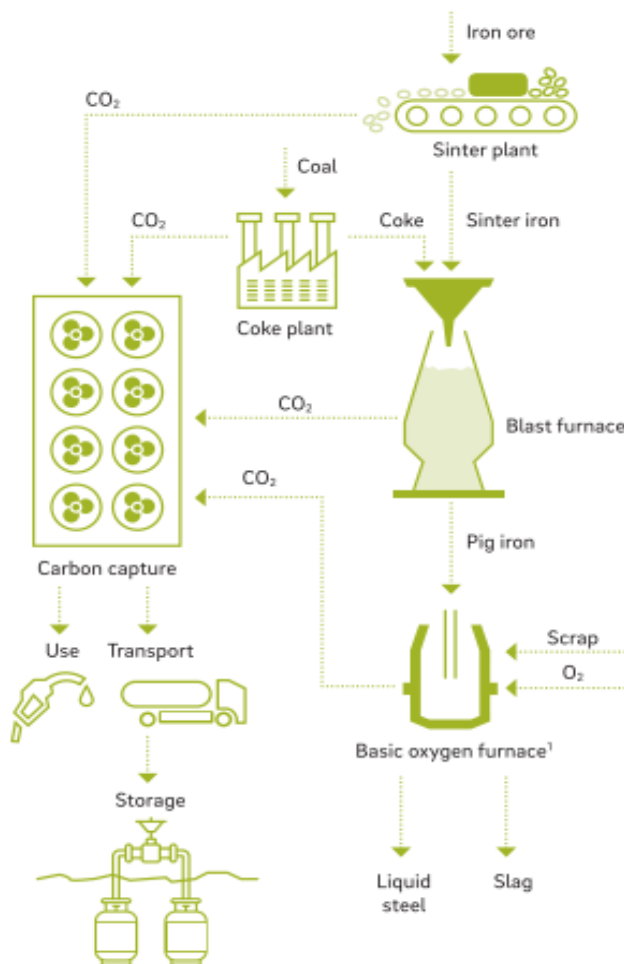


Figure 1.8: Carbon capture and storage technology (Berger, 2020)

The CO₂ capture process is complex and involves transport and storage at special sites, which currently do not guarantee large amounts of storage. Other problems with CO₂ capture are that

electricity is consumed for the process, which can be a source of indirect emissions, and although emissions can be reduced by around 90 %, fossil fuels continue to be used, making the process unsustainable in the long term (Arasto et al., 2013).

- Hydrogen in Blast Furnaces

An option to be adopted to reduce emissions from blast furnaces is the use of hydrogen as a reducing agent, to decrease the need for coke. Several alternatives are proposed in the literature, and some are starting to be introduced. (Yilmaz et al., 2017) demonstrated that the insertion of pure hydrogen in gaseous form into the blast furnace to replace part of the carbon monoxide from the coke. The insertion of 27,5 kg of hydrogen per tonne of hot metal results in a saving of 120 kg of coke per tonne of HM. This would guarantee a decrease in CO₂ emissions of about 20 %, or 460 kg of CO₂ per tonne of steel produced. There are no blast furnaces that are implementing this solution, due to the problems caused by replacing coke with hydrogen without changing the production process. Hydrogen has very different physical properties from carbon monoxide, in particular its density is very low, which makes it difficult to use inside the blast furnace, as the hydrogen molecules tend to escape to the top, while the iron ore reduction process takes place at the bottom. Moreover, hydrogen is highly flammable, and it is not known whether its use inside a blast furnace could cause safety problems. In addition to the technological difficulties that limit its use, the presence of coke in existing blast furnaces is essential to ensure their proper functioning (Porta, 2020).

The use of hydrogen gas does not represent an industrial alternative, while the technique of inserting Hot Briquetted Iron into blast furnaces is already employed. HBI contains a high percentage of Fe, more than 90 %, and this makes it possible to reduce the use of other reducing agents. The introduction of 100 kg of HBI per tonne of hot metal produced, cuts the use of reducing agents by 25 kg, and a reduction in coke by up to 18 kg per tonne of crude steel. The presence of a minimum percentage of coke must always be guaranteed. The use of HBI also guarantees an increase in plant productivity of up to 10 %. The utilisation of the reducing gas is lower because HBI is a pre-reduced material. An increase in the calorific value of the reducing gas has been verified due to the higher CO and H₂ content (Griesser, 2020).

- Direct Reduced Iron

One solution that is becoming popular for the decarbonisation of the steel industry is the production of reduced iron in the DRI plant, which converts raw iron ore into iron sponge, characterised by high porosity, purity, and high reactivity to oxygen. The iron sponge produced requires further treatment for complete transformation into steel, which in most cases takes place in the electric arc furnace. Direct Reduced Iron in the form of Hot Briquetted Iron can also be used inside blast furnaces to reduce the use of coke, and consequently greenhouse gas emissions (Chevrier et al., 2021).

DRI technology is already on the market, but currently the production of reduced iron accounts for a very low percentage in the global scenario. In the year 2020, 106 million tonnes of reduced iron were produced, of which only 0,6 million tonnes in the European Union (Worldsteel, 2021). There are different types of DRI plants, which vary according to the reducing reactors used, the main systems being the shaft furnace, rotary furnace, and fluidised bed reactor. The main worldwide supplier of direct reduction plants is Midrex Technologies (Porta, 2020).

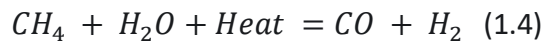
The reduction process takes place at high temperatures between 800 and 1100 °C. It is important that the temperature is kept below the melting temperature of the metal, at 1200°C. The reducing gas, after being preheated, enters the shaft furnace, where iron ore in the form of pellets is also placed in the upper part, allowing the reduction reactions to take place. Afterwards, the reacted iron ore passes into the lower part of the shaft, where it cools down. Alternatively, DRI can exit the reduction furnace hot and be transformed into Hot Briquetted Iron by a mechanical pressing process. Reduced iron in the form of HBI is less reactive and porous respect DRI, so it is easily transported and stored.

between hematite and hydrogen is endothermic, and needs more heat than mixing with carbon monoxide, which produces an exothermic reduction reaction. The design of the heater depends on the available energy sources, either an electric heater or a hydrogen burner can be used. These plants are at an advanced stage of development (Chevrier, 2020).

1.7 State of the art hydrogen production

About 70 million tonnes of hydrogen are currently produced worldwide, 76 % of which is from natural gas, and 23 % from coal, which is used almost exclusively in China. Hydrogen production via natural gas has a carbon footprint of 10 tonCO₂/tonH₂ produced, while the specific emissions of hydrogen produced via coal average 19 tonCO₂/tonH₂. This means that hydrogen production is responsible for the emission of around 800 million tonnes of CO₂ each year. The leading technology for dedicated hydrogen production in the ammonia and methanol industries and in refineries using natural gas is Steam Methane Reforming which produces the so-called 'Grey Hydrogen'. The 'Green Hydrogen' obtained by the electrolysis process accounts for only 2 % of world hydrogen production (Energy Agency, 2019).

Steam Methane Reforming is a process involving the endothermic reaction,



in which natural gas and pressurised steam are combined to produce a syngas containing carbon monoxide and hydrogen. Carbon monoxide is then converted into carbon dioxide and hydrogen using the water-gas shift reactor. The reforming process takes place at temperatures above 700 °C and pressures between 3 and 25 bar. The heat required for the reaction is provided by the combustion of natural gas (Valenzuela & Zapata, 2007).

'Black Hydrogen' is produced from coal through the gasification process. The typical gasification reaction is endothermic, converting carbon into carbon monoxide and hydrogen. Also in this case, CO is further converted into CO₂ and H₂ through the water-gas shift reaction.

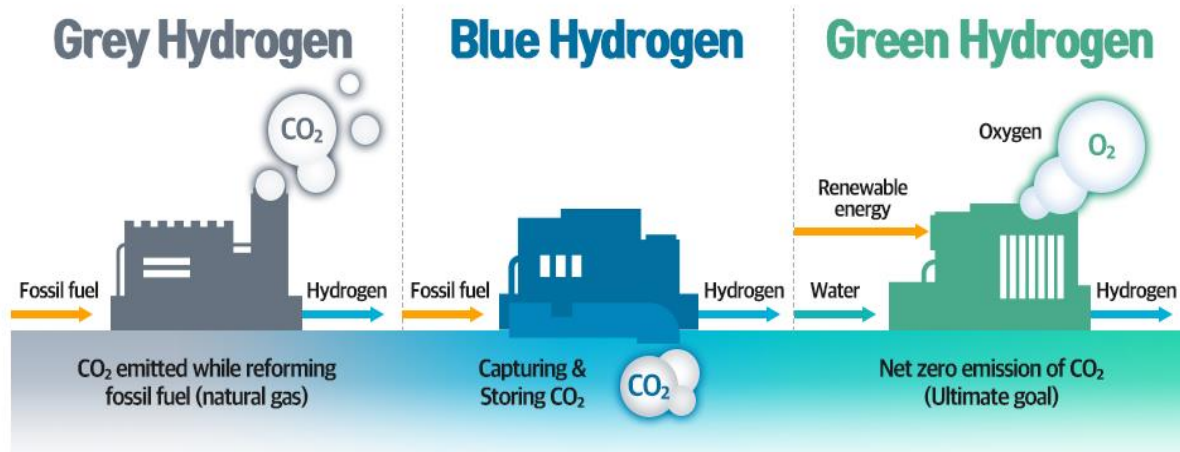


Figure 1.101: Grey, blue and green hydrogen production differences (POSCO Newsroom, 2020)

Carbon Capture and Storage technology can be combined with the methanation process to reduce CO₂ emissions, obtaining 'Blue Hydrogen'. The other existing technology using natural gas is Autothermal Reforming, in which O₂ and CH₄ are combined to produce syngas through an exothermic reaction. This process is able to capture almost 95 % of the emitted carbon dioxide (Hydrogen Council, 2020). However, the latter process is not used in industry due to low efficiency, and the need to purify the hydrogen produced.

1.7.1 Green hydrogen production

Green hydrogen currently plays a marginal role, but its growth in the coming years will be exponential, due to the key role hydrogen can play in the decarbonisation scenario in many fields, such as transport, oil refining, steel and chemical industry, and the energy sector. Currently, the cost of low-carbon hydrogen, produced by electrolysis, has an average cost in Europe of around \$6.000/ton, which is very high compared to grey hydrogen. The cost of green hydrogen is highly influenced by the cost of renewable energy, which will decrease in the coming years, especially for photovoltaics and wind power. As large-scale electrolyser production increases, the cost of installing this technology will also decrease, making green hydrogen competitive on the market.

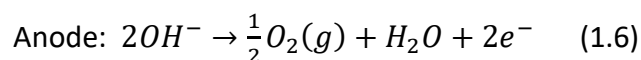
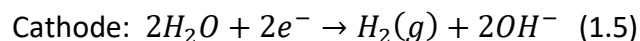
Hydrogen also represents a solution for the volatility of renewable energy sources, as the possibility of producing, storing and transporting hydrogen makes it possible to greatly increase energy flexibility and optimise the energy production of photovoltaic and wind power plants, facilitating their growth (H2IT, 2019).

Several projects to produce hydrogen from renewable resources are emerging in many remote areas with great potential for solar and wind energy, such as Patagonia, New Zealand, North Africa, the Middle East, Mongolia, much of Australia, China and the United States, where hydrogen can be produced from cheap electricity (Energy Agency, 2019).

The principle of water electrolysis is based on the separation of the H_2O molecule into H_2 and O_2 applying electricity. There are four types of electrolyzers, which use different physico-chemical processes, depending on the temperature and pressure at which they operate, and the type of electrolyte used. The main electrolyzers are the Alkaline and the Polymer Electrolyte Membrane (PEM), which are already commercially available, while the Anion Exchange Membrane (AEM) and Solid Oxide are in the research and development phase (International Renewable Energy Agency, 2020).

- Alkaline Electrolyser

The cathode is formed from nickel and covered with platinum. Metals such as nickel or copper, covered with metal oxides such as manganese oxide, tungsten, or ruthenium, are used for the anode (Ancona et al., 2019). The system is immersed in the electrolyte, which is an alkaline solution containing between 20 and 40 % KOH by weight. The reactions that take place are as follows.



In the cathode, water is split into hydrogen gas and OH^- ions thanks to the DC electrons supplied. The OH^- ions produced are released into the electrolyte, which transports them to the anode, where they are oxidised (Bessarabov & Millet, 2017).

The hydrogen produced is dissolved in the alkaline solution and separated through a gas-liquid separator located outside the electrolyser. This limits the operating pressure of alkaline electrolyzers to 30 bar. The operating temperature varies between 70 and 90 °C.

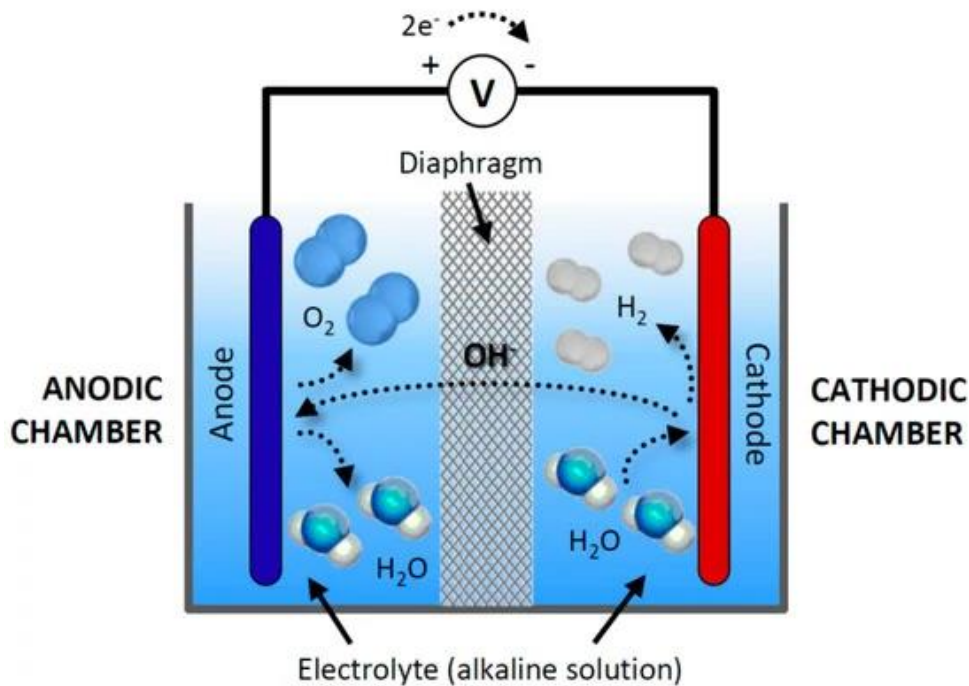


Figure 1.11: General scheme and operation of an alkaline electrolysis cell (Rodríguez & Amores, 2020)

Compared to other technologies, alkaline electrolyzers have high durability, can work up to 60.000 hours, and technological maturity, leading low specific costs. The cost of alkaline electrolysis systems is currently in the range of \$600-1000/kW for large power installations, in order of MW. The main disadvantages of this technology are the low current density, which is currently 0,2-0,8 A/cm², and the operating problems under dynamic conditions. At present, hydrogen production is limited to an operating range of between 20 % and 100 % of rated power, to avoid the safety risk due to the formation of possible flammable mixtures (Rodríguez & Amores, 2020). The new research projects use zero-gap electrodes, which consist of thinner diaphragms and different types of electrocatalysts to increase the current density to the levels used by PEM electrolyzers (higher than 2 A/cm²) (International Renewable Energy Agency, 2020).

- Polymer Electrolyte Membrane Electrolyser (PEM)

PEM electrolyzers consist of a PFSA proton exchange polymer membrane, which acts as a solid electrolyte. The material used for the polymer membrane, which allows the electrode and gas separation, is Nafion. The thickness of the membrane is very thin, about 0,2 mm, which allows for high conversion efficiencies compared to alkaline electrolyzers. The high chemical-

mechanical resistance of the polymer membrane allows PEM electrolyzers to work at high pressures, up to 70 bar (International Renewable Energy Agency, 2020).

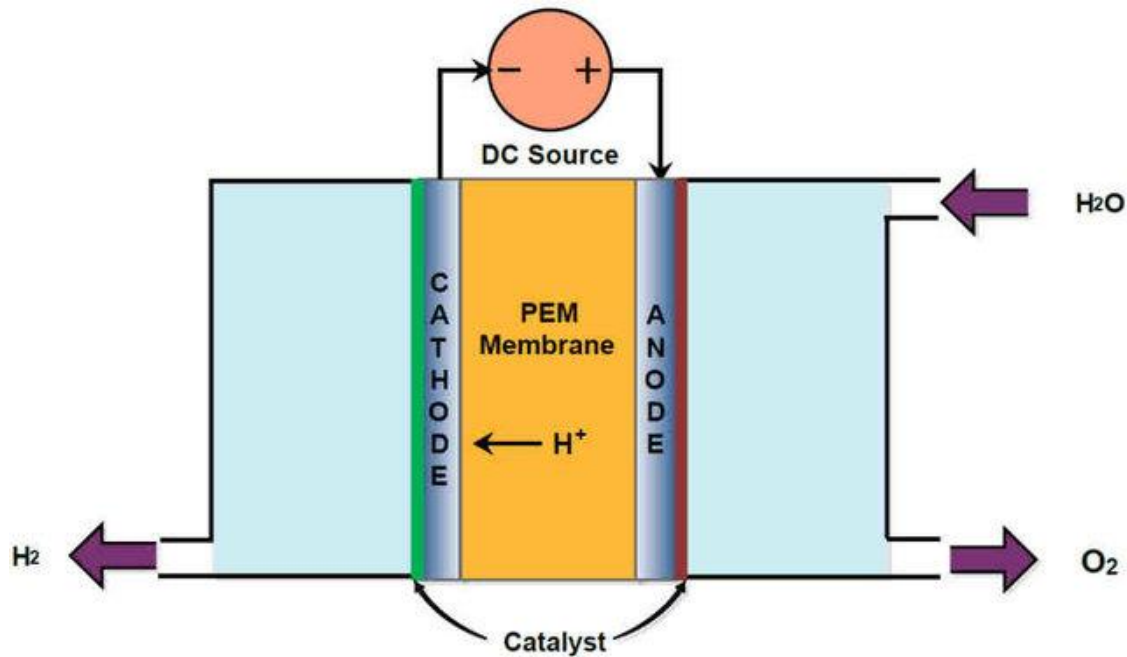
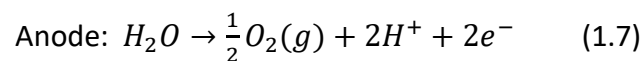


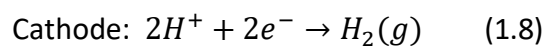
Figure 1.12: General scheme and operation of an PEM electrolysis cell (Rashid et al., 2015)

The catalysts are based on platinum, iridium, ruthenium, and rhodium. The operating temperature is between 50 and 80 °C. The typical current density of PEM varies between 1 and 2 A/cm².

Water is introduced into the anode, where the oxidation reaction takes place and H⁺ ions are produced.



The H⁺ ions produced cross the polymer membrane, flowing towards the cathode, where they react with the electrons, which reach the cathode via an external circuit, producing pure hydrogen.



Compared to alkaline cells, polymer cells show higher efficiency and higher reliability. The use of a solid electrolyte instead of a caustic solution also increases safety (Ancona et al., 2019). The main disadvantage of PEM electrolyzers is the limited life of the membranes. At present, PEM electrolyzers are growing on the market, but their cost is much higher than alkaline electrolyzers, ranging between \$1000 and \$1500/kW, and the electrolyzers on the market are small (Valenzuela & Zapata, 2007).

- Solid Oxide Electrolyser (SOEC)

In this type of cell, electrolysis takes place at high temperatures between 700 and 1000 °C. Under these conditions, the kinetics is faster, and the reaction is easily reversible, allowing the use of non-precious metals for the electrodes. The electrical energy required to split the water molecule at these temperatures is less than the electrical energy required at normal temperatures, because part of the energy required is provided by heat (Valenzuela & Zapata, 2007). SOEC electrolyser needs less than 50 kWh per kg of produced hydrogen.

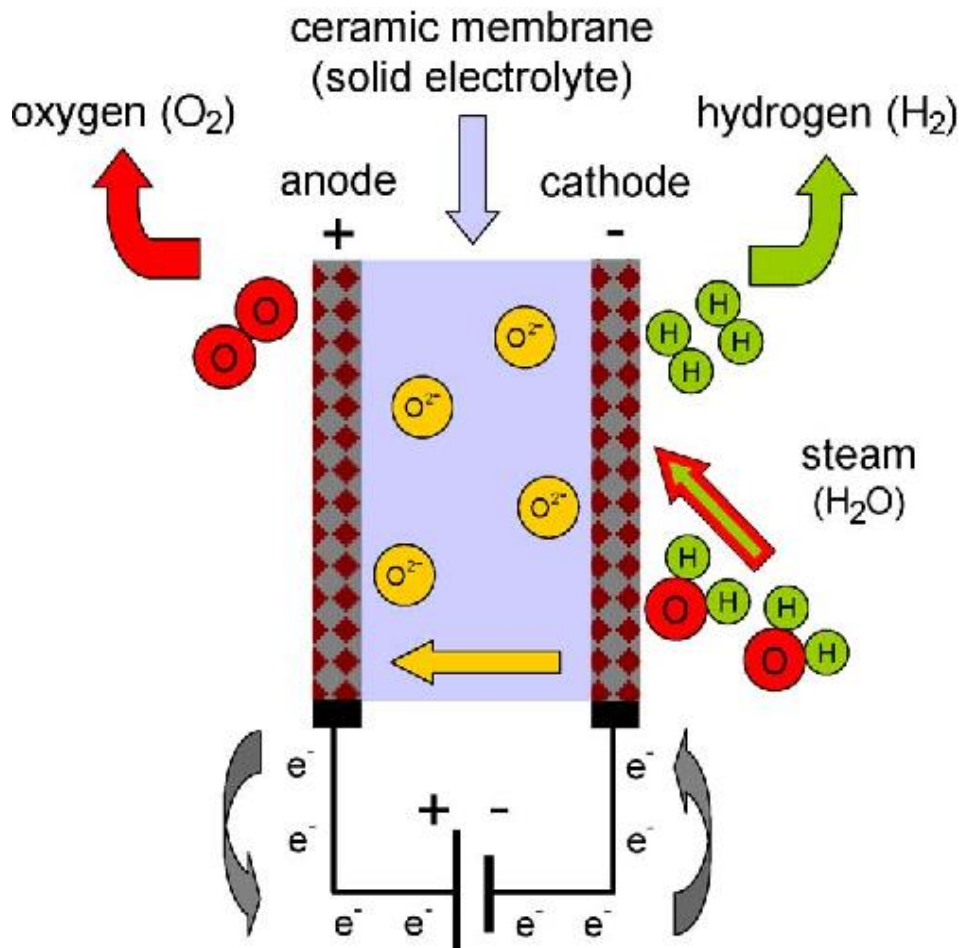
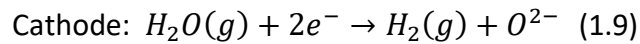


Figure 1.13: General scheme and operation of an SOEC electrolysis cell (Ursúa et al., 2012)

Solid oxide electrolyzers are characterised by ceramic multilayers consisting of a dense electrolyte placed between two porous electrodes. Water vapour is fed to the cathode and when a potential is applied, it diffuses into the reactive sites and is dissociated into hydrogen gas and O^{2-} ions. The hydrogen produced diffuses to the cathode surface, where it is collected, while the O^{2-} ions migrate through the electrolyte to the anode, where they are oxidised to oxygen gas (Ancona et al., 2019).

The reactions that take place are as follows:



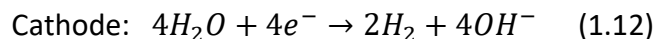
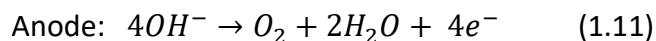
Compared to PEM and alkaline electrolyzers, these systems do not require purification of the water. The solid electrolyte must possess a high ionic conductivity, which, at high temperatures, allows the migration of O^{2-} ions from the cathode to the anode.

The main disadvantages of SOEC electrolyzers are the fast degradation of the electrodes, and the very short lifetime, less than 20,000 hours. Currently, SOECs are only developed in small sizes, in the kilowatt range. The installation cost of these electrolyzers is over \$2000/kW. Although SOECs represent an option for the future, they need substantial technological improvements to be commercialised on a large scale.

- Anion Exchange Membrane Electrolyser (AEM)

AEM is a developing technology, and its main feature is the use of inexpensive transition metal catalysts instead of noble metal catalysts such as platinum, ruthenium and iridium (Cossar et al., 2019).

The process of electrolysis of water into hydrogen and oxygen is possible due to the two half-reactions occurring at the anode and cathode.



The reduction reaction of water takes place at the cathode, where it combines with electrons from the external circuit to split water into hydrogen molecules and OH^- ions. The hydroxyl ions diffuse into the AEM electrolyte and reach the anode, where they react to form oxygen and water molecules. Oxygen and hydrogen are produced in gaseous form (Vincent & Bessarabov, 2018).

This technology is not yet commercially viable, the energy efficiency, robustness and stability of the membrane must be improved. The specific production cost of the AEM cell is much higher than for other electrolyzers.

1.8 Hydrogen transportation and energy carriers

At present, hydrogen is a regional product, more than 80 % of the hydrogen gas is used in the same site where it is produced. The small percentage of hydrogen that is transported, and

travels short distances, due to the lack of adequate infrastructure and high transportation costs. Despite this, hydrogen in the near future will be a very important energy carrier to transport energy produced in remote locations with large renewable resources to highly populated areas, where the demand for energy is very high (IRENA, 2022).

Hydrogen can be transported on a global scale in three ways, by ship, by pipeline or by truck. There is not a best way for transport at the moment, the optimal choice depends on the end use of the hydrogen, the distance travelled and the type of route (Hydrogen Council, 2021). In general, for distances of less than 1500 km and for small volumes of hydrogen, transporting hydrogen gas via pipelines is the cheapest option. The cost of transport in natural gas pipelines increases linearly with the distance. For the transport of large hydrogen volumes, hydrogen pipelines are the best solution, up to distances of 4000 km. For short distances, small volumes and fluctuating demand for hydrogen, the best option is transport by truck (IRENA, 2022). To cover long distances, shipping is the most suitable solution. Hydrogen in ambient conditions has a low volume density, which prevents it from being transported in large quantities. The main energy carriers to increase the energy density of hydrogen are Ammonia, Liquefied Hydrogen and Liquid Organic Hydrogen Carriers. Each of these carriers requires three stages, the transformation of hydrogen gas into the form and conditions suitable for transport, the transport stage, and the reconversion of the carrier into pure hydrogen gas.

- Pipeline

Projects named 'Power to Gas', or P2G are emerging, which consist in producing hydrogen through electrolysis and feeding it into natural gas pipelines for storage and transport. The study carried out by (Altfeld & Pinchbeck, n.d.) shows that a small percentage of hydrogen, less than 10 % by volume, can be introduced into some parts of the natural gas transport system. Despite this, there are many parts of the system that suffer from hydrogen-related problems. The gas turbines currently in operation have a hydrogen tolerance of 1 % by volume. This value can be increased up to 5 % through structural modifications. Gas engines also have a very low hydrogen tolerance of less than 2 %. Other energy problems arise from the energy density of hydrogen, which is much lower than that of natural gas. Placing hydrogen inside a gas pipeline would reduce the energy transported. Hydrogen also has a higher combustion speed than natural gas, which entails safety risks. In general, the upper limit of hydrogen that can be

introduced into the pipeline is relative to the component with the lower tolerance (Energy Agency, 2019).

Due to this series of structural and energy issues, as well as a safety risk, it is currently very difficult to foresee the use of pipelines to transport hydrogen in the near future. The alternative solution is the construction of new dedicated pipelines for hydrogen, but this alternative needs time and a large production, distribution, and utilisation chain.

- Liquid Hydrogen LH₂

Hydrogen exists in different states; under normal atmospheric conditions, hydrogen is in gaseous form and has a very low density of 0,081 kg/m³. Hydrogen has an excellent gravimetric energy density with a lower heating value (LHV) of 120 MJ/kg, but has a very low volumetric energy density (Aziz, 2021). Liquid hydrogen boiling temperature is -252,9 °C at atmospheric pressure and the density is 70,8 kg/m³ (Wijayanta et al., 2019).

The maritime transport of liquefied hydrogen is being developed, there are already ships capable of transporting it, but the volumes transported are very low. The transport principle is similar to that of liquefied natural gas LNG, but the cryogenic transport conditions of temperature and pressure as well as the equipment are different. The storage and transport tanks have spheric shape to reduce the heat exchange surface area.

The main drawback of liquid hydrogen transport is the liquefaction temperature of -253 °C. Liquefaction occurs by cooling a gas to form a liquid. This process uses a system of compressors, heat exchangers, expansion motors and valves to achieve cooling. The simplest liquefaction process is the Linde or Joule Thompson Expansion Cycle (Amos, 1999). This process involves a high energy consumption, which is equivalent to 30-36 % of the energy contained in the hydrogen, and a high cost of the liquefaction and storage system, which must ensure that cryogenic conditions are maintained. In theory, the energy required to liquefy H₂ at ambient pressure, using liquid helium as the cooling medium, is about 3960 kJ/kg. However, in industrial applications, this specific energy consumption increases to around 12,5 and 15 kWh/kgH₂ (International Renewable Energy Agency (IRENA), 2022a).

Another problem related to liquid hydrogen is the phenomenon of boiloff during storage and transport. This phenomenon consists of the evaporation of part of the hydrogen, usually between 0,2 % and 0,3 % per day, due to several factors, including ortho-to-para conversion,

mixing or pumping energy, radiant heating, convection heating or conduction heating (Amos, 1999).

Liquid hydrogen requires the regasification process before it can be utilised. Since re-gasified H₂ has a high purity, storage, and transport of H₂ in liquid form are considered more appropriate for systems requiring high H₂ purity, such as fuel cells for power generation and H₂-based vehicles. The cost of conversion and naval transport of liquefied hydrogen is estimated to be \$2/kgH₂ (Energy Agency, 2019).

- Liquid Organic Hydrogen Carrier (LOHC)

LOHC are liquid hydrogen carriers under ambient conditions, can be hydrogenated and dehydrogenated reversibly, allowing hydrogen to be stored and transported over long distances (Niermann et al., 2021). The ideal characteristics that are searched for in LOHCs are a high hydrogen storage density, a low enthalpy of reaction, a low degradation rate, non-toxicity, and a high melting point to remain in liquid form at low temperatures. Almost all existing LOHCs have low hydrogen densities of between 5 and 7 % by weight, meaning that each tonne of organic carrier transports between 50 and 70 kg of H₂ (Hurskainen & Itonen, 2020).

The organic hydrocarbon chain consists of hydrogenation through an exothermic reaction requiring temperatures between 100 and 250 °C and operating pressures between 10 and 50 bar. After the transportation phase, dehydrogenation takes place, to separate the hydrogen and the carrier liquid, which is returned to the starting point and hydrogenated again. The dehydrogenation reaction is endothermic, requiring large amounts of heat, equivalent to 30-40 % of the energy contained in the hydrogen. Dehydrogenation takes place in the presence of a catalyst, at high temperatures, between 150 and 400 °C, at low pressures, close to atmospheric pressure (Niermann et al., 2021).

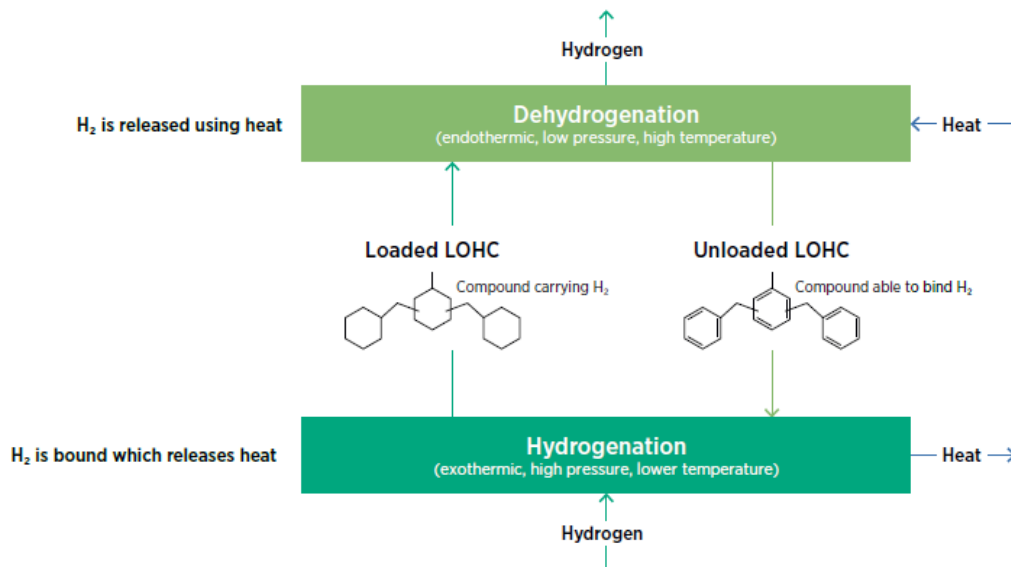


Figure 1.14: Liquid organic hydrogen carrier supply chain (International Renewable Energy Agency (IRENA), 2022a)

The transport of hydrogen by LOHCs has advantages. With physical and chemical properties very similar to those of crude oil, these organic hydrocarbons are compatible with existing transport infrastructures, ensuring safety and competitive transport costs. Toluene and Dibenzyl Toluene have great potential for large-scale production (Rao & Yoon, 2020). Toluene can be converted into MCH, which in liquid form can contain 5,2 % hydrogen by weight. The hydrogenation reaction takes place at temperatures above 180 °C and pressure of around 2 bar.



The hydrogenation reaction takes place in the presence of a catalyst. Methylcyclohexane is produced in gaseous form and is then cooled to room temperature where it is in the liquid phase (Wijayanta et al., 2019).

One aspect that needs to be improved is the dehydrogenation process, which requires a lot of energy, decreasing the thermodynamic efficiency of the system. Although these molecules do not suffer from Boil-Off during transport, unlike Ammonia and liquid Hydrogen, due to their stability, the hydrogenation and dehydrogenation processes have losses, estimated to be 0,1 % per production cycle. The amount of hydrogen contained in the molecule is also very low. LOHC production plants are now entering the commercialisation phase, their production is currently very low. A plant with a capacity of 5 ton/day is being built in Germany (International Renewable Energy Agency (IRENA), 2022a).

(Energy Agency, 2019) estimated that the cost of transporting hydrogen via LOHC is \$0,6 per kg of Hydrogen.

- Liquid Ammonia

A very promising hydrogen carrier is Ammonia. It is synthesised using hydrogen and nitrogen gas as reagents, can be stored for long periods of time, up to months. Ammonia is characterised by a high gravimetric density, consisting of 17,8 % by weight of hydrogen and 82,2 % of nitrogen. It also has a high volumetric hydrogen density of 123 kg per cubic meter, at a pressure of 10 bar, which is higher than other energy carriers, such as methanol and liquefied hydrogen, which contain 99 and 71 kgH₂/m³ respectively (Makhloufi & Kezibri, 2021). The boiling point at atmospheric pressure is -33,35 °C. NH₃ is very toxic with a pungent smell. There are strict protocols to ensure safety.

Ammonia market is developed worldwide. Ammonia is the most produced chemical, in 2020 more than 180 million tonnes of NH₃ were produced, most of it in China and Russia. A large part of ammonia is used for fertiliser production, which means that its use is related to population growth. World production is estimated to grow by 2,3 % each year, up to 600 tonnes in 2050. The main compounds that use ammonia are urea, ammonium nitrate, and ammonium sulphate. Ammonia is also used in the mining industry, for the manufacture of nitro-glycerine and TNT. NH₃ is used to produce synthetic fibres such as nylon in the textile industry (Torino, 2021).

Ammonia has been identified as one of the best alternatives as a green fuel for shipping. The International Maritime Organisation (IMO) has a target to reduce greenhouse gas emissions by at least 50 % by 2050 (K. Kim et al., 2020). The technologies that can use ammonia as a fuel are combustion engines, fuel cells and gas turbines.

Two-stroke combustion engines are the most common technology for deep sea shipping. They are a mature technology, and have been commercialised for a long time, using fossil fuels such as diesel or gasoline. The use of ammonia in the ICE is a new idea and is under development. The company MAN has launched the first ammonia ICE prototype on the market, which has few differences to conventional engines. The ammonia combustion process is described in the equation.



Fuel and oxygen of air are the inputs to the combustion, which produces nitrogen, water and heat. The problem with ammonia is its low flammability, so a pilot fluid is needed to increase flammability. Fossil fuels such as HMO could be used, but to completely cut emissions, hydrogen should be used.

Another technology being investigated as a potential ship propulsion is fuel cells. It is at a preliminary stage compared to ICE. Currently they represent more a theoretical idea than a real possibility (Sophie & Ness, 2021).

Currently, ammonia production is based on the use of fossil fuels. 73 % of NH_3 is produced using natural gas, 22 % from coal and 5 % from oil. Only 1 % of ammonia is produced using renewables (International Renewable Energy Agency (IRENA), 2022a). Each year, ammonia production is responsible for the emission of about 300 tonnes of carbon dioxide. Specific emissions from NH_3 plants using natural gas and coal are 2,7 and 3,4 tonnes of CO_2 per tonne of NH_3 , respectively (Morgan, 2013).

Approximately 10 % of the ammonia produced is an internationally traded commodity, which can be transported using LNG carriers and pipelines (IRENA, 2022). Almost 40 ports around the world have ammonia export terminals, while about 90 ports have ammonia import terminals. If the end product is hydrogen in gaseous form, is possible to hydrogenate NH_3 through cracking and purification plants (Osman et al., 2020). The process of reconversion (cracking) and purification of hydrogen consumes a huge quantity of thermal and electrical energy. The efficiency of these systems is very low, around 70 %, and the cracking process requires heat, as the dissociation reaction takes place at high temperatures between 550 and 750 °C, while the purification plant is very energy-intensive, consuming between 5 and 8 kWh/kg H_2 . Furthermore, ammonia, like liquefied hydrogen, is subject to Boil-Off, which consists of the evaporation of a small percentage of the liquid (0,08 %) during transport and storage.

1.9 Conventional ammonia production process

Around 85 % of the world's ammonia production occurs via the Haber Bosch process. Traditional ammonia production plants are divided into two areas, syngas production and ammonia synthesis. Nitrogen is taken from the air through air separation units (ASU), while hydrogen is obtained through the steam methane reforming (SMR) process of natural gas (Frattini et al., 2016).

A syngas containing H_2 and N_2 is heated to temperatures between 500 and 650 °C and is compressed to a pressure in the range of 100-300 bar. These conditions are necessary due to the high dissociation energy of the nitrogen triple bond of 941 kJ/mol. The iron catalyst is fundamental for the reaction, gaseous hydrogen and nitrogen reacts on the surface of the hot iron to form gaseous ammonia.

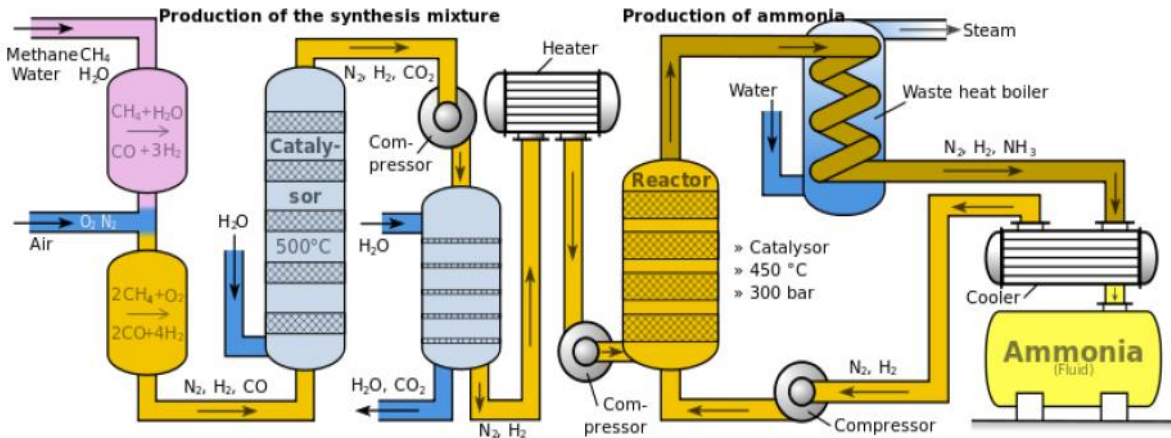
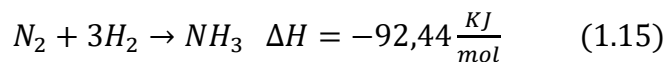


Figure 1.15: Haber-Bosch conventional process (Process, n.d.)

The ammonia synthesis reaction is the following (Morgan, 2013).



This reaction is exothermic, releasing 2,7 GJ of heat per tonne of NH_3 produced. The conversion of the reagents does not exceed 25-30 % per cycle, so the recirculation of unconverted nitrogen and hydrogen in the synthesis reactor is necessary. This enables an overall conversion of 99 % to be achieved. The syngas consists of 99,5 % hydrogen and nitrogen and the remaining 0,5 % inert gases such as argon, the presence of which does not affect the synthesis reaction, but the recirculation leads to their accumulation, so they must be removed.

The traditional process is based on steam reforming of natural gas to obtain the hydrogen needed for the synthesis reaction. The reaction that takes place is the following.



This reaction involves methane and water vapour, producing hydrogen and carbon monoxide; it is endothermic, needing high temperatures to take place, around 700 °C. It is very important to remove impurities present after the reaction, such as sulphur, water vapour and carbon dioxide. Emissions from this process are 0,3-0,4 m³ of CO_2 per m³ of H_2 produced. The efficiency of the process does not exceed 75 % (Volpe, 2021).

1.10 Green ammonia production and transport

Green ammonia can be produced using solely electricity, which is generated from renewable sources such as photovoltaics and wind power. The combination of electrolyzers and the Haber-Bosch process is called Power-to-Ammonia (P2A) technology.

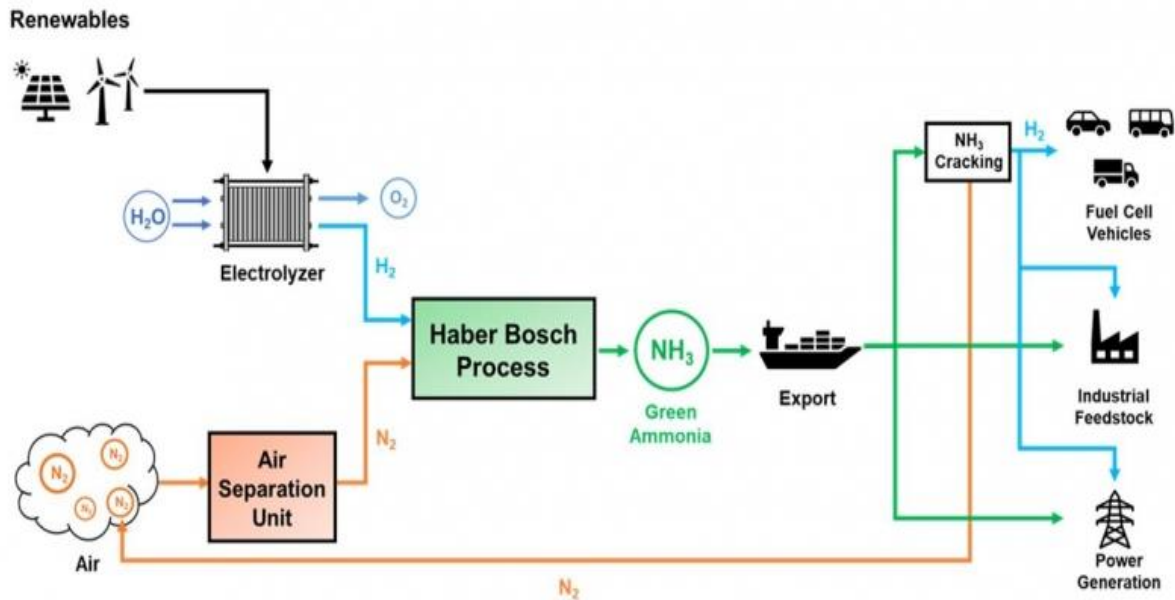


Figure 1.16: Green ammonia production and storage process (Alternative Green and Cost-Effective Processes for Ammonia Production – Green Ammonia, n.d.)

A basic Power to Ammonia plant is divided into the electrolysis plant to produce hydrogen, which can be fed by a desalination plant, that converts salt water into fresh water, suitable for electrolysis; a dedicated plant for the extraction of nitrogen from air, called the Air Separation Unit, and the Haber-Bosch plant for the synthesis of ammonia. The ammonia liquefaction and storage plant is a facility that is installed according to the function of the plant (Ikäheimo et al., 2018).

The description of the electrolyzers is given in section 1.7.1, the other parts of the process are described in this paragraph.

1.10.1 Desalinator

Water is an indispensable resource, and it is starting to shortage in many parts of the planet, where severe drought crisis is taking place. The continuous supply of drinkable water is becoming extremely complicated due to rapid population growth, urbanisation, and

industrialisation. For these reasons and for environmental and social purposes, the water needed for the electrolysis process should be produced using desalinators.

The electrolysis process requires large amounts of water during its operation. Theoretically, the specific consumption is 10-11 litres of water per kg of hydrogen produced, but considering the losses and efficiency of the plants, the real water consumption is closer to 15 litres per kg of H₂. The water used in the electrolysis process has specific properties, it must have a high level of purity. The resistivity must be above 1 MΩ/cm (Teknik, 2021).

Seawater has an average salinity of 35.000 parts per million, while the salinity of brackish water varies between 1000 and 11.000 ppm.

Desalination plants are divided into two types, thermal distillation, and membrane separation. The former technology uses heat to vaporise the water and separate it from the salt component, while membrane processes create a potential difference across the membrane using electric pumps (Osman et al., 2020).

Thermal plants produce water with very high purity levels, without the need for pre-treatment. The great disadvantage of this type of plant is energy consumption, both thermal and electrical, for this reason they are often used in combination with thermal power plants, which release large amounts of heat.

- Multi-Stage Flash Desalination (MSF)

More than 90 % of the world's thermal systems are MSF systems. This technology guarantees the production of water with a very high degree of purity.

The MSF process consists of preheating the incoming sea water to a temperature of 90 °C, before entering the instantaneous vaporisation cell, where the water evaporates and separates from the organic residues, which are extracted.

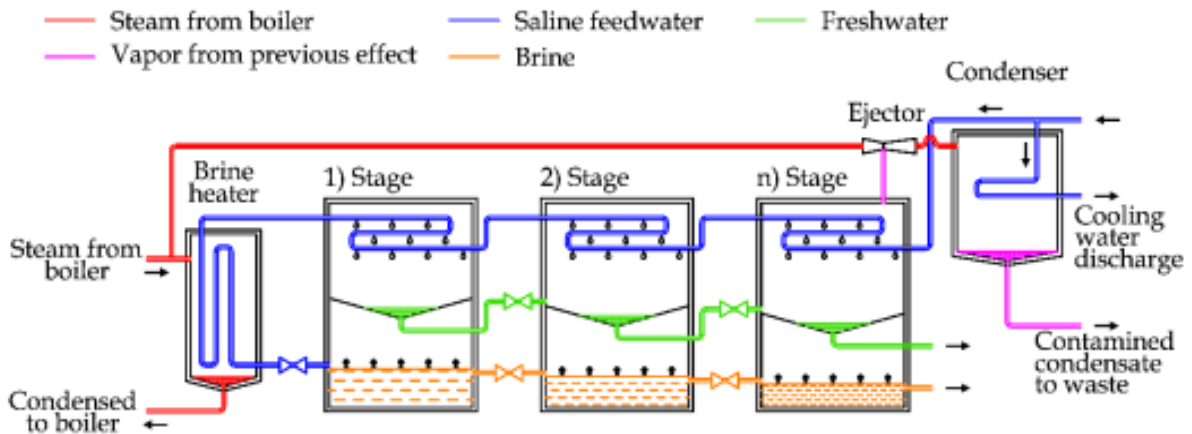


Figure 1.17: Multi flash stage desalination process (Curto et al., 2021)

The incoming saline water is used as cooling water for the condenser and then as a raw source to produce fresh water.

Due to the pressure drop, the introduction of heated saline water produces the 'flashing effect', causing the saline water rapidly boils inside the cell, producing steam (Curto et al., 2021). The vaporisation cells are placed in series forming a multi-stage configuration (Giorgetti, Cappella, 2013). On average, the number of stages is between 18 and 25. These plants have a high energy consumption, 12 kWh of thermal energy per cubic metre of water, and 6 kWh/H₂O of electrical energy.

MSF plants can reach large capacities, one of the largest MSF plants in the world, located in the United Arab Emirates has a daily production of 455,000 m³ (Morgan, 2013).

- Multiple-Effect Distillation

MED technology uses a thermal process very similar to the process used by the MSF. The main difference consists in the evaporation cell, that is not a flash, but an effect reactor, which is located below tubes through which steam flows and is condensed, releasing heat to the incoming saline water.

There are different configurations of these plants. The basic scheme comprises a steam supply system, heat exchangers, and a condenser. Salt water is used in the heat exchangers to condense the fresh water produced, preheats, and enters the main line to be evaporated.

It is common to combine a Rankine cycle with the desalination plant to create electricity using the steam generated. MED technology uses a cascade system of chambers, each characterised by a lower pressure than the previous chamber, which allows the water to evaporate at a lower

temperature. At the end of the chambers is the condenser, which liquefies the fresh water produced. MED plants can have a variable range of effect chambers, this depends on the degree of purity of the water and the production efficiency of the plant, as well as the physical and chemical characteristics of the incoming water. This technology is not applicable for large plants, currently the maximum capacity achieved is 20.000 m³ of water per day (Curto et al., 2021).

- Reverse Osmosis

Reverse osmosis is the only membrane technology commercialised for large plants. This technology exploits the chemical principle of osmosis, reversing its natural reaction. Salt water is pressed and passes through a semi-permeable membrane, which filters the water, separating it from impurities. The level of impurities in the water is higher than with thermal methods, so reverse osmosis technology requires pre and post chemical treatment to achieve a high level of purity. Chemical pre-treatments use substances such as barium and strontium sulphate, which aim to eliminate large particles that could congest the membrane, and inhibit the phenomenon of fouling, or the precipitation of poorly soluble minerals in the water.

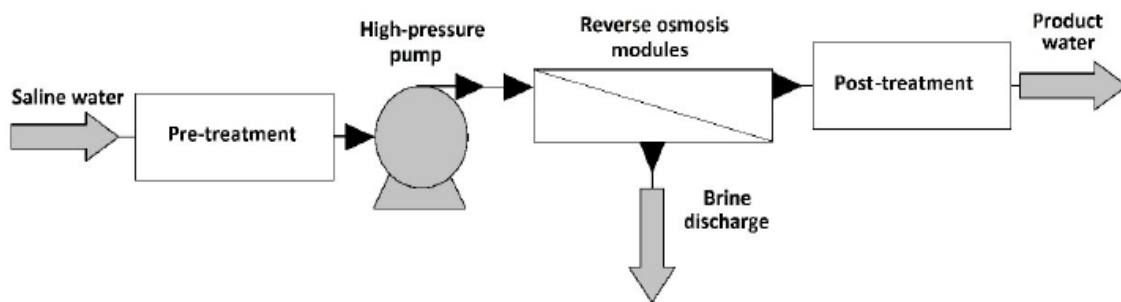


Figure 1.18: Reverse osmosis process (SOURCE)

This type of process does not require thermal energy, only electrical energy, which is needed to pump the water at high pressures. The pressures applied are between 15 and 25 bar for brackish water, and between 50 and 80 bar for salt-water, which contains much higher salt concentrations. The specific energy consumption of the RO system is between 2 and 4 kWh/m³ of H₂O, and it is influenced by the quality of the feed water, the operating pressures, and the efficiency of the system. For this reason, desalination plants powered by energy from renewable sources, particularly wind power, are being developed (Giorgetti, Cappella, 2013).

The design and operation of a wind-driven RO system is a challenging and complicated task due to the intermittent and fluctuating wind speed. For this reason, energy storage systems are implemented for remote areas, and grid support in integrated plants (Teknik, 2021).

Reverse osmosis plants are large, typically having a capacity of 200.000 m³/day to 300.000 m³/day. The largest plant built has double the capacity.

1.10.2 Air separation units

Nitrogen is the most abundant element in the atmosphere. Air is 78 % nitrogen, in the form of the diatomic bond N₂, which is an inert gas under ambient conditions. Because of this property, nitrogen is used extensively in the chemical industry and in shipping. One characteristic of nitrogen is its low reactivity, which makes it suitable as a blanketing and purging gas. In addition, nitrogen is used as a reagent in some chemical processes, including the Haber-Bosch process (Ivanova & Lewis, 2012). The three technologies developed to produce nitrogen are cryogenic distillation, polymer separation membrane and pressure swing adsorption. Cryogenic distillation technology is the most widespread in the market, being used by about 70 % of the world's nitrogen production plants.

- Cryogenic Air Separation Unit

The cryogenic distillation plant is the most developed on the market, guaranteeing the production of nitrogen with high purity on large scale capacities. This technology exploits the different liquefaction points of air components. Cryogenic systems fractionate air in a distillation process involving different components, decreasing the temperature to -160 °C (Ebrahimi et al., 2015).

The process is highly nonlinear and tremendously complex and involves numerous fluid flows and components. The first process is the compression of incoming air, and the removal of water, carbon dioxide and other contaminants present. The gas obtained is a mixture of nitrogen and oxygen and argon. The second process consists of cooling the gas to cryogenic conditions using a heat exchanger. Subsequently, the mixture reaches the distillation unit, which separates the oxygen and nitrogen streams. The two streams return to the heat exchanger and are finally compressed to the required pressure.

There are many different configurations of this plant, the process undergoes small variations depending on the product required and the purity desired. Cryogenic distillation plants can have different methods of pressurising the products, a different number of distillation columns, and the state of the products, which can be either liquid or gaseous. When the nitrogen produced has to be liquefied, an external refrigeration source must be installed, which increases the cost and complexity.

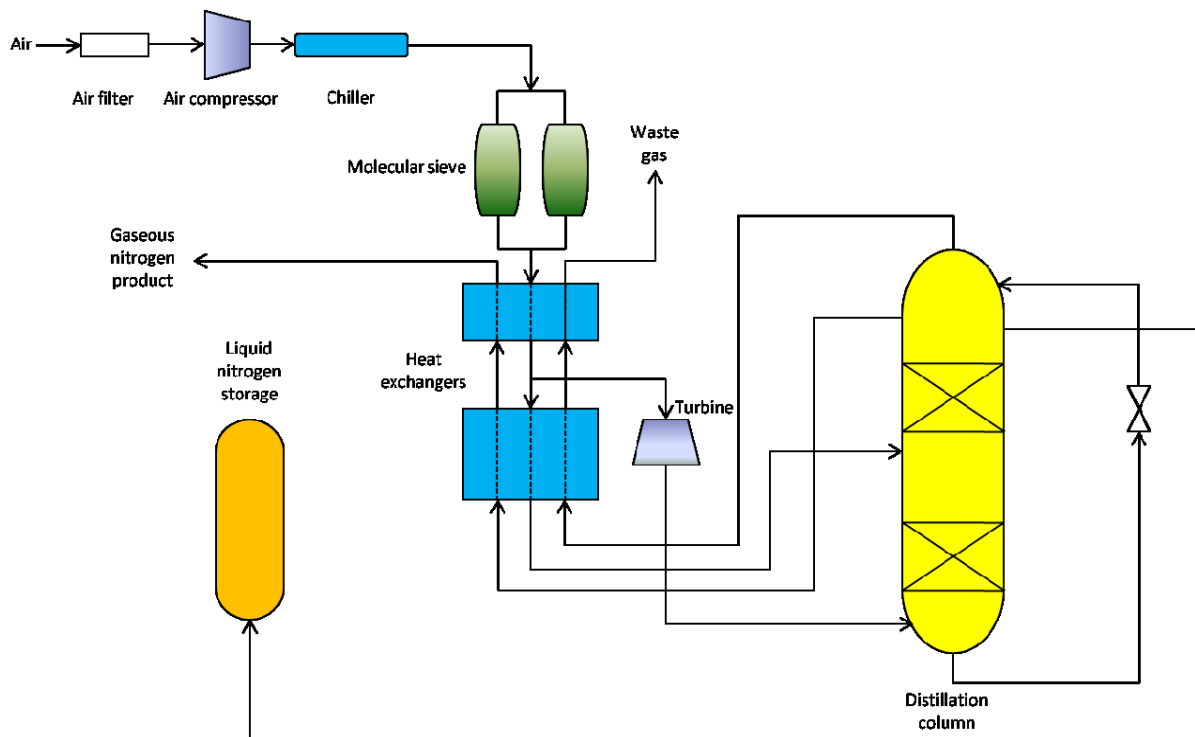


Figure 1.192: Simplified flowsheet of cryogenic air separation unit (Morgan, 2013)

The main components common to all cryogenic plants are the heat exchanger whose purpose is to cool the incoming air stream by exchanging heat with the product streams that have been refrigerated. The nitrogen and oxygen produced leaves the heat exchanger from near ambient temperature. The other indispensable components are the distillation column, which separates the air components according to their boiling point, and a series of compressors (Mehrpooya et al., 2015). Most configurations use two distillation columns, a high-pressure column producing ultra-pure nitrogen gas and a low-pressure column producing oxygen and nitrogen. The distillation column products are compressed with multi-stage intercooler compressors (Jones et al., 2011).

The capacity of Cryogenic Air Separation Units is very large, up to 400.000 m³/h. The purity of the products in these plants is over 99,99 %. Cryogenic distillation systems have lower energy consumption than other ASU technologies.

- Pressure Swing Adsorption PSA

The PSA process is the alternative to cryogenic distillation, especially for small plants with capacities up to 5000 m³/h and for applications requiring nitrogen purity levels below 99,99 %. Depending on the use, the PSA works using different materials. For oxygen production this technology exploits the properties of zeolites, which when under pressure form a dipole capable of capturing the nitrogen molecule. The zeolite is arranged to form a bed reactor. When air passes through the bed, the nitrogen is captured by the zeolite, which works at a minimum of 1,5 atm. The other air components, mainly oxygen, pass (Ebrahimi et al., 2015). The zeolitic bed becomes saturated with nitrogen after a certain period and must be regenerated to continue working. This is done by decreasing the operating pressure below atmospheric pressure, allowing the zeolite to return to its normal polarity, releasing the nitrogen molecules that were captured (Prakash Rao & Michael Muller, 2007).

When the purpose is nitrogen production, PSA plants use carbon molecular sieves that contain pores and cavities in which nitrogen adsorbs more slowly than oxygen (Ivanova & Lewis, 2012). At high pressures, the oxygen is removed from air that is enriched with nitrogen, while at low pressures, the oxygen is removed from the adsorber (Morgan, 2013). Adsorption and desorption cycles allow the PSA to work continuously.

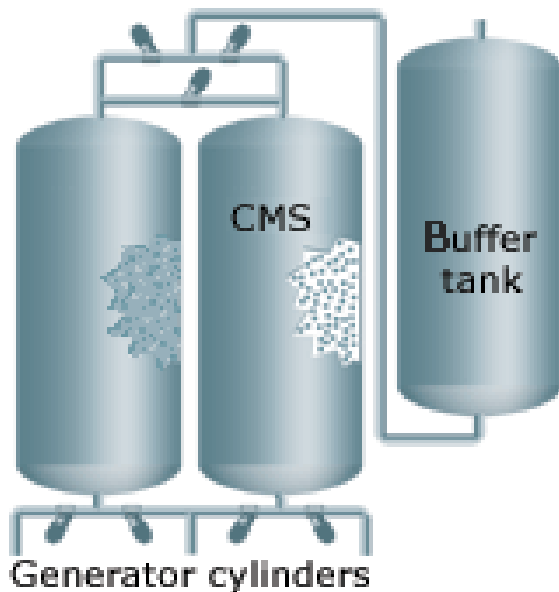


Figure 1.20: Pressure swing adsorption plant (Seshan, 1989)

The PSA plant consists of two cylinders containing carbon molecular sieves, and a buffer to store the nitrogen produced. Compressed air enters one of the cylinders, inside which oxygen

is adsorbed by the sieves at high pressure. The nitrogen-enriched gas leaving the cylinder is stored in the buffer. The presence of two cylinders allows alternating work. When one cylinder is saturated with oxygen it is desorbed by decreasing the pressure inside. A complete PSA system includes an air compressor, and an air refrigeration cycle (Seshan, 1989). The specific consumption is 0,75 kg/m³.

- Separation Membrane

Membrane nitrogen generators extract available nitrogen from compressed air. According to (Omega Air) these generators use hollow-fibre membrane technology to separate nitrogen from other components in the compressed air. The membrane uses the principle of selective permeation to produce nitrogen purity. Each gas has a characteristic permeation speed, which is a function of its ability to diffuse through a membrane. Oxygen is a fast gas and is selectively diffused through the membrane wall, while nitrogen travels along the inside of the fibre. Most of the slow gas, and a small amount of fast gas, continues to travel through the fibre until it reaches the end of the membrane separator, where the nitrogen gas produced is directed to the application. While the oxygen gas is discharged from the membrane separator at atmospheric pressure.

These generators operate at pressures between 5 and 24 bar, with operating temperatures between 35 and 55 °C. The nitrogen produced has purity levels lower than those achieved by other technologies, it can be as low as 99,5 %. The production capacity is very small compared to cryogenic distillation; these plants have flow rates of less than 1000 m³ of N₂ per hour.

These types of separators are not suitable for applications requiring high purity and large production flows. The main applications are the coating of pharmaceutical products, and inertisation of flammable liquids.

1.10.3 Hydrogen storage

Hydrogen is gaining in importance as energy carrier, for this reason the storage of hydrogen is a key point to ensure its growth globally. Depending on its use, hydrogen can be stored in different ways, such as compressed gas and liquid gas. There are new techniques still being studied or engineered, such as chemical (metal hydrides, ammonia, hydrocarbons) and physical (nanotubes) absorption of hydrogen (Arca et al., 2007). Of these methods only gaseous storage

and liquid storage are used for large-scale stationary applications. Liquefaction plants need cryogenic storage technologies, which keep the temperature of hydrogen below boiling point. Ammonia production plants require many storage systems, for both intermediate and final products. In particular, the intermediate hydrogen buffer, which separates electrolytic production with ammonia production in the Haber-Bosch process, is very important. These plants favour the use of pressure storage tanks for hydrogen gas.

- Liquid Storage

Liquid hydrogen has a much higher volume density than hydrogen gas and metal hydrides. As a liquid, the density of hydrogen is $70,8 \text{ kg/m}^3$, compared to the density of 39 kg/m^3 of hydrogen gas at 700 bar. One problem with storing hydrogen in liquid form is the Boil-Off phenomenon, which consists of the evaporation of part of the liquid by heat transfer with the environment, due to ortho-to-para conversion, mixing or pumping energy, radiant heating, convection heating or conduction heating. This phenomenon also occurs with double-walled insulated storage systems. The evaporation rate depends on the external temperature, the insulating material, and the shape of the tank, and can vary between 0,2 % and 0,007 %. Furthermore, the storage of hydrogen in liquid form requires a large amount of energy for liquefaction, and for maintaining cryogenic conditions of $-252,9 \text{ }^\circ\text{C}$, such as re-liquefaction of the evaporated gas (Morgan, 2013). Hydrogen liquefaction is a complicated process using a combination of heat exchangers, compressors, expanders, and throttling valves.

Cryogenic containers, also called Dewars have a double-walled structure and the space between the walls is evacuated to almost eliminate heat transfer completely by convection and conduction. Several layers of reflective heat screening, such as aluminised plastic mylar or perlite, are inserted between the walls to prevent radiant heat transfer between the inner and outer walls. To further improve thermal insulation, an additional outer wall can be added with liquid nitrogen on the inside, which reduces the temperature difference with the external environment, decreasing the heat exchanged (Amos, 1999). Liquid hydrogen tanks are spherical in shape, because this shape has the smallest heat transfer surface area per unit volume. Increasing the tank dimensions, the volume increases faster than the surface area, reducing boil-off. Cylindrically shaped tanks can also be used, as they are easier and cheaper to construct

than spherical tanks and their volume to surface area ratio is slightly higher than that of spherical ones.

- Hydrogen Liquefaction

The hydrogen liquefaction process plays an important role in the hydrogen value chain, as it enables the storage and transport of hydrogen in liquid form. Hydrogen is in liquid form at a temperature of $-253\text{ }^{\circ}\text{C}$ and at atmospheric pressure (Aziz, 2021).

There are many processes for hydrogen liquefaction. The first liquefaction cycle was invented in 1899 by Dewar who compressed the gas to 180 bar and cooled it to $-250\text{ }^{\circ}\text{C}$, then liquefied it in a flask (Aasadnia & Mehrpooya, 2018). Hydrogen liquefaction for small-scale plants is achieved with a Brayton refrigeration cycle that uses helium as a coolant. This technology is characterized by low investment costs but lower process efficiency and thus higher operating costs. For larger plants, a Claude hydrogen cycle is used, which is characterized by higher investment but lower operating costs (Ohlig & Decker, 2014). Existing plants are energy intensive and produce on a relatively small scale. For example, the Leona liquefaction plant in Germany, one of the newest plants, has a capacity of 5 tons per day and requires about 11,9 kWh/kg of liquefied hydrogen. The United States has plants with consumption between 12 and 15 kWh/kg of LH_2 (Stolzenburg et al., 2013).

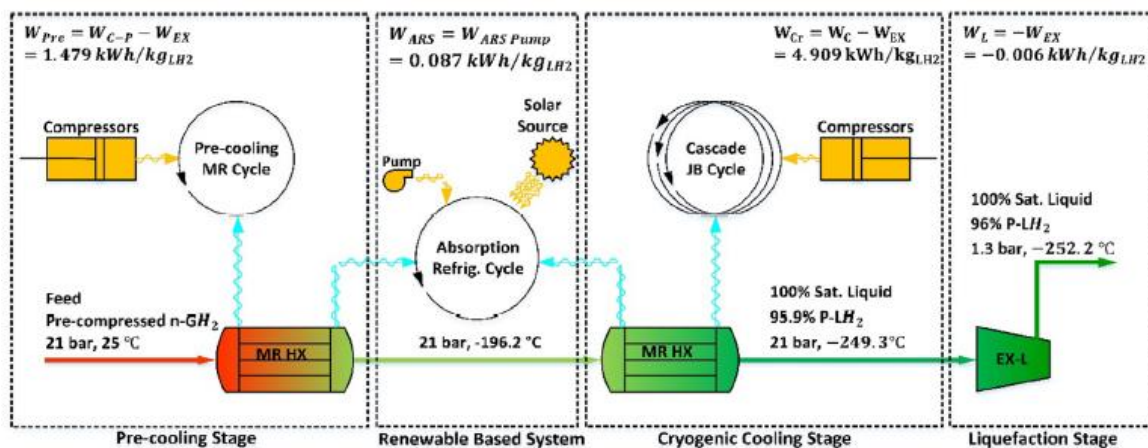


Figure 1.21: Hydrogen liquefaction process based on joule thomson refrigeration cycle and solar adsorption chilling (Aasadnia & Mehrpooya, 2018)

Refrigeration plants are composed of five subsystems, after gas compression there is the chilling stage, which lowers the temperature of the gas from room temperature by about twenty degrees. The next stage is the precooling of hydrogen gas, which is the part that varies most in different plants, as the cooling medium changes, liquid nitrogen, mixed refrigerants, or

natural gas liquids can be used. According to the study by (Noh et al., 2022), the use of a liquid natural gas based pre-cooling system can improve process-specific consumption, decreasing SEC to 5,6 kWh/kgH₂. The gas comes out of precooling at a temperature of about -200 °C, and is further cooled in a refrigeration cycle, such as the Joule Tomphson cascade cycle or Brayton cycle, which bring the gas temperature very close to the critical liquefaction temperature of minus 250 °C. The last step consists in expanding the hydrogen to reservoir pressure, very close to atmospheric pressure. Under these conditions, the hydrogen is liquid. Innovative processes that lower the energy consumption of the process to 5-6 kWh/kgH₂ are being researched.

- Compressed Gas Storage

Compression is the most common method of storing hydrogen. The density of hydrogen stored in compressed form depends strongly on the storage pressure. At a pressure of 100 bar, the volumetric density of stored hydrogen is 7,8 kg/m³ at ambient temperature. To achieve a higher density, the storage pressure must be increased; at 700 bar, the density of hydrogen reaches 39 kg/m³ (Aziz, 2021). Spherical or cylindrical metal tanks are used for stationary applications. Compressed hydrogen is used in many applications, including vehicles, hydrogen filling stations and in some industrial processes. In particular in industrial environment, hydrogen produced on site is usually stored at 250 bar. The transport sector uses hydrogen at 350 bar, particularly for heavy vehicles. For automobiles, the goal is to increase the pressure to 700 bar to ensure fast charging and increase the autonomy.

A high amount of energy is required to compress hydrogen in a multi-stage compression system. However, the advantage is the simplicity of this technology, only requiring a multistage compressor and a pressure vessel.

A problem with large storage tanks is the leakage of gas remaining in the empty tank at the end of the discharge cycle. In small containers this may not be a problem, but in larger containers it can represent a large amount of gas. One option that is used is to use a liquid such as brine to fill the container volume and displace the remaining hydrogen gas (Amos, 1999).

Compressed hydrogen can also be stored underground, in large caverns of porous, impermeable rock, but salt caverns can also be used.

1.10.4 Ammonia synthesis unit

The Haber-Bosch process does not change in the green process, but the synthesis of ammonia occurs through the reaction of nitrogen and hydrogen, in 1:3 proportions, in the presence of a heterogeneous iron-based catalyst, activated with aluminium and potassium oxides to increase the reaction speed. The reaction is exothermic ($\Delta H = -92 \text{ KJ/mol}$) and takes place under high temperature and pressure conditions of 500-600 °C and 150-300 bar, respectively, necessary to cleave the nitrogen triple bond.

The synthesis plant is characterised by the same components as the conventional process, a system of catalytic synthesis reactors, cooling units, units for separating the ammonia from the unconverted syngas, and compression and recycling systems for the unconverted syngas.

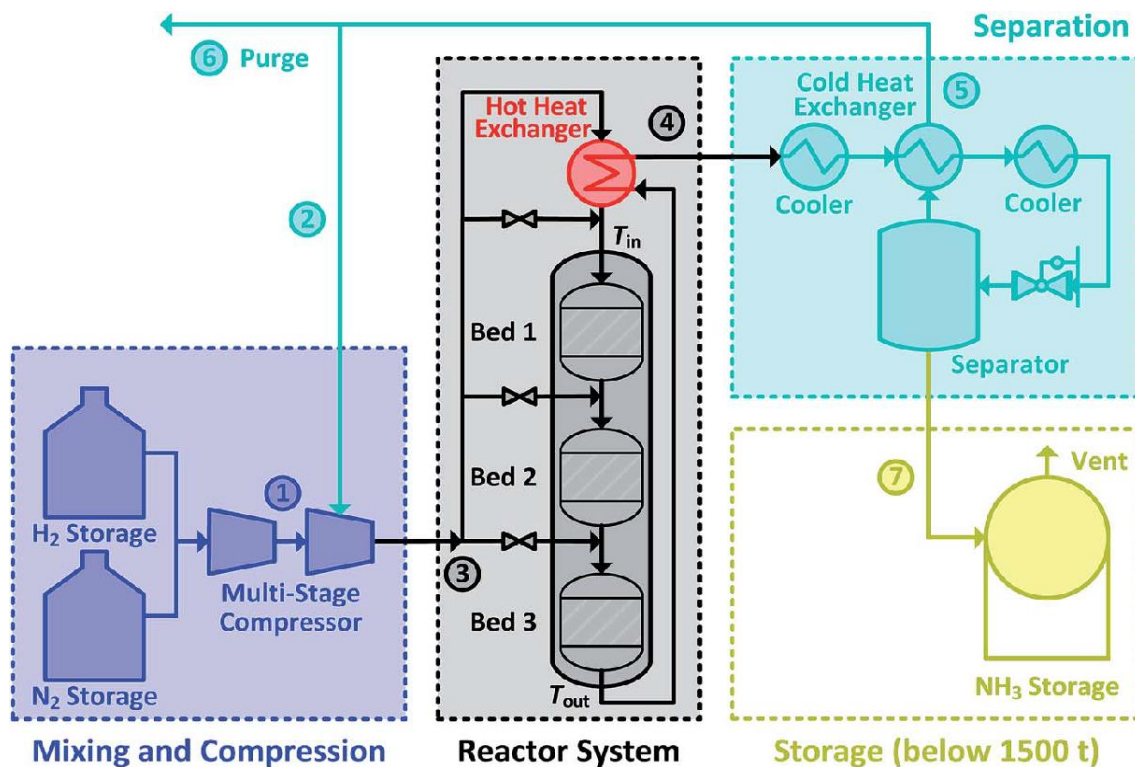


Figure 1.22: Ammonia synthesis loop scheme (Cheema & Krewer, 2018)

The syngas, after being compressed, is pre-heated by means of a heat exchanger, which utilises the output gases from the previous process. The processed gases are cooled in water heat exchangers, which allow the production of water vapour that feeds a turbine for electricity production. Finally, the ammonia produced goes to the liquefaction plant, while N_2 and H_2 are recompressed. The maximum percentage of ammonia produced per cycle is 25-30 % of the syngas (Cheema & Krewer, 2018). In the power to ammonia synthesis cycle, the only inert gas is argon from the air separation unit, together with nitrogen, unlike the conventional process,

where the inert gases include methane produced by reforming. The concentration of Ar in the synthesis cycle is controlled by venting a small amount of gas from the recycle stream.

The most important problem with the power-to-ammonia process is the non-flexibility of the synthesis plant, being always powered by fossil fuels, which provide continuity of power, unlike renewable energy. Currently there are no synthesis processes capable of working under dynamic conditions. The most common method of powering the Haber Bosch process with electrolysis is the use of large hydrogen buffers, which guarantee the presence of hydrogen for a given period. Another option used is the coupling of the electricity grid, which, however, has the disadvantage of having indirect emissions, due to the electricity production methods (Smith et al., 2020). The analysis of the operational flexibility of the Haber-Bosch process conducted by the paper (Cheema & Krewer, 2018) had positive results regarding the work of the synthesis plant under dynamic conditions, achieved by changing operational variables within certain ranges, which when exceeded lead to reactor damage. In particular, the best results have been obtained by varying the mixture of hydrogen and nitrogen and increasing the concentration of the Inert gas. Synthesis was ensured by reducing the amount of hydrogen input by 67 %. This can guarantee the continued operation of the synthesis reactor even at times of hydrogen shortage due to the lack of renewable energy. The sensitivity study described by the paper (Verleysen et al., 2021) indicated that the most impactful parameter on reactor flexibility is inlet temperature, followed by H₂:N₂ mixture concentration.

Much more studies and research need to take place in this area to improve flexibility of power-to-ammonia plants and decrease production costs by simplifying processes, which to date are complex and require expensive storage facilities.

1.10.5 Ammonia storage

Maritime transport of ammonia takes place under cryogenic conditions, hence NH₃ after being produced in gaseous form in the Haber-Bosch process is liquefied and stored in special tanks that maintain cryogenic conditions. Liquid ammonia can be stored under both high pressure and low pressure.

- High Pressure Storage

Pressure storage of ammonia takes place at an ambient temperature of 20 °C and a high pressure of 8,58 bar. In this state, NH₃ has an energy density of 13,77 MJ/l. Although the pressure required to keep ammonia in a liquid state is 8,58 bar, the tanks have higher operating pressures, up to 17 bar, to prevent ammonia from boiling when the ambient temperature rises. The storage system consists of a cylindrical or spherical pressure tank and is made of carbon steel. The system does not lose the stored fuel and does not require energy to maintain the pressurized state of the fuel in the tank, this reduces operating costs significantly, compared with low-pressure storage tanks. The size of this type of tank is small, they can store up to a maximum of 270 tons, so this option is not feasible for large storage volumes (Bartels, 2008). A drawback of this type of tank is the amount of steel needed, which is 2,8 tons per ton of liquid ammonia stored (Nayak-Luke et al., 2021).

- Low Pressure Storage

The most widely used technology for storing ammonia in large quantities involves keeping NH₃ under cryogenic conditions, with temperatures below -33 °C and atmospheric pressure. Ammonia under these conditions has an energy density of 15,37 MJ/l, higher than ammonia stored under high pressure. The tanks are large and can store up to 60.000 tons of ammonia. These types of tanks need to support only the static pressure of the fluid, for this reason they use less metal, 1 ton of steel is used for every 45 tons of ammonia. This makes them more economical for large sizes (Bartels, 2008). Tanks can be single-walled or double-walled, with the former being constructed with external insulation, while double-walled tanks have insulation that fills the space between the two walls (Nayak-Luke et al., 2021). Ammonia in this state suffers from Boil-Off, which is the evaporation of a small percentage of NH₃ due to several causes, including convective heat exchange with the tank walls. The rate of evaporation depends on several factors such as the shape and material of the tank and the outside temperature. On average, the evaporation rate is between 0,1 % and 0,02 %.

The storage facility has a refrigeration system, which keeps the ammonia in a cryogenic condition. The refrigeration process requires energy.

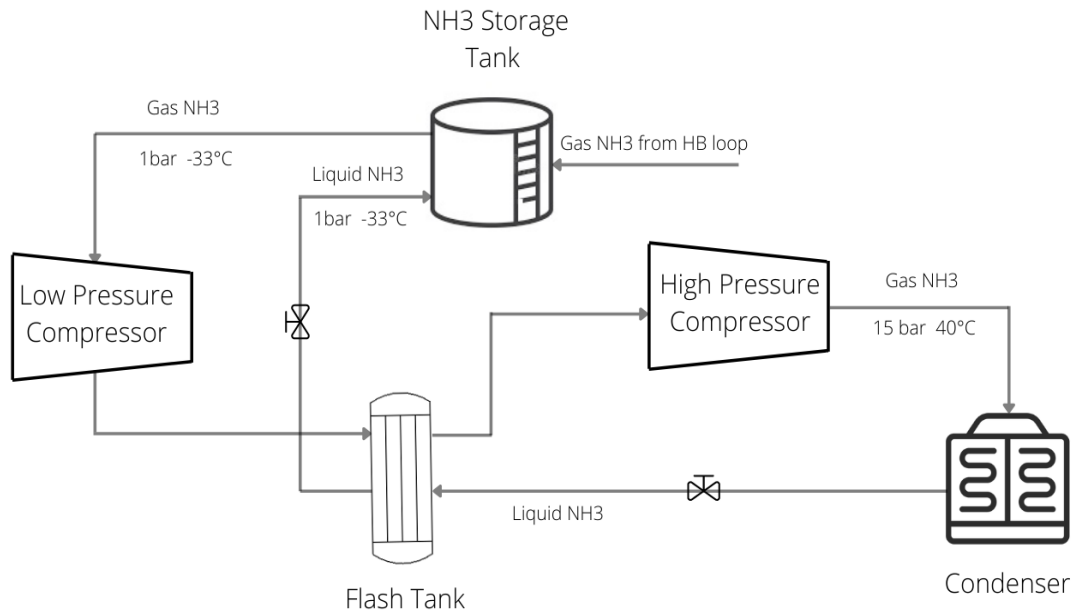
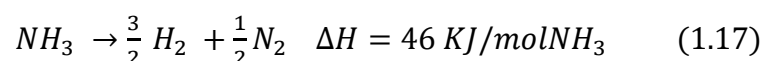


Figure 1.23: Liquid ammonia liquefaction and storage process (the Author)

The liquefaction process involves the gaseous ammonia entering a low-pressure compressor, which compresses the gas that then passes through a flash tank to be cooled. Next, the NH_3 enters in a high-pressure compressor, preparing the ammonia in the condition to be liquefied in the condenser. The outgoing ammonia is partly liquid and partly solid, it again passes through the flash tank, which is responsible for separating the two phases (Gezerman, 2015). The liquid ammonia is sent to the buffer where it expands at tank pressure, while the gaseous NH_3 passes through the compressor one more time to restart the refrigeration cycle. The Boil-Off ammonia is recirculated and liquefied in this process.

1.10.6 Ammonia cracking

Cracking is the splitting of a complex molecule with catalysts and heat, into simpler molecules. The cracking process involves the decomposition of ammonia into hydrogen and nitrogen through an endothermic reaction, which requires a thermal energy of 46 kJ per mole of NH_3 .



The plants can operate at temperatures between 400 and 500 °C, with a conversion efficiency of less than 99 %, using a nickel catalyst. It is possible to work at higher temperatures, up to 900 °C, and at high pressures of 40 bar, increasing the conversion efficiency up to 99,5 % (J. Kim

et al., 2022). The energy required by the cracking process is thermal, so it can be provided by burning some of the hydrogen produced, or other renewable energy sources.

The process of ammonia separation and hydrogen purification is divided into several steps, as is demonstrated in the scheme below.

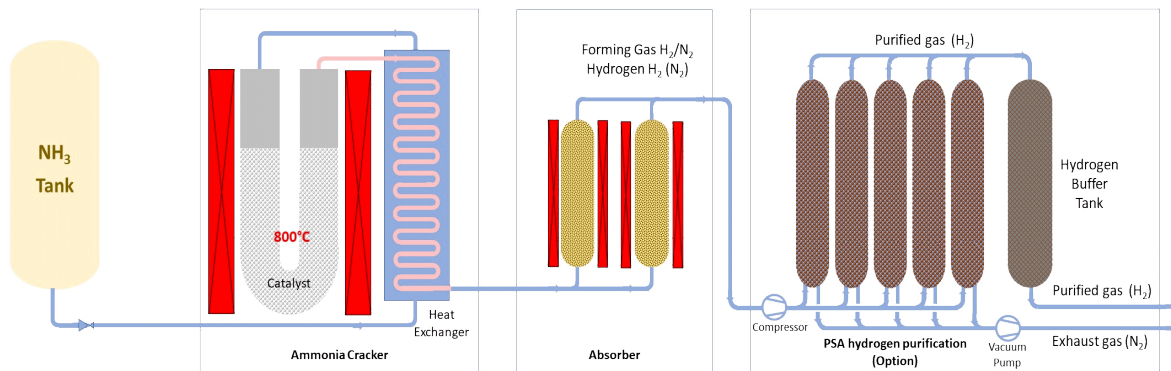


Figure 1.24: Ammonia cracking and hydrogen purification process (Crystec et al.)

The ammonia gas is pre-heated in a heat exchanger and vaporizer and then cracked in the main furnace unit. After the cracking step, the gas mixture exiting the cracker, which includes hydrogen, nitrogen, and undecomposed ammonia, is sent to an ammonia recovery unit after an intermediate compression step. The unreacted ammonia is recovered. To obtain high-purity hydrogen, a system is used to remove residual nitrogen in the product. This system can be cryogenic or Pressure Swing Adsorption (Makhloufi & Kezibri, 2021).

The most common process for purifying hydrogen is Pressure Swing Adsorption (PSA), which is based on a physical process that utilizes the different adsorption properties of various gases to separate them. To separate nitrogen from hydrogen and generate high-purity hydrogen, porous materials such as molecular sieves or zeolite are employed (Crystec et al.).

Currently, cracking plants are only commercialised for small and medium size.

References Chapter 1

- Aasadnia, M., & Mehrpooya, M. (2018). Conceptual design and analysis of a novel process for hydrogen liquefaction assisted by absorption precooling system. *Journal of Cleaner Production*, 205, 565–588. <https://doi.org/10.1016/j.jclepro.2018.09.001>
- Alternative green and cost-effective processes for Ammonia production – Green Ammonia.* (n.d.). 4–7.
- Altfeld, K., & Pinchbeck, D. (n.d.). *Admissible hydrogen concentrations in natural gas systems.* www.gas-for-energy.com
- Amos, W. A. (1999). Costs of Storing and Transporting Hydrogen. *Other Information: PBD: 27 Jan 1999; PBD: 27 Jan 1999; PBD: 27 Jan 1999, November*, Medium: ED; Size: vp. <http://www.osti.gov/bridge/servlets/purl/6574-OBMIES/webviewable/>
- Ancona, M. A., Branchini, L., Catena, F., Pascale, A. De, & Melino, F. (2019). *Sistemi ibridi di accumulo per l' incremento dello sfruttamento della risorsa rinnovabile nell' ambito delle comunità energetiche (anno 1 di 3)*. 1–136.
- Arasto, A., Tsupari, E., Kärki, J., Sihvonen, M., & Lilja, J. (2013). Costs and potential of carbon capture and storage at an integrated steel mill. *Energy Procedia*, 37, 7117–7124. <https://doi.org/10.1016/j.egypro.2013.06.648>
- Armijo, J., & Philibert, C. (2020). Flexible production of green hydrogen and ammonia from variable solar and wind energy: Case study of Chile and Argentina. *International Journal of Hydrogen Energy*, 45(3), 1541–1558. <https://doi.org/10.1016/j.ijhydene.2019.11.028>
- Aziz, M. (2021). *Transportation , and Safety.*
- Bartels, J. R. (2008). A feasibility study of implementing an Ammonia Economy. *Digital Repository @ Iowa State University, December*, 102. <http://lib.dr.iastate.edu/cgi/viewcontent.cgi?article=2119&context=etd>
- Berger, R. (2020). *The Future of Steelmaking.* 16. <https://www.mynewsdesk.com/rolandberger/pressreleases/europes-steel-industry-must-invest-over-eur-100-billion-in-co2-reduction-2995086>
- Bhaskar, A., Assadi, M., & Somehsaraei, H. N. (2020). Decarbonization of the iron and steel industry with direct reduction of iron ore with green hydrogen. *Energies*, 13(3), 1–23. <https://doi.org/10.3390/en13030758>
- Cheema, I. I., & Krewer, U. (2018). Operating envelope of Haber-Bosch process design for power-to-ammonia. *RSC Advances*, 8(61), 34926–34936. <https://doi.org/10.1039/c8ra06821f>
- Chevrier, V. (2020). Ultra-Low CO₂ Ironmaking: Transitioning to the Hydrogen Economy - Midrex Technologies, Inc. *Metec & 5th Estad*, 1–15. <https://www.midrex.com/tech-article/ultra-low-co2-ironmaking-transitioning-to-the-hydrogen-economy/>

- Chevrier, V., Lorraine, L., & Michishita, H. (2021). *MIDREX[®] Process : Bridge to Ultra-low CO₂ Ironmaking*. 39.
- Cossar, E., Barnett, A. O., Seland, F., & Baranova, E. A. (2019). The performance of nickel and nickel-iron catalysts evaluated as anodes in anion exchange membrane water electrolysis. *Catalysts*, 9(10). <https://doi.org/10.3390/catal9100814>
- Cracker, A., & Trading, C. T. (n.d.). *ContentContactAbout Products Applications CareerLanguage ▾ us ▾ ▾ Ammonia Cracker , hydrogen generator Crystec Technology Trading GmbH Ammonia Cracker for the Generation of Forming Gas . ContentContactAbout Products Applications CareerLanguage ▾*. 1–8.
- Curto, D., Franzitta, V., & Guercio, A. (2021). A review of the water desalination technologies. *Applied Sciences (Switzerland)*, 11(2), 1–36. <https://doi.org/10.3390/app11020670>
- Ding, H., Zheng, H., Liang, X., & Ren, L. (2020). Getting ready for carbon capture and storage in the iron and steel sector in China: Assessing the value of capture readiness. *Journal of Cleaner Production*, 244, 118953. <https://doi.org/10.1016/j.jclepro.2019.118953>
- Ebrahimi, A., Meratizaman, M., Reyhani, H. A., Pournali, O., & Amidpour, M. (2015). Energetic, exergetic and economic assessment of oxygen production from two columns cryogenic air separation unit. *Energy*, 90, 1298–1316. <https://doi.org/10.1016/j.energy.2015.06.083>
- Elements. (2020). *Il contributo delle Comunità Energetiche alla decarbonizzazione*. 42–46. <https://doi.org/10.12910/EAI2020-032>
- Energ, S., & Publicado, U. U. (2022). *El consumo de energía en Argentina durante 2021 fue el más alto de la historia*. 1–8.
- Energy Agency, I. (2019). The Future of Hydrogen. In *The Future of Hydrogen*. OECD. <https://doi.org/10.1787/1e0514c4-en>
- Fan, Z., & Friedmann, S. J. (2021). Low-carbon production of iron and steel: Technology options, economic assessment, and policy. *Joule*, 5(4), 829–862. <https://doi.org/10.1016/j.joule.2021.02.018>
- Frattini, D., Cinti, G., Bidini, G., Desideri, U., Cioffi, R., & Jannelli, E. (2016). A system approach in energy evaluation of different renewable energies sources integration in ammonia production plants. *Renewable Energy*, 99, 472–482. <https://doi.org/10.1016/j.renene.2016.07.040>
- Gezerman, A. O. (2015). Exergy analysis and purging of an ammonia storage system. *International Journal of Exergy*, 17(3), 335–351. <https://doi.org/10.1504/IJEX.2015.070502>
- Griesser, A. (2020). *Using HBI in Blast Furnaces*. 1–11.
- H2IT. (2019). Piano Nazionale di Sviluppo – Mobilità Idrogeno Italia. *Associazione Italiana Idrogeno e Celle a Combustibile*, 1–162.

- Home, E., Energoclub, M., Rinnovabili, F. E., Consumi, F. E. R., & Pompe, F. V. (n.d.). *Potenziale nazionale FER Potenziale nazionale delle fonti energetiche rinnovabili*. 3–7.
- Hurskainen, M., & Ihonen, J. (2020). Techno-economic feasibility of road transport of hydrogen using liquid organic hydrogen carriers. *International Journal of Hydrogen Energy*, 45(56), 32098–32112. <https://doi.org/10.1016/j.ijhydene.2020.08.186>
- Hydrogen Council. (2020). *Path to hydrogen competitiveness A cost perspective*. January.
- Hydrogen Council. (2021). *Hydrogen Insights*. February, 58. <https://hydrogencouncil.com/wp-content/uploads/2021/02/Hydrogen-Insights-2021.pdf>
- Ikäheimo, J., Kiviluoma, J., Weiss, R., & Holttinen, H. (2018). Power-to-ammonia in future North European 100 % renewable power and heat system. *International Journal of Hydrogen Energy*, 43(36), 17295–17308. <https://doi.org/10.1016/j.ijhydene.2018.06.121>
- Ingegneria, D., Guccione, R., Di, L., Messa, M., & Massa, G. (2018). *Ilva, tre scenari per la riconversione dello stabilimento*.
- International Renewable Energy Agency (IRENA). (2022a). *Global hydrogen trade to meet the 1.5 °C climate goal: Part III – Green hydrogen supply cost and potential*.
- International Renewable Energy Agency (IRENA). (2022b). *GREEN HYDROGEN FOR INDUSTRY*.
- International Renewable Energy Agency, T. (2020). *GREEN HYDROGEN COST REDUCTION SCALING UP ELECTROLYSERS TO MEET THE 1.5°C CLIMATE GOAL H 2 O 2*. www.irena.org/publications
- IRENA. (2020). Reaching Zero With Renewables. *The International Renewable Energy Agency (IRENA)*, 216.
- IRENA. (2022). *Geopolitics of the energy transformation: the hydrogen factor*.
- Iron and Steel Technology Roadmap. (2020). *Iron and Steel Technology Roadmap*. <https://doi.org/10.1787/3dcc2a1b-en>
- Ivanova, S., & Lewis, R. (2012). Producing nitrogen via pressure swing adsorption. *Chemical Engineering Progress*, 108(6), 38–42.
- Jones, D., Bhattacharyya, D., Turton, R., & Zitney, S. E. (2011). Optimal design and integration of an air separation unit (ASU) for an integrated gasification combined cycle (IGCC) power plant with CO₂ capture. *Fuel Processing Technology*, 92(9), 1685–1695. <https://doi.org/10.1016/j.fuproc.2011.04.018>
- Kim, J., Huh, C., & Seo, Y. (2022). End-to-end value chain analysis of isolated renewable energy using hydrogen and ammonia energy carrier. *Energy Conversion and Management*, 254(December 2021), 115247. <https://doi.org/10.1016/j.enconman.2022.115247>
- Kim, K., Roh, G., Kim, W., & Chun, K. (2020). A preliminary study on an alternative ship propulsion system fueled by ammonia: Environmental and economic assessments. *Journal of Marine Science and Engineering*, 8(3). <https://doi.org/10.3390/jmse8030183>

- Makhloufi, C., & Kezibri, N. (2021). Large-scale decomposition of green ammonia for pure hydrogen production. *International Journal of Hydrogen Energy*, 46(70), 34777–34787. <https://doi.org/10.1016/j.ijhydene.2021.07.188>
- Mastronardi, L. J., Caratori, L., Vila Martinez, J. P., Lapun, P. G., Barbaran, G., Vallés Puertas, D. G., Ramírez, G. A., Kempel, D., Christensen, J., Rivas, I. A., Natale, H. O., Rocío, R., Miranda, M. E., Bobillo, E., Ramón, M., Rivero, V., & Koutoudjian, G. (2019). *Escenarios Energéticos 2030 Documento de Síntesis*. <http://datos.minem.gob.ar/dataset/escenarios-energeticos>
- Mehrpooya, M., Sharifzadeh, M. M. M., & Rosen, M. A. (2015). Optimum design and exergy analysis of a novel cryogenic air separation process with LNG (liquefied natural gas) cold energy utilization. *Energy*, 90, 2047–2069. <https://doi.org/10.1016/j.energy.2015.07.101>
- Ministero della Transizione Ecologica, & Dipartimento per l’Energia ed il Clima. (2021). *La Situazione Energetica Nazionale del 2020*. 1–174.
- Ministero dello Sviluppo Economico; Ministero dell’Ambiente e della Tutela del Territorio e del Mare; Ministero delle Infrastrutture e dei Trasporti. (2019). *Piano Nazionale Integrato per l’Energia e il Clima (National Energy and Climate Plan)*. 294. https://www.mise.gov.it/images/stories/documenti/it_final_necp_main_en.pdf<https://www.mise.gov.it/index.php/it/198-notizie-stampa/2040668-pniec2030>
- Morgan, E. R. (2013). Techno-economic feasibility study of ammonia plants powered by offshore wind. *University of Massachusetts - Amherst, PhD Dissertations*, 432. http://scholarworks.umass.edu/open_access_dissertations/697
- Nayak-Luke, R. M., Forbes, C., Cesaro, Z., Bañares-Alcántara, R., & Rouwenhorst, K. H. R. (2021). Techno-Economic Aspects of Production, Storage and Distribution of Ammonia. In *Techno-Economic Challenges of Green Ammonia as an Energy Vector*. Elsevier Inc. <https://doi.org/10.1016/b978-0-12-820560-0.00008-4>
- Niermann, M., Timmerberg, S., Drünert, S., & Kaltschmitt, M. (2021). Liquid Organic Hydrogen Carriers and alternatives for international transport of renewable hydrogen. *Renewable and Sustainable Energy Reviews*, 135(August 2020), 110171. <https://doi.org/10.1016/j.rser.2020.110171>
- Noh, W., Park, S., Kim, J., & Lee, I. (2022). Comparative design, thermodynamic and techno-economic analysis of utilizing liquefied natural gas cold energy for hydrogen liquefaction processes. *International Journal of Energy Research*, 46(9), 12926–12947. <https://doi.org/10.1002/er.8064>
- Ohlig, K., & Decker, L. (2014). The latest developments and outlook for hydrogen liquefaction technology. *AIP Conference Proceedings*, 1573(February), 1311–1317. <https://doi.org/10.1063/1.4860858>
- Oliveira, A. M., Beswick, R. R., & Yan, Y. (2021). A green hydrogen economy for a renewable energy society. *Current Opinion in Chemical Engineering*, 33, 1–7. <https://doi.org/10.1016/j.coche.2021.100701>

- Osman, O., Sgouridis, S., & Sleptchenko, A. (2020). Scaling the production of renewable ammonia: A techno-economic optimization applied in regions with high insolation. *Journal of Cleaner Production*, 271, 121627. <https://doi.org/10.1016/j.jclepro.2020.121627>
- Parif, A. di. (2016). Paris Agreement_2015_ITA. *Gazzetta Ufficiale Dell'Unione Europea*, 4–18.
- POSCO Newsroom. (2020). *POSCO to establish hydrogen production capacity of 5 million tons*. 22–25. <https://newsroom.posco.com/en/posco-to-establish-hydrogen-production-capacity-of-5-million-tons/>
- Prakash Rao, & Michael Muller. (2007). Industrial Oxygen: Its Generation and Use. 2007 *ACEEE Summer Study on Energy Efficiency in Industry*, 124–135. http://aceee.org/files/proceedings/2007/data/papers/78_6_080.pdf
- Process, T. H. (n.d.). *The Haber Process SIII Production of Ammonia through the Haber-Bosch Process*. 23–24.
- Rambhujun, N., Salman, M. S., Wang, T., Prathana, C., Sapkota, P., Costalin, M., Lai, Q., & Aguey-Zinsou, K.-F. (2020). Renewable hydrogen for the chemical industry. *MRS Energy & Sustainability*, 7(1). <https://doi.org/10.1557/mre.2020.33>
- Rao, P. C., & Yoon, M. (2020). Potential liquid-organic hydrogen carrier (Lohc) systems: A review on recent progress. *Energies*, 13(22). <https://doi.org/10.3390/en13226040>
- Rashid, M. M., Mesfer, M. K. Al, Naseem, H., & Danish, M. (2015). Hydrogen Production by Water Electrolysis: A Review of Alkaline Water Electrolysis, PEM Water Electrolysis and High Temperature Water Electrolysis. *International Journal of Engineering and Advanced Technology*, 3, 2249–8958.
- Rb, P., & Universitario, R. (2020). *Politecnico di Torino Politecnico di Torino*. October, 87316161.
- Renewable Energy Agency, I. (2020). *Green hydrogen: A guide to policy making*. www.irena.org
- Rodríguez, J., & Amores, E. (2020). Cfd modeling and experimental validation of an alkaline water electrolysis cell for hydrogen production. *Processes*, 8(12), 1–17. <https://doi.org/10.3390/PR8121634>
- Samsatli, S., & Samsatli, N. J. (2019). The role of renewable hydrogen and inter-seasonal storage in decarbonising heat – Comprehensive optimisation of future renewable energy value chains. *Applied Energy*, 233–234(November 2018), 854–893. <https://doi.org/10.1016/j.apenergy.2018.09.159>
- Seshan, K. (1989). Pressure swing adsorption. *Applied Catalysis*, 46(1), 180. [https://doi.org/10.1016/S0166-9834\(00\)81410-4](https://doi.org/10.1016/S0166-9834(00)81410-4)
- Sharma, S., & Ghoshal, S. K. (2015). Hydrogen the future transportation fuel: From production to applications. *Renewable and Sustainable Energy Reviews*, 43, 1151–1158. <https://doi.org/10.1016/j.rser.2014.11.093>

- Siamo, D., & Alternativi, E. (n.d.). *Generatori di azoto a membrana - serie NM-GEN*. 1–6.
- Sigal, A., Leiva, E. P. M., & Rodríguez, C. R. (2014). Assessment of the potential for hydrogen production from renewable resources in Argentina. *International Journal of Hydrogen Energy*, 39(16), 8204–8214. <https://doi.org/10.1016/j.ijhydene.2014.03.157>
- Smith, C., Hill, A. K., & Torrente-Murciano, L. (2020). Current and future role of Haber-Bosch ammonia in a carbon-free energy landscape. *Energy and Environmental Science*, 13(2), 331–344. <https://doi.org/10.1039/c9ee02873k>
- Sophie, A., & Ness, S. (2021). *Conceptual Design of Ammonia- fueled Vessels for Deep-sea Shipping*. June.
- Stocaggio, D. I., Idrogeno, D., Materiali, E., Nanostrutturati, I., Chimica, D., Perugia, U., Elce, V., Industriale, I., & Tecnica, F. (2007). Valutazioni Energetiche Ed Economiche Sulle Varie Tecnologie. *Quantum*.
- Stolzenburg, K., Berstad, D., Decker, L., Elliott, A., Haberstroh, C., Hatto, C., Klaus, M., Mortimer, N. D., Mubbala, R., Mwabonje, O., Nekså, P., Quack, H., Rix, J. H. R., Seemann, I., & Walnum, H. T. (2013). Efficient Liquefaction of Hydrogen: Results of the IDEALHY Project. *Proceedings of the Energie – Symposium, Stralsund/Germany, November, November*, 1–8. https://www.idealhy.eu/uploads/documents/IDEALHY_XX_Energie-Symposium_2013_web.pdf
- Studio di impatto ambientale di un grande impianto di dissalazione ad osmosi inversa : focus su recupero energetico , scarichi a mare e LCA*. (2013).
- Sustainable, E. U., Strategy, D., Council, E., & Sds, E. U. (2010). *Strategy*. 7–9.
- Teknik, E. I. (2021). *An Industrial Perspective on Ultrapure Water Production for Electrolysis*.
- Torino, P. D. I. (2021). *Technical-economic analysis of the electrosynthesis of ammonia - Thesis*. March.
- Torino, P. D. I., Ruggeri, B., Gomez, E., Cecconi, S., Di, A., Ambientale, S., & Energetica, E. D. (2021). *sostenibilità energetica / ambientale confrontata con l' u tilizzo del gas naturale*.
- Ursúa, A., Gandía, L. M., & Sanchis, P. (2012). Hydrogen production from water electrolysis: Current status and future trends. *Proceedings of the IEEE*, 100(2), 410–426. <https://doi.org/10.1109/JPROC.2011.2156750>
- Valenzuela, M. A., & Zapata, B. (2007). Hydrogen production. *Hydroprocessing of Heavy Oils and Residua*, 313–338. https://doi.org/10.1299/jsmemag.119.1169_182
- Ventosità, D. I., & Varie, M. A. (n.d.). *Il Tuo Consulente Personale per il Risparmio Energetico*. 1–14.
- Verleysen, K., Parente, A., & Contino, F. (2021). How sensitive is a dynamic ammonia synthesis process? Global sensitivity analysis of a dynamic Haber-Bosch process (for flexible seasonal energy storage). *Energy*, 232. <https://doi.org/10.1016/j.energy.2021.121016>
- Vincent, I., & Bessarabov, D. (2018). Low cost hydrogen production by anion exchange

- membrane electrolysis: A review. *Renewable and Sustainable Energy Reviews*, 81(August 2016), 1690–1704. <https://doi.org/10.1016/j.rser.2017.05.258>
- Vogl, V., Åhman, M., & Nilsson, L. J. (2018). Assessment of hydrogen direct reduction for fossil-free steelmaking. *Journal of Cleaner Production*, 203, 736–745. <https://doi.org/10.1016/j.jclepro.2018.08.279>
- Wijayanta, A. T., Oda, T., Purnomo, C. W., Kashiwagi, T., & Aziz, M. (2019). Liquid hydrogen, methylcyclohexane, and ammonia as potential hydrogen storage: Comparison review. *International Journal of Hydrogen Energy*, 44(29), 15026–15044. <https://doi.org/10.1016/j.ijhydene.2019.04.112>
- Worldsteel. (2021). *World Steel in Figures Report 2021*. 1–29. <https://www.worldsteel.org/en/dam/jcr:976723ed-74b3-47b4-92f6-81b6a452b86e/World%2520Steel%2520in%2520Figures%25202021.pdf>
- Yilmaz, C., Wendelstorf, J., & Turek, T. (2017). Modeling and simulation of hydrogen injection into a blast furnace to reduce carbon dioxide emissions. *Journal of Cleaner Production*, 154, 488–501. <https://doi.org/10.1016/j.jclepro.2017.03.162>

Chapter 2

Supply chain design

2.1 Purpose of the work

The scope of the thesis is the evaluation of the technical and economic feasibility of producing green hydrogen through wind energy produced in the Chubut region, part of Patagonia Argentina, and characterised by a highly windy desert climate. The work carried out involved the design of the hydrogen production and storage plant, the maritime transport chain from the city of Comodoro Rivadavia to the city of Taranto, in Italy, the storage and reconversion in the port of arrival. The objective of the work is the analysis of the total costs and the evaluation of the hydrogen levelized cost, to identify the processes and factors that most influence LCOH, to individuate possible improvements and optimisations that can lower the final cost, so that it can be competitive in the hydrogen market.

To size the production process, it was necessary to calculate the hydrogen demand of Italian steel industry.

2.2 Hydrogen Demand

To quantify the hydrogen demand required for the decarbonization of the Italian steel industry, it is essential to estimate the demand for reduced iron. According to what has been explained in the introduction chapter, the total demand in reduced iron is divided according to its end use, either directly in the electric arc furnace or as a reducing agent in the blast furnace, in the form of hot briquetted iron.

The Journal (Guccione et al., 2018), related to the day July 6, 2018, published a paper about the development of a national plan for the re-qualification of Ilva steel industry in Taranto, which was discussed by the government. Specifically, the proposal was to open two steel production lines of 2,5 million tons/year, for a total of 5 million tons/year, articulated on direct reduction (DRI) and electric arc furnace (EAF). Based on the latest paper from the (Worldsteel, 2021), Italy produced 20,4 tons of steel in 2020, 3 less than in 2019 (due to Covid Pandemic). National steel production is divided according to process into 15,3 % through oxygen furnaces and 84,7 % through with electric furnaces (recycling 100 % scrap). Italy produced 3,6 million tons of Pig Iron (Blast Furnace Product) in 2020, compared to 4,6 million tons in 2019, while national DRI

production is null. Based on these data, the national demand for HBI and DRI is calculated. For the decarbonisation of blast furnaces pig iron production process, 100 kgHBI/tonHM is assumed to be used.

HBI demand for Blast Furnace

<i>BF Pig Iron Italy Production</i>	4.600.000	ton/year
<i>HBI in BF</i>	100	kgHBI/tonHM
<i>Annual HBI Production</i>	460.000	ton/year

Table 2.1: Annual demand of HBI for use in the blast furnace

To calculate the direct reduced iron necessary for the electric arc furnace the percentage of DRI and scrap has to be selected, since the amount of DRI fed can vary from 0 to 100 %. In this work a mix consisting of 60 % DRI and 40 % scraps has been assumed.

DRI demand for Electric Arc Furnace

<i>DRI-EAF steel annual production</i>	5.000.000	ton/year
<i>Reduced Iron</i>	60 %	
<i>Scrap</i>	40 %	
<i>Annual DRI Production</i>	3.000.000	ton/year

Table 2.2: Annual demand of reduced iron for use in electric arc furnace

By adding up the demand of the blast furnaces and electric furnaces, the annual amount of 3.460.000 tonnes of reduced iron produced by the DRI plant is obtained.

Hydrogen has two roles in the steel plant, it is required in pure form as a reducing gas for iron ore, but it can also be used as a source of thermal energy to support the reduction reaction of the shaft furnace, to further decrease the carbon footprint of the process.

- Demand of pure hydrogen as reducing gas

The paper (Fan & Friedmann, 2021) published a forecast of NG and H₂ utilisation for different levels of hydrogen penetration in reduction syngas, basing its simulation analysis on data from an existing MIDREX plant.

<i>H₂ replacement rate</i>	<i>Base Case - 0%</i>	<i>Scenario 1 - 30%</i>	<i>Scenario 2 - 100%</i>
<i>NG [m³/ton_{DRI}]</i>	266,7	186,7	0
<i>H₂ [m³/ton_{DRI}]</i>	0	240	800
<i>NG [kg/ton_{DRI}]</i>	14,8	10,3	0
<i>H₂ [kg/ton_{DRI}]</i>	0	21,6	71,9
<i>CO₂ Abatement [kgCO₂/ton_{DRI}]</i>	0	113,8	379,2

Table 2.3: NG-H₂ mixing scenarios for reducing gas

Two scenarios have been considered in this work, the first, currently industrially feasible, involves replacing 30 % natural gas with green hydrogen. The specific hydrogen consumption is 21,6 kg per tonne of reduced iron. The second, futuristic scenario assumes the use of pure hydrogen as reducing gas, in this case 71,9 kg of hydrogen per tonne of DRI is needed. The annual demand for pure hydrogen for the crude iron reduction process, calculated by multiplying the specific hydrogen consumption by the total amount of reduced iron, is 74.636 tonH₂/year in Scenario 1, and 248.788 tonH₂/year in Scenario 2.

- Hydrogen demand for thermal energy production

With the purpose of making the DRI plant greener, the heat requirement of the plant has been calculated, assuming that it could be met through the combustion of hydrogen, which unlike natural gas does not emit CO₂, but only water vapour. The processes that need thermal energy are identified; according to the study (Bhaskar et al., 2020), 436 kWh/ton_{DRI} are required for the electrical heating of raw iron to a temperature of 800 °C. The reduction reaction of iron oxide with H₂, which is endothermic, requires 334 kWh/ton_{DRI}, while preheating the hydrogen in the furnace requires 160 kWh/ton. The hydrogen requirement can be calculated using the following formula.

$$H_2 \left[\frac{kg_{H_2}}{ton_{DRI}} \right] = \frac{\text{Thermal Demand} \left[\frac{MJ}{ton_{DRI}} \right]}{LHV_{H_2} \left[\frac{MJ}{kg_{H_2}} \right]} * \frac{1}{H_2 \text{ Boiler Efficiency}} \quad (2.1)$$

The thermal demand has been transformed from kWh to MJ. Dividing by the Low Heating Value of hydrogen, which is 120 MJ/kg, and considering the efficiency of a hydrogen boiler, assumed to be 90 %, the amount of hydrogen required for each process is computed.

Quantity of H₂ needed to provide thermal heating

<i>Heating Iron Ore Pellets (800°C)</i>	14,5	kgH ₂ /ton _{DRI}
<i>Hydrogen Pre-Heating (500°C)</i>	5,3	kgH ₂ /ton _{DRI}
<i>Endothermic Reaction</i>	11,1	kgH ₂ /ton _{DRI}

Table 2.4: Quantity of hydrogen needed to provide thermal energy for processes

The annual requirement of hydrogen as a heat source for the DRI plant has been calculated for the two scenarios analysed. The heat required for the endothermic reaction is only needed in the second scenario, where the only reducing gas is hydrogen. In the first scenario, the heat emitted by the exothermic reaction between hematite and carbon monoxide balances the heat requirement of the endothermic reaction between hydrogen and hematite. In scenario 1, specific hydrogen demand for heating is 19,8 kgH₂/ton_{DRI}, for a total of 68.508 tonnes of hydrogen per year. Demand rises in the second scenario, where 30,9 kgH₂/ton_{DRI} is required, for a total of 106.914 tonnes of hydrogen per year.

The total hydrogen demand of the DRI Plant for the two scenarios is summed in table 2.5.

<i>H₂ Demand</i>	<i>Scenario 1 (70% NG - 30% H₂)</i>	<i>Scenario 2 (100% H₂)</i>
<i>Reducing agent</i>	74.636 tonH ₂ /y	248.788 tonH ₂ /y
<i>Thermal energy</i>	68.508 tonH ₂ /y	106.914 tonH ₂ /y
<i>Total H₂ Demand</i>	143.144 tonH ₂ /y	355.702 tonH ₂ /y

Table 2.5: Total demand of hydrogen in the two analysed scenarios

The complete decarbonisation of the DRI plant (Scenario 2) results in a significant increase in hydrogen use. For the same amount of reduced iron produced in the DRI plant, the demand for hydrogen in the second scenario is more than twice as high as in the first scenario, where natural gas is used as a reducing agent together with green hydrogen. The specific consumption goes from 41,4 kg H₂ per tonne of reduced iron in the first scenario, to 102,8 kg H₂ per tonne of DRI in the second scenario.

The deep decarbonisation assumed in the second scenario guarantees CO₂ emissions cut of 256,4 kg CO₂ per tonne of reduced iron produced with respect the first scenario, corresponding to a DRI plant pollution reduction of 887.144 tonnes of CO₂ per year.

2.3 Ammonia production supply chain

To satisfy the demand for hydrogen, the technical-economic analysis of two carriers, liquid hydrogen and ammonia, has been carried out, studying their production, storage, transport and conversion costs. In this section, the NH_3 carrier is addressed.

As the production of green ammonia is a new technology, several possible configurations of the production process have been evaluated to decide which one is the most suitable for the study.

The ammonia production chain is characterised by an electrolysis plant producing hydrogen in gaseous form, fed by a desalinator. Nitrogen is produced via the Air Separation Unit. The hydrogen and nitrogen produced are mixed in a 3:1 molar proportion and are compressed and heated to reach the inlet conditions of the Haber-Bosch ammonia synthesis plant. The ammonia synthesized is liquefied and stored in liquid form in dedicated tanks, before being loaded into ocean transport vessels.

Three processes have been evaluated, which differ in the presence of hydrogen and nitrogen buffers and in the pressure at which the mixing of N_2 and H_2 takes place for syngas formation. The Haber-Bosch system can only work continuously and at maximum load. Intermediate buffers have been designed to ensure the supply of wind energy, which is a volatile source, to power the plant.

The figure below shows the first alternative, which involves the presence of two storage tanks, one for hydrogen and one for nitrogen, at the outlet pressure of the gases from the electrolyser and ASU respectively. Mixing takes place at low pressure and the syngas is compressed to a pressure of 200 bar before entering the synthesis plant.

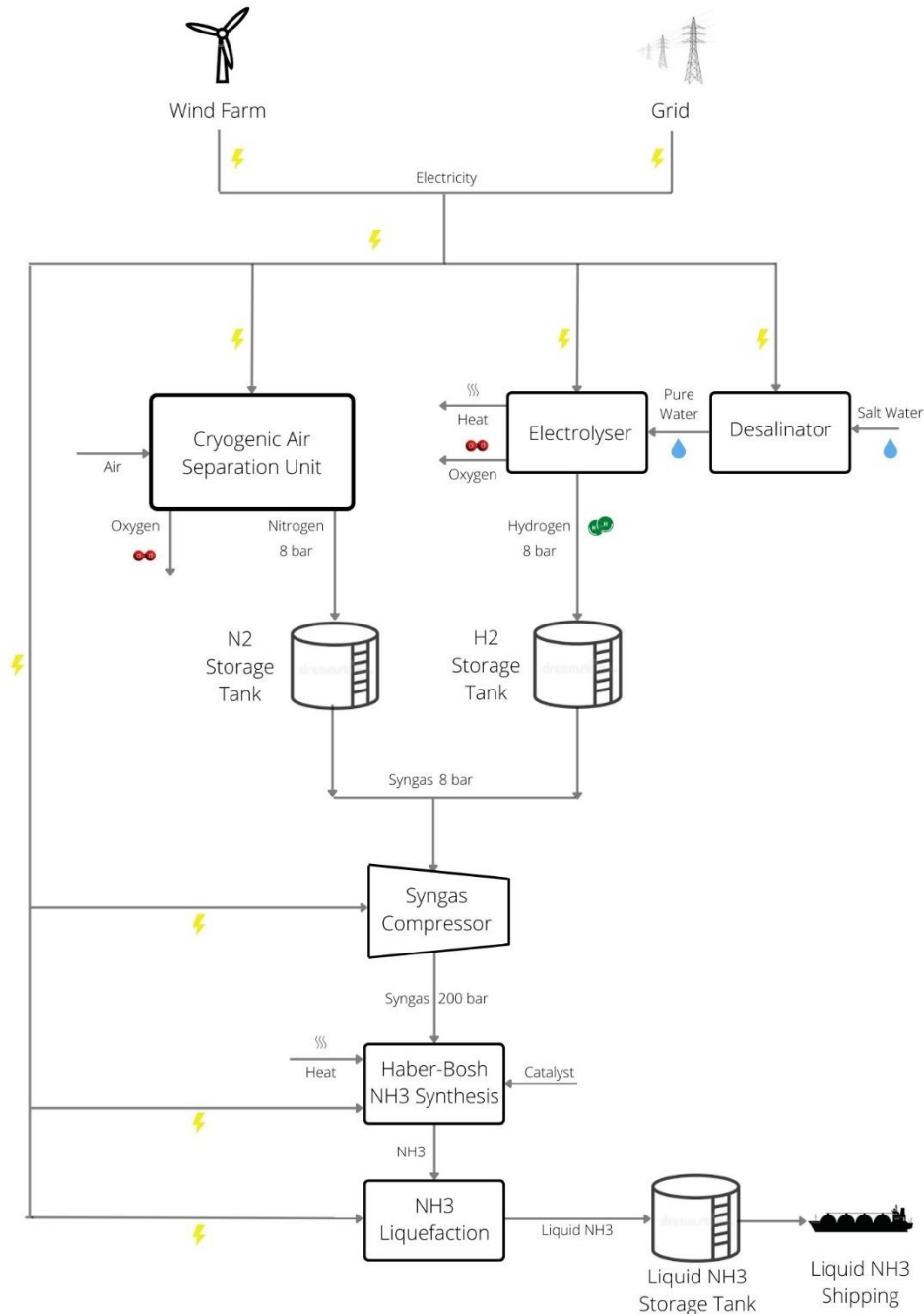


Figure 2.1: Ammonia production process - Option 1 (the Author)

This process is not technically feasible, as storing hydrogen at low pressures would require the use of huge volumes, greatly increasing storage costs.

The second option involves a single syngas buffer, which allows the Haber-Bosch plant to be separated from the electrolyser and ASU. Syngas formation occurs immediately after H₂ and N₂ are produced. The syngas is compressed to a pressure of 200 bar and stored.

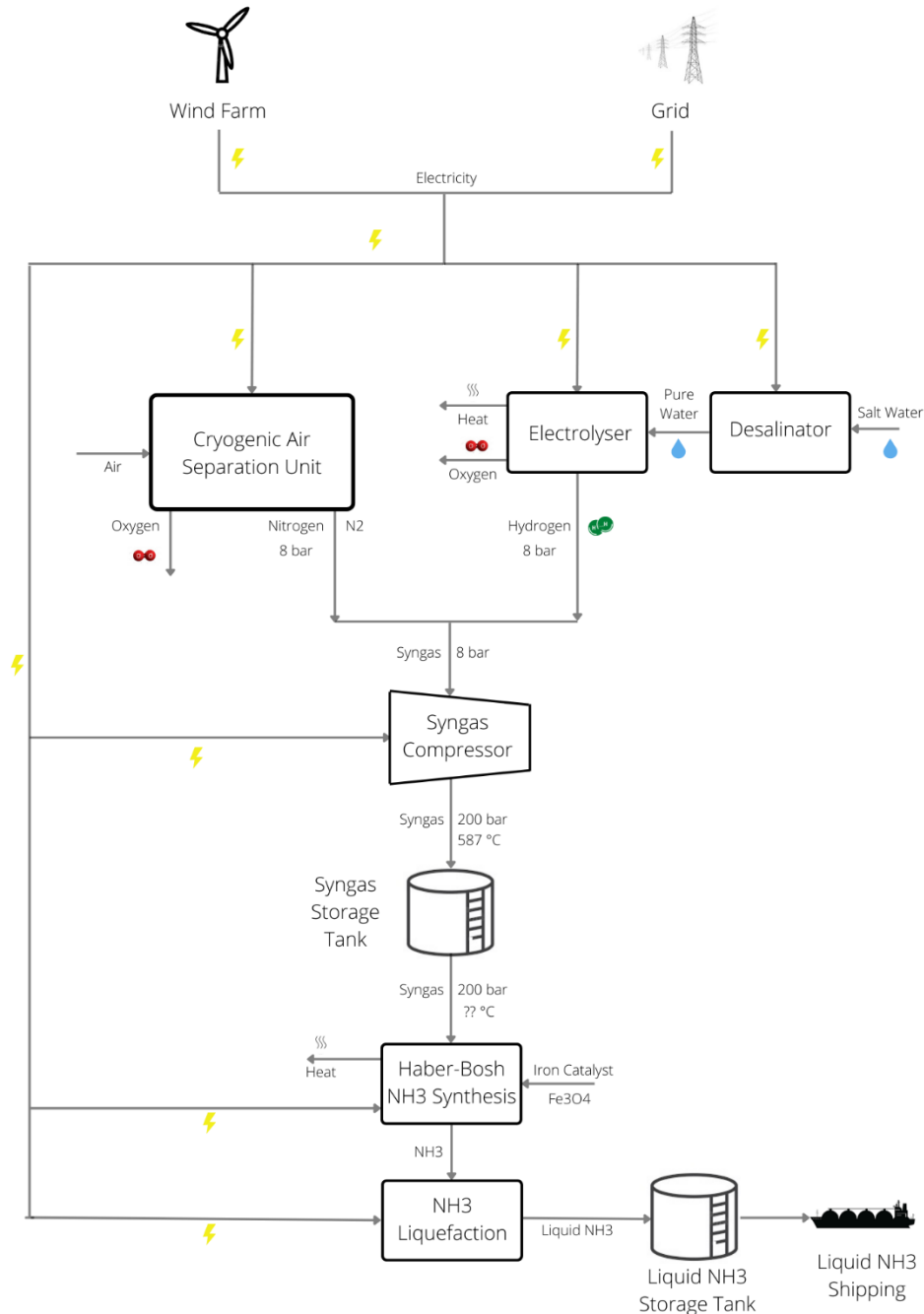


Figure 2.2: Ammonia production process - Option 2 (the Author)

This option is very promising, as it involves the installation of only one buffer and one compressor train. At present, this solution is not feasible on industrial scale. Hydrogen and nitrogen have different chemical and physical properties, which makes their storage complicated and expensive, since for the synthesis of ammonia, H₂ and N₂ must be mixed in the correct proportions.

The third option involves the use of only one intermediate hydrogen buffer, placed after the compressor train. There is no N_2 buffer because the ASU, as well as the Haber-Bosch plant, are also connected to the electricity grid, which ensures continuity of energy supply.

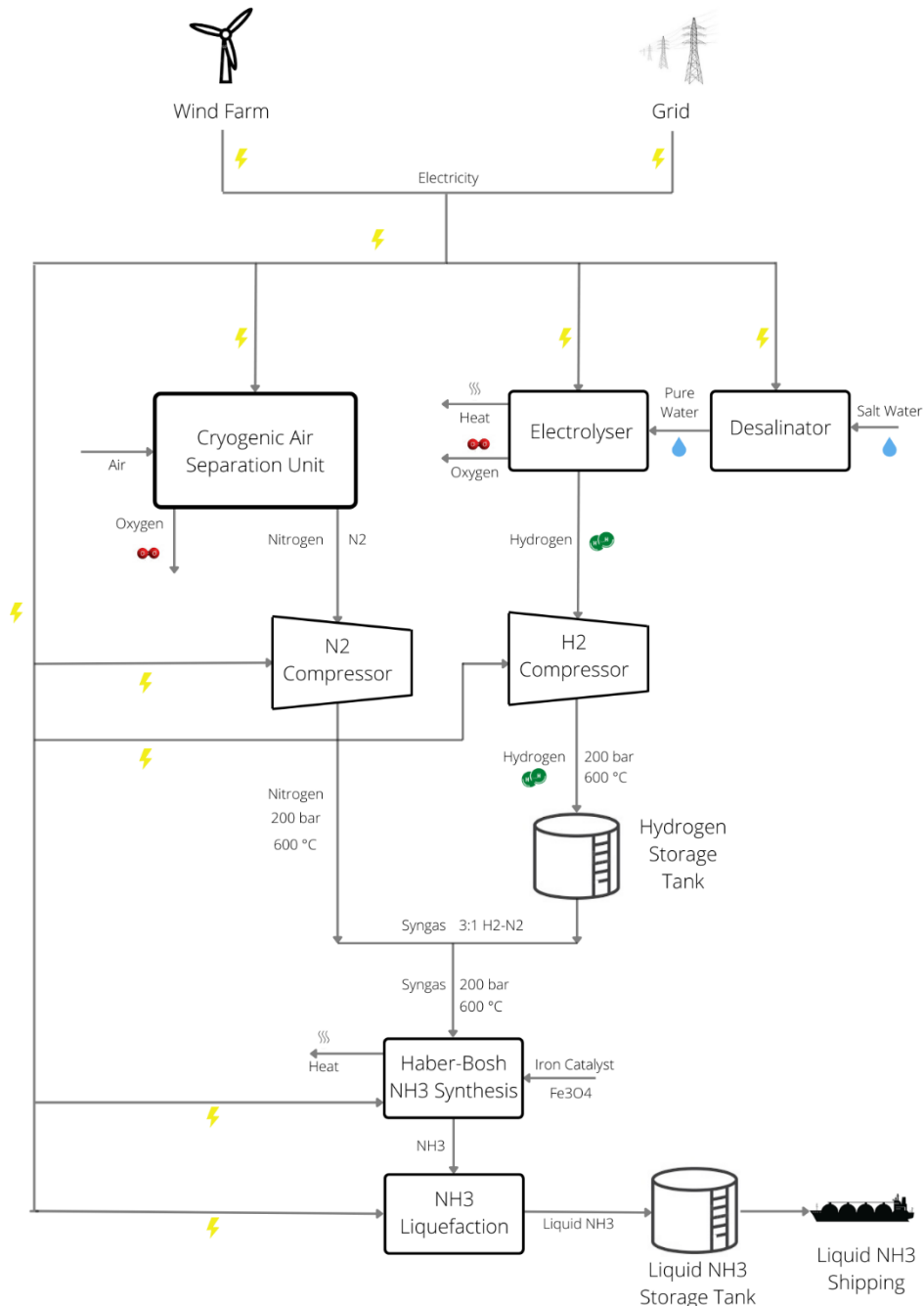


Figure 2.3: Ammonia production process - Option 3 (the Author)

This layout has been chosen for the dimensioning of the production chain, which involves, after the synthesis of ammonia, its liquefaction and storage in special cryogenic tanks, sited in the loading terminal of the Port of Comodoro Rivadavia.

2.3.1 Electricity

The wind farm is located in the Chubut region of eastern Patagonia. According to the paper (Armijo & Philibert, 2020), the Capacity Factor is steadily exceeding 45 %. In some areas of this region, near to city of Comodoro Rivadavia, a net CF of over 60 % can be achieved. For this thesis, a CF of 54 % has been used, in accordance with the paper (Correa et al., 2022).

Electricity for electrolysis and desalination can be provided only by the wind power plant, ensuring capacity factor of 54 %, or by a wind-grid mix, where grid integration can be chosen, varying from 0 to 46 %. In contrast, the rest of the production chain, which includes the ASU, the ammonia synthesis and liquefaction plant are always supplied by a wind-grid mix, which guarantees a total capacity factor of 100 %. According to (Ministerio de Energía, 2019), the price of wind power is \$42/MWh, while grid-supplied electricity costs \$60/MWh, and has indirect CO₂ emissions of 344 g/kWh (Energ et al., 2021). Electricity in Italy is taken from the electricity grid, its cost has been considered \$224/MWh, the average national price in January 2022. The indirect emissions of grid energy in Italy are 312 gCO₂/kWh (Qualenergia, 2019).

The following sections illustrate the technological choices and design of the various plants involved in the ammonia production and storage process.

2.3.2 Balance of the process

The stages of ammonia production, storage in liquid form at ports of departure and arrival, sea transport, and reconversion into hydrogen are characterised by mass losses, which cause an overproduction of hydrogen and ammonia compared to the final hydrogen demand of the steel industry. For the production chain, which involves the hydrogen production, compression and storage process, nitrogen production, ammonia synthesis and its liquefaction, a loss rate of 2 % by mass has been considered. This is mainly due to the ammonia synthesis process, which requires continuous recirculation of the syngas, since only 25-30 % is synthesised in each cycle, the continuous recirculation causes losses. The maritime transport phase is characterised by two sources of losses, which are the Boil-Off of ammonia during transport and the ammonia used as fuel for the ships, which have a specific consumption of about 120 kgNH₃/km.

Finally, the ammonia cracking and hydrogen purification plant is very inefficient. The paper (Ishimoto et al., 2020) calculates the efficiency of the plant to be 69,5 %, which means that for every 100 kg of hydrogen that enters in the form of ammonia, 69,5 kg of pure hydrogen are

produced. The paper (Makhloufi & Kezibri, 2021) reports a hydrogen decomposition process efficiency of 68,5 % in its study. (US Department of Energy, 2006) reports an overall conversion efficiency of 65 % for a cracking and purification plant.

The following table shows the mass balance of hydrogen and ammonia during all the stages described above, for both scenarios.

Scenario 1 (70 % NG - 30 % H₂)

<i>Hydrogen Demand for DRI Plant</i>	143.144.352	kgH ₂
<i>Related Ammonia</i>	806.447.054	kgNH ₃
<i>Cracking Plant Efficiency</i>	69,5 %	
<i>Hydrogen Entering Cracking Plant</i>	205.963.096	kgH ₂
<i>Ammonia Entering Cracking Plant</i>	1.160.355.473	kgNH ₃
<i>Ammonia Used as Maritime Fuel</i>	85.637.558	kgNH ₃
<i>Transportation Annual Boil-Off</i>	7.838.416	Kg NH ₃
<i>Ammonia Stored in Loading Terminal</i>	1.253.831.447	kgNH ₃
<i>Production Plant Efficiency</i>	2,0 %	
<i>Total Ammonia Production</i>	1.278.908.076	kgNH ₃
<i>Total Annual Nitrogen Production</i>	1.051.901.893	kgN ₂
<i>Total Hydrogen Production</i>	227.006.184	kgH ₂
<i>Overproduction</i>	58,6 %	

Table 2.6: Mass balance of hydrogen and ammonia for the entire supply chain, scenario 1

In scenario 1, the overproduction of hydrogen compared to final demand is 58,6 %, a very large value, which leads to an increase in the final hydrogen cost, due to large losses during the transport phase, where ammonia is used as fuel, and the hydrogen reconversion phase, which is highly inefficient.

Scenario 2 (100 % H₂)

<i>Hydrogen Demand for DRI Plant</i>	355.701.840	kgH ₂
<i>Related Ammonia</i>	2.003.954.028	kgNH ₃
<i>Cracking Plant Efficiency</i>	69,5 %	
<i>Hydrogen Entering Cracking Plant</i>	511.801.209	kgH ₂
<i>Ammonia Entering Cracking Plant</i>	2.883.387.091	kgNH ₃
<i>Ammonia Used as Maritime Fuel</i>	171.275.117	kgNH ₃
<i>Transportation Annual Boil-Off</i>	15.676.833	Kg NH ₃
<i>Ammonia Stored in Loading Terminal</i>	3.070.339.040	kgNH ₃
<i>Production Plant Efficiency</i>	2,0 %	
<i>Total Ammonia Production</i>	3.131.745.821	kgNH ₃
<i>Total Annual Nitrogen Production</i>	2.575.860.938	kgN ₂
<i>Total Hydrogen Production</i>	555.884.883	kgH ₂
<i>Overproduction</i>	56,3 %	

Table 2.7: Mass balance of hydrogen and ammonia for the entire supply chain, scenario 2

For the second scenario, overproduction is also very high, at 56,3 % by mass. The causes are the same as those explained for the first scenario.

2.3.3 Electrolyser

Both alkaline and PEM electrolysers have been considered to study their technological and economic impact on the final cost of hydrogen.

The table 2.8 shows the data of the electrolysers, which have been taken from data sheets of the company (Nel Hydrogen). For the alkaline electrolyser, the A1000 series product has been considered.

<i>Technical Data</i>	<i>Alkaline</i>	
<i>Operating Temperature</i>	70	°C
<i>Operating Pressure</i>	30	bar
<i>Net Production Rate</i>	785	Nm ³ /h
<i>Net Production Rate</i>	1694,5	kgH ₂ /day
<i>Operation Dynamic Range</i>	15-100 %	
<i>Power Consumption at Stack</i>	4,1	kWh/Nm ³
<i>Power Consumption at Stack</i>	45,6	kWh/kgH ₂
<i>Power Consumption at System</i>	48	kWh/kgH ₂
<i>Level (atmospheric pressure)</i>		
<i>Delivery Pressure</i>	30	bar
<i>Electrolyte</i>	25%	KOH
<i>Feed Water Consumption</i>	1	lt/Nm ³
<i>Feed Water Consumption</i>	11,1	kg/kgH ₂
<i>Stack Lifetime</i>	80.000	h
<i>Stack Degradation Rate</i>	0,13	%/1000h
<i>Heat Produced in the reaction</i>	1791,4	kWh/m ³

Table 2.8: Technical specifications alkaline electrolyser

The alkaline electrolyser operates at a temperature of 70 °C and a pressure of 30 bar. The single unit has a capacity of almost 800 m³/h. The specific consumption of the stack is 45,6 kWh/kgH₂, while the system specific consumption is slightly higher at 48 kWh/kgH₂, a value in line with that published by (IRENA, 2020). The ideal specific water consumption is 11,1 kgH₂/kgH₂O. The stack life is 80.000 h according to (Armijo & Philibert, 2020), while the specific heat produced by the electrolysis reaction is 1791 kWh/ m³ of H₂ at operating temperature.

The table 2.9 shows the technical data of the PEM electrolyser, referring to product M2000 of Nel Hydrogen.

<i>Technical Data</i>	<i>PEM</i>	
<i>Operating Temperature</i>	50	°C
<i>Operating Pressure</i>	30	bar
<i>Net Production Rate</i>	1698	Nm ³ /h
<i>Net Production Rate</i>	4247	kgH ₂ /day
<i>Operation Dynamic Range</i>	10-100%	
<i>Power Consumption at Stack</i>	4,5	kWh/Nm ³
<i>Power Consumption at Stack</i>	48	kWh/kgH ₂
<i>Power Consumption at System</i>	50,0	kWh/kgH ₂
<i>Level (atmospheric pressure)</i>		
<i>Delivery Pressure</i>	30	bar
<i>Electrolyte</i>		PEM
<i>Feed Water Consumption</i>	0,9	lt/Nm ³
<i>Feed Water Consumption</i>	10,0	kg/kgH ₂
<i>Stack Lifetime</i>	65.000	h
<i>Stack Degradation Rate</i>	0,25	%/1000h
<i>Heat Produced in the reaction</i>	1635,2	kWh/m ³

Table 2.9: Technical specifications PEM electrolyser

The operating conditions for the PEM electrolyser are 30 bar and 50 °C, with a daily capacity of 4247 kgH₂/d each unit. The specific consumption of the stack is 48 kWh/kgH₂, which increases to 50 kWh/kgH₂ at system level, these data are congruent with the publication of (International Renewable Energy Agency, 2020), which indicates a specific consumption of an alkaline electrolyser ranging between 50-78 kWh/kgH₂ and a consumption for a PEM of 50-83 kWh/kgH₂. The same paper predicts a reduction in specific consumption for both types of electrolysers to a level below 45 kWh/kgH₂ by 2050. The paper (Tractebel Engineering, 2017) reports specific consumptions of alkaline and PEM electrolysers above 20 MW of 51 kWh/kg and 58 kWh/kg respectively.

The ideal water consumption is 10 kgH₂O per kg H₂ produced, while the stack life is 65.000 h (IRENA, 2020). Heat production is 1635,2 kWh/m³ of H₂, released at the operating temperature of the stack (Teknik, 2021).

The specific electricity consumption (SEC) of electrolysers at operating pressure is higher than the relative consumption at ambient pressure reported in the fact sheet. The following

experimental formula, used in a study developed by CONICET, has been used to calculate the specific consumption at operating conditions, where SEC_0 refers to the specific consumption at ambient pressure and P is the operating pressure of the electrolyser.

$$SEC [kWh] = SEC_0 * \left(1 + \frac{97070 * P^2 + 550600 * P - 771500}{P^3 + 6713 * P^2 + 396500 * P + 541500} \right) * 100 \quad (2.2)$$

The result of this formula is a specific electricity consumption of alkaline at 30 bar of 50,7 kWh/kgH₂, and a specific consumption of PEM at 30 bar of 52,8 kWh/kgH₂.

To size the electrolysis plant, the plant's availability and the capacity factor of the electricity mix consisting of wind and grid has been considered. Assuming that the plant can be shut down 14 days in a year for maintenance and contingencies, the availability is calculated by dividing the operating days by the total days, and results in 96 %. The CF of the electrolyser is given by the following formula:

$$CF_{TOT}[\%] = CF_{electricity} * Availability \quad (2.3)$$

The CF of the electricity mix depends on the choice, it can vary from a minimum of 54 % if only the wind plant is used, to a maximum of 100 %, considering full grid integration.

The capacity of the electrolyser has been calculated using the following formula, which considers the total CF and the amount of hydrogen produced per year.

$$Plant Capacity \left[\frac{tonH_2}{day} \right] = \frac{Annual H_2 Produced [tonnes]}{CF_{TOT} * 365} \quad (2.4)$$

The same formula can be used to calculate the hourly capacity of the plant, using 8760 (h) instead of 365 (days).

The power output of the plant is calculated using the following formula, which considers the total energy consumed by the plant, the total CF, and the total hours per year.

$$Power [KW] = \frac{Annual Electricity Consumed [kWh]}{CF_{TOT} * 8760 [h]} \quad (2.5)$$

The table 2.10 shows data for the two production scenarios, considering four case studies, relating to the type of electrolyser, Alkaline or PEM, and the type of power supply, which can be either exclusively through wind power, guaranteeing a capacity factor of 54 %, or through full grid integration, which increases the electrical capacity factor to 100 %.

<i>Option</i>	<i>Scenario 1</i>	<i>Scenario 2</i>
<i>Annual Hydrogen Produced [ton]</i>	227.006	555.885
<i>Total Electricity Consumed [GWh]</i>		
<i>Alkaline</i>	11.503	28.169
<i>PEM</i>	11.982	29.342
<i>Plant Power [GW]</i>		
<i>Wind Energy (CF 54%) - Alkaline</i>	2,53	6,19
<i>Wind + Grid Energy (CF 100 %) - Alkaline</i>	1,37	3,34
<i>Wind Energy (CF 54%) - PEM</i>	2,63	6,43
<i>Wind + Grid Energy (CF 100 %) - PEM</i>	1,42	3,48
<i>Plant Capacity [tonH₂/day]</i>		
<i>Only Wind Energy – CF 54%</i>	1.197	2.933
<i>Wind + Grid Energy – CF 100 %</i>	647	1.583

Table 2.10: Electrolyser plant power and capacities for different scenarios, (NH₃ supply chain)

The capacity factor is a significant dimensioning parameter. There is a big difference in power between the case where only wind power is used, and the case of grid integration, this will also be reflected in the final hydrogen cost and process emissions. The power in the case of full grid integration drops to about half the power of the case without grid. The difference between the alkaline and PEM electrolyser is small, and depends on the specific plant energy consumption, which is slightly higher in the case of PEM.

The total thermal energy released by the electrolysers at operating temperature has been calculated. In first scenario the alkaline electrolyser produces 36.326 GWh_{th}, while the PEM 33.158 GWh_{th}. In second scenario the total heat produced increases to 89.054 GWh_{th} in case of alkaline electrolyser and 81.289 GWh_{th} considering PEM. This heat cannot be reused in the ammonia production process because it is released at low a temperature, but it could be used to pre-heat gases or fluids in other industrial processes, or for district heating.

2.3.4 Desalinators

The purpose of the desalination plant is to purify salt water and make it available in pure form for the electrolyser. Reverse Osmosis desalinators have been adopted for this process, as they only require electricity to operate, unlike desalinators using MFS and MED technology, which require thermal energy in addition to electricity.

Electricity, as in the case of the electrolyser, comes both from the wind plant and from the grid, which can be integrated, ensuring a capacity factor increase of up to 100%.

The operation process of the RO desalinator is explained in the introductory chapter. Pre and post chemistry treatment of the water are necessary to achieve the required standards. The purification process consists of four phases, the pre-treatment removes suspended solids, the reintegration phase to desalinise, followed by the polishing phase to achieve a high-water quality, and finally a recovery phase for the used wastewater.

The dimensioning of the plant has been based on the specific water consumption of the electrolysers. The alkaline has an ideal water consumption of 11,1 kg H₂O per kg H₂ produced, the PEM consumes slightly less, 10 kg H₂O/kgH₂. For the calculation, an efficiency of 70 % has been considered, to take into account the real case, where inefficiencies and losses are present in both the electrolyser and the desalinator. The real consumption is therefore 14,30 kgH₂O/kgH₂ for the PEM and 15,89 kgH₂O/kgH₂ for the alkaline. These values are very similar to literature values. (Shi et al., 2020) calculated a specific consumption of 17 kgH₂O/kgH₂ for electrolysers driven by electricity from wind power, while (International Renewable Energy Agency, 2020) explains that due to some inefficiencies in the process, the ratio of water consumed can range between 18 kg and 24 kg of water per kilo of hydrogen.

By multiplying the specific consumption of the electrolysers by the total hydrogen produced, the total amount of water required for the electrolysis process can be calculated. The capacity of the desalinator has been calculated by considering the availability of the plant, considered to be 96 %, which when multiplied by the capacity factor of the energy mix, as in formula (2.3) used in the previous paragraph, results in the total capacity factor of the plant. By dividing the total amount of water by the total CF and the number of hours, or annual days, as explained in formula (2.4), the capacity of the plant can be obtained. Finally, using formula (2.5), the capacity of the desalination plant has been found by dividing the total electricity used by the total CF and the number of annual hours. According to the paper (Teknik, 2021), the specific consumption of a reverse osmosis plant is 1,534 kWh per m³ of produced water. The study carried out by (Caldera et al., 2016) uses a specific consumption of the RO plant varying in the range of 3-4 kWh/m³ H₂O. The paper (Cappella & Giorgetti, 2013) specifies a range of specific RO system consumption between 2,5 and 4 kWh/m³ H₂O. For this study, an intermediate value of 2,5 kWh/kg H₂O has been assumed.

The table 2.11 shows the values for both scenarios considered.

<i>Option</i>	<i>Scenario 1</i>	<i>Scenario 2</i>
<i>Annual Water Demand [ton]</i>		
<i>Alkaline</i>	3.608.084	8.835.350
<i>PEM</i>	3.247.275	7.951.815
<i>Total Electricity Used [MWh]</i>		
<i>Alkaline</i>	9.020	22.088
<i>PEM</i>	8.118	19.879
<i>Plant Power [MW]</i>		
<i>Wind Energy (CF 54%) + Alkaline</i>	1,99	4,86
<i>Wind + Grid Energy (CF 100 %) + Alkaline</i>	1,07	2,63
<i>Wind Energy (CF 54%) + PEM</i>	1,79	4,38
<i>Wind + Grid Energy (CF 100 %) + PEM</i>	0,97	2,36
<i>Plant Capacity [m³/day]</i>		
<i>Wind Energy (CF 54%) + Alkaline</i>	19.069	46.695
<i>Wind + Grid Energy (CF 100 %) + Alkaline</i>	10.297	25.215
<i>Wind Energy (CF 54%) + PEM</i>	17.162	42.025
<i>Wind + Grid Energy (CF 100 %) + PEM</i>	9.267	22.694

Table 2.11: Desalinator plant power and capacities for different scenarios, (NH₃ supply chain)

The capacity factor is a very influential factor on both plant power and capacity, which in the case of full grid utilisation is approximately half as much as in the case of using only wind power; this results in substantially lower installation and maintenance costs for the plant. The choice of electrolyser is not influential, as the values vary slightly.

2.3.5 Hydrogen compressor

Hydrogen is produced at pressure of 30 bar in both alkaline and PEM electrolysers. To be stored, hydrogen must be compressed to increase its volumetric density and store a larger quantity. Hydrogen can be compressed to large pressures of up to 1000 bar. The Haber-Bosch process uses syngas at 200 bar, which is the storage pressure chosen in the thesis.

There are two types of hydrogen compressors, they can be either volumetric or centrifugal. For large compression ratios, reciprocating compressors are used, consisting of a motor that moves a piston, which compresses the hydrogen. Ionic compressors operate in a similar way, but instead of a piston they use ionic liquids. Centrifugal compressors are preferred for applications

requiring large flow rates and low compression ratios, their operation consists of turning a turbine at high speeds to compress the gas. The high cost of hydrogen compressors compared to air and gas compressors is due to the fact that hydrogen has a very low molecular weight, so they must rotate at higher speeds to achieve the same compression ratio (Department of Energy, 2022). The use of centrifugal compressors, which are suitable for low compression ratios and high flow rates, has been considered in this work.

To calculate the compressor power, it is necessary to know the specific energy consumption, which is calculated using the theoretical formula 2.6.

$$W_C = \frac{c_{pH_2} * T_{in}}{\eta_{is}} * \left(\beta^{\frac{k-1}{k}} - 1 \right) * \frac{1}{\eta_{el}} \left[\frac{kJ}{kg} \right] \quad (2.6)$$

The specific work W_C , of the compressor, expressed in KJ/kg°K, depends on the inlet temperature of the hydrogen, and the compression ratio, β , which is calculated as the ratio of the outlet pressure over the inlet pressure. The isentropic efficiency is 80 %, while the electrical efficiency is 95 %. The specific heat C_P of hydrogen is 14,403 KJ/kg°K. The specific heats ratio, k , is calculated using the following formula, where C_P and C_V are the specific heats at constant pressure and volume, and are respectively 14,401 and 10,18 KJ/kg°K.

$$K = \frac{C_P}{C_V} = \frac{C_P}{C_P - R} = 1,405 \quad (2.7)$$

The specific work of the compressor is expressed in kWh/kg°K. To do this, the conversion from KJ to kWh is used, which is 0,0002777778 kWh/KJ. To calculate the outlet temperature of compressed hydrogen, the formula 2.8 has been used:

$$T_{OUT} [^{\circ}K] = T_{IN} + \frac{W_C}{C_P} \quad (2.8)$$

By knowing the specific consumption of the compressor, the total energy consumed is divided by the annual hours and the capacity factor of the electricity mix to calculate its power. The table 2.12 shows the results of energy consumed and compressor capacity for the different cases analysed.

<i>Option</i>	<i>Scenario 1</i>	<i>Scenario 2</i>
<i>Specific Compressor Work [KJ/Kg]</i>		
<i>Alkaline</i>	4.496	4.496
<i>PEM</i>	4.234	4.234
<i>Specific Compressor Work [KWh/Kg]</i>		
<i>Alkaline</i>	1,25	1,25
<i>PEM</i>	1,18	1,18
<i>Outlet Temperature [°C]</i>		
<i>Alkaline</i>	382	382
<i>PEM</i>	344	344
<i>Total Electricity Consumption [MWh]</i>		
<i>Alkaline</i>	298.455	730.846
<i>PEM</i>	281.060	688.250
<i>Power Plant [MW]</i>		
<i>Wind Energy (CF 54%) + Alkaline</i>	63	154
<i>Wind + Grid Energy (CF 100 %) + Alkaline</i>	34	83
<i>Wind Energy (CF 54%) + PEM</i>	59	145
<i>Wind + Grid Energy (CF 100 %) + PEM</i>	32	78

Table 2.12: Specific compression work, electricity consumption and compressor power for different scenarios

The table 2.12 illustrates that the configuration with the alkaline electrolyser requires slightly more compression work than the PEM, this is due to the higher inlet temperature. The output temperature in the alkaline configuration is also higher than PEM configuration. The energy consumed and the compressor power are similar in alkaline and PEM configurations, while they change depending on the energy supply case, being almost double in case of wind energy compared to energy mix configuration.

The calculated specific work values are similar to the ones found in the literature. The paper (Grouset et al., 2019) uses a very similar formula, and obtains slightly higher results than this work, but totally in alignment. The paper (Tractebel Engineering & Inicio, 2017) also obtains specific work values congruent with the results obtained in this work. The work to compress hydrogen from atmospheric pressure up to 200 bar in the Tractebel is estimated to be 5 kWh/kg, very similar to the value calculated by the previous formula of 5,83 kWh/kg.

2.3.6 Hydrogen storage buffer

The hydrogen buffer is engineered to ensure the continuity of ammonia synthesis in the absence of energy from the wind power plant. Its purpose is to decouple the production of hydrogen, which is strongly linked to wind power, from the production of ammonia, which on contrast is characterised by continuous operation, guaranteed by total grid integration. The sizing of the buffer is linked to the choice of grid use as integration to renewable energy.

The hydrogen gas tank is placed after the compressor in the production chain, where the hydrogen is compressed to a pressure of 200 bar, which is necessary for the synthesis of ammonia in the Haber-Bosch process. The hydrogen leaving the tank is mixed with nitrogen at a pressure of 200 bar and is fed into the synthesis plant. Compressed hydrogen tank does not require energy.

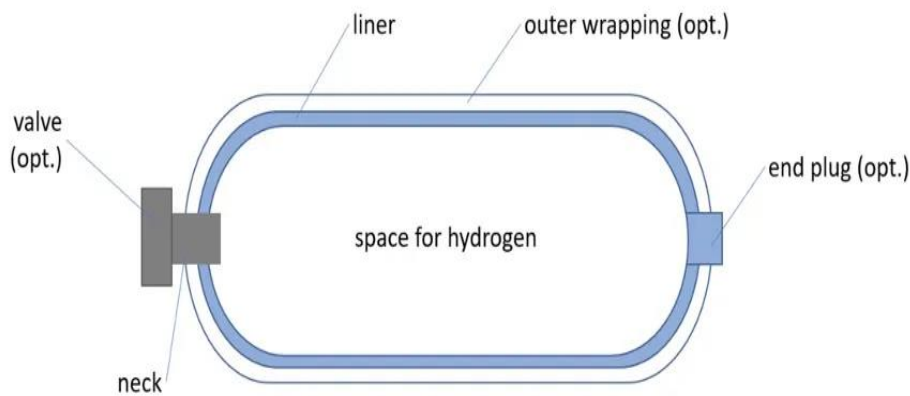


Figure 2.4: Compressed hydrogen storage tank (Hyfindr)

The compressed hydrogen tank consists of a liner, which holds the hydrogen inside the tank. An outer cover creates a layer of thermal insulation. Hydrogen is inserted into and withdrawn from the tank using a valve in the tank neck (Hyfindr).

The sizing of the storage tank has been done considering the hourly capacity of the electrolyser, and the equivalent hours of energy supply, which can be found by multiplying the capacity factor of electricity by the annual hours.

$$h_{eq} = 8760 * CF_{el} \quad (2.9)$$

The average hours of energy absence are calculated by subtracting the equivalent hours from the total hours of the year and assumed to be constant over that period.

$$h_{NO\,el} = \frac{8760 - h_{eq}}{365} \quad (2.10)$$

An oversizing factor of 200 % of the average number of hours when no electricity is supplied has been considered to ensure that the peak hours of non-production are covered. The size of the plant is such that it covers hydrogen production for a total of hours equal to twice the average hours of no energy supply. This calculation has been carried out in the absence of a historical record of wind power production trends in the province of Chubut.

$$Tank\ size\ [kgH_2] = h_{NO\,el}[h] * 200\% * Hydrogen\ flow\ rate\ \left[\frac{kgH_2}{h}\right] \quad (2.11)$$

From this formula, it is possible to find the tank capacity to cover twice the daily average number of hours of no hydrogen production. The table 2.13 shows the storage hours and tank size according to capacity factor, also an intermediate case of 21 % grid integration has been considered to show how the tank size vary with respect to the capacity factor.

<i>Option</i>	<i>Scenario 1</i>	<i>Scenario 2</i>
<i>Hours of Storage [h]</i>		
<i>CF 54 %</i>	22,08	22,08
<i>CF 75 %</i>	12	12
<i>CF 100 %</i>	0	0
<i>Tank Size [tonH₂]</i>		
<i>CF 54 %</i>	1102	2698
<i>CF 75 %</i>	431	1052
<i>CF 100 %</i>	0	0

Table 2.131: Hours of storage and tank size based on capacity factors

As shown in the table 2.13, the capacity factor is very relevant for the sizing of the storage tank. Grid integration decreases the capacity of the reservoir to zero in the case of full integration, with a capacity factor of 100 %.

The tank is well insulated, but there are heat losses due to convective exchange with the walls, resulting in a slight decrease in temperature. A temperature decrease rate of 0,5 °C per hour of storage has been assumed.

2.3.7 Cryogenic air separation unit

For the synthesis of ammonia, nitrogen must be produced. Ammonia consists of 17,75 % hydrogen by weight and 82,25 % nitrogen, which means that in scenario 1, the demand for nitrogen is 1.051.902 tonnes per year, while in scenario 2, it increases to 2.275.861 tonnes.

To produce nitrogen, which is extracted from the air, the cryogenic separator has been chosen, which is commercially developed for large plants and guarantees a very high purity of N₂ and high volumetric flow rates. In addition, the cryogenic separator has lower energy consumption than PSA technology, which is used for applications that do not require very high purity standards, as ammonia synthesis does. The operation of the cryogenic separator is explained in the introduction chapter.

In the production process evaluated in this work, the ASU works continuously, as there is no intermediate nitrogen buffer. This choice allows cost savings in storage and allows a smaller separation plant to be dimensioned. The drawback of this choice are the indirect CO₂ emissions related to energy from the grid. The electrical capacity factor for ASU is always 100 %.

The sizing of the cryogenic separation unit is calculated considering the availability of the plant. Assuming that there is an average of 14 days when the plant does not operate due to technical failures or preventive maintenance, the plant availability is 96 %, and coincides with the total capacity factor. By dividing the total nitrogen produced in the year by the total capacity factor and the annual hours, it is possible to calculate the hourly capacity of the plant, as explained by formula 2.4.

Cryogenic ASU consumes electricity and uses refrigerants to lower the air temperature and reach the boiling points of nitrogen, oxygen, and argon, which are 77,4 °K, 90,2 °K and 87,3 °K respectively. The specific consumptions reported in the literature give a large range of results, as cryogenic distillation plants have different configurations depending on the final product, which can be oxygen, nitrogen or both. The paper (Young et al., 2021) carried out a technical-economic analysis of a cryogenic ASU with the purpose of producing both nitrogen and oxygen. The specific consumption of this plant is 1,45 kWh/kgN₂ produced. The paper (Becker et al., 2015) reports that the consumption of existing industrial air separation plants used in the ammonia synthesis process varies between 0,15 and 0,25 kWh per m³ of N₂ produced at a pressure of 8 bar. Considering that the density of nitrogen gas under these conditions is 1,251 kg/m³, the specific consumption varies between 0,12 and 0,20 kWh/kgN₂. The paper (Nayak-Luke et al., 2021) claims that the electricity demand of an air separation unit (ASU) largely

depends on the plant size and the degree of refrigeration recovery, leading to a range of 0,5-0,8 kWhel per kgN₂. The paper (Cesaro et al., 2021) adopts an electricity consumption value equal to 0,119 kWh/kgN₂. In this work, an average value of 0,4 kWh/kgN₂ to produce nitrogen at the pressure of 8 bar has been chosen.

The table 2.14 shows the daily capacity values, total energy consumption and power output of the ASU plant for the different scenarios.

<i>Option</i>	<i>Scenario 1</i>	<i>Scenario 2</i>
<i>ASU Plant Capacity [tonN₂/day]</i>	2.997	7.339
<i>Total Electricity Consumption [GWh]</i>	421	1.030
<i>ASU Plant Power [MW]</i>	50	122

Table 2.14: Plant capacity, annual electricity consumption and plant power for both scenarios

In this case, the capacity factor does not affect the plant sizing and consumption parameters, as it is fixed at 100 %. The decision to fully integrate the electricity grid for the ASU is due to the fact that this plant, unlike electrolysis, consumes low amount of electricity, and emissions are contained, in return for significant cost savings due to the undersize of the ASU and the non-use of the intermediate nitrogen buffer.

2.3.8 Nitrogen compressor

To mix the syngas, hydrogen and nitrogen must be at the same pressure of 200 bar. For the compression of nitrogen, an air compressor can be used, as air is approximately 79 % nitrogen, the molecular weight and density of the two gases are very similar and do not cause problems in operation. There are two main types of air compressors, centrifugal compressors, where the compression is related to the speed of rotation of the compressor, and positive displacement compressors, which perform mechanical compression, often using pistons. In this work, the use of a centrifugal compressor has been considered. Its main characteristic is the discharge pressure that increases in relation to the increase in the rotational speed, while the air flow remains constant and independent of the speed. They are normally multi-stage. The centrifugal compressor consists of a bladed disc called impeller, set into rotation at high speed. Due to the centrifugal force imparted by the impeller, air is drawn in from the centre of the impeller and accelerated radially with a certain increase in dynamic pressure. The air, once it leaves the impeller, is conveyed into a diffuser consisting of diverging channels, which forms the stator part of the machine, which converts kinetic energy into pressure energy (Fang et al., 2014).

To calculate the specific energy of the compressor, the same formula of the hydrogen compressor has been used.

$$W_C \left[\frac{kJ}{kg} \right] = \frac{c_{pN_2} * T_{in}}{\eta_{is}} * \left(\beta^{\frac{k-1}{k}} - 1 \right) * \frac{1}{\eta_{el}} \quad (2.12)$$

The specific heat of nitrogen is 1,04 KJ/kg°K, while the specific heat ratio k is 1,41. The inlet temperature of the compressor is 298 °K, the compression ratio is 25, the inlet and outlet pressure are 8 and 200 bar respectively. The isentropic efficiency of the compressor is equal to 80 %, while the electrical efficiency is 0,95. The calculated specific work is 601 KJ/kg, which is equivalent to 0,17 kWh/kg, much lower than the compression work of hydrogen, this is due to the lower specific heat and lower inlet temperature.

The nitrogen outlet temperature is calculated using the formula 2.13, and is 876 °K, or 603 °C.

$$T_{OUT} [°K] = T_{IN} + \frac{W_C}{C_p} \quad (2.13)$$

The hourly capacity of the compressor is calculated by dividing the annually compressed nitrogen by the annual hours and the total CF, which in this case corresponds with the compressor availability, assumed to be 96 %. The compressor power is calculated by dividing the energy consumed by the total CF and the number of annual hours. The table 2.15 shows the compressor capacity, annual energy consumption and power.

<i>Option</i>	<i>Scenario 1</i>	<i>Scenario 2</i>
<i>Compressor Capacity [tonN₂/h]</i>	125	306
<i>Total Electricity Consumption [GWh]</i>	185	452
<i>Compressor Power [MW]</i>	22	54

Table 2.15: Compressor capacity, electricity consumption and power, for both scenarios

The nitrogen compressor is not influenced by the capacity factor, which is 100 %, due to the total integration of the grid with wind power. The energy required to compress nitrogen is much lower than the energy used to compress hydrogen, this is reflected in a small power of the compressor, 22 MW in the first scenario and 54 MW in the second one.

2.3.9 Ammonia synthesis plant

The ammonia synthesis plant receives inlet syngas, consisting of 17,75 wt% H₂ and 82,25 wt% N₂, at certain pressure and temperature conditions. The inlet pressure of the syngas is 200 bar, while the inlet temperature is calculated using the following formula, where MW indicates the molar weight and T indicates the temperature.

$$T_{SYNGAS} [^{\circ}C] = \frac{MW_{N_2} * T_{N_2} + MW_{H_2} * T_{H_2}}{MW_{N_2} + MW_{H_2}} \quad (2.14)$$

The temperature of N₂ is 603 °C, the temperature of H₂ varies depending on the electrolyser chosen. If the PEM electrolyser is used, the temperature of the hydrogen leaving the storage tank is 344 °C, which leads to a syngas temperature of 557 °C, while with the alkaline electrolyser, the hydrogen temperature rises to 371 °C, which results in a syngas temperature of 561 °C.

The amount of syngas entering the Haber-Bosch plant is equal to the sum of hydrogen and nitrogen. In scenario 1, the total syngas synthesised annually amounts to 1.278.908 tonnes, while in the second scenario, 3.131.746 tonnes. The total losses of the production process have been considered in the synthesis phase, as this is the most inefficient process, and they are supposed to be 2 %. This is due to the fact that at each synthesis cycle only 20 % of syngas is converted to ammonia, due to thermodynamic limitations (Osman et al., 2020), and the syngas recirculation process results in mass losses.

The design of the synthesis plant is based on the assumption of continuous operation. This choice is due to the technological limitation of the Haber-Bosch process, which is not suitable for alternating or low-load operation (Cheema & Krewer, 2018). Continuity of production is ensured by the total integration of the grid to the wind power, which increases the capacity factor by up to 100 %. A 14 days plant shutdown for preventive maintenance and technical faults have been considered. The plant availability is 96 %, which corresponds to the total capacity factor. The hourly capacity of the plant is calculated by dividing the annually produced ammonia by the total CF and the annual hours, as explained in formula 2.4.

The synthesis process takes place in the presence of an iron catalyst that can increase the reaction speed by increasing the conversion per step of the ammonia synthesis cycle. If the activity of the catalysts is sufficiently high, ammonia synthesis can be achieved at lower temperatures and pressures, with higher overall energy efficiency. Iron catalysts are the most used for ammonia synthesis. These catalysts are derived from iron oxides, of which there are three types, that are Fe₂O₃, Fe₃O₄ and Fe₁xO, known as hematite, magnetite and wüstite respectively (Humphreys et al., 2021). Usually, the weight percentage of the catalyst is around 2-10 %. In this thesis work, the minimum value was used, 2 wt. %, as the reaction takes place at high temperatures and pressures.

At each synthesis cycle there is a small pressure drop in the syngas, which according to (Morgan, 2013) is 6 % of the inlet pressure, in this case 12 bar. It is then necessary to recompress the syngas by means of a compressor to bring it back to the ideal synthesis conditions. The specific work of compressing the syngas is found using formula 2.12. The specific heat ratio is 1,4 while the compression ratio is very low at 1,06. The isentropic and electrical efficiencies are the same as those used for other compressors. The specific heat of the syngas is calculated using the formula 2.15, and is 3,41 KJ/Kg°K.

$$C P_{SYNGAS} \left[\frac{KJ}{Kg^{\circ}K} \right] = \frac{C P_{N_2} * M W_{N_2} + C P_{H_2} * M W_{H_2}}{M W_{N_2} + M W_{H_2}} \quad (2.15)$$

The specific work of compressing syngas is 67,36 KJ/kg, equivalent to 0,02 kWh/kg.

To calculate the total energy used to recompress the syngas, the formula 2.16 has been used, which considers the syngas conversion factor per cycle of 20 %.

$$Power\ Consumption\ [kWh] = \frac{W_c \left[\frac{kWh}{kg} \right] * Total\ Syngas\ Synthetised\ [kg]}{Conversion\ Rate\ [%]} \quad (2.16)$$

The NH₃ synthesis reaction is exothermic, which means that it releases an amount of heat equal to 2,6 MJ per kg NH₃ produced (Ikäheimo et al., 2018), which corresponds to 0,722 kWh_{th}/kg NH₃, calculated using the conversion factor 3,6 MJ/kWh. The amount of heat produced annually at the synthesis temperature of ammonia has been calculated. In this work, the heat produced is considered as loss, but can potentially be used to produce steam in a Rankine cycle for electricity production, or it can be used for heating fluids needed in other industrial processes in the port. The ammonia leaving the Haber-Bosch plant is at a pressure of 140 bar and a temperature of 25 °C. The table 2.16 provides the values of the parameters discussed above.

<i>Option</i>	<i>Scenario 1</i>	<i>Scenario 2</i>
<i>Annual NH₃ Produced [ton]</i>	1.253.831	3.070.339
<i>Plant Capacity [ton/h]</i>	149	364
<i>Total Catalyst Used [ton Fe₃O₄]</i>	25.077	61.407
<i>Annual Electricity Used [GWh]</i>	119	291
<i>Total Heat Produced [GWh_{th}]</i>	906	2217
<i>Plant Power [MW]</i>	14	34,5

Table 2.16: Technical data of Haber-Bosch synthesis plant for both scenarios

The synthesis plant has a big capacity, in the second scenario it exceeds 360 tonnes per hour, while the synthesis process is low in energy, as the only source of electricity is to recompress the syngas after each synthesis cycle, so the power of the plant is also small. This partly explain

the choice to feed the plant with an energy mixture of wind and grid. The process produces large amounts of heat, which could be used in other industrial or civil applications.

2.3.10 Ammonia liquefaction and storage

After being produced in the Haber-Bosch process in gaseous form, ammonia must be stored in liquid form, prior to transport by shipping. The liquid ammonia storage plant is complex. The diagram 2.5 shows the process of liquefaction and storage of ammonia, which liquefies at a temperature of $-33\text{ }^{\circ}\text{C}$ and a pressure of 1 bar. Under these conditions, its density is $681,9\text{ kg/m}^3$. As explained in the paper (Gezerman, 2015), the storage plant requires dedicated equipment, including a multi-stage compressor, a condenser, a flash tank heat exchanger and storage tanks made of cryogenic materials.

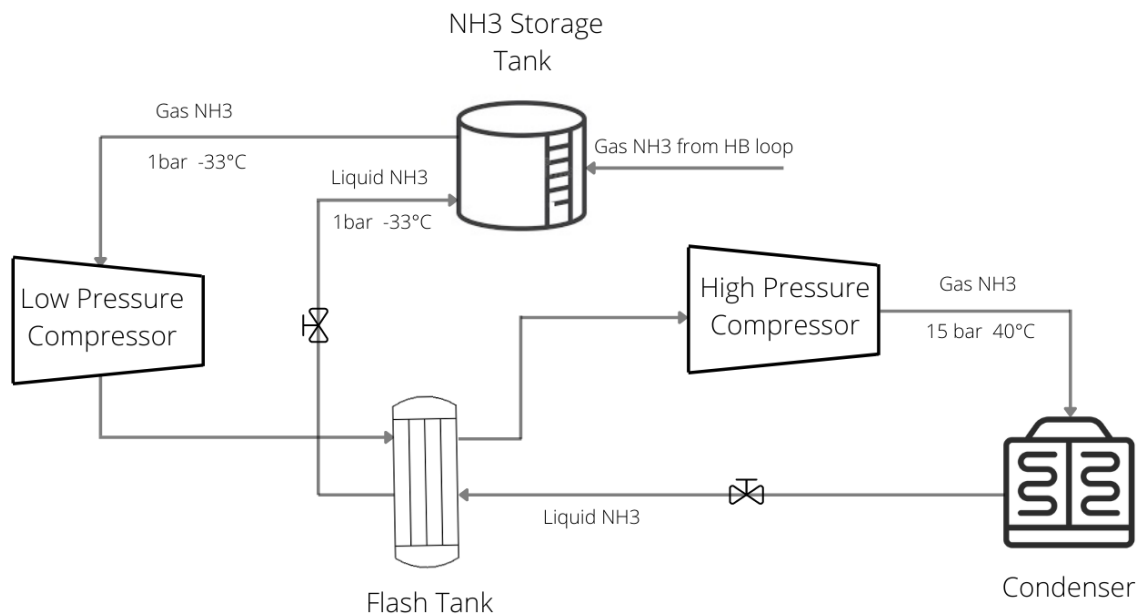


Figure 2.5: Ammonia refrigeration cycle and cryogenic storage (the Author)

The ammonia exits the synthesis circuit at a pressure of 140 bar and a temperature of $25\text{ }^{\circ}\text{C}$. It then enters the storage tank, where it expands to atmospheric pressure and is cooled by a two-stage ammonia refrigeration circuit. After filling the tank, the boil-off vapour is continuously cooled by the refrigeration system.

The boiling ammonia vapour is first compressed to an intermediate pressure of approximately 4 bar before flowing into a flash tank for cooling. A second-stage compressor further compresses the gas to a pressure that allows the ammonia to condense in the air-cooled

condenser. The condensed ammonia enters the flash tank, expands, and is separated into liquid and vapour. The vapour passes back through the second stage and the liquid at the bottom of the flash tank is sent back to the storage tank where it expands at tank pressure (Bartels, 2008). The specific energy required by the liquefaction plant is 0,0378 kWh/kgNH₃, according to the paper (UMAS, 2020), and multiplied by the ammonia stored annually plus the amount of ammonia that evaporates, the electricity consumed annually by the plant can be calculated. The ammonia stored annually in the port of Comodoro Rivadavia is 1.253.831 tonnes in scenario 1, while it rises to 3.070.399 tonnes in scenario 2. The ammonia flow rate entering the storage tank is 3.572 tonnes/day in scenario 1 and 8.747 tonnes/day in scenario 2. It is possible to choose the tank capacity and number of units, to decide the total amount of ammonia that can be stored, to ensure a minimum of 20 days of storage two cylindrical tanks with a capacity of 50.000 tonnes have been chosen in scenario 1, and 4 tanks of the same capacity in scenario 2; guaranteeing 28 and 23 days of storage respectively, in case serious problems or damages in the hydrogen and ammonia production chain.

The NH₃ vaporisation during the storage period occurs for the Boil-Off phenomenon, that can be calculated starting from the amount of heat exchanged between the fluid and the tank, using the following formula (Morgan, 2013).

$$Q [W] = U * A * \Delta T \quad (2.17)$$

U represents the Heat Transfer Coefficient, and in this case is 0,32 W/kg°K, A is the internal surface area of the tank, assumed to be cylindrical in shape with a diameter/height ratio of 0,75, and ΔT is the temperature difference between the fluid and the environment. The area of cylindrical tank is calculated as below.

$$A_{tank} = 2 * \pi * \frac{d}{2} * h + 2 * \pi * \frac{d^2}{4} \quad (2.18)$$

D represents the diameter of the tank, while h is the height. The ambient temperature has been assumed to be 10 °C. Heat Q is calculated in Watts, and is converted to KJ/s through the formula 2.19.

$$Q = W * 0.001 \left[\frac{KJ}{s * W} \right] \quad (2.19)$$

By obtaining the heat in KJ/s, it is possible to calculate the amount of ammonia that evaporates by dividing the heat transferred by the heat of vaporisation of the ammonia, which is ΔH = 1370 [KJ/kg].

$$NH3_{vap} = \frac{Q}{\Delta H} \left[\frac{kg}{s} \right] \quad (2.20)$$

NH_{3vap} is then multiplied by the total time of storage, to calculate the total amount of ammonia that evaporates inside a tank during the storage period.

The Boil-Off percentage is calculated using the formula 2.21, where NH_{3tot} represents the amount of total ammonia that is present inside the tank, and NH_{3vap} is referred to NH₃ vaporized in one day.

$$BoilOff = \frac{NH_3vap}{NH_3tot} [\%] \quad (2.21)$$

Finally, the total ammonia that evaporates annually during the storage phase is calculated by multiplying ammonia vaporized during a day of storage for the annual days. The evaporated ammonia is not lost, but is fed back into the refrigeration cycle and liquefied. The table 2.17 shows the main ammonia storage data for both scenarios.

<i>Option</i>	<i>Scenario 1</i>	<i>Scenario 2</i>
<i>Annual NH₃ Stored [ton]</i>	1.246.124	3.054.923
<i>Tank filling rate [ton/h]</i>	3.550	8.703
<i>Capacity of tank [ton]</i>	50.000	50.000
<i>Number of tanks</i>	2	4
<i>Days of storage ensured [d]</i>	28,2	23
<i>Heat Transfer Q [W]</i>	134.635	134.635
<i>Daily NH₃ Evaporated per tank [kg]</i>	8491	8491
<i>BoilOff [%/d]</i>	0,02%	0,02%
<i>Annual Ammonia Evaporated [kg]</i>	6.198.304	12.396.609
<i>Annual Energy Consumption [GWh]</i>	47,6	116,5
<i>Power Plant [MW]</i>	5,6	13.8

Table 2.17: Technical and energetic results for storage and refrigeration cycle, scenarios 1 and 2

The Boil-Off percentage is 0,02 %, slightly lower than the values found in the literature. (UMAS, 2020) speaks of a Boil-Off of 0,1 %, (Nayak-Luke et al., 2021) estimates a Boil-Off ranging between 0,03 % and 0,1 %. (Bartels, 2008) estimates a Boil-Off of 0,1 %. The Boil-Off causes the yearly evaporation of about 6.200 tonnes of NH₃ in scenario 1 and 12.400 tonnes in scenario 2.

2.4 Ammonia transportation and cracking

The ammonia transport, storage and reconversion chain include the NH₃ storage facility, which is part of the terminal infrastructure of the port of departure, in which there is also the

ammonia pumping plant from the storage tanks to the vessel docked at the quay, which must guarantee the stability of the vessel during the entire loading operation. In addition, the terminal is characterised by the technical and logistical support infrastructure that guarantees its functionality. In the transport phase, vessels are considered for ocean navigation, arriving at the final port, where an unloading terminal is present, having a similar structure to the loading one. The arrival port is characterised by the presence of the ammonia cracking plant, which separates the molecule of NH_3 obtaining hydrogen, which is purified in the hydrogen purification plant, and then sent as a product to the reduced iron production plant. The picture 2.6 illustrates all the steps of the transport chain.

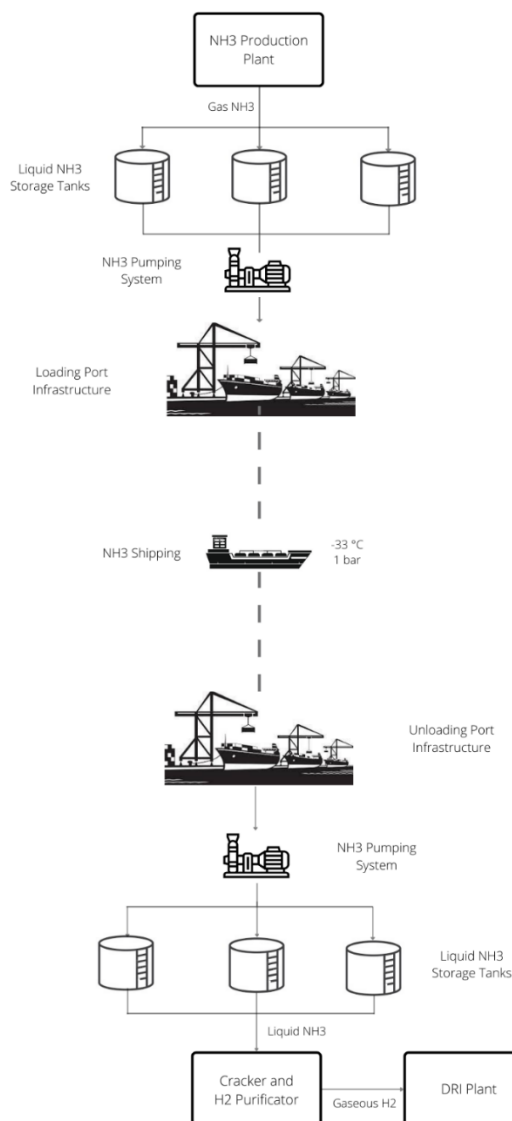


Figure 2.6: NH_3 storage, transport, and reconversion supply chain (the Author)

The ammonia transport process is long and complex, requiring significant infrastructures in the loading and unloading terminal, and logistical management to ensure a perfect connection

between the ammonia production part and the hydrogen utilisation part, which are more than 13.000 km distant. In the following sections, the operation, design, and energy required for all infrastructures and processes that are part of the transport chain will be discussed.

2.4.1 Loading terminal

Terminal facilities include piers and docks with articulated loading or unloading arms for the transfer of ammonia between ship and land. The docks must be equipped to accommodate ships of more than 250-300 m in length. It also includes pipelines used to transport NH₃ between the terminal's storage and processing facilities and the loading arms, the NH₃ is pumped through cryogenic pump system. The NH₃ is maintained at about -33 °C to keep it in a liquid state. The loading/unloading arms and pipes are insulated to prevent heat build-up from the air and minimise ammonia vaporisation. A specialised work jetty is designed for loading and unloading liquefied ammonia to and from ships and onshore tanks. There are support infrastructures necessary for the processes of entry/exit of the ship from the port, berthing of the ship at the quay, as well as logistics co-ordination offices, which manage and follow all ship loading operations.

The design and consumption analysis of the ammonia liquefaction and cryogenic storage plant are addressed in section 2.3.10. The other energy-intensive plant in the loading terminal is the cryogenic pumping system, which is responsible for moving liquid NH₃ from the storage tank to the vessel's tanks. The formula 2.22 has been used to calculate the pump power.

$$P \text{ [kW]} = \frac{q \left[\frac{\text{m}^3}{\text{h}} \right] * \rho \left[\frac{\text{kg}}{\text{m}^3} \right] * g \left[\frac{\text{m}^2}{\text{s}} \right] * h [\text{m}] * p [\text{Pa}]}{\eta * 3600000} \quad (2.22)$$

The power is calculated in kW, depending on the hourly volume flow q , which according to the paper (Ishimoto et al., 2020) is 3.800 ton/h, which equals 5.573 m³/h, knowing that the density of liquid NH₃ ρ is 681,9 kg/m³. The gravity acceleration g is equal to 9,81 m/s, the pump head h has been assumed to be 0,1 m, and the pumping pressure p is equal to 100.000 Pa. The energy efficiency of the pump η has been assumed to be 0,9.

The calculated pump power is 115 MW. By dividing the power by the hourly flow rate of 3.800.000 kg/h, the specific energy consumption of the pumping plant can be calculated, which is 0,0303 kWh/kg ammonia. The specific energy consumption of all other loading processes has been assumed to be 30 % of the energy required for pumping. This means that the specific energy consumed in the loading terminal is 0,0394 kWh/kgNH₃.

The total specific consumption of the terminal, considering the liquefaction plant, which requires a consumption of 0,0378 kWh/kg, the pumping plant and auxiliary operations is 77,2 kWh per tonne NH₃, very close to the value given in the paper (Ishimoto et al., 2020), which reports a specific terminal consumption of 80 kWh/kgNH₃.

The annual energy consumed by the loading terminal is 49 GWh in scenario 1 and 121 GWh in scenario 2.

2.4.2 Oceanic transport

Liquid ammonia can be transported under different conditions. It can be pressurised to about 8 bar at room temperature or cooled to -33°C at ambient pressure. The most widely used option for ship transport is the second, because pressurised storage is not suitable for high volumes. By increasing tank capacity, pressurised storage requires large quantities of steel, which increases the weight of the ship and the transport costs (International Renewable Energy Agency (IRENA), 2022).

The ocean transport of ammonia currently takes place using LPG tankers, because the design conditions for storing ammonia and LPG are similar due to their boiling points that are respectively -33 °C for NH₃ and -42,1 °C for LPG. In accordance with the paper (Seo & Han, 2021), three different vessel sizes have been considered, depending on the total amount of ammonia stored. The ship dimensions are related to the cargo capacity that can be 84.000 m³, 60.000 m³ or 24.000 m³. The vessel's loading capacity is 94 % of the total capacity, due to a 98 % fill limit at the supply entrance, to avoid overpressure in the tank, and a remaining heel in the tank at the demand entrance of 4 % (Salmon et al., 2021).

Cargo ships currently have internal combustion engines using marine diesel, also called HFO, as fuel, which is characterised by a lower heating value of 40,9 MJ/kg, and specific emissions of 3,21 kg of CO₂ per kg of HFO burned (Winnes & Fridell, 2009). In this work has been considered the use of internal combustion engines with NH₃ as fuel, which are at an advanced stage of development, so much so that the company MAN has recently launched its first two-stroke ICE prototype on the market. Ammonia has a lower LHV than HFO, at 18,6 MJ/kg, but does not cause CO₂ emissions during its combustion. However, it is necessary to use a small percentage of HFO as a pilot fluid to increase the flammability of ammonia, which according to (Seo & Han, 2021) is 3 %.

For ocean transport, two types of losses must be taken into account, the evaporated NH₃ by Boil-Off, and the ship's fuel consumption, which in the case of this work is ammonia (J. Kim et al., 2022). Ammonia used as fuel is considered as a loss in the chain. Boil-Off is mainly generated by the temperature difference between the cargo and the atmosphere. The release of BOG into the atmosphere results in a loss of energy, so it is necessary to re-liquefy the gas, but in this work, the ammonia evaporated during transport is considered as loss.

- Shipment duration and calculation of required vessels

The total duration of the shipping is divided in four steps. After the loading process, the ocean transport of the ship takes place to the port of arrival, where the ship stops for the ammonia unloading. The vessel is then ready to return to the port of departure unloaded.

The loading time is calculated considering the capacity of the ship, which is 94 % of the total capacity, and the flow rate of the pumping system that transfers the liquid ammonia from the storage tanks to the vessel tanks, which is 5.573 m³/h. The formula for calculating the loading time is:

$$\text{Loading Time [h]} = \frac{\text{Ship Capacity [m}^3\text{]}}{\text{Pump Volumetric Flow Rate } \left[\frac{\text{m}^3}{\text{h}} \right]} \quad (2.23)$$

The total time the ship spends in the port, considering the phase of entry, mooring, preparation for loading and exit from the port has been estimated to be 50 % more than the loading phase. The distance between the port of Comodoro Rivadavia and the port of Taranto has been calculated using the website 'classic.searoutes.com', it is 7.226 nautical miles, which corresponds to 13.383 km. By setting the sailing speed, which for a cargo vessel can vary between 15 and 20 knots, the shipping time is calculated.

$$\text{Shipping Duration [h]} = \frac{\text{Maritime Distance [km]}}{\text{Ship Speed } \left[\frac{\text{km}}{\text{h}} \right]} \quad (2.24)$$

By setting the sailing speed to 17 knots, which corresponds to 31,5 km/h, the sailing time is 425 h. The unloading time in the arrival terminal is calculated using the same formula as in the loading terminal, while the return time is calculated using formula 2.24. It should be noted that the maritime distance of the outward voyage is slightly less than the return voyage, since in the latter case the route includes the passage through the Messina strait. The distance covered on the return travel is 13.399 km.

The total time needed for the transport is given by the sum of the four phases described. Knowing the total time, the yearly number of trips done by a ship can be calculated. By multiplying the carrying capacity of a ship by the number of trips made in a year, it is possible to calculate the annually amount of ammonia that can be transported by one vessel.

$$\text{Annual NH}_3 \text{ carried per ship [m}^3\text{]} = \text{ship capacity [m}^3\text{]} * \text{travels per year} \quad (2.25)$$

By dividing the total ammonia produced in the port of departure by the ammonia transported per ship per year, the number of ships needed to ensure transport can be calculated.

$$\text{Number of vessels} = \frac{\text{Annual NH}_3 \text{ Produced [m}^3\text{]}}{\text{Annual NH}_3 \text{ transported per ship [m}^3\text{]}} + 1 \quad (2.26)$$

The purchase of one ship over the minimum number has been considered to ensure continuity of transport during maintenance and repair operations. The table 2.18 shows the obtained results.

Option	Scenario 1			Scenario 2		
	Small Vessel	Medium Vessel	Big Vessel	Small Vessel	Medium Vessel	Big Vessel
Capacity	22.560	56.400	78.960	22.560	56.400	78.960
Ship Speed [knots]	17	17	17	17	17	17
Loading Time [h]	6,1	15,2	21,3	6,1	15,2	21,3
Transportation Time [h]	425,06	425,06	425,06	425,06	425,06	425,06
Unloading Time [h]	6,1	15,2	21,3	6,1	15,2	21,3
Transportation Time [h]	425,59	425,59	425,59	425,59	425,59	425,59
Total time [h]	862,79	881,01	893,15	862,79	881,01	893,15
Total time [d]	35,95	36,71	37,21	35,95	36,71	37,21
Number of trips per year	10	9	9	10	9	9
Annual NH ₃ transported per ship [m ³]	225.600	507.600	710.640	225.600	507.600	710.640
Minimum Number of Ships required	9	5	4	20	10	7

Table 2.18: Vessel ship duration, number of trips per year and required number of vessels needed, for small, medium, and big ship size

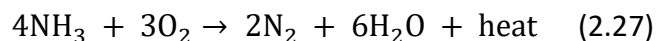
The duration of the transport depends exclusively on the speed of the ship, what changes is the duration of the loading and unloading phases, which increases as the capacity of the ship increases. The difference between using a small and a large vessel is slightly more than a day,

this means that the number of trips per vessel are similar whether using small or large vessels. There is a big difference between the total capacity of ammonia transported, which in the case of a large vessel is three times larger than when using a small vessel. This affects the number of ships needed to fulfil the shipping service, from 9 ships of 24.000 m³ capacity, to only 4 ships of 84.000 m³, in first scenario, while in second one the number of vessels required diminish from 20 of small size to 7 of big size. From a logistical point of view, without considering the economic aspect, the adoption of large or medium-sized vessels is convenient compared to the use of small vessels.

The time between one trip and the next has been calculated by dividing the total number of days in a year by the number of total trips made. In the case of large vessels, the time interval between one trip and the next is 13,5 days in scenario 1, and decreases to 6,76 days in scenario 2. Turning to small ships, the frequency of trips is 4,56 days in scenario 1 and 1,92 days in scenario 2. The logistical organisation of transport is also more complex by adopting small ships.

- Vessel fuel consumption and fuel tank design

The engines used for ship propulsion are two-stroke internal combustion engines. ICEs are thermal energy machines that convert the energy of fuels such as diesel and gas into mechanical energy through internal combustion. The ammonia ICE is a relatively new concept and has not yet been tested on full-scale ships. MAN Energy Solutions recently launched a prototype on the market (Altfeld & Pinchbeck, 2019). The ammonia combustion process follows the process described in the equation 2.27.



Fuel and air are the inputs to the combustion, which produces nitrogen, water, and heat.

NO_x emissions can be reduced with the exhaust gas after-treatment technology, which use the selective catalytic reduction system.

The ship's fuel consumption (FC) has been calculated by initially calculating the specific fuel consumption (SFC) of an ammonia-fuelled internal combustion engine. According to the calculations developed in the paper (Sophie & Ness, 2021), the SFC is:

$$SFC \left[\frac{\text{kg}}{\text{kWh}} \right] = \frac{1}{LHV \cdot \eta} \quad (2.28)$$

The LHV of ammonia is 18,6 MJ/kg, which is equivalent to 5,17 kWh/kg NH₃. Considering an engine efficiency of 48 % (J. Kim et al., 2022), the specific fuel consumption is 0,40 kg/kWh.

Knowing the specific fuel consumption, it is possible to calculate the fuel consumption, using a formula that links engine power P , with ship speed V , and specific fuel consumption (SFC).

$$FC \left[\frac{kg}{km} \right] = \frac{P * SFC}{V} \quad (2.29)$$

To use the above formula, it is necessary to calculate the power of the ship, correlating it with its deadweight and speed. the '*Formula dell'Ammiragliato*' has been used, which is developed as follows (Codegone, 1958).

$$P [HP] = \frac{D^{2/3} * V^3}{A} \quad (2.30)$$

Power is expressed in horse-power and is given by the experimental formula that correlates the deadweight of the ship raised to $2/3$ by the cube of the speed, expressed in knots. A is the admiralty coefficient, that for tankers varies between 600 and 750. In this work, an intermediate value of 675 has been considered. To calculate the deadweight of the ship, a net to deadweight ratio of 0,75 has been assumed, meaning that the weight of the cargo is equal to 0,75 the total weight of the loaded ship. The ship vessel has been set to 17 knots.

Given the ship's fuel consumption, measured in kg/km, to know the total fuel consumption of a ship per trip it is necessary to multiply FC by the total distance travelled by the ship for the round trip. The amount of fuel required is calculated in kg of NH_3 , and to convert this to m^3 it is necessary to divide by the density of ammonia, which is $681,9 \text{ kg}/m^3$. The tank capacity is dimensioned to hold 20 % more fuel than is needed. The formula 2.31 summarises the calculations described.

$$Tank Capacity [m^3] = \frac{FC \left[\frac{kg}{km} \right] * Round Trip Distance [km]}{NH_3 Density \left[\frac{kg}{m^3} \right]} * 1,2 \quad (2.31)$$

The annual ammonia used as fuel is calculated by multiplying the NH_3 burned in one trip, by the total number of trips done in the year to ensure the shipping service.

As explained above, the internal combustion engine uses a small percentage by weight of marine diesel as a pilot fuel. The sizing of the HFO tank, which is characterised by an LHV of $40,9 \text{ MJ}/kg$, and a density of $1010 \text{ kg}/m^3$, is calculated using the formula 2.32.

$$Pilot Fuel Tank [m^3] = \frac{3 \% * NH_3 Trip Consumption [kg]}{HFO Density \left[\frac{kg}{m^3} \right]} * 1,2 \quad (2.32)$$

The annual HFO needed is calculated by multiplying the HFO consumed by a vessel per trip, by the total number of trips made in the year. The table 2.19 shows the results of the calculations described in the section.

Option	Scenario 1			Scenario 2		
	Small Vessel	Medium Vessel	Big Vessel	Small Vessel	Medium Vessel	Big Vessel
<i>Cargo Ship Capacity [m³]</i>	22.560	56.400	78.960	22.560	56.400	78.960
<i>Deadweight [ton]</i>	20.512	51.279	71.790	20.512	51.279	71.790
<i>Ship Speed [knots]</i>	17	17	17	17	17	17
<i>Ship Power [MW]</i>	4	7,4	9,2	4	7,4	9,2
<i>Fuel Consumption [kg/km]</i>	51,4	94,6	118,4	51,4	94,6	118,4
<i>Round Trip Fuel Consumption [tons]</i>	1.376	2.534	3.172	1.376	2.534	3.172
<i>Fuel Tank Volume [m³]</i>	2421	4460	5582	2421	4460	5582
<i>Annual Fuel NH₃ Consumed [ton]</i>	110.072	91.240	85.638	261.422	205.290	171.275
<i>Percentage of Ammonia Consumed as Fuel</i>	8,5%	7,1%	6,7%	8,1%	6,5%	5,5%
<i>HFO Tank Capacity [m³]</i>	49,04	90,3	113,1	49,04	90,3	113,1
<i>Annual HFO Consumed [ton]</i>	3302	2737	2569	7843	6159	5138

Table 2.19: Ship power, NH₃ consumption, fuel tank size, HFO pilot fuel consumption, for small, medium and large size vessels

The table shows that the choice of vessel size influences the consumption of ammonia and HFO. At the same speed, the power of the ship increases as its weight increases, so the specific fuel consumption also increases, from 51 kg/km for small ships to 118 kg/km in large ships. Consequently, the fuel tank increases in capacity. The interesting result concerns the annual consumption of ammonia as fuel, which is much higher for small vessels than for large vessels. This is explained because although large vessels are characterized by higher specific fuel consumption, the number of annual trips and vessels involved is much lower, which saves large quantity of fuel and reduces transport costs. By choosing to use small vessels, the percentage of NH₃ wasted increases by 2% compared to the use of large vessels. A similar result is obtained

for pilot fuel. The adoption of large ships saves ammonia and decreases CO₂ emissions related to the combustion of marine diesel.

The calculated engine power is lower than the power used in the paper (Seo & Han, 2021), where a ship with a capacity of 84.000 m³ uses an engine of 16 MW, while in this study for a ship of the same size the calculated engine power is 9,2 MW. The paper (Sophie & Ness, 2021) gives an indication of the specific engine power of 36 KW/m³. Using this figure in the case study, for a ship with a capacity of 84.000 m³, with an engine size of 650 m³, the calculated engine power would be 23,4 MW. These results have not been considered, as they are experimental.

- Boil-Off calculation

The Boil-Off during the transport phase has been calculated using the same formulas as for the storage tank in the loading terminal. The shape and size of the transport tanks are different, as is the storage time, resulting in a slightly different Boil-Off percentage.

Unlike the ammonia evaporated in the storage plant, which was cooled in the liquefaction cycle and hence was not lost, the ammonia evaporated during the transport phase is considered as a leakage and is released from the tanks through escape valves. According to the paper (K. Kim et al., 2020), it would be possible to use the vaporised NH₃ as fuel for the ICE engine. This represents an interesting but currently undeveloped solution. A further option is to recycle the ammonia within a liquefaction process in the ship, but in this work, the vaporised NH₃ is considered as a loss.

The liquid ammonia is transported at a temperature below boiling point, -33 °C, and at ambient pressure. The utilisation of four parallelepiped tanks per vessel, all the same size, has been assumed. The height of the tanks is 18 m, and the ratio of the long side to the short side of the base is 2. The surface area is calculated using the formula 2.33.

$$A_{tank} = 2 * L * l + 2 * (L + l) * h \quad (2.33)$$

L and l represent the long and short sides of the base, while h is the height of the tank. The Heat Transfer Coefficient U and the Heat of Vaporization ΔH are the same adopted for the land storage tanks. The ambient temperature has been set to 10 °C. The table 2.20 shows the percentage of Boil-Off and NH₃ annually evaporated for each vessel size considered.

Option	Scenario 1			Scenario 2		
	Small Vessel	Medium Vessel	Big Vessel	Small Vessel	Medium Vessel	Big Vessel
<i>Cargo Ship Capacity [m³]</i>	22.560	56.400	78.960	22.560	56.400	78.960
<i>Number of Tanks</i>	4	4	4	4	4	4
<i>Capacity per Tank [m³]</i>	5.640	14.100	19.740	5.640	14.100	19.740
<i>Tank Height [m]</i>	18	18	18	18	18	18
<i>Tank's Surface Area [m²]</i>	1978,5	3704	4722,3	1978,5	3704	4722,3
<i>Total Vessel Length [m]</i>	120,2	190	224,8	120,2	190	224,8
<i>Heat Transfer Q [W]</i>	27.224	50.968	64.979	27.224	50.968	64.979
<i>NH₃ Evaporation Rate [kg/h]</i>	71,54	133,9	170,75	71,54	133,9	170,75
<i>Boil-Off [%/d]</i>	0,045%	0,033%	0,03%	0,045%	0,033%	0,03%
<i>NH₃ Evaporated per Round Trip [kg]</i>	121.629	227.712	290.312	121.629	227.712	290.312
<i>Annual NH₃ Losses [ton/year]</i>	9.730	8.198	7.838	23.110	18.445	15.677

Table 2.20: Total vessel length, NH₃ evaporation rate, NH₃ evaporated annually, for all the vessel size

The total length of vessels has been assumed to be 20 % longer than the total length of containers. It goes from a length of 120 m for small ships to a length of 225 m for larger ships, values in line with those of existing vessels, which can reach lengths of 250-300 m. The vaporisation flow rate increases as the size of the tanks increases, from 71,5 kg/h for small ships to 171 kg/h for large ships. The contrasting result concerns the calculated Boil-Off percentage, which decreases as the tank surface area increases, with the result that the annual ammonia lost through vaporisation drops from 23.110 tonnes with small vessels to 15.677 tonnes with large vessels in scenario 2, while in scenario 1 the annual BOG decreases from 9.730 ton/year with small vessels to 7.838 ton/year in big vessels. The calculated BOG percentage is in accordance with the values found in the literature, (J. Kim et al., 2022) uses a BOG percentage of 0,036 %. (Ishimoto et al., 2020) adopts a BOG of 0,2 %.

Also from the NH₃ transport losses, the choice of using large vessels is convenient compared to using small or medium-sized vessels, since the ammonia evaporated is lower.

- CO₂ emissions saving with respect the use of maritime diesel fuel

The amount of marine diesel that would be needed for oceanic transport has been calculated if standard ships were used, with an ICE engine propelled by HFO. An engine efficiency of 48 % (Sophie & Ness, 2021), and LHV of 40,9 MJ/kg has been taken into account for the calculation of the specific HFO consumption. The density of HFO is 1010 kg/m³. The SFC is 0,183 kg/kWh, which is lower than for ammonia. The engine power is the same as in the NH₃ case since it depends on the speed of the ship and its deadweight. The calculation of FC uses formula 2.29. The table 2.21 shows the results. The CO₂ emissions are calculated considering the specific consumption of the maritime diesel equal to 3,21 kgCO₂/kgHFO.

<i>Option</i>	<i>Scenario 1</i>			<i>Scenario 2</i>		
	<i>Small Vessel</i>	<i>Medium Vessel</i>	<i>Big Vessel</i>	<i>Small Vessel</i>	<i>Medium Vessel</i>	<i>Big Vessel</i>
<i>Cargo Ship Capacity [m³]</i>	22.560	56.400	78.960	22.560	56.400	78.960
<i>Vessel Power [MW]</i>	4	7,4	9,2	4	7,4	9,2
<i>Ship Speed [knots]</i>	17	17	17	17	17	17
<i>Fuel Consumption [kg/km]</i>	23,36	43,04	53,86	23,36	43,04	53,86
<i>Round Trip HFO Consumption [ton]</i>	626	1.153	1.442	626	1.153	1.442
<i>Fuel Tank Volume [m³]</i>	743	1369	1714	743	1369	1714
<i>Annual HFO Consumption [ton]</i>	50.057	41.493	38.945	118.886	93.359	77.890
<i>Annual CO₂ Emissions [ton]</i>	160.684	133.192	125.014	381.625	299.683	250.028

Table 2.21: Fuel consumption and CO₂ emission for HFO ship transportation, for all size vessels

The results in the table show that the specific fuel consumption is lower in the case of marine diesel, due to its higher calorific value. Consequently, the tank size is smaller than in the case of NH₃. The emissions produced annually exceed 120 tonnes in scenario 1, and 250 tonnes in scenario 2. The use of ammonia as fuel proves to be an environmentally friendly choice.

2.4.3 Unloading Terminal

Ammonia arriving in Italy is stored in the unloading terminal in the port of Taranto. The general structure of the terminal is very similar to that described for the departure terminal, it includes the storage and liquefaction facility for NH_3 , the system for pumping liquid ammonia from the ship to the land tanks, and the auxiliary infrastructure for docking and unloading operations. The main difference is that in the arrival terminal, the ammonia arrives already liquefied, and only the percentage of evaporated NH_3 must be reliquefied, this implies less energy expenditure in the storage phase.

The ammonia stored annually is less than the NH_3 at the departure terminal, this is due to losses of NH_3 as fuel and through evaporation during the transport phase. The ammonia flow from the tank to be converted into hydrogen required by the steelworks is 3346 tonnes per day in scenario 1 and 8315 tonnes in scenario 2. It is possible to select the size of each tank and the number of tanks used, to ensure a suitable storage duration, higher than 20 days. In scenario 1, if 2 storage tanks of 40.000 tonnes are used, the supply of ammonia is guaranteed for 23,9 days. In scenario 2, 4 tanks of 50.000 tonnes each are used, guaranteeing the supply of NH_3 for 24,1 days.

The Boil-Off calculation is the same as for the loading terminal, what changes is the ambient temperature, which is set at 20 °C in Taranto.

The specific consumption of the refrigeration system is 0,0378 kWh/kg NH_3 , and that of the pumping system is 0,0303 kWh/kg NH_3 . An energy over-consumption of 30 % is considered, because of the energy consumption of the terminal's auxiliary equipment. The total specific energy consumption of the unloading terminal is therefore 77,2 kWh/kg NH_3 . The electricity consumed at the arrival terminal is taken entirely from the electricity grid, which is responsible for an indirect CO_2 consumption of 312 g CO_2 /kWh (Qualenergia, 2019). The CF of electricity is 100 %. The table 2.22 shows the results obtained.

<i>Option</i>	<i>Scenario 1</i>	<i>Scenario 2</i>
<i>Annual NH₃ Storage [ton]</i>	1.160.355	2.883.387
<i>Daily NH₃ Cracker Demand [ton/day]</i>	3346	8315
<i>Storage Tank Capacity [ton]</i>	40.000	50.000
<i>Number of Storage Tanks</i>	2	4
<i>Day of Storage Ensured [day]</i>	23,9	24,1
<i>Boil-Off [%/d]</i>	0,02%	0,02%
<i>Annual NH₃ Evaporated [kg/year]</i>	6.583.755	15.279.541
<i>Annual Energy Consumption Refrigeration Process [kWh]</i>	248.866	577.567
<i>Annual Terminal Energy Consumption [kWh]</i>	45.672.881	113.493.320

Table 2.22: Storage Boil-Off, NH₃ evaporated and energy consumption in unloading terminal, scenarios 1 and 2

The Boil-Off percentage, calculated with a cylindrical tank shape, is equivalent to 0,02 %. In scenario 1 it is slightly higher because smaller tanks are used. The energy consumed annually for the re-liquefaction of the evaporated ammonia is only a small percentage of the total energy consumed in the loading terminal, while the energy consumed for pumping and discharging the ammonia is significant, amounting to 45,7 GWh in scenario 1 and 113,5 GWh in scenario 2.

2.4.4 Cracking and purification plants

The goal of this work is the production of hydrogen gas for the decarbonisation of a direct iron reduction plant. The ammonia transported and stored at the port of arrival is to be decomposed into hydrogen and nitrogen. The hydrogen obtained must then be purified to a high level of purity of more than 99,99 % using a PSA plant. The hydrogen conversion process is very inefficient, according to the paper (Ishimoto et al., 2020) only 69,5 % of the hydrogen contained in the incoming ammonia molecule is separated and purified as a final product. The figure 2.7 illustrates the decomposition and purification process.

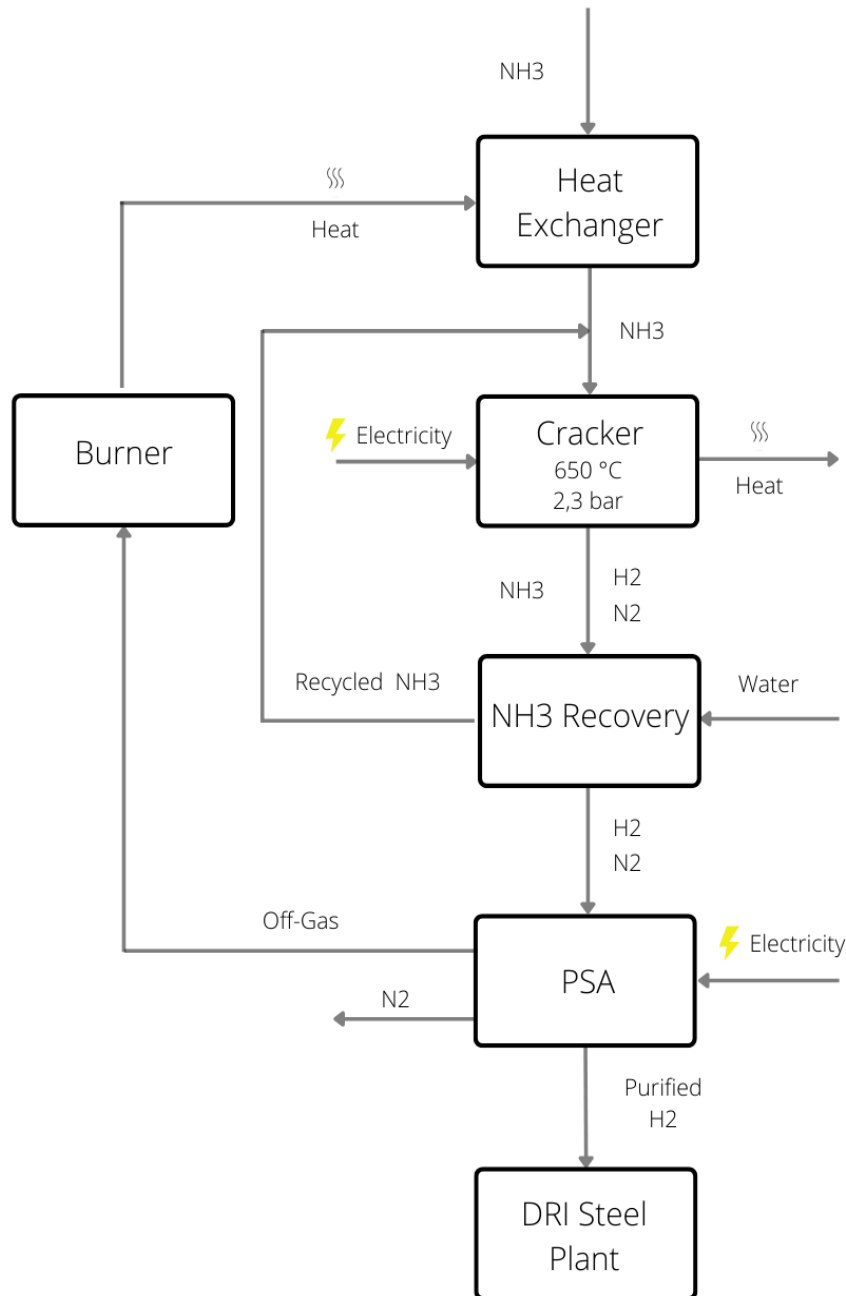
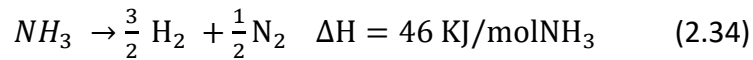


Figure 2.7: Ammonia cracking and hydrogen purification process (the Author)

The catalytic cracking of ammonia into hydrogen is about 98-99 % efficient at temperatures below 425 °C. At temperatures above 600 °C, ammonia starts to thermally decompose without the need for a catalyst. The ammonia conversion rate depends on temperature, pressure and the catalysts used. In this work the following process has been considered. After being pre-heated in a heat exchanger, the ammonia enters the cracker where the decomposition reaction of NH₃ into H₂ and N₂ takes place, at a temperature of 650 °C and a pressure of 2,3 bar, in the presence of a nickel-based catalyst (Makhloufi & Kezibri, 2021).



The reaction is endothermic. The heat required for decomposition is 2,7 MJ/kgNH₃, and is provided by a burner using part of the hydrogen leaving the PSA and residual NH₃ and N₂ (Alboshmina, 2019).

Before passing through the pressure swing adsorption plant, the stream exiting the cracker passes through an ammonia recovery plant, where the undecomposed NH₃ is separated from the H₂ and N₂ stream via a water absorption process and returns to the cracker to be decomposed. The PSA plant separates the nitrogen from the hydrogen stream to obtain a hydrogen stream with a purity of more than 99,99 %. Some of the hydrogen produced is sent to the burner where it produces the heat necessary for the cracking reaction.

The hourly capacity of the cracker has been calculated considering the ammonia decomposed annually and the plant's availability. A plant shutdown period of 14 days in a year has been assumed for preventive maintenance and repair of the plant due to possible breakdowns. The hourly flow of NH₃ entering the plant is found by means of the formula 2.35.

$$\text{NH}_3 \text{ Flow Rate } \left[\frac{\text{kg}}{\text{h}} \right] = \frac{\text{Annual NH}_3 \text{ Decomposed } [\text{kg}]}{\text{Plant Availability } [\%] * 8760 [\text{h}]} \quad (2.35)$$

To calculate the amount of hydrogen and nitrogen input, NH₃ must be multiplied by the weight percentage, which is 17,75 % H₂ and 82,25 % N₂. The efficiency of the cracker is 99 %. The mixture of N₂ and H₂ enters the PSA plant, where hydrogen and nitrogen are separated. The efficiency of the PSA plant is 75 % (Ishimoto et al., 2020). Part of the Off-Gas stream, consisting of 5,1 % H₂ and 94,9 % N₂ is directed to the burner, characterized by an efficiency of 90 %, to be combusted and provide the heat necessary to bring the ammonia to the temperature of 650 °C, at which it is decomposed in the cracker.

To calculate the amount of Off-Gas required for the endothermic reaction, the total heat required has been calculated according to the following formula.

$$\text{Total Heat } [\text{MJ}] = \text{Specific Heat } \left[\frac{\text{MJ}}{\text{kgNH}_3} \right] * \text{Total NH}_3 \text{ Decomposed } [\text{kg}] \quad (2.36)$$

The specific heat has been transformed by dividing the heat expressed in KJ/mol by the molar weight of ammonia, which is 17,03 g/mol. The specific heat required for the endothermic decomposition reaction is 2,70 MJ/kgNH₃.

To calculate the amount of Off-Gas, a mixture consisting of 5,1 wt% hydrogen and 94,9 wt% nitrogen is considered. Considering that the LHV of H₂ is 120 MJ/kg and that of nitrogen is null,

the LHV of the Off-Gas is calculated using the following formula and is equal to 6,14 MJ/kg of Off-Gas.

$$LHV_{OFFGAS} \left[\frac{MJ}{kg} \right] = \frac{LHV_{H_2} * \%_{H_2} + LHV_{N_2} * \%_{N_2}}{\%_{H_2} + \%_{N_2}} \quad (2.37)$$

The total amount of Off-Gas required is calculated by dividing the total heat required by the LHV of the Off-Gas. A burner efficiency of 90 % is considered.

The cracker mostly has a heat energy demand, which is satisfied by burning some of the hydrogen produced. The electrical energy consumed by the cracker is very low, at 0,002 kWh/kg ammonia (J. Kim et al., 2022). The paper (Nordio et al., 2021) analyses the processes and configurations of pressure swing absorption plants in detail. By varying the process configuration and the materials used for absorption, the paper classified 17 options, where the specific electricity consumption varies between 4 and 12 kWh/kg. The PSA system considered includes two membrane modules in series, the first operating at high pressure and the second at low pressure, an electrochemical hydrogen compressor and a vacuum pump. The specific energy consumed by this type of PSA is 5,62 kWh/kg.

<i>Option</i>	<i>Scenario 1</i>	<i>Scenario 2</i>
<i>Annual Ammonia Entering the Cracker [ton]</i>	1.160.355	2.883.387
<i>Hourly Plant Capacity [ton/h]</i>	137,7	342,3
<i>H₂ Flow Rate Entering PSA [ton/h]</i>	24,45	60,8
<i>N₂ Flow Rate Entering PSA [ton/h]</i>	113,3	281,5
<i>H₂ Purified Flow Rate [ton/h]</i>	17,42	43,3
<i>Total Heat needed for NH₃ Cracking [MJ]</i>	3.134.070.327	7.787.904.773
<i>Annual Off-Gas Used for Combustion [ton/y]</i>	566.896	1.408.689
<i>Electricity Consumption by Cracker [GWh]</i>	2,32	5,77
<i>Electricity Consumption by PSA [GWh]</i>	804,5	1999

Table 2.23: Process mass balance, thermal and electrical energy consumption

The table shows the inefficiency of the hydrogen purification process. Scenario 1 has an input flow rate of 24,5 ton/h, which decreases to 17,4 ton/h of purified hydrogen. To meet the thermal energy demand of the cracker, 567 thousand tonnes of Off-Gas are burnt annually in Scenario 1 and 1409 thousand tonnes in Scenario 2. PSA is an energy-intensive process, consuming 805 GWh of electricity annually in scenario 1, rising to 2000 GWh in scenario 2. The

electricity is supplied entirely from the grid, ensuring an electricity CF equal to 100 %, and causing indirect greenhouse gas emissions.

2.5 *CO₂ saved and emitted during production and transportation phases*

Greenhouse gas emissions from the NH₃ production, ocean transport and H₂ conversion steps have been calculated to quantify the impact renewable energy has in the supply chain. CO₂ emissions associated with wind energy are null, as only the production phase is considered, while indirect emissions produced by the Argentine and Italian grids are 344 gCO₂/kWh and 312 gCO₂/kWh, respectively. To know the total emissions, it is necessary to calculate the annual electricity consumption of each process.

When an electricity mix between wind and grid is used, the following formula is applied to calculate the specific electricity emissions.

$$\text{Specific } CO_2 \left[\frac{g}{kWh} \right] = \frac{CO_2 \text{Grid} \left[\frac{g}{kWh} \right] * CF_{GRID} [\%]}{CF_{WIND} + CF_{GRID} [\%]} \quad (2.38)$$

In the configuration selected in the thesis work, the wind CF is 54 %, while the grid CF can be varied from 0 to 46 % for the electrolyser, desalinator and hydrogen compressor. The other processes, starting from the ASU and arriving at the NH₃ liquefaction plant must work with the total CF equal to 100 %, which means that the grid CF is fixed 46 %. In the second case, the specific emissions of the electricity mix are 158,24 gCO₂/kWh, calculated using formula 2.38. The processes that take place in the arrival port and the cracking-purification plant are entirely grid-fed, so the specific emissions are 312 gCO₂/kWh. During the transport phase, CO₂ emissions are related to the combustion of the pilot fuel, which emits 3,21 gCO₂/gHFO.

The tables 2.24 and 2.25 report the total carbon dioxide emitted and saved in the production, transport, and conversion phases, comparing the case where all energy comes from the grid. The production of H₂ takes place with an alkaline electrolyser; choosing PEM would slightly change the absolute emission values, as they have different energy consumption.

Option	Scenario 1		
	Only Wind CF 54 %	Wind + Grid CF 100 %	Only Grid CF 100 %
<i>Specific Emissions H₂ Production [gCO₂/kWh]</i>	0	158,24	344
<i>Specific Emissions NH₃ Production-Storage [gCO₂/kWh]</i>	158,24	158,24	344
<i>Specific Emissions H₂ Reconversion [gCO₂/kWh]</i>	312	312	312
<i>Annual CO₂ Total Emissions [ton CO₂]</i>	399.147	2.268.148	4.612.621
<i>CO₂ Saved H₂ Production [ton CO₂]</i>	4.062.951	2.193.994	0
<i>CO₂ Saved for NH₃ production-storage [ton]</i>	150.427	150.479	0
<i>CO₂ Saved Maritime Transportation [ton CO₂]</i>	116.767	116.767	116.767
<i>Total CO₂ Saved [ton]</i>	4.330.146	2.461.240	116.767

Table 2.24: Processes specific emissions, annual CO₂ emissions and emissions saved for scenario 1

The table 2.24, related to Scenario 1, shows that the use of wind energy saves more than 4 million tonnes of CO₂ compared to the hypothetical case of using the electricity grid, while wind-grid energy combination guarantees an emission cut of 2,4 million tonnes of CO₂. The emissions saved during the transport phase have a relatively small value to total emissions and are equivalent to 116.767 tonCO₂/year.

Option	Scenario 2		
	Only Wind CF 54 %	Wind + Grid CF 100 %	Only Grid CF 100 %
<i>Emissions H₂ Production [gCO₂/kWh]</i>	0	158,24	344
<i>Emissions NH₃ Production-Storage [gCO₂/kWh]</i>	158,24	158,24	344
<i>Specific Emissions H₂ Reconversion [gCO₂/kWh]</i>	312	312	312
<i>Annual CO₂ Total Emissions [ton CO₂]</i>	983.186	5.559.932	11.300.976
<i>CO₂ Saved H₂ Production [ton CO₂]</i>	9.949.214	5.372.576	0
<i>CO₂ Saved NH₃ production-storage [ton CO₂]</i>	368.341	368.468	0
<i>CO₂ Saved Maritime Transportation [ton CO₂]</i>	233.534	233.534	233.534
<i>Total CO₂ Saved [ton]</i>	10.551.090	5.974.578	233.534

Table 2.25: Processes specific emissions, annual CO₂ emissions and emissions saved for scenario 2

The decision to feeding the electrolyser only through wind power, which is the most energy-intensive plant of the whole process, eliminates a huge amount of CO₂, in the second scenario

would lead to a cut of almost more than 5 million tonnes compared to the grid-wind power case, and even almost 10,5 million tonnes of CO₂ compared to grid use alone. Emissions from NH₃ production and storage are far lower. This, together with the economic aspect, is the reason why the chain from ASU to hydrogen storage are powered by the wind-grid mix. Maritime transportation emissions are caused using maritime diesel as a pilot fuel. Using NH₃ as the main fuel saves about 230.000 tonnes of CO₂ per year, compared to using HFO as the main fuel.

Considering all the lifetime of the project of 20 years, the wind configuration led to CO₂ emissions saving of 86.602.911 tonnes in scenario 1, and to 211.021.799 tonnes in scenario 2.

2.6 Liquid hydrogen production supply chain

The second energy carrier investigated to meet the hydrogen demand of steel industry is liquefied hydrogen. The processes studied in this work are H₂ production, liquefaction, and storage in the terminal at the port of Comodoro Rivadavia, transport under cryogenic conditions by specialised ships, and storage in liquid form in the unloading terminal at the port of Taranto. The demand for hydrogen from the steel industry is the same considered for the ammonia supply chain. The figure 2.8 illustrates the supply chain of LH₂.

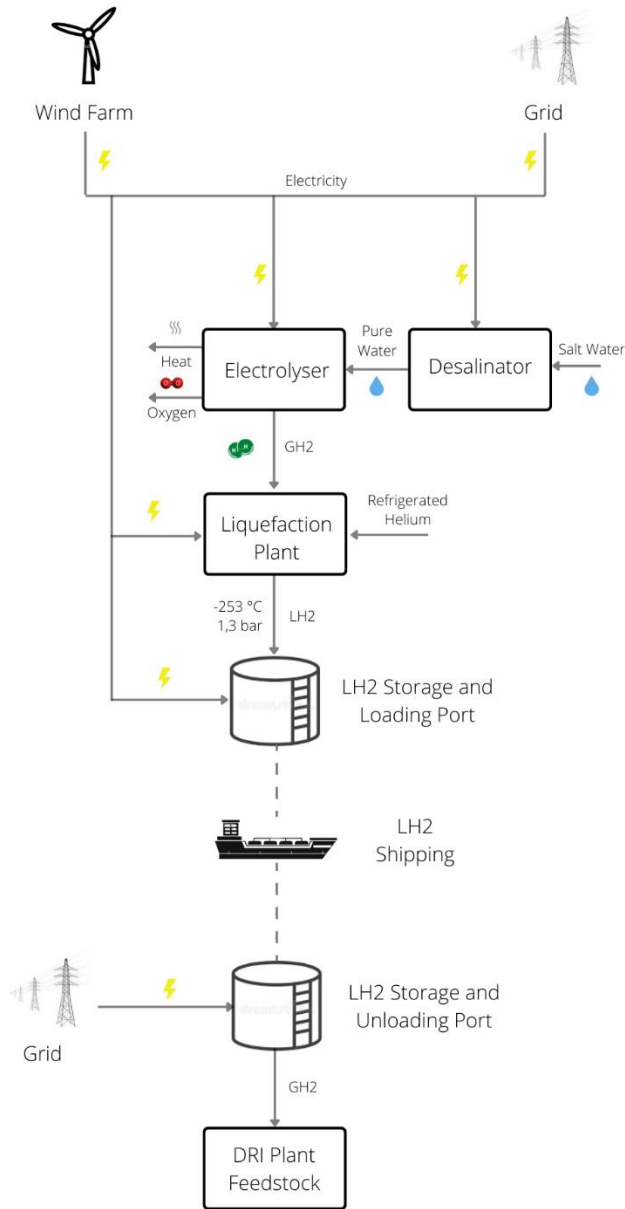


Figure 2.8: LH₂ supply chain (the Author)

Hydrogen is produced via the electrolysis plant, which can be alkaline or PEM technology, fed by a desalinator using reverse osmosis technology. The hydrogen gas produced by the electrolyser enters a liquefaction plant, which brings it to cryogenic conditions and allows it to be liquefied and stored in special tanks. Maritime transport is done by specialised vessels, which unload LH₂ at the arrival terminal, where the hydrogen is again stored in cryogenic tanks, before being re-gasified and sent to the direct iron reduction plant.

The process of producing liquefied hydrogen is much simpler than that of producing ammonia, involves less components and does not require intermediate buffers. The desalination, electrolysis and liquefaction processes are connected and work in series. The only storage facility required is for liquefied hydrogen in the terminal, which allows the production and transport phases to be separated. With this configuration, there are no processes requiring a continuous power supply, as is necessary for the ammonia synthesis plant. The analysis of the electricity utilised for the processes is explained in section 2.3.1.

2.6.1 Balance of the process

Balancing the hydrogen flow in all processes is useful for analysing the losses and overproduction required to obtain the desired amount of product. Electrolyser mass losses are assumed to be 0,5 %. The liquefaction process, comprising different stages, is characterised by a loss rate of 1,67 % (Stolzenburg et al., 2013). In this work liquefaction plant losses of 0,5 % have been considered on industrial experience. Losses in the cryogenic LH₂ storage tanks have been assumed to be 0,5 % by mass, related to the recycling of the vaporised hydrogen by Boil-Off and to the loading and unloading processes of the liquefied hydrogen from the tanks to the ships. Sources of loss during the transport phase are related to the Boil-Off of hydrogen, which is released into the atmosphere via safety valves, and the hydrogen needed as fuel for ship propulsion. The table 2.26 shows the mass balance considering the losses analysed.

Option	Scenario 1		Scenario 2	
	H ₂ Fuel	NH ₃ Fuel	H ₂ Fuel	NH ₃ Fuel
<i>Hydrogen Demand for DRI Plant [kg]</i>	143.144.352	143.144.352	355.701.840	355.701.840
<i>Losses in Unloading Storage</i>	0,5 %	0,5 %	0,5 %	0,5 %
<i>Hydrogen Entering Unloading Storage [kg]</i>	143.860.074	143.860.074	357.480.349	357.480.349
<i>Hydrogen used as fuel [kg]</i>	6.248.192	0	12.496.385	0
<i>Boil-Off During Shipping [kg]</i>	3.547.428	3.547.428	7.094.856	7.094.856
<i>Total Hydrogen Transported [kg]</i>	153.655.694	147.407.502	377.071.591	364.575.206
<i>Loading Storage Losses</i>	0,5 %	0,5 %	0,5 %	0,5 %
<i>Total Hydrogen Storage Loading Terminal [kg]</i>	154.423.973	148.144.540	378.956.948	366.398.082
<i>Liquefaction Process Losses</i>	0,5 %	0,5 %	0,5 %	0,5 %
<i>Total Hydrogen Liquefied [kg]</i>	155.196.093	148.885.262	380.851.733	368.230.072
<i>Electrolyser Losses</i>	0,5 %	0,5 %	0,5 %	0,5 %
<i>Total Hydrogen Produced [kg]</i>	155.972.073	149.629.689	382.755.992	370.071.222
<i>Overproduction</i>	9,0 %	4,5 %	7,6 %	4,0 %

Table 2.26: mass balance of liquid hydrogen supply chain, scenarios 1 and 2 (LH₂ supply chain)

Total hydrogen losses are much lower than in the case of liquid ammonia, mainly since liquid hydrogen does not have to be decomposed, and the production chain involves far fewer processes, which limits losses. In the case of using hydrogen as a marine fuel, the required overproduction is 9,0 % in scenario 1, and drops to 4,5 % if the use of ammonia as a fuel is considered. Also in the second scenario the hydrogen used as fuel accounts for 3,6 % of total production, passing from an overproduction of 7,6 % in case of H₂ used as fuel, to 4,0 % in case of use NH₃ as maritime fuel.

2.6.2 Electrolyser

The electrolysers are the same as those used in the ammonia synthesis process, described in section 2.3.3. The difference lies in the operating pressure at which they work. The liquefaction plant requires the hydrogen input to be at a pressure of 21 bar (Aasadnia & Mehrpooya, 2018),

so both the alkaline electrolyser and PEM are set to work at an operating pressure of 21 bar. The alkaline electrolyser (A1000 Nel Hydrogen series data) works at a temperature of 70 °C, and the specific consumption of the system at ambient pressure is 48 kWh/kg H₂, which increases with increasing pressure. At 21 bar, the specific consumption is 50,2 kWh/kg H₂, and is calculated using formula 2.2. The ideal water consumption is 11,1 kg H₂O/kg H₂.

The PEM electrolyser (data from the M2000 Nel Hydrogen series) operates at a temperature of 50 °C and a pressure of 21 bar. The specific consumption of the system at ambient pressure is 50 kWh/kg H₂ and increases to 52,3 kWh/kg H₂ at 21 bar. The ideal water consumption is 10 kg H₂O/kg H₂. Mass losses are assumed to be 0,5 %.

Total CF is determined using formula 2.3, while hourly and daily capacity are calculated using formula 2.4, in the former case dividing by the number of annual hours (8760) and in the latter by the number of days (365). The number of days of plant shutdown is assumed to be 14, which results in availability of 96 %. The power of the electrolyser is calculated using the formula 2.5. The annual electricity used is consumed by multiplying the specific consumption by the total amount of hydrogen produced. The table 2.27 shows the results for the alkaline and PEM electrolyser for both production scenarios.

Option	Scenario 1		Scenario 2	
	H ₂ Fuel	NH ₃ Fuel	H ₂ Fuel	NH ₃ Fuel
Annual H ₂ Production [ton]	155.972	149.630	382.852	370.071
Annual H ₂ Liquefaction Plant [ton]	152.196	148.885	382.756	368.230
<i>Total Electricity Consumed [GWh]</i>				
Alkaline	7.787	7.470	19.109	18.475
PEM	8.111	7.781	19.904	19.245
<i>Plant Power [GW]</i>				
CF 54 % + Alkaline	1,71	1,64	4,20	4,06
CF 100 % + Alkaline	0,92	0,89	2,27	2,19
CF 54 % + PEM	1,76	1,71	4,35	4,23
CF 100 + PEM	0,96	0,92	2,36	2,28
<i>Plant Capacity [ton/day]</i>				
CF 54%	810	778	1994	1926
CF 100 %	438	420	1078	1041

Table 2.27: Electrolyser plant power and capacities for different scenarios, (LH₂ supply chain)

The amount of hydrogen produced annually is by far less than the amount required in the NH₃ supply chain, this is explained by lower losses in the production and transport chain. The power of the electrolyser is lower than 2 GW for all the configurations evaluated in the scenario 1, while it reaches the maximum value of 4,35 GW in the scenario 2 for the configuration with CF 54 % and PEM electrolyser. The annual energy consumed increases by about 300 GWh when using the PEM electrolyser instead of the alkaline in scenario 1, while it increases by about 800 GWh in scenario 2. The capacity factor is a very important parameter for the plant's output and capacity. In the case of using electricity generated exclusively by wind power, with a CF of 54 %, the capacity of the electrolysis plant is almost twice as high as in the case where the grid integrates wind power, and the CF of the mix is 100 %. The same is true for plant power. The impact of the choice of fuel on the sizing and consumption of the electrolysis plant is very low. As shown in the table, the values are very similar.

2.6.3 Desalinator

The desalination plant has the task of supplying the water to the electrolyser with the correct grade of purity. A reverse osmosis desalinator has been adopted, the operation of which is explained in paragraph 2.3.4. Although the ideal amount of water used by the alkaline and PEM electrolysers is 11,1 and 10 kg H₂O per kg H₂, respectively, an overproduction of 30 % is considered to overcome the inefficiency of the electrolysis plant and flow losses. The specific water consumption is therefore 14,3 and 15,89 kgH₂O per kg H₂ for the PEM and alkaline electrolyser respectively.

The plant availability is 96 %, and the total CF is calculated by multiplying the CF of electricity by the availability. Hourly and daily capacity are calculated using formula 2.4. Plant power is calculated using formula 2.5. The specific consumption of the reverse osmosis desalinator is 2,5 kWh/m³. No thermal energy is required. The table 2.28 shows the values of plant capacity, annual energy consumption and plant power for both scenarios.

Option	Scenario 1		Scenario 2	
	H ₂ Fuel	NH ₃ Fuel	H ₂ Fuel	NH ₃ Fuel
<i>Annual Water Production [ton]</i>				
<i>Alkaline</i>	2.479.053	2.378.245	6.083.603	5.881.989
<i>PEM</i>	2.191.129	2.140.420	5.475.243	5.293.790
<i>Total Electricity Consumed [MWh]</i>				
<i>Alkaline</i>	6.197	5.946	15.209	14.705
<i>PEM</i>	5.578	5.351	13.688	13.234
<i>Plant Power [MW]</i>				
<i>CF 54 % + Alkaline</i>	1,4	1,3	3,3	3,2
<i>CF 100 % + Alkaline</i>	0,7	0,7	1,8	1,8
<i>CF 54 % + PEM</i>	1,2	1,2	3	2,9
<i>CF 100 % + PEM</i>	0,7	0,6	1,6	1,6
<i>Plant Capacity [m³/day]</i>				
<i>CF 54% + Alkaline</i>	13.102	12.569	32.152	31.086
<i>CF 100 + Alkaline</i>	7.075	6.787	17.362	16.786
<i>CF 54% + PEM</i>	11.792	11.312	28.936	27.977
<i>CF 100 % + PEM</i>	6.367	6.109	15.626	15.108

Table 2.28: Desalinator plant power and capacities for different scenarios, (LH₂ supply chain)

The total amount of water produced is by far less than the water needed in the ammonia production chain. In scenario 1, there is a reduction of 1 million tonnes of water, while in scenario 2, the reduction is 2,8 million tonnes of water.

The choice of fuel has no significant impact on the design of the desalination plant. Plant capacity, energy consumed, and power output are not significantly affected by this choice.

The capacity factor determines a great variation in sizing. Selecting 100 % CF reduces the power and capacity of the electrolyser by almost half respect the case in which only wind energy is used.

The alkaline electrolyser requires more water, which leads to a slight increase in the electricity used, the power of the system and its capacity. The difference is very small compared to the case of the PEM.

In scenario 1, the configuration requiring the higher plant output is alkaline and CF 54 %, resulting in a desalination power of 1,4 MW, while the configuration with CF 100 % and PEM

requires a desalination power of 0,6 MW. In the second scenario, the plant capacity increases to 3,3 MW in the first case and 1,6 MW in the second case.

2.6.4 Liquefaction plant

Hydrogen produced in gaseous form enters the liquefaction plant to be stored in liquid form. The boiling temperature of hydrogen is $-252,9\text{ }^{\circ}\text{C}$ at ambient pressure, lower than NH_3 , which becomes liquid at a temperature of $-33\text{ }^{\circ}\text{C}$.

There are many different hydrogen liquefaction processes, some of which have been described in the introductory chapter, such as the Linde-Hampson cycle and the Claude cycle. For this work has been considered a process similar to the one described in the paper (Aasadnia & Mehrpooya, 2018), which involves a refrigeration cycle using a mixed refrigerant, which pre-cools the hydrogen gas from a temperature of $25\text{ }^{\circ}\text{C}$ to a temperature of $-196,2\text{ }^{\circ}\text{C}$. The energy used in this phase includes compressors and pumps. Next, further refrigeration occurs in a cascade Joule-Brayton cycle that cools the hydrogen gas from $-196,2\text{ }^{\circ}\text{C}$ to $-249,3\text{ }^{\circ}\text{C}$ in the cryogenic section of the plant, which is the most energy-intensive part. Finally, the hydrogen passes through a turbine that expands it to a temperature of 1,3 bar at which the hydrogen liquefies and can be stored in cryogenic tanks. The turbine has a very low energy consumption. The specific energy consumed per kilogram of LH_2 produced is 6,47 kWh, which is higher than the ideal value of 2,89 kWh, due to the exergy efficiency of the plant, estimated to be 45,5 %, which is significantly higher than the exergy efficiency of currently existing hydrogen liquefiers. A very similar value of energy consumption has been also evaluated in the paper (Stolzenburg et al., 2013), in which a liquefaction process divided into five parts is described and calculates the specific energy consumption to be 6,4 kWh/kg H_2 , which increases to 6,76 kWh/kg H_2 considering losses. Existing plants are characterised by much higher energy consumption, ranging between 10 and 15 kWh/kg H_2 .

The liquefaction plant considered in the thesis work and illustrated in the following figure involves the compression of hydrogen to a pressure of 80 bar. GH_2 then passes through a chiller that lowers its temperature to approximately $6\text{ }^{\circ}\text{C}$, before being pre-cooled with a mixed refrigerant consisting of nitrogen, methane, ethane, propane and butene, which brings the hydrogen to a temperature of $-193\text{ }^{\circ}\text{C}$. Deeper refrigeration takes place via the Brayton cycle that brings the temperature of the gas to $-246,2\text{ }^{\circ}\text{C}$. Finally, the last stage is expansion in a turbine that brings the gas temperature down to $-252,9\text{ }^{\circ}\text{C}$ at a pressure of 1,3 bar, in which the

hydrogen is liquefied (Stolzenburg et al., 2013). The figure 2.9 shows the H₂ liquefaction process considered.

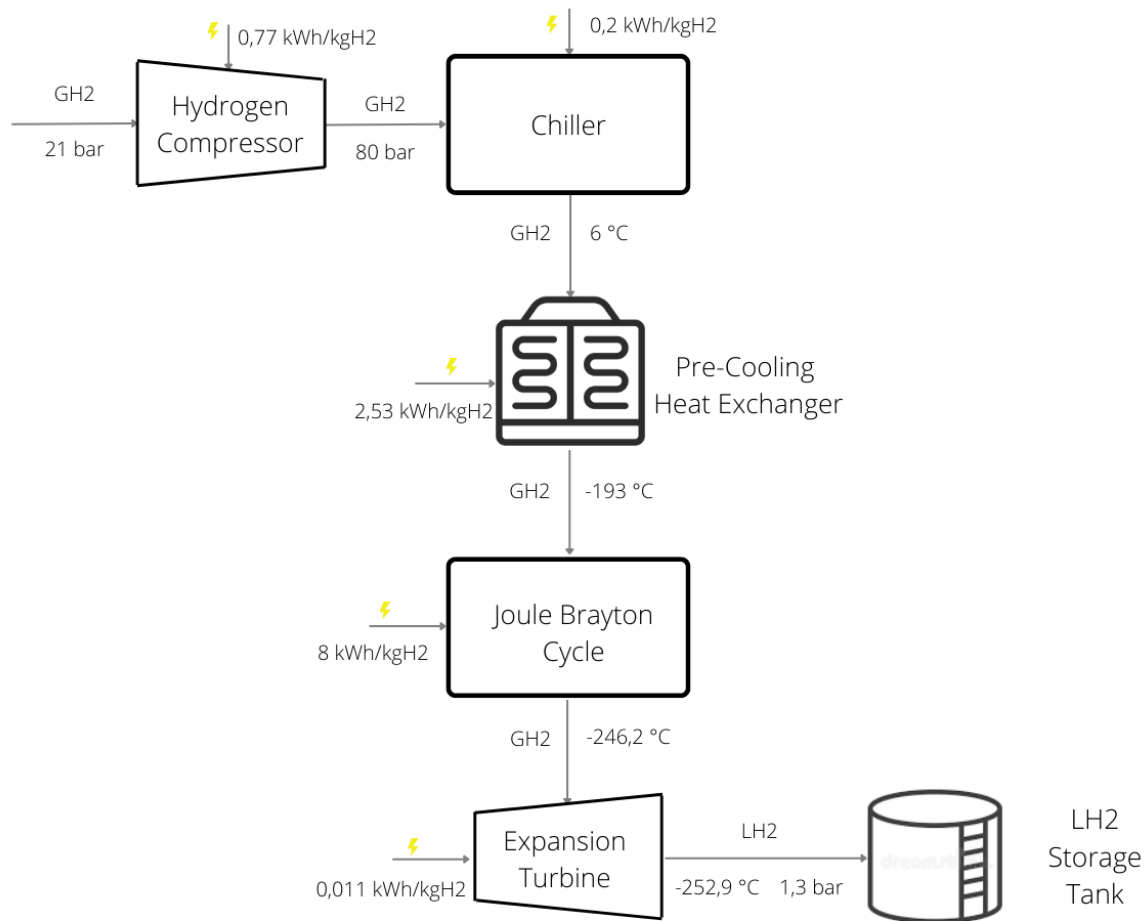


Figure 2.9: Hydrogen liquefaction process (the Author)

In this work, the specific consumption value used in the '*Hydrogen Delivery Scenario Analysis Model*' or HDSAM has been used, which is 11,52 kWh/kgH₂. Since the ideal consumption for hydrogen liquefaction is 2,89 kWh/kg, the exergy efficiency of the system is 25 %. For the calculation of the partial consumption of the different components, the paper (Aasadnia & Mehrpooya, 2018) has been considered. Formula 2.6 has been applied to calculate the energy consumption of the compressor, resulting in an SEC of 0,77 kWh/kgH₂.

The HDSAM program also considers mass losses to be 0,5 %, a figure that has been highlighted in industrial processes. Inefficiencies are lower than the value used of 1,67 %, in agreement with the paper (Stolzenburg et al., 2013). In this work mass losses of 0,5 % have been considered, following the industrial experience.

According to the paper (Noh et al., 2022), the equivalent working hours of the plant are 8000 h, so the availability is 91,3 %. The total CF of the liquefaction plant is obtained by multiplying

the availability by the CF of the electricity, which depends on the electricity mix used. Daily capacity is calculated by dividing the total amount of hydrogen liquefied in a year by the total CF and the annual days (365). The total energy consumed by the plant is calculated by multiplying the SEC by the total amount of hydrogen processed, it also includes the re-liquefaction of the vaporized hydrogen during the storage period. The following table summarises the results for scenarios 1 and 2.

<i>Option</i>	<i>Scenario 1</i>		<i>Scenario 2</i>	
	<i>H₂ Fuel</i>	<i>NH₃ Fuel</i>	<i>H₂ Fuel</i>	<i>NH₃ Fuel</i>
<i>Total Hydrogen Liquefied [ton]</i>	155.196	148.885	380.852	368.230
<i>Liquid Hydrogen Stored [ton]</i>	154.424	148.145	378.957	366.398
<i>Annual Energy Consumption [GWh]</i>	1829	1756	4483	4338
<i>Plant Capacity [ton/day]</i>				
<i>CF - 54 %</i>	862	827	2116	2046
<i>CF - 100 %</i>	457	447	1142	1105
<i>Plant Power [MW]</i>				
<i>CF - 54 %</i>	423	407	1038	1004
<i>CF - 100 %</i>	228	219	560	542

Table 2.29: Hydrogen liquefaction plant capacity, total energy consumption and plant power, Scenarios 1 and 2

Like the other elements of the process, the liquefaction plant is also greatly influenced by the capacity factor. The choice of maritime fuel does not imply great changes in the calculated values. The total energy spent on hydrogen liquefaction rises from over 1800 GWh in scenario 1, to almost 4500 GWh in scenario 2. After the electrolyser, the liquefaction process is the most energy intensive. The liquefaction plant is not influenced by the type of electrolyser selected, because the quantity of hydrogen processed is the same for both alkaline and PEM, and the hydrogen inlet conditions are the same.

2.6.5 Liquid hydrogen storage

Liquefied hydrogen is stored in dedicated cryogenic tanks located in the port of departure. The tanks must be constructed to maintain the cryogenic conditions of hydrogen, with temperatures below -253 °C, at a pressure close to ambient. Paragraph 1.7.3 of the introductory chapter describes the structure and properties of this type of tank. A mass loss

rate of 0,5 % has been assumed, due to both the recirculation of hydrogen gas in the liquefaction plant and the vessel loading operations.

As with the liquid NH₃ tanks, the capacity and number of LH₂ tanks can be decided to ensure a proper storage duration, chosen to be over 20 days to ensure the transportation of hydrogen if a big failure happens in the production chain. The storage period is calculated by dividing the total capacity of the tanks by the flow rate of liquefied hydrogen, expressed in m³/h. The density of liquefied hydrogen is 70,8 kg/m³.

The Boil-Off rate has been determined using the same procedure as for liquid ammonia. The LH₂ tanks are spherical in shape, with a capacity of 50.000 m³ and a diameter of 45,7 m. The surface area of the tank is calculated using the formula 2.39.

$$A [m^2] = 4 * PI * \left(\frac{d}{2}\right)^2 \quad (2.39)$$

The heat transfer coefficient U is 0,01 W/m²°K, while the heat of vaporisation ΔH is 443,17 KJ/kg (Aziz, 2021). The ambient temperature is 10 °C. Using formula 2.17, the heat exchanged is calculated, while using 2.20, the rate of evaporated hydrogen can be founded, it is equal to 0,04 kg/s, which corresponds to 140 kg of hydrogen per hour of storage. The Boil-Off rate is calculated by dividing the amount of hydrogen evaporated in one day by the amount of hydrogen stored in one tank. The annually evaporated hydrogen is calculated by multiplying the daily evaporated hydrogen per the total amount of day in a year.

The energy required by this storage plant is 11,52 kWh per kg of H₂, the electricity totally used to cool the liquefied hydrogen is calculated in the previous paragraph.

Option	Scenario 1		Scenario 2	
	H ₂ Fuel	NH ₃ Fuel	H ₂ Fuel	NH ₃ Fuel
Storage Tank Filling Rate [m ³ /h]	274	263	672	650
Tank Capacity [m ³]	50.000	50.000	50.000	50.000
Number of tanks	3	3	7	7
Days of Storage Ensured	22,81	23,78	21,69	22,43
Boil-Off Rate [%/day]	0,095%	0,095%	0,095%	0,095%
Annual Evaporated Hydrogen [kg]	3.683.654	3.683.654	8.595.194	8.595.194

Table 2.30: Liquid hydrogen storage tank, days of storage ensured, Boil-Off rate and annual H₂ evaporated, scenarios 1 and 2

The table 2.30 shows the inlet flow rates of hydrogen into the tanks, in scenario 1 it is about 270 m³/h, while in scenario 2 it rises to 670 m³/h. It has been decided to maintain the same

tank size of 50.000 m³, which corresponds to 3540 tonnes of liquid hydrogen. To ensure a storage duration of more than 20 days in scenario 1, 3 tanks are required, while in scenario 2 the number increases to 7. The calculated Boil-Off rate is 0,095 %, value larger than for NH₃. The calculated Boil-Off is in line with the values reported in the literature, the paper (Ishimoto et al., 2020) considers a BOG of 0,1 %, (Al-Breiki & Bicer, 2020) reports a hydrogen vaporisation rate during the production phase of 1,189 %. The paper (Niermann et al., 2021) reports a Boil-Off of 1,35 % for cryogenic tanks. (Johnston et al., 2022) uses a BOG during storage of 0,1 %. The amount of H₂ evaporated annually, calculated by multiplying the daily H₂ evaporated per the annual days, is about 3.680 tonnes in Scenario 1 and exceeds 8.595 tonnes in Scenario 2. The liquid hydrogen storage facility is part of the port's loading terminal, which is described in the next section.

2.6.6 Loading terminal

The transport of liquid hydrogen is not yet developed worldwide, there are few ports in the world with infrastructure capable of storing and distributing hydrogen, and ships for the maritime transport of liquefied hydrogen have not yet been commercialised on a large scale. The liquid hydrogen transport chain is at a preliminary stage of development, unlike the ammonia transport chain, which is a technology that has been developed for many years. The building of adequate port infrastructure is essential to facilitate the expansion of this technology.

Kawasaki built a terminal at LH₂ that houses a spherical liquefied hydrogen tank with a volume of 2.500 m³, and a specially designed loading arm system for the transfer of liquefied hydrogen between land and ship facilities. The tank is equipped with a double-shell structure with vacuum insulation, which prevents heat transfer with the outside environment (Ovcina, 2021). LH₂ must be kept at approximately -253 °C to remain in a liquid state, which is why the loading/unloading arms and pipes are insulated to prevent heat build-up from the air and minimise hydrogen vaporisation.

The port terminal is conceptually similar to LNG storage terminals and is characterised by a facility that transfers liquid hydrogen from fixed land-based storage tanks via a cryogenic line with loading arms, to a flexible end of a ship moored at a dock. The location of the tanks is very important, proximity to the quay results in reduced installation costs, and ensures easier handling of the cryogenic pipeline.



Figure 2.10: LH₂ loading terminal facilities (Eria, 2020)

The docks must be equipped to accommodate ships longer than 300 metres. They also include pipelines used to transport LH₂ between the terminal storage. There are also support infrastructures required for the processes of ship entry/exit from the port, for the docking of the ship at the quay and for the logistics coordination offices, which manage and follow all ship loading operations.

The design of the storage facility and the study of the energy required for the hydrogen liquefaction plant have been treated in the previous sections. It is necessary to calculate the energy consumed by the terminal infrastructure, for the ship loading process and for auxiliary processes. The paper (Ishimoto et al., 2020) considers an energy use for loading processes of 198 kWh per tonne of hydrogen handled. The paper (Ozawa et al., 2017) considers an energy utilisation of 0,055 kWh per m³ hydrogen, which corresponds to 0,78 kWh/ton H₂, a value considered too low. For the thesis work, a SEC of 198 kWh/kg H₂ has been assumed.

The terminal's annual energy consumption for loading operations in the terminal is 30.424 MWh in scenario 1, and increases to 74.660 MWh in scenario 2. The energy used during the loading phase is negligible respect the energy required for the hydrogen liquefaction plant.

2.6.7 Oceanic transport

The transport phase consists of oceanic navigation of tankers dedicated to transporting liquefied hydrogen under cryogenic conditions. The port of departure is Comodoro Rivadavia, a city facing the Atlantic ocean in the Chubut region of eastern Patagonia, and the port of arrival is in Taranto, an Italian city located in the mediterranean sea.

Dedicated ships with a capacity of 160.000 m³ have been considered for transport, as proposed by the paper (Eria, 2020). The document (Niermann et al., 2021) considers a maximum ship capacity to be 173.400 m³. In this work the first option has been adopted. The usable capacity of the ship is 94 %, so the maximum amount of hydrogen that can be transported by the ship is 150.400 m³.

- Shipment duration and calculation of required vessels

Maritime transport is composed of loading the ship, transport to the port of arrival, where the ship is unloaded, before returning empty to the terminal of departure. A duration of 36 hours has been considered for the loading and unloading of the ship, in accordance with the paper (Johnston et al., 2022). The sailing duration is calculated by dividing the total distance by the cruising speed of the ship, assumed to be 17 knots. The total distance is the same as that used in the case of NH₃ and is equal to 7.226 nautical miles. By adding up the durations of these four phases, it is possible to know the total duration of a roundtrip. The number of trips a ship can make in a year is obtained by dividing the annual number of days by the number of days needed for a single trip. Finally, the number of ships required for the transport service is calculated by dividing the total amount of hydrogen stored by the amount of hydrogen that a single ship can transport annually and adding one, like in the formula 2.26. The table 2.31 shows the results of the calculations described.

<i>Option</i>	<i>Scenario 1</i>	<i>Scenario 2</i>
<i>Vessel Capacity [m³]</i>	150.400	150.400
<i>Vessel Speed [knots]</i>	17	17
<i>Loading Time [h]</i>	36	36
<i>Transportation Time [h]</i>	425,1	425,1
<i>Unloading Time [h]</i>	36	36
<i>Transportation Time [h]</i>	425,6	425,6
<i>Total Time [h]</i>	922,7	922,7
<i>Total Time [d]</i>	38,44	38,44
<i>Number of trips per year</i>	9	9
<i>Totan LH₂ transported per ship [m³]</i>	1.353.600	1.353.600
<i>Minimum Number of Ships required</i>	3	5

Table 2.31: LH₂ transport duration, annual vessel capacity transported, number of vessels required, scenarios 1 and 2

The total duration of a trip is 38,44 days, one ship is able to make 9 trips per year, transporting 1.353.600 m³ of LH₂. The minimum number of ships required to provide the shipping service is 3 in scenario 1 and 5 in scenario 2.

- Vessel fuel consumption and fuel tank design

To make the hydrogen value chain totally carbon free, the use of fuels that do not cause greenhouse gas emissions into the atmosphere has been evaluated. Two different cases have been developed, in which the fuel used can be either hydrogen or ammonia. There are currently no hydrogen-powered ship propulsion systems, and research is at a preliminary stage, while internal combustion engines using NH₃ as fuel are at an advanced stage of development and close to commercialisation. Calculations concerning the use of hydrogen are theoretical and are aimed at estimating the amount of hydrogen hypothetically required to power transport. Fuel consumption is calculated starting with the Specific Fuel Consumption [kg/kWh] using the formula 2.28, which correlates the lower calorific value of fuel and engine efficiency. Engine power is instead calculated using the 'Ammiragliato' formula 2.30, which correlates power [HP] with ship speed [knots] and deadweight [tons], which is calculated considering a net-dead weight ratio of 0,25. Finally, the fuel consumption [kg/km] is obtained from formula 2.29, where the engine power is multiplied by the SFC and divided by the ship's speed.

Finally, the capacity of the fuel tank is found by multiplying the fuel consumption by the total distance the ship must travel in the round trip. The tank capacity is oversized by 20 % compared to the required fuel. In the case of both NH₃ and H₂, the use of HFO as pilot fluid is considered.

<i>Option</i>	<i>Scenario 1</i>		<i>Scenario 2</i>	
	H ₂	NH ₃	H ₂	NH ₃
<i>Low Heating Value [MJ/kg]</i>	120	18,6	120	18,6
<i>Engine Efficiency</i>	48 %	48 %	48 %	48 %
<i>Specific Fuel Consumption [kg/kWh]</i>	0,06	0,4	0,06	0,4
<i>Vessel Dead-Weight [ton]</i>	42.593	42.593	42.593	42.593
<i>Vessel Speed [km/h]</i>	31,5	31,5	31,5	31,5
<i>Vessel Power [MW]</i>	6,5	6,5	6,5	6,5
<i>Fuel Consumption [kg/km]</i>	13	83,6	13	83,6
<i>Fuel Tank Volume [m³]</i>	5.883	3.941	5.883	3.941
<i>Annual Fuel Consumed [ton]</i>	6.248	40.311	12.496	80.622
<i>Percentage of Annual Hydrogen Produced</i>	4,0 %	0 %	3,3 %	0 %

Table 2.32: Vessel power, transportation fuel consumption, fuel tank capacity, annual fuel consumption, scenarios 1 and 2

The specific fuel consumption is lower in the case of hydrogen, which is due to its higher calorific value. Engine power is the same in both cases, as the calculation only takes the physical properties of the ship into account. Fuel consumption per km is also lower in the H₂ case than in the NH₃ case, from 13 kg/km to 83,6 kg/km. On the other hand, the tank size is smaller in the case of NH₃, since the density of liquid ammonia is much higher than the density of LH₂. In scenario 1, the annual hydrogen used as fuel is just over 6 thousand tonnes, this figure increases to 12.500 tonnes in scenario 2. In the case of ammonia, the annual amount used as fuel is 40 thousand tonnes in Scenario 1 and doubles in Scenario 2.

- Boil Off Calculation

Hydrogen evaporation also occurs during transport, but unlike during storage, the hydrogen evaporated by boil off is lost and released into the atmosphere through safety valves. The hydrogen gas increases the pressure inside the tanks, and when the pressure reaches a threshold level, the Boil-Off valves are opened. Boil-Off is caused by heat loss, sloshing, flashing and the conversion from ortho to para-hydrogen, and depends on several engineering factors, such as thermal insulation and the shape and size of the tank. To decrease the rate of Boil-Off,

it is important to reduce the surface-to-volume ratio, and to use good insulation with low thermal conductivity, to reduce the heat exchanged with the surroundings. According to the paper (Wijayanta et al., 2019), the Boil-Off rate varies between 0,06 and 2,0 %, for tanks of less than 100 m³ capacity, and decreases as the tank volume increases.

The usable capacity of the ship is 150.400 m³, and four tanks of spherical shape and equal size have been assumed. Each tank has a volume of 37.600 m³, and a diameter of 41,6 m. The internal surface area is 5427,6 m². The total length of the cargo is 170 m, so the total length of the ship is probably more than 200 m. The ambient temperature has been assumed to be 10 °C. Using formulas 2.17, 2.20 and, 2.21, the heat exchanged [W], the hydrogen evaporation rate [kg/s], and the Boil-Off percentage are calculated.

<i>Option</i>	<i>Value</i>
<i>Tank Capacity [m³]</i>	37.600
<i>Tank Surface Area [m²]</i>	5.428
<i>Heat Transfer Q [W]</i>	14.269
<i>H₂ Vaporisation Rate [kg/h]</i>	115,9
<i>Boil-Off [%/day]</i>	0,105%
<i>H₂ Evaporated per Round Trip per tank [kg]</i>	197.079
<i>Annual H₂ Losses Scenario 1 [kg]</i>	3.547.428
<i>Annual H₂ Losses Scenario 2 [kg]</i>	7.094.856

Table 2.33: Boil-Off hydrogen during transport

The evaporation rate is 115,9 kg/h, which is equivalent to 197.079 kg per round trip. The Boil-Off rate is 0,105 %/day, which is in line than the values found in the literature. The (Al-Breiki & Bicer, 2020) paper uses a value of 0,52 %. The paper (Johnston et al., 2022) considers a transportation BOG equals to 0,2 %/day. The paper (Ozawa et al., 2017) reports a mean Boil-Off during transportation of 0,3 %/day. The annual amount of hydrogen lost through evaporation is calculated by multiplying the hydrogen evaporated per trip by the total number of annual trips. In first scenario 3.547 tonnes of hydrogen are lost, and in the second one 7.095 tonnes.

- CO₂ emissions saving with respect the use of maritime diesel fuel

To quantify the benefits of using green fuels such as ammonia and hydrogen, the amount of marine diesel that would be required for ocean transport was calculated if standard ships with

an ICE engine powered by HFO were used. An engine efficiency of 48 % (Sophie & Ness, 2021) and an LHV of 40,9 MJ/kg has been considered for the calculation of specific HFO consumption. The density of HFO is 1010 kg/m³. The SFC is 0,183 kg/kWh, lower than that of ammonia, but higher than the specific consumption of hydrogen. The engine power is the same as for NH₃ and H₂, since it depends on the speed of the ship and its deadweight capacity. The calculation of FC uses formula 2.29.

<i>Option</i>	<i>Scenario 1</i>	<i>Scenario 2</i>
<i>Cargo Ship Capacity [m³]</i>	150.400	150.400
<i>Vessel Power [MW]</i>	6,5	6,5
<i>Ship Speed [knots]</i>	17	17
<i>Fuel Consumption [kg/km]</i>	38,03	38,03
<i>Round Trip HFO Consumption [kg]</i>	1.018.450	1.018.450
<i>Fuel Tank Volume [m³]</i>	1210	1210
<i>Annual HFO Consumption [ton]</i>	27.498	45.830
<i>Annual CO₂ Emissions [ton]</i>	88.269	147.115

Table 2.34: Fuel consumption and CO₂ emission for HFO ship transport

The specific fuel consumption is 38 kg/km, higher than hydrogen due to the lower LHV, but lower than ammonia for the same reason. The tank capacity is 1210 m³, lower than H₂ and NH₃, because the density of HFO is higher. The annual consumption of marine diesel is 27.500 tonnes in scenario 1, and would contribute to the emission of almost 90.000 tonnes of CO₂. In scenario 2, annual HFO consumption is almost 46.000 tonnes, which would increase CO₂ emissions to 147.000 tonnes.

2.6.8 Unloading terminal

The unloading terminal has a similar structure to the loading terminal, they share the infrastructure and main processes. When the ship docks at the quay, unloading operations begin via an unloading arm. To keep the hydrogen in liquid form, dedicated equipment is used to maintain cryogenic conditions inside, and to minimise heat exchange with the environment as much as possible. The liquid hydrogen is transferred from the ship's tanks to the terminal tanks, which store the hydrogen before it is sent to the direct reduction plant. The storage conditions for hydrogen are -253 °C at ambient pressure. A mass loss rate of 0,5 % has been assumed during the storage phase, due to both the recirculation of gaseous hydrogen in the

liquefaction plant and the transfer of liquid hydrogen from the ship's tanks to the reservoirs. The annually stored hydrogen is 143.860 tonnes in scenario 1, and increases to 357.480 tonnes in scenario 2.

The flow rate of hydrogen sent to the DRI plant is 17,2 t/h in scenario 1, and 42,74 tH₂/h in scenario 2. The storage tanks have a capacity of 50.000 m³, and a diameter of 45,7 m. The choice on the number of tanks adopted depends on the storage time to be guaranteed, in the case of the thesis it was decided to have a minimum time of 20 days. For the Boil-Off calculation, the formulas described in section 2.3.9 have been used. The heat exchanged Q is 17.912 W, while the evaporation rate is 145,5 kg/h. The ambient temperature is set to 20 °C.

The energy consumption for the unloading terminal is 0,198 kWh/kg H₂, the same as for the loading terminal, while the liquefaction of evaporated hydrogen by Boil-Off requires a specific energy of 11,52 kWh/kg H₂.

<i>Option</i>	<i>Scenario 1</i>	<i>Scenario 2</i>
<i>DRI Plant flow rate [m³/h]</i>	243	604
<i>Number of tanks</i>	3	6
<i>Days of storage guaranteed</i>	25,7	20,7
<i>Boil-Off Rate [%/d]</i>	0,099%	0,099%
<i>Annual Evaporated Hydrogen [kg]</i>	3.823.771	7.647.541
<i>Annual Energy Consumption [MWh]</i>	72.500	158.812

Table 2.35: Unloading storage terminal tanks, Boil-Off rate and electricity consumed

To ensure a minimum of 20 days of storage, 3 tanks are required in scenario 1 and 6 in scenario 2. The rate of evaporated hydrogen is 0,04 kg/s, which equals 145,5 kg/h. The Boil-Off rate during the storage period is 0,1 %, which implies the evaporation of 3.824 tonnes of hydrogen in scenario 1 and 7.658 tonnes in scenario 2. The annual energy consumed at the unloading terminal is 72,5 GWh in scenario 1, and rises to 158,8 GWh in scenario 2.

2.7 CO₂ saved and emitted during production and transportation phases

To quantify the impact of renewable energy in the supply chain, greenhouse gas emissions from the hydrogen production, storage in liquid form, maritime transport and storage at the port of arrival have been calculated. CO₂ emissions associated to wind energy are zero, as only the production phase is considered, while indirect emissions from the Argentine and Italian networks are 344 gCO₂/kWh and 312 gCO₂/kWh respectively. To know the total emissions, it is

necessary to calculate the annual electricity consumption of each process. When using a mix of wind and grid electricity, the formula 2.38 is applied to calculate the specific electricity emissions.

In the selected configuration, the CF of the wind power plant is 54 %, while the CF of the grid can vary from 0 to 46 % for the electrolysis, desalination and H₂ liquefaction processes. The selection of grid integration in the energy mix is an operator decision. Only the loading processes at the terminal need a continuous supply of electricity, given by an electric CF of 100 %. The unloading and liquefaction operations of the evaporated hydrogen in the arrival terminal are supplied exclusively by grid energy, characterised by emissions of 312 gCO₂/kWh. During the transport phase, CO₂ emissions are related to the combustion of the pilot fuel, which emits 3,21 gCO₂/gHFO.

The tables 2.36 and 2.37 show the total carbon dioxide emissions released and saved in the production, transport, and conversion phases, comparing the case where all energy comes from the grid. H₂ production takes place with an alkaline electrolyser; the choice of PEM would change the absolute values of emissions, as they have a different energy consumption.

<i>Option</i>	<i>Scenario 1</i>		
	Only Wind CF 54 %	Wind + Grid CF 100 %	Only Grid CF 100 %
<i>Specific Emissions H₂ Production and Storage [gCO₂/kWh]</i>	0	158,24	344
<i>Specific Emissions Port Facilities Argentina [gCO₂/kWh]</i>	158,24	158,24	344
<i>Specific Emissions Port Facilities Italia [gCO₂/kWh]</i>	312	312	312
<i>Annual CO₂ Total Emissions [ton CO₂]</i>	28.036	1.550.585	3.343.577
<i>CO₂ Saved H₂ Production [ton CO₂]</i>	3.309.889	1.787.340	0
<i>CO₂ Saved for LH₂ storage [ton]</i>	5.652	5.652	0
<i>CO₂ Saved Maritime Transportation [ton CO₂]</i>	87.667	87.667	87.667
<i>Total CO₂ Saved [ton]</i>	3.403.208	1.880.659	87.667

Table 2.36: Processes specific emissions, annual CO₂ emissions and emissions saved for scenario 1

The most polluting processes in the LH₂ chain are the hydrogen production and liquefaction phase, as they are the most energy-intensive, while loading and unloading at the platform do

not contribute significantly to emissions. The use of wind power alone saves 1.561.628 tonnes of CO₂ annually compared to the case of grid integration in scenario 1. Emissions related to the transport phase depend on the use of marine diesel as a pilot fuel, the emissions saved compared to the case where only HFO is used as fuel are 87.667 tonnes, a degree of magnitude lower than the emissions related to production. Compared to the assumption of power supply only via the electricity grid, 3.403.208 tCO₂/year would be saved in the case of wind power., and 1.880.659 tonCO₂/year in the case of wind–grid mix electricity.

<i>Option</i>	<i>Scenario 2</i>		
	Only Wind CF 54 %	Wind + Grid CF 100 %	Only Grid CF 100 %
<i>Specific Emissions H₂ Production and Storage [gCO₂/kWh]</i>	0	158,24	344
<i>Specific Emissions Port Facilities Argentina [gCO₂/kWh]</i>	158,24	158,24	344
<i>Specific Emissions Port Facilities Italia [gCO₂/kWh]</i>	312	312	312
<i>Annual CO₂ Total Emissions [ton CO₂]</i>	62.567	3.798.098	8.197.155
<i>CO₂ Saved H₂ Production [ton CO₂]</i>	8.120.719	4.385.188	0
<i>CO₂ Saved for LH₂ storage [ton]</i>	13.869	13.869	0
<i>CO₂ Saved Maritime Transportation [ton CO₂]</i>	145.912	145.912	145.912
<i>Total CO₂ Saved [ton]</i>	8.280.500	4.544.969	145.912

Table 2.37: Processes specific emissions, annual CO₂ emissions and emissions saved for scenario 2

In the second scenario, total emissions increase in relation to the increased volumes of hydrogen produced. The single use of wind power reduces CO₂ emissions by 3.848.639 tonnes per year, compared to using the grid-wind power mix. The emissions saved during the transport phase amount to 145.912 tonnes CO₂. Compared to a hypothetical case of only grid power, up to 8.280.500 tonnes CO₂/year would be saved in the case of wind power, and 4.544.969 would be saved in case of wind-grid power mix.

Considering the project life of 20 years, the total amount of carbon dioxide saved is 68.064.163 tonCO₂ in scenario 1 and 165.609.995 tonCO₂ in scenario 2.

References Chapter 2

- Aasadnia, M., & Mehrpooya, M. (2018). Conceptual design and analysis of a novel process for hydrogen liquefaction assisted by absorption precooling system. *Journal of Cleaner Production*, 205, 565–588. <https://doi.org/10.1016/j.jclepro.2018.09.001>
- Al-Breiki, M., & Bicer, Y. (2020). Comparative cost assessment of sustainable energy carriers produced from natural gas accounting for boil-off gas and social cost of carbon. *Energy Reports*, 6, 1897–1909. <https://doi.org/10.1016/j.egy.2020.07.013>
- Alboshmina, N. A. H. (2019). *Ammonia cracking with heat transfer improvement technology*. 1–165. <https://orca.cardiff.ac.uk/126553/1/2019AlboshminaNAPhD.pdf>
- Altfeld, K., & Pinchbeck, D. (n.d.). *Admissible hydrogen concentrations in natural gas systems*. www.gas-for-energy.com
- Armijo, J., & Philibert, C. (2020). Flexible production of green hydrogen and ammonia from variable solar and wind energy: Case study of Chile and Argentina. *International Journal of Hydrogen Energy*, 45(3), 1541–1558. <https://doi.org/10.1016/j.ijhydene.2019.11.028>
- Aziz, M. (2021). *Transportation, and Safety*.
- Bartels, J. R. (2008). A feasibility study of implementing an Ammonia Economy. *Digital Repository @ Iowa State University, December*, 102. <http://lib.dr.iastate.edu/cgi/viewcontent.cgi?article=2119&context=etd>
- Becker, F. G., Cleary, M., Team, R. M., Holtermann, H., The, D., Agenda, N., Science, P., Sk, S. K., Hinnebusch, R., Hinnebusch A, R., Rabinovich, I., Olmert, Y., Uld, D. Q. G. L. Q., Ri, W. K. H. U., Lq, V., Frxqwu, W. K. H., Zklfk, E., Edvhg, L. V, Wkh, R. Q., ... ح, فاطمی. (2015). No 主観的健康感を中心とした在宅高齢者における健康関連指標に関する共分散構造分析Title. In *Syria Studies* (Vol. 7, Issue 1). https://www.researchgate.net/publication/269107473_What_is_governance/link/548173090cf22525dcb61443/download%0Ahttp://www.econ.upf.edu/~reynal/Civilwars_12December2010.pdf%0Ahttps://think-asia.org/handle/11540/8282%0Ahttps://www.jstor.org/stable/41857625
- Bhaskar, A., Assadi, M., & Somehsaraei, H. N. (2020). Decarbonization of the iron and steel industry with direct reduction of iron ore with green hydrogen. *Energies*, 13(3), 1–23. <https://doi.org/10.3390/en13030758>
- Caldera, U., Bogdanov, D., & Breyer, C. (2016). Local cost of seawater RO desalination based on solar PV and wind energy: A global estimate. In *Desalination* (Vol. 385, pp. 207–216). <https://doi.org/10.1016/j.desal.2016.02.004>
- Cesaro, Z., Ives, M., Nayak-Luke, R., Mason, M., & Bañares-Alcántara, R. (2021). Ammonia to power: Forecasting the levelized cost of electricity from green ammonia in large-scale power plants. *Applied Energy*, 282(July 2020). <https://doi.org/10.1016/j.apenergy.2020.116009>
- Cheema, I. I., & Krewer, U. (2018). Operating envelope of Haber-Bosch process design for

- power-to-ammonia. *RSC Advances*, 8(61), 34926–34936.
<https://doi.org/10.1039/c8ra06821f>
- Correa, G., Volpe, F., Marocco, P., Muñoz, P., Falagüerra, T., & Santarelli, M. (2022). Evaluation of levelized cost of hydrogen produced by wind electrolysis: Argentine and Italian production scenarios. *Journal of Energy Storage*, 52, 105014.
<https://doi.org/10.1016/J.EST.2022.105014>
- Department of Energy. (2022). Gaseous Hydrogen Compression . *Hydrogen and Fuel Cell Technologies Office*, i. <https://www.energy.gov/eere/fuelcells/gaseous-hydrogen-compression>
- Energ, D., Secretar, R., Energ, P., & Frecuencia, F. T. (2021). *Información adicional Otros recursos de este dataset. 2011, 2009–2010.*
- Eria. (2020). Review of Hydrogen Transport Cost and Its Perspective (Liquefied Hydrogen). *Demand and Supply Potential of Hydrogen Energy in East Asia - Phase 2*, 16(16), 60–89.
[https://www.eria.org/uploads/media/Research-Project-Report/RPR_2020_16/11_Chapter-4-Review-of-Hydrogen-Transport-Cost-\(Liquefied-Hydrogen\)_0801.pdf](https://www.eria.org/uploads/media/Research-Project-Report/RPR_2020_16/11_Chapter-4-Review-of-Hydrogen-Transport-Cost-(Liquefied-Hydrogen)_0801.pdf)
- Fan, Z., & Friedmann, S. J. (2021). Low-carbon production of iron and steel: Technology options, economic assessment, and policy. *Joule*, 5(4), 829–862.
<https://doi.org/10.1016/j.joule.2021.02.018>
- Fang, X., Chen, W., Zhou, Z., & Xu, Y. (2014). *ScienceDirect Empirical models for efficiency and mass flow rate of centrifugal compressors ` le empirique pour l ' efficacite ´ et le de ´ bit massique de Mode compresseurs centrifuges. 1.*
- Gezerman, A. O. (2015). Exergy analysis and purging of an ammonia storage system. *International Journal of Exergy*, 17(3), 335–351.
<https://doi.org/10.1504/IJEX.2015.070502>
- Grouset, D., Ridart, C., Grouset, D., Ridart, C., Energy, L., Together, S., Compression, W., Grouset, D., & Ridart, C. (2019). *Lowering Energy Spending Together With Compression , Storage , and Transportation Costs for Hydrogen Distribution in the Early Market To cite this version : HAL Id : hal-01877835 Chapter 6 Lowering energy spending together with compression , storage and t.*
- Guide, F. A. Q., & Tank, H. (n.d.). *Hydrogen Tank – FAQ Guide. 0*, 1–16.
- Humphreys, J., Lan, R., & Tao, S. (2021). Development and Recent Progress on Ammonia Synthesis Catalysts for Haber–Bosch Process. *Advanced Energy and Sustainability Research*, 2(1), 2000043. <https://doi.org/10.1002/aesr.202000043>
- Ikäheimo, J., Kiviluoma, J., Weiss, R., & Holttinen, H. (2018). Power-to-ammonia in future North European 100 % renewable power and heat system. *International Journal of Hydrogen Energy*, 43(36), 17295–17308. <https://doi.org/10.1016/j.ijhydene.2018.06.121>
- Ingegneria, D., Guccione, R., Di, L., Messa, M., & Massa, G. (2018). *Ilva, tre scenari per la riconversione dello stabilimento.*

- International Renewable Energy Agency (IRENA). (2022). *Global hydrogen trade to meet the 1.5 °C climate goal: Part III – Green hydrogen supply cost and potential*.
- International Renewable Energy Agency, T. (2020). *GREEN HYDROGEN COST REDUCTION SCALING UP ELECTROLYSERS TO MEET THE 1.5°C CLIMATE GOAL H 2 O 2*.
www.irena.org/publications
- IRENA. (2020). Green Hydrogen Cost Reduction. In */publications/2020/Dec/Green-hydrogen-cost-reduction*. */publications/2020/Dec/Green-hydrogen-cost-reduction%0Ahttps://www.irena.org/-/media/Files/IRENA/Agency/Publication/2020/Dec/IRENA_Green_hydrogen_cost_2020.pdf*
- Ishimoto, Y., Voldsund, M., Nekså, P., Roussanaly, S., Berstad, D., & Gardarsdottir, S. O. (2020). Large-scale production and transport of hydrogen from Norway to Europe and Japan: Value chain analysis and comparison of liquid hydrogen and ammonia as energy carriers. *International Journal of Hydrogen Energy*, 45(58), 32865–32883.
<https://doi.org/10.1016/j.ijhydene.2020.09.017>
- Johnston, C., Ali Khan, M. H., Amal, R., Daiyan, R., & MacGill, I. (2022). Shipping the sunshine: An open-source model for costing renewable hydrogen transport from Australia. *International Journal of Hydrogen Energy*, 47(47), 20362–20377.
<https://doi.org/10.1016/j.ijhydene.2022.04.156>
- Kim, J., Huh, C., & Seo, Y. (2022). End-to-end value chain analysis of isolated renewable energy using hydrogen and ammonia energy carrier. *Energy Conversion and Management*, 254(December 2021), 115247.
<https://doi.org/10.1016/j.enconman.2022.115247>
- Kim, K., Roh, G., Kim, W., & Chun, K. (2020). A preliminary study on an alternative ship propulsion system fueled by ammonia: Environmental and economic assessments. *Journal of Marine Science and Engineering*, 8(3). <https://doi.org/10.3390/jmse8030183>
- Makhloufi, C., & Kezibri, N. (2021). Large-scale decomposition of green ammonia for pure hydrogen production. *International Journal of Hydrogen Energy*, 46(70), 34777–34787.
<https://doi.org/10.1016/j.ijhydene.2021.07.188>
- Ministerio de Energía. (2019). *Adjudicaciones del Programa RenovAr*. 9–10.
<https://public.tableau.com/profile/datosenergia#!/vizhome/AdjudicacionesRenovARMINEMArgentina/AdjudicacionesRenovArArgentina>
- Morgan, E. R. (2013). Techno-economic feasibility study of ammonia plants powered by offshore wind. *University of Massachusetts - Amherst, PhD Dissertations*, 432.
http://scholarworks.umass.edu/open_access_dissertations/697
- Nayak-Luke, R. M., Forbes, C., Cesaro, Z., Bañares-Alcántara, R., & Rouwenhorst, K. H. R. (2021). Techno-Economic Aspects of Production, Storage and Distribution of Ammonia. In *Techno-Economic Challenges of Green Ammonia as an Energy Vector*. Elsevier Inc.
<https://doi.org/10.1016/b978-0-12-820560-0.00008-4>
- Nel Hydrogen. (n.d.). *Atmospheric Alkaline Electrolyser | Nel Hydrogen*. Retrieved August 9,

- 2022, from <https://nelhydrogen.com/product/atmospheric-alkaline-electrolyser-a-series/>
- Niermann, M., Timmerberg, S., Drünert, S., & Kaltschmitt, M. (2021). Liquid Organic Hydrogen Carriers and alternatives for international transport of renewable hydrogen. *Renewable and Sustainable Energy Reviews*, 135(August 2020), 110171. <https://doi.org/10.1016/j.rser.2020.110171>
- Noh, W., Park, S., Kim, J., & Lee, I. (2022). Comparative design, thermodynamic and techno-economic analysis of utilizing liquefied natural gas cold energy for hydrogen liquefaction processes. *International Journal of Energy Research*, 46(9), 12926–12947. <https://doi.org/10.1002/er.8064>
- Nordio, M., Wassie, S. A., Van Sint Annaland, M., Pacheco Tanaka, D. A., Viviente Sole, J. L., & Gallucci, F. (2021). Techno-economic evaluation on a hybrid technology for low hydrogen concentration separation and purification from natural gas grid. *International Journal of Hydrogen Energy*, 46(45), 23417–23435. <https://doi.org/10.1016/j.ijhydene.2020.05.009>
- of Energy, U. S. D. (2006). Potential Roles of Ammonia in a Hydrogen Economy. *Energy*, January 2006, 1–23. https://www.hydrogen.energy.gov/pdfs/nh3_paper.pdf
- Osman, O., Sgouridis, S., & Sleptchenko, A. (2020). Scaling the production of renewable ammonia: A techno-economic optimization applied in regions with high insolation. *Journal of Cleaner Production*, 271, 121627. <https://doi.org/10.1016/j.jclepro.2020.121627>
- Ovcina, J. (2021). Kawasaki Heavy Industries builds the world's 1st liquefied hydrogen receiving terminal. *Offshore Energy*, 1–6. <https://www.offshore-energy.biz/kawasaki-heavy-industries-builds-the-worlds-1st-liquefied-hydrogen-receiving-terminal/>
- Ozawa, A., Inoue, M., Kitagawa, N., Muramatsu, R., Anzai, Y., Genchi, Y., & Kudoh, Y. (2017). Assessing Uncertainties of Well-To-Tank Greenhouse Gas Emissions from Hydrogen Supply Chains. *Sustainability*, 9(7), 1101. <https://doi.org/10.3390/su9071101>
- Qualenergia, R. (2019). *CO2, quanto sono sporchi i mix elettrici dei diversi Stati Ue | QualEnergia.it*. <https://www.qualenergia.it/articoli/co2-quanto-sono-sporchi-i-mix-elettrici-dei-diversi-stati-ue/>
- Razionale, M., & Mario, M. (1958). *M I S S I , L I*.
- Salmon, N., Bañares-Alcántara, R., & Nayak-Luke, R. (2021). Optimization of green ammonia distribution systems for intercontinental energy transport. *IScience*, 24(8). <https://doi.org/10.1016/j.isci.2021.102903>
- Seo, Y., & Han, S. (2021). Economic evaluation of an ammonia-fueled ammonia carrier depending on methods of ammonia fuel storage. *Energies*, 14(24). <https://doi.org/10.3390/en14248326>
- Shi, X., Liao, X., & Li, Y. (2020). Quantification of fresh water consumption and scarcity footprints of hydrogen from water electrolysis: A methodology framework. *Renewable Energy*, 154, 786–796. <https://doi.org/10.1016/j.renene.2020.03.026>

- Sophie, A., & Ness, S. (2021). *Conceptual Design of Ammonia-fueled Vessels for Deep-sea Shipping*. June.
- Stolzenburg, K., Berstad, D., Decker, L., Elliott, A., Haberstroh, C., Hatto, C., Klaus, M., Mortimer, N. D., Mubbala, R., Mwabonje, O., Nekså, P., Quack, H., Rix, J. H. R., Seemann, I., & Walnum, H. T. (2013). Efficient Liquefaction of Hydrogen: Results of the IDEALHY Project. *Proceedings of the Energie – Symposium, Stralsund/Germany, November, November, 1–8*. https://www.idealhy.eu/uploads/documents/IDEALHY_XX_Energie-Symposium_2013_web.pdf
- Studio di impatto ambientale di un grande impianto di dissalazione ad osmosi inversa : focus su recupero energetico , scarichi a mare e LCA*. (2013).
- Techno-economic assessment of*. (2020). March.
- Teknik, E. I. (2021). *An Industrial Perspective on Ultrapure Water Production for Electrolysis*.
- Tractebel Engineering, & Inicio. (2017). *Early business cases for H2 in energy storage and more broadly power to H2 applications*. June.
- Wijayanta, A. T., Oda, T., Purnomo, C. W., Kashiwagi, T., & Aziz, M. (2019). Liquid hydrogen, methylcyclohexane, and ammonia as potential hydrogen storage: Comparison review. *International Journal of Hydrogen Energy, 44*(29), 15026–15044. <https://doi.org/10.1016/j.ijhydene.2019.04.112>
- Winnes, H., & Fridell, E. (2009). Particle emissions from ships: Dependence on fuel type. *Journal of the Air and Waste Management Association, 59*(12), 1391–1398. <https://doi.org/10.3155/1047-3289.59.12.1391>
- Worldsteel. (2021). *World Steel in Figures Report 2021*. 1–29. <https://www.worldsteel.org/en/dam/jcr:976723ed-74b3-47b4-92f6-81b6a452b86e/World%2520Steel%2520in%2520Figures%25202021.pdf>
- Young, A. F., Villardi, H. G. D., Araujo, L. S., Raptopoulos, L. S. C., & Dutra, M. S. (2021). Detailed Design and Economic Evaluation of a Cryogenic Air Separation Unit with Recent Literature Solutions. *Industrial and Engineering Chemistry Research, 60*(41), 14830–14844. <https://doi.org/10.1021/acs.iecr.1c02818>

Chapter 3

Economic analysis

3.1 Description of used parameters

The aim of the economic analysis is to calculate the levelized cost of hydrogen, LCOH, to compare the production, storage and transport costs of the two considered carriers, ammonia and liquid hydrogen. The levelized cost of hydrogen is an economic indicator very important in the feasibility study, as it allows the calculation of the actual value of investment and operating costs of a plant over its lifetime (Lazard, 2021). In particular, LCOH represents an economic assessment of the average cost required to finance and maintain a hydrogen production, storage, and transport supply chain during its lifetime, in relation to the total amount of hydrogen generated during the same time interval. The levelized cost of hydrogen hence constitutes a reference value for the selling price per unit of H₂ produced. It represents product tariff at which an investor would precisely break even after paying the required rates on return on capital, given the costs incurred during the lifetime of a technology. LCOH also makes it possible to compare projects using different technologies, different sizes and different economic parameters. The formula 3.1 is used to calculate LCOH.

$$LCOH \left[\frac{\$}{kgH_2} \right] = \frac{\sum_{t=0}^n \frac{(I+O\&M+E+Other\ Costs)}{(1+r)^t}}{\sum_{t=0}^n \frac{H_2}{(1+r)^t}} \quad (3.1)$$

The levelized cost of hydrogen always considers investment costs, I, and operating and maintenance costs, O&M, while only in some cases does it consider other costs, mainly electricity, E, but also the cost of fuels, refrigeration liquids and materials needed for chemical reactions, such as catalysts.

The fixed costs of the project are the capital expenditure (CAPEX) and the fixed cost of operation and maintenance (OPEX). CAPEX is an investment cost that occurs during the construction of the project before it is commissioned and is expressed in \$/kW of installed capacity. Capital expenditure does not consider financial costs (interest rates) or the financing structure. OPEX is an annual expense divided into fixed and variable parts. Fixed OPEX is expressed in \$/kW of installed capacity and includes expenses such as plant management, land rent, taxes, administrative costs and plant maintenance. Variable OPEX, on the other hand, is

expressed in \$/KWh (Sustainable Energy Handbook, 2016), includes the costs of electricity, chemicals, process water, labour costs, fuel costs and unexpected repair costs. The construction of the plant has been assumed to occur during year zero, so CAPEX is only present during this year, while fixed and variable OPEX costs begin from the year one until the last year of the project.

The sum of all costs over the life of the plant is actualized using the discount rate r , which allows the value of an investment to be estimated based on expected future cash flows. The discount rate plays a key role in the valuation of an investment, it must be chosen considering the real, risk-free discount rate referred to other possible, alternative investments, inflation over the entire life of the project reflecting the loss of purchasing power of the invested capital over the same period, and a premium to be allocated to equity as a measure of the rate of return expected from a risky investment. Commonly the Weighted Average Cost of Capital (WACC), which is the average cost that is paid for capital borrowed or sold, can be used as the discount rate, or values used in similar projects can be applied (Hayes & Scott, 2011). Future cash flows are reduced by the discount rate. A lower discount rate leads to a higher present value. This means that when the discount rate is higher, money in the future will be worth less than at present. The following parameters have been considered for the calculation of LCOH:

- Discount Rate, r : 7 %
- Plants Lifetime, n : 20 years (with a few exceptions, such as electrolyser stacks and compressors)
- Wind Electricity Cost: \$42/MW
- Grid Electricity Cost (Argentina): \$60/MWh
- Grid Electricity Cost (Italy): \$224/MWh

In the following paragraphs, the economic calculations for each component of the NH_3 and LH_2 process are addressed.

3.2 Ammonia supply chain

The final levelized cost of the final hydrogen delivered to the steel industry is obtained by summing up all levelized costs of the hydrogen and nitrogen production processes, ammonia synthesis and liquefaction, storage, transport, cracking and purification. To calculate the LCOH for hydrogen production, it is necessary to calculate the costs of electrolysis and desalination.

3.2.1 Electrolyser

For the calculation of the LCOH of the electrolyser, the CAPEX, the fixed OPEX and the cost of electricity have been considered. According to the paper (International Renewable Energy Agency, 2020), the CAPEX of the alkaline electrolyser varies between \$500 - \$1000/kW, for systems larger than 10 MW, while the nominal cost of the stacks is \$270/kW. The investment cost of the PEM is higher, varying between 700 - 1400 \$/kW, and the cost of the stacks is 400 \$/kW. The paper (Tractebel Engineering, 2017) considers a CAPEX cost of \$750/kW for systems larger than 20 MW, and OPEX of 4 % of CAPEX for alkaline electrolysers, while large PEMs are characterised by a CAPEX of \$1,200/kW. The following values have been considered in this work.

<i>Option</i>	<i>Alkaline</i>	<i>PEM</i>
<i>CAPEX System [\$/kW]</i>	900	1100
<i>CAPEX stack replacement [\$/kW]</i>	360	440
<i>CAPEX auxiliares [\$/kW]</i>	540	660
<i>OPEX [% of CAPEX sistema]</i>	4,0 %	4,0 %
<i>OPEX [\$/kW]</i>	36	44

Table 3.1: CAPEX and OPEX considered for alkaline and PEM electrolysers

The costs presented in the table 3.1 refer to scenario 1, relating to the annual production of 227.006.184 kgH₂. In scenario 2, production increases to 555.884.883 kgH₂, resulting in an increase in electrolyser capacity. A scaling factor has been considered that correlates the investment cost with the plant size. The formula 3.2 has been adopted, and the exponent n has been taken as 0,9. S₀ and S₁ are the electrolyser powers in scenario 2 and 1, C₀ and C₁ represent the investment costs.

$$C_1 = C_0 * \left(\frac{S_1}{S_0}\right)^n \quad (3.2)$$

The CAPEX in scenario 2 becomes \$823/kW for the alkaline electrolyser and \$1006/kW for the PEM electrolyser.

The power output of the electrolysis plant depends on the capacity factor considered, resulting in investment and operating costs. The cost of electricity is also calculated by multiplying the specific cost of energy, which depends on the grid mix used, by the total amount of energy used in a year. Stack life is 80.000 hours for alkaline electrolysers and 65.000 for PEMs; when this

limit is exceeded, the stack must be replaced with a new unit. For the calculation of the hydrogen produced during the life of the system, the degradation rate has been considered, which for alkaline electrolyzers is 0,013 % per 1000 hours of operation, and for PEMs is 0,025 %/1000 h. For the calculation of LCOH it has been assumed that hydrogen production starts in year 1, as year 0 is considered for the construction of the plant. The electricity cost of the energy mix is calculated using the formula 3.3.

$$Electricity\ Cost\ \left[\frac{\$}{kWh}\right] = \frac{Grid\ Cost\ \left[\frac{\$}{kWh}\right]*CF_{GRID} + Wind\ Cost\ \left[\frac{\$}{kWh}\right]*CF_{WIND}}{CF_{GRID} + CF_{WIND}} \quad (3.3)$$

The costs of CAPEX, OPEX and Electricity in the table 3.2 represent the input values in equation 3.1 which allows LCOH to be calculated.

Option	Scenario 1			
	Alkaline		PEM	
	CF 54 %	CF 100 %	CF 54 %	CF 100 %
Power [GW]	2,53	1,37	2,63	1,42
CAPEX Stack [\$]	\$854.735.867	\$461.557.368	\$1.106.351.898	\$597.430.025
CAPEX Auxiliaries [\$]	\$1.421.188.039	\$767.441.541	\$1.791.236.407	\$967.267.660
OPEX System [\$]	\$91.036.956	\$49.159.956	\$115.903.532	\$62.587.907
Electricity Cost [\$]	\$483.144.051	\$578.392.450	\$503.275.053	\$602.492.135

Table 3.2: Electrolyser cost analysis, scenario 1 (NH₃ supply chain)

The CAPEX and OPEX of the system are related to the power of the electrolyser, which depends on the capacity factor, in the mix configuration they decrease by almost half compared to the wind configuration. The cost of electricity increases in the mix energy configuration, as the specific cost per kWh increases compared to the cost of wind power.

In this section the levelized cost of hydrogen production is evaluated, it is relative to the amount of hydrogen produced by the electrolyser during the lifetime of the project. In scenario 1 the annual production is 227.006.184 kg, and in scenario 2 is 555.884.883 kg per year. The purpose is to verify the economic competitiveness of the hydrogen produced. The LCOH of the final product will be discussed later, and refers to the final hydrogen sent to the steel industry, which is much lower than the hydrogen produced in Argentina due to the large inefficiencies and mass losses in the transport and conversion chain, 143.144.352 kg per year in scenario 1, and 355.701.840 kg per year in scenario 2.

The table 3.3 shows the composition of the levelized cost of hydrogen for the four evaluated configurations.

<i>LCOH Composition</i>	<i>Scenario 1</i>			
	Alkaline		PEM	
	CF 54 %	CF 100 %	CF 54 %	CF 100 %
<i>CAPEX Stack [\$ /kg]</i>	0,512	0,382	0,703	0,539
<i>CAPEX Auxiliaries [\$ /kg]</i>	0,592	0,321	0,774	0,421
<i>OPEX System [\$ /kg]</i>	0,418	0,227	0,547	0,297
<i>Electricity Cost [\$ /kg]</i>	2,219	2,670	2,374	2,862
<i>LCOH Electrolyser [\$ /kg]</i>	3,741	3,601	4,398	4,119

Table 3.3: Electrolyser LCOH composition, scenario 1 (NH₃ supply chain)

The choice of electrolyser influences LCOH, as the PEM is characterised by higher investment and operation costs and consumes more electricity than the alkaline electrolyser. The capacity factor does not particularly influence the final cost, as the lower investment cost in the case of grid-wind mix is counterbalanced by the higher cost of electricity. The results show the great importance of the cost of electricity. By varying the price of electricity, or the consumption of the electrolyser, it is possible to strongly influence the LCOH.

The hydrogen production costs slightly diminish in scenario 2, as illustrated in the following table.

<i>LCOH Composition</i>	<i>Scenario 2</i>			
	Alkaline		PEM	
	CF 54 %	CF 100 %	CF 54 %	CF 100 %
<i>Electrolyser Power [GW]</i>	6,19	3,34	6,45	3,48
<i>CAPEX Stack [\$ /kg]</i>	0,468	0,350	0,643	0,493
<i>CAPEX Auxiliaries [\$ /kg]</i>	0,541	0,294	0,708	0,385
<i>OPEX System [\$ /kg]</i>	0,382	0,207	0,500	0,272
<i>Electricity Cost [\$ /kg]</i>	2,219	2,670	2,374	2,862
<i>LCOH Electrolyser [\$ /kg]</i>	3,611	3,521	4,225	4,011

Table 3.4: Electrolyser LCOH composition, scenario 2 (NH₃ supply chain)

The decrease in the levelized cost of hydrogen in scenario 2 is very small despite the scaling factor considered. LCOH decreases by less than \$200/tonH₂ in each configuration, with respect the first scenario.

3.2.2 Desalinator

The reverse osmosis desalination plant uses only electrical energy for operation, which is considered in the economic analysis together with the investment and operating costs. According to (Toth, 2020), the investment cost of an RO plant can vary between 900 and 2500 $\$/\text{m}^3/\text{day}$, in this work the average value of 1700 $\$/\text{m}^3/\text{day}$ has been used. The fixed OPEX costs are 4 % of the investment cost, in particular $\$68/\text{m}^3/\text{day}$. The electricity cost is obtained by multiplying the annual energy consumed by the specific energy cost, which depends on the wind-grid mix selected. The levelized cost of water is calculated by considering the plant's water production during its 20-year life cycle. This value changes with the choice of electrolyser, as the alkaline has a specific water consumption of 15,89 $\text{kgH}_2\text{O}/\text{kgH}_2$, while the PEM consumes 14,3.

The CAPEX, OPEX and electricity cost shown in the table 3.5 are the results of economic calculations and are the input values in the LCOW equation.

Option	Scenario 1			
	Alkaline		PEM	
	CF 54 %	CF 100 %	CF 54 %	CF 100 %
Annual Water Production [tons]	3.608.084	3.608.084	3.247.275	3.247.275
Plant Capacity [m^3/day]	19.069	10.297	17.162	9.267
CAPEX [\\$]	\\$32.416.614	\\$17.504.971	\\$29.174.952	\\$15.754.474
OPEX [\\$]	\\$1.296.665	\\$700.199	\\$1.166.998	\\$630.179
Cost of Electricity [\\$]	\\$378.849	\\$453.536	\\$340.964	\\$408.182
Cost of Water [$\$/\text{m}^3$]	1,312	0,778	1,312	0,778

Table 3.5: Desalinator cost analysis, scenario 1 (NH_3 supply chain)

The cost of water is not influenced by the choice of electrolyser, although the capacity of the RO plant is larger in the case of the alkaline electrolyser. The cost of water is strongly influenced by the capacity factor, it goes from $\$1,312/\text{m}^3$ in the case of wind to $\$0,778/\text{m}^3$ in the case of wind-grid mix, this is due to the decrease of the plant capacity, and consequently the investment cost, which accounts for 64 % of LCOW in the case of wind configuration and 59 % in the case of energy mix configuration. LCOW results are the same in scenario 2.

The calculated water cost is in line with what is reported in the literature. (Toth, 2020) reports a water cost ranging between 0,5 and 1,2 $\$/\text{m}^3$. The paper (Curto et al., 2021) reports a cost

range between 0,45 and 1,72 \$/m³H₂O, for Seawater Reverse Osmosis plants. The paper (Teknik, 2021) calculated a water cost of \$0,669/m³ for a Reverse Osmosis plant. The paper (Fúnez Guerra et al., 2020) uses a water cost of \$2,500/m³ in its study, which is higher than the result obtained in this thesis, but coherent.

3.2.3 Levelized cost of produced hydrogen

LCOH for hydrogen production refers to the costs of the electrolysis plant and the water desalination plant, and it is referred to the hydrogen produced in the electrolysis plant. The graph 3.1 shows LCOH for different case studies.

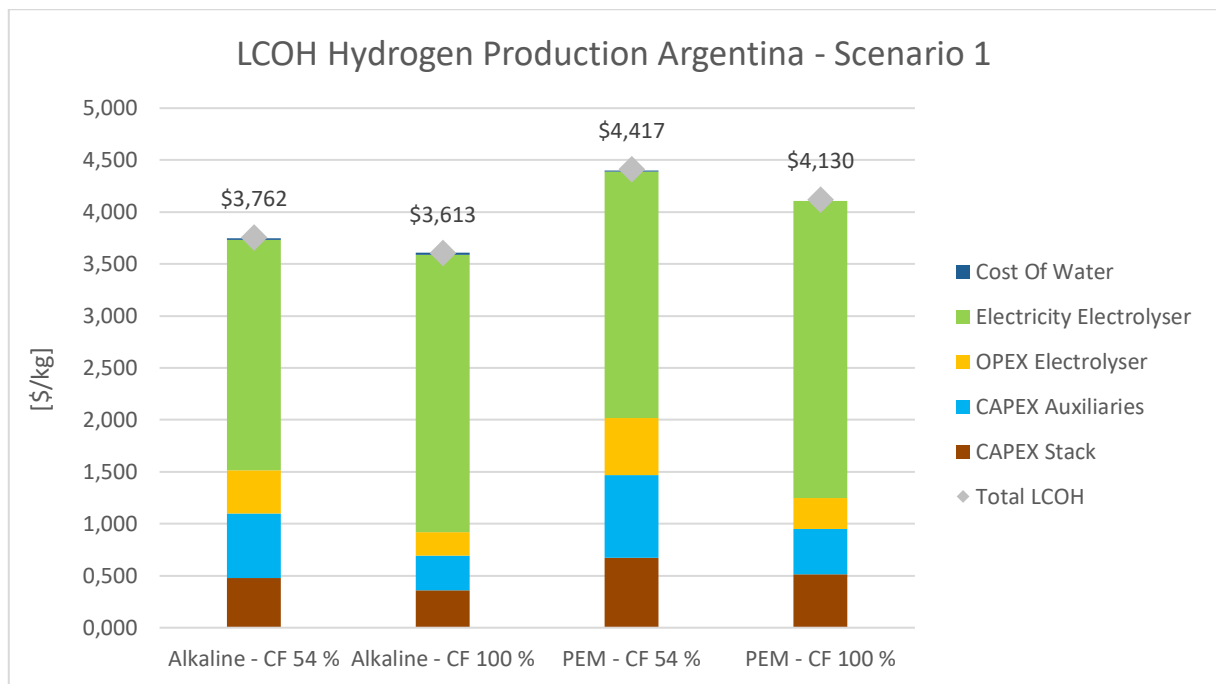


Figure 3.1: Levelized cost of hydrogen production, (NH₃ supply chain)

The cost of producing hydrogen is highly influenced by the cost of electricity, so it depends on the energy supply configuration. The energy mix configuration lowers the cost of energy by roughly \$0,500/kg compared to the wind configuration. On the other hand, the investment and operating costs are higher in the wind configuration, which is due to the larger power requirement of the electrolysis plant. The cost of water is almost negligible to the total cost of hydrogen.

The selection of PEM electrolyser causes the installation cost to increase respect using an alkaline electrolyser, this is due to the higher specific cost of investment. Consequently, operating costs also increase. The difference in H₂ cost production between alkaline and PEM

electrolyser is \$0,654/kgH₂ in the case of the wind configuration and \$0,515/kgH₂ in the case of the mix configuration.

The most cost-effective configuration involves alkaline and energy mix, LCOH is \$3,613/kgH₂, while the most expensive configuration is for PEM and wind power, resulting in an LCOH of \$4,417/kgH₂.

In scenario 2, LCOH related to hydrogen production are slightly lower respect the values calculated in scenario 1, the most economic and the most expensive configurations remain the same of scenario 1, LCOH of alkaline electrolyser and wind-grid energy mix is \$3,533/kgH₂, while the LCOH related to PEM and wind energy is \$4,244/kgH₂.

LCOH calculated in this paper agrees with values presented in the literature. According to the analysis of (Dinh et al., 2021), who calculated the production of green hydrogen with electricity produced offshore, LCOH of green hydrogen is €5,000/kgH₂, the paper (Hou et al., 2017) utilizes a hydrogen price ranging between 2 and 9 €/kg for his study in Denmark. The paper (Nagasawa et al., 2019) uses a green hydrogen price between 3 and 4 \$/kg in its study. The paper (Babarit et al., 2018) calculates a LCOH between 3,5 and 5,7 \$/kg in the long run. Furthermore, the study carried out by (Correa et al., 2022) on a case study similar to the one carried out in this work obtains a levelized cost of hydrogen produced in Argentina by wind energy of €4,570/kgH₂.

3.2.4 Hydrogen compressor

The calculation of the levelized cost of hydrogen in the case of the compressor involves the calculation of the CAPEX, the fixed OPEX and the cost of electricity. The investment cost has been calculated using the formula 3.4, provided by (Tractebel Engineering, 2017), which is divided into site cost, that depends on the capacity Q, and compression system cost, that depends on the capacity Q, the compression ratio P_{out}/P_{in}, and the output pressure P_{out}.

$$CAPEX = A \left(\frac{Q}{Q_{ref}} \right)^a + B \left(\frac{Q}{Q_{ref}} \right)^b * \left(\frac{P_{out}}{P_{in}} \right)^c * \left(\frac{P_{out}}{P_{ref}} \right)^d \quad (3.4)$$

The capacity Q of the compressor plant is expressed in kg/h. The parameters of the equation are given in the table 3.6.

<i>Parameter</i>	<i>Value</i>	<i>Unit</i>
<i>A</i>	100.000	\$
<i>B</i>	300.000	\$
<i>a</i>	0,66	-
<i>b</i>	0,66	-
<i>c</i>	0,25	-
<i>d</i>	0,25	-
<i>Qref</i>	50	kg H ₂ /h

Table 3.6: Compressor CAPEX equation's parameter

The OPEX of the compressor is 4 % of the CAPEX, while the electricity cost is calculated by multiplying the specific cost of the wind-grid mix by the total amount of electricity consumed annually.

The CAPEX, OPEX and energy cost results shown in the table 3.7 have been calculated using the formulas described and are used as input data in the equation to calculate LCOH.

<i>Option</i>	<i>Scenario 1</i>			
	<i>Alkaline</i>		<i>PEM</i>	
	CF 54 %	CF 100 %	CF 54 %	CF 100 %
<i>Plant Capacity [kg/h]</i>	49.903	26.948	49.903	26.948
<i>Compression Ratio</i>	6,67	6,67	6,67	6,67
<i>CAPEX [\$]</i>	\$41.105.018	\$27.369.995	\$41.105.018	\$27.369.995
<i>OPEX [\$]</i>	\$1.644.201	\$1.094.800	\$1.644.201	\$1.094.800
<i>Cost of Electricity [\$]</i>	\$12.535.102	\$15.006.308	\$11.804.512	\$14.131.687

Table 3.7: H₂ Compressor cost analysis, scenario 1

The CAPEX and OPEX of the compressor depend on the capacity of the system, in wind configuration they have a higher value. The investment cost for the Alkaline and PEM configurations is the same, since the formula used for CAPEX is based on the ratio of the output pressure to the input pressure. The electricity cost is slightly higher in the alkaline configuration, this is due to the fact that more energy is required for compression, 1,25 kWh/kgH₂ versus 1,18 kWh/kgH₂ in the PEM configuration.

The LCOH calculation refers to the final hydrogen delivered over the lifetime of the plant. According to (Correa et al., 2022), the life of the hydrogen compressor is 10 years, which means

that the investment cost must be repeated in the eleventh year to ensure a total project life of 20 years.

The compressor is an energy-intensive component, and most of the levelized cost of hydrogen is due to energy costs. The compression LCOH is \$0,140/kgH₂ for the alkaline configurations and drops to \$0,134/kgH₂ in the PEM configurations.

The capacity factor has small influence on the levelized cost of hydrogen, as the higher investment cost in the wind configuration is balanced by the lower cost of energy compared to the wind-grid mix configuration, in particular \$42/MWh compared to \$50/MWh.

In scenario 2, the LCOH values are slightly lower than in scenario 1, this is due to the investment cost that does not grow in a linear trend with respect the quantity of hydrogen processed.

3.2.5 Hydrogen storage buffer

The hydrogen storage tank is used to separate the production of hydrogen from the synthesis of ammonia. The electrolyser is able to follow the load profile of wind power and operate at loads below the nominal load, while the ammonia synthesis process operates continuously at a nominal load, which is why it is supplied by a wind-grid mix that guarantees a capacity factor of 100 %. The size of the tank must be sufficient to ensure a continuous supply of hydrogen for the Haber-Bosch process. If a supply from the wind-grid mix would be adopted, there would be no need for the storage facility.

The storage tank does not use energy to operate, the levelized cost of hydrogen depends only on the investment cost and fixed operating costs. The paper (Tzimas et al., 2003) reports costs of pressure tanks that increase non-linearly with increasing storage pressure. A pressure tank of 140 bar has a specific cost of \$400/kg, increasing the pressure to 540 bar the price becomes \$2100/kg. (Parks et al., 2014) indicates a storage cost of compressed hydrogen at 250 bar of \$450/kg. In this paper, the CAPEX provided in (Tractebel Engineering, 2017) has been adopted, which is \$470/kg for a pressure of 200 bar. The same paper identifies an OPEX of 2 % of the CAPEX, and a plant life of 30 to 40 years. In scenario 2 a scaling factor has been considered, using equation 3.2 and considering an exponent of 0,9, a specific CAPEX of \$430/kgH₂ has been calculated.

The storage CAPEX is calculated by multiplying the specific investment cost by the capacity of the storage tank. The calculation of the storage tank capacity is explained in chapter 2.3.5.

The values of CAPEX, OPEX and energy cost in the table 3.8 are the input values in equation 3.1 for calculating LCOH.

Option	Scenario 1		Scenario 2	
	CF 54 %	CF 75 %	CF 54 %	CF 75 %
Tank Size [kg]	1.101.855	431.161	2.698.186	1.055.812
Hours of Storage	22,08	12	22,08	12
CAPEX [\$]	\$517.872.079	\$202.645.596	\$1.160.219.794	\$453.999.050
OPEX [\$]	\$10.357.442	\$4.052.912	\$23.204.396	\$9.079.981

Table 3.8: Economic analysis of compressed hydrogen storage tank

The cost of hydrogen storage is strongly dependent by the capacity factor since it influences the size of the tank. In the wind configuration, the buffer has a size of more than 1000 tonnes of H₂, as it must guarantee storage for 22 hours. In the case of wind-grid supply with 100 % CF there is no need for a hydrogen buffer, so LCOH is not affected by the intermediate storage cost.

The levelized cost of hydrogen, referring to the amount of final hydrogen delivered to the steel plant during the entire project life for the wind configuration is \$0,414/kgH₂ in scenario 1, while in scenario 2 it decreases to \$0,373/kgH₂.

3.2.6 Air separation unit

Cryogenic ASU produces nitrogen through cryogenic distillation, uses electricity to compress the air and cool it, as well as using heat exchangers with coolant to bring the nitrogen and oxygen to their respective boiling points.

In the economic analysis for the LCON calculation, CAPEX, OPEX, which also includes the cost of the refrigerant, and the cost of electricity have been considered. The investment cost has been estimated from the figure of (Morgan, 2013), who calculated a specific CAPEX of \$1500/kgN₂/h. To discount the value to the year 2022, the following formula has been applied, which relates the investment cost to the cost index that adjusts the value considering the effect of time. The indices are taken from the Chemical Engineering Plant Cost Index (CEPCI) scale.

$$\frac{C_1}{C_0} = \frac{I_1}{I_0} \quad (3.5)$$

The I₁ index refers to the year 2022, and is equal to 797,6, while the I₀ index refers to 2013, the year in which the benchmark has been calculated, and is equal to 567,3. The discounted

investment cost C_1 is therefore equal to \$2109/kgN₂/h. This value is referred to scenario 1. The equation 3.2 has been used to calculate the specific CAPEX for the scenario 2, always using a cost exponent equal to 0,9. The CAPEX in scenario 2 is equal to \$1928/kgN₂/h. This values are in accordance also with the value proposed in the paper (Cesaro et al., 2021), which is 1450 \$/kgN₂/h. Operating costs are considered to be 4 % of CAPEX, in accordance with (UMAS, 2020). For the electricity calculation, the grid-wind mix cost of \$50/MWh has been multiplied by the electricity consumed annually. The cost of electricity does not change because for ASU and the others plant in the NH₃ production chain the CF is assumed to be 100 %, to ensure the continuity of production.

The levelized cost of nitrogen is calculated on the basis of the nitrogen produced during the life of the plant. The CAPEX, OPEX and energy cost results shown in the table 3.9 have been calculated using the formulas described and are used as input data in the equation to calculate LCON.

<i>Option</i>	<i>Scenario 1</i>	<i>Scenario 2</i>
<i>Annual Nitrogen Produced [tons/y]</i>	1.051.902	2.575.861
<i>Plant Capacity [kg/h]</i>	124.870	305.776
<i>CAPEX [\$]</i>	\$263.342.224	\$589.554.226
<i>OPEX [\$]</i>	\$10.533.689	\$23.582.169
<i>Cost of Electricity [\$]</i>	\$21.155.851	\$51.805.715
<i>LCON [\$/kgN₂]</i>	0,0538	0,0509

Table 3.9: ASU cost analysis, scenario 1 and 2

The levelized cost of nitrogen is \$53,8/tonneN₂in scenario 1 and it slightly decrease to \$50,9/kgN₂in scenario 2. The paper (Ebrahimi et al., 2015) estimated a production cost of N₂ of between \$10 and \$30 per tonne of nitrogen, which is lower than the value calculated in this thesis. The value of LCON calculated using the economic data for the cryogenic distillation plant described in the paper (Young et al., 2021) is \$0,1833/kgN₂, which is significantly higher than the value calculated in this paper, this is due to the fact that the plant considered is designed for the production of both nitrogen and oxygen and is more complex and energy intensive.

The article (EU Nitrogen Market Report, 2022) reports the export and import prices of nitrogen in EU countries, they varied between 0,1 and 0,2 \$/m³ in 2021, which considering the nitrogen density of 1,251 kg/m³, is equivalent to 0,08, and 0,16 \$/kgN₂, values in line with the cost of nitrogen calculated in this paper.

For the calculation of the levelized cost of hydrogen, nitrogen production costs are referred to the final hydrogen produced for the steel plant. In this case, LCOH is \$0,395/kgH₂ in scenario 1, and \$0,368/kgH₂ in scenario 2.

3.2.7 Nitrogen compressor

The nitrogen compressor is present in the ammonia production chain after the ASU, its task is to compress the nitrogen to a pressure of 200 bar for mixing with hydrogen to form the syngas that enters the ammonia synthesis plant. As explained in section 2.3.7, a centrifugal air compressor is used to compress the nitrogen.

The calculation of the LCON includes investment, operating and electricity costs. For the investment cost, the value presented in the document (Mongird et al., 2020) of \$130/kW has been considered. This cost is for the year 2012, and has been discounted to the year 2022 using formula 3.5, resulting in \$183/kW. To calculate the CAPEX, the specific investment cost is to be multiplied by the compressor power, which is calculated by dividing the annual energy consumed by the number of annual hours and the capacity factor of the compressor. The operating costs have been assumed to be 4 % of the CAPEX, as for the hydrogen compressor. The electricity cost is obtained by multiplying the electricity mix price of \$50/MWh by the electricity consumed annually. The life of the compressor is less than 20 years, as reported in the literature. The study carried out by (Sonavane et al., 2015) shows that compressor components are subject to low and high cycle fatigue, erosion, corrosion, creep, accumulated stress and damage, resulting in performance degradation that can lead to failure. In accordance with the paper (Air Compressor Purchasing Guide, 2015) a life of 15 years has been considered, which implies an additional investment cost during the 16th year of the project.

The table 3.10 shows the economic calculations for the nitrogen compressor. The CAPEX, OPEX and energy cost results shown in the table have been calculated using the formulas described and are used as input data in the equation to calculate LCON.

<i>Option</i>	<i>Scenario 1</i>	<i>Scenario 2</i>
<i>Compressor Power [kW]</i>	21.969	53.796
<i>CAPEX [\$]</i>	\$4.015.338	\$9.832.620
<i>OPEX [\$]</i>	\$160.614	\$393.305
<i>Electricity Cost [\$]</i>	\$9.289.171	\$22.747.001

Table 3.10: Nitrogen compressor cost analysis, scenario 1 and 2

The levelized cost of compressing N₂, referred to the final hydrogen delivered to steel industry is very low, at \$69,6/ton N₂, and is strongly influenced by the cost of electricity, which accounts for 93 %. Since this cost is negligible compared to the others, it can be considered within the cost of nitrogen production.

3.2.8 Haber-Bosch plant

The ammonia synthesis plant converts the syngas of H₂ and N₂ into NH₃ in the presence of the Fe₃O₄ catalyst. The plant does not need thermal energy since the input syngas has a sufficient temperature for the reaction to happen. The levelized cost of ammonia includes the investment cost, relative to the first year of the project, the operating costs, the cost of the electricity needed to recompress the unreacted syngas, and the cost of the hematite.

The investment cost is related to the plant capacity and can vary between \$3000/kgNH₃/h and \$4500/kgNH₃/h, as reported by (Ikäheimo et al., 2018), which also adopts an operating cost of 2 % of CAPEX. The paper (Morgan, 2013) shows a graph relating the investment cost of the synthesis plant to its capacity. For a plant with a capacity of more than 500 tonNH₃/day, the reported cost is \$180.000/tonNH₃/day, and refers to 2010. Using formula 3.5, the specific cost is discounted, which becomes \$260.654/tonNH₃/day. The study carried out by (Cesaro et al., 2021) takes into account 3300 \$/kgNH₃/h as the investment cost.

In this work the value of \$3000/kgNH₃/h has been considered, and the operating costs are considered to be 4 % of the CAPEX. Also (Armijo & Philibert, 2020) considers the same paper in his study. For scenario 2 the scale factor is considered, adopting the scale exponent equal to 0,9. The specific CAPEX in scenario 2 is \$2743/kgNH₃/h. The capacity of the synthesis plant can be calculated by dividing the annually produced ammonia by the capacity factor of the plant and the number of annual hours.

According to the paper (Fúnez Guerra et al., 2020), the life of the catalytic bed is 80.000 h, after which it must be replaced. The replacement cost is 30 % of the initial investment cost. In this work, the replacement has been considered to occur in the eleventh year of the project life. For the cost of electricity, the grid wind mix specific cost of \$50/MWh has been considered. For magnetite, the current market price of \$114 per tonne has been used.

LCOA is related to the total amount of ammonia synthesised during the life of the plant, which is 20 years. The CAPEX, OPEX and energy cost results shown in the table 3.11 have been calculated using the formulas described and are used as input data in the equation to calculate LCOA.

<i>Option</i>	<i>Scenario 1</i>	<i>Scenario 2</i>
<i>Ammonia Flow Rate [kg/h]</i>	148.840	364.475
<i>CAPEX [\$]</i>	446.521.171	999.646.117
<i>OPEX [\$]</i>	17.860.847	39.985.845
<i>Electricity Cost [\$]</i>	5.919.307	14.494.994
<i>Catalyst Cost [\$]</i>	2.858.736	7.000.373
<i>LCOA [\$/kgNH₃]</i>	0,0597	0,0551

Table 3.11: Ammonia synthesis plant economic analysis, scenarios 1 and 2

The LCONH₃ of ammonia production is \$59,7/tonNH₃ in scenario 1 and it slightly decreased in scenario 2 to \$55,1/tonNH₃. Most of the costs are related to CAPEX, which accounts for about 65 % of the final cost. Variable operating costs are low as electricity is only used for syngas recompression, and hematite has an economic market price.

The contribution of the Haber-Bosch process to the LCOH of the final hydrogen produced is \$0,523/kgH₂ in scenario 1, and \$0,476/kgH₂ in scenario 2.

3.2.9 Levelized cost of ammonia production process

The total investment cost for the green ammonia production process is the sum of the CAPEX of the plants involved. The pie chart 3.2 compares the weight of the investment costs of each plant for the cheapest configuration in scenario 1, which includes the alkaline electrolyser and the complete integration of the electricity grid into the energy mix. The total CAPEX is \$1,99 billion.

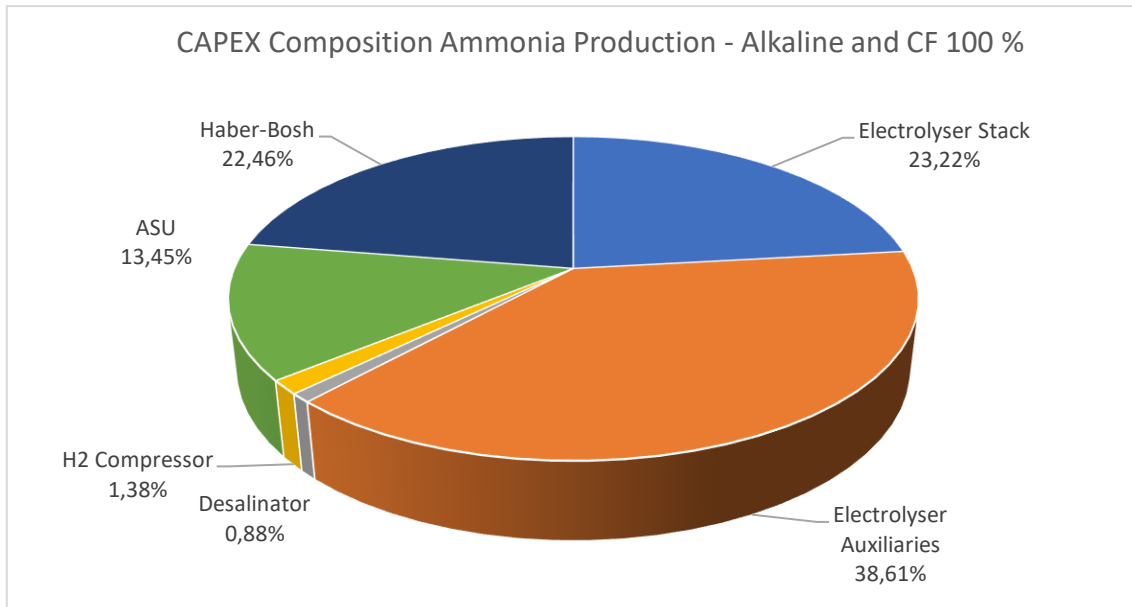


Figure 3.2: CAPEX composition of ammonia production processes for cheapest configuration

Slightly more than 60 % of the total investment cost is related to the electrolyser, the Haber-Bosch plant accounts for one fourth of the investment, and the ASU has a weight of 13,5 %. The compressor and desalinator have a negligible weight in the total costs.

The following graph shows the composition of CAPEX in the most expensive configuration in scenario 1, which includes PEM and wind energy. In this configuration, the total investment cost rises to \$4,2 billion.

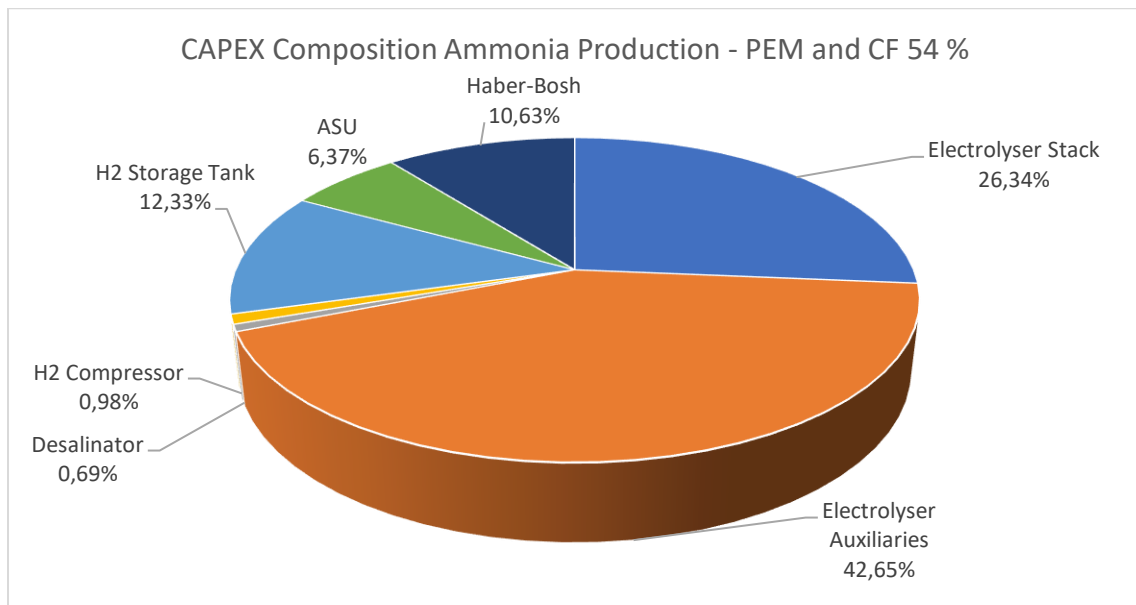


Figure 3.3: CAPEX composition of ammonia production processes for most expensive configuration

The PEM is characterised by higher investment cost respect alkaline electrolyser, in this configuration the electrolyser CAPEX accounts for 69 % of the total investment. With the wind

configuration there is also contribution of the hydrogen buffer, which was not present in the previous configuration, and accounts for 12,3 % of total investment. The CAPEX of the Haber-Bosch and the ASU remain the same as in the previous case, since they are independent of the configuration selected.

The following graphs aim to show the LCOH construction of the ammonia production process, including all the plants involved. The LCOH calculation is referred to the final hydrogen provided to the steel industry during the whole lifetime of the project, that is set to 20 years. The annual hydrogen delivered is 143.144.352 kg in scenario 1 and 355.701.840 kg in scenario 2.

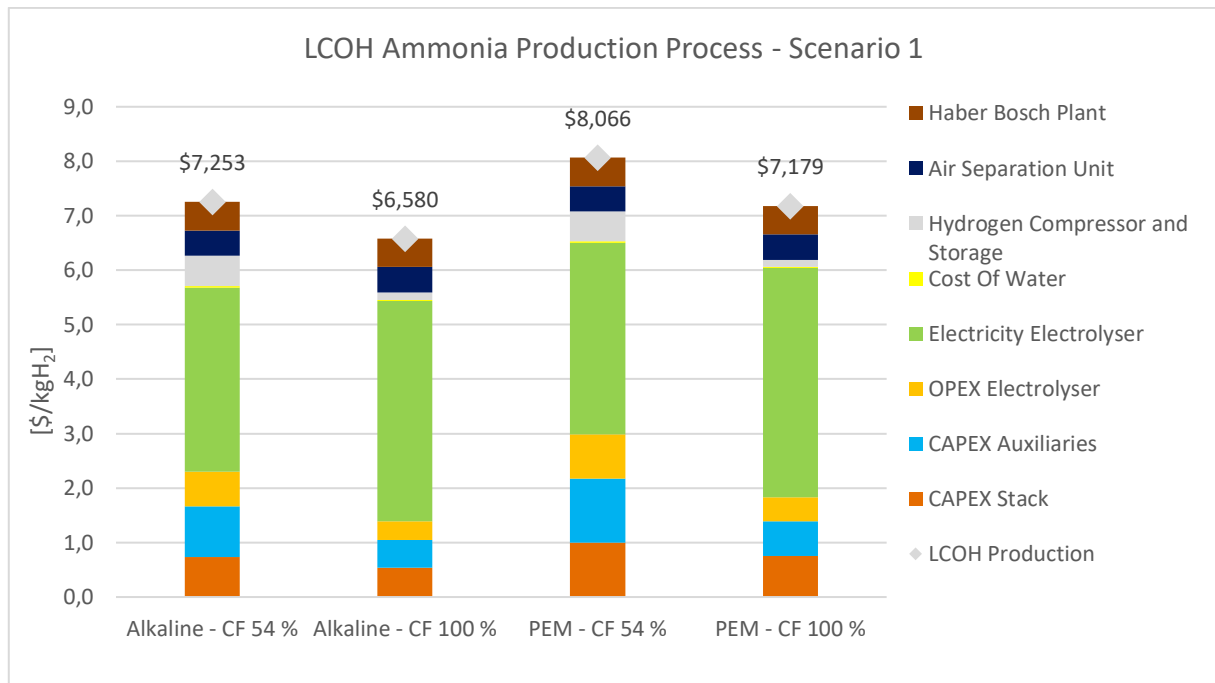


Figure 3.4: Levelized cost of final hydrogen related to ammonia production process, scenario 1

The levelized cost of hydrogen relative to ammonia production is very high, this is due to the inefficiencies of the transport and reconversion process, forcing an overproduction of hydrogen and ammonia of more than 50 %. Most of the cost is related to the production of hydrogen, in particular the energy consumed by the electrolyser, which exceeds \$3,500/kgH₂ in each configuration.

The processes that are influenced by the capacity factor, apart from hydrogen production, are hydrogen compression and storage CGH₂. In the case of CF of 54 % LCOH of hydrogen compression and storage is \$0,554/kgH₂, while it is \$0,140/kgH₂ in the case of 100 % CF. The cost of nitrogen production and ammonia synthesis are the same for all case studies, as they are independent of the type of electrolyser, and are subjected to 100 % CF. The cost of nitrogen

production is \$0,465/kgH₂ and the cost related to ammonia synthesis is \$0,523/kgH₂. The hydrogen compression cost is higher for the alkaline configuration.

The cheapest configuration remains alkaline and energy mix, while the most expensive is PEM and wind. Compared to the levelized cost of hydrogen production, the cost of ammonia does not increase significantly, the conversion of hydrogen into ammonia is cost-effective.

The following graph reports the LCOH of the final hydrogen related to ammonia production in scenario 2.

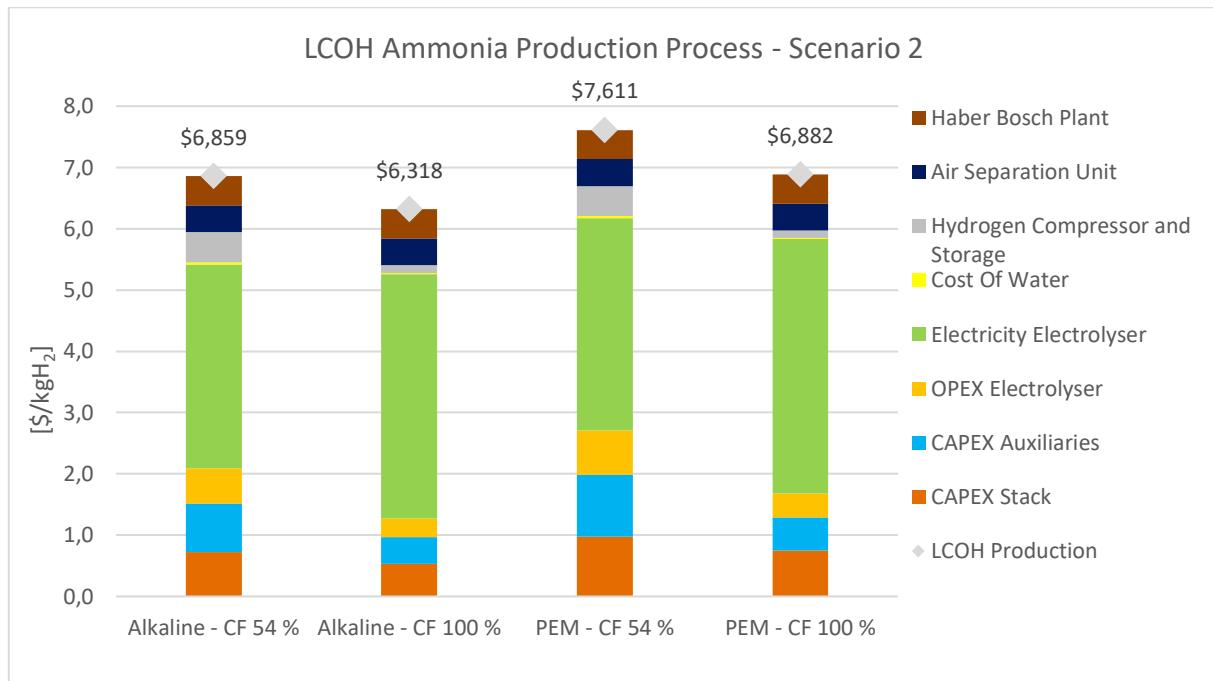


Figure 3.5: Levelized cost of final hydrogen related to ammonia production process, scenario 2

In scenario 2 LCOH for ammonia production are slightly lower than the values calculated in scenario 1, this is due to the scale factor considered that lowers the investment specific investment costs and consequently the operating costs.

In order to lower the cost of producing ammonia, it is necessary to reduce the cost of the electricity needed for electrolysis, by decreasing the cost of wind and grid power, and improving electrolysis technology, which is currently very energy intensive. Another cost that influences the cost reduction is the CAPEX of electrolyzers.

3.2.10 *Liquid ammonia storage and loading terminal facility*

The economic analysis of the loading terminal has been approached by considering the costs of the NH₃ liquefaction and storage plant, and the construction costs of the loading facilities of

the port terminal. The installation cost of the storage plant, which also includes the ammonia liquefaction process, is \$1,060/kgNH₃ stored, according to (UMAS, 2020), which also uses fixed operating costs of 3 % of the CAPEX that is calculated by multiplying the specific cost by the amount of ammonia that can be stored. This value is very similar to the data obtained from the paper (Nayak-Luke et al., 2021), for which the specific cost of storing liquefied NH₃ is \$1,040/kgNH₃.

The investment cost for the construction of the loading terminal refers to the study conducted by (Ishimoto et al., 2020), who reported a CAPEX of \$286 million for a plant with a capacity of 75.000 m³, for the entire terminal (which also includes the storage facility). Using the formula 3.6, that combines the formulas 3.2 and 3.5, the investment cost has been adjusted to the new plant capacity and the year of the investment.

$$C_1 = C_0 * \left(\frac{I_1}{I_0}\right) * \left(\frac{S_1}{S_0}\right)^n \quad (3.6)$$

C_0 is the investment cost to be adjusted, I_1 and I_0 are the CEPCI scale values for the year 2022 and 2015, which are respectively 797,6 and 556,8. The relationship of investment cost with plant capacity is governed by a cost exponent n , the value of which varies depending on the type of component. Its value is often around 0,6 and it is possible to use the six-tenths rule in the absence of other information. In this work the cost exponent has been selected equal to 0,67. S_0 and S_1 are the plant capacities, calculated in m³. In scenario 1, the plant capacity is 146.649 tonnes NH₃, the specific infrastructure cost is \$5,360/kgNH₃. In scenario 2, the plant capacity is 293.298 m³, and the specific cost decreases to \$4,532/kgNH₃ (between scenario 1 and scenario 2 has been considered a scale exponent of 0,9).

The operating costs for the loading terminal have been assumed to be 3 % of the investment cost, they include labour costs, infrastructure maintenance costs, administrative costs, and the insurance rate.

The economic calculations of the LCOA are related to the ammonia totally stored during the project life of 20 years, and include investment costs, operating costs, the cost of the electricity needed for liquefying the NH₃ and pumping the ammonia from the storage tanks to the ship. The cost of electricity relates to a specific cost of the wind-grid mix of \$50/MWh. The CAPEX, OPEX and energy cost results shown in the table 3.12 have been calculated using the formulas described and are used as input data in the equation to calculate LCOH. The following table summarises the economic calculations.

<i>Option</i>	<i>Scenario 1</i>	<i>Scenario 2</i>
<i>Storage Capacity [ton]</i>	100.000	200.000
<i>Storage Plant CAPEX [\$]</i>	106.000.000	212.000.000
<i>Port Infrastructure CAPEX [\$]</i>	536.000.000	906.400.000
<i>OPEX Terminal [\$]</i>	19.260.000	33.552.000
<i>Refrigeration Electricity Cost [\$]</i>	2.394.429	5.858.998
<i>Loading Terminal Electricity Cost [\$]</i>	2.481.429	6.076.436

Table 3.12: Loading storage ammonia terminal plant economic analysis, scenarios 1 and 2

The levelized cost of ammonia for storage and port activities at the departure terminal is strongly influenced by the cost of installation of the terminal infrastructure and the operating costs. The cost of electricity for refrigeration is similar to the cost of energy required for terminal loading operations, both of which have a relative weight in the unit cost composition. Using formula 3.5, the investment cost increases non-linearly with respect the capacity of the facility, due to the scale factor.

The contribution of the storage facility and the loading terminal to the levelized cost of hydrogen is calculated using formula 3.1 with the final hydrogen sent to the steel plants as denominator. In scenario 1 LCOH is \$0,592/kgH₂, while in scenario 2 it drops to \$0,425/kgH₂.

3.2.11 Maritime transport

The economic study of the maritime transport involves the investment cost of building or purchasing dedicated vessels for the transportation liquid ammonia in cryogenic conditions, with a propulsion system using ammonia as fuel. Operation and repair costs are also considered, as well as the cost of pilot fuel, used to improve the performance of the internal combustion engine.

For the investment cost, the paper (Seo & Han, 2021) has been considered, it shows the average cost of LNG carriers from 2016 to 2020. For small size vessels with capacity of 24.000 m³ the cost is \$42 million, for medium size vessel of 60.000 m³ the cost is \$63,02 million and for big size vessel with capacity of 84.000 m³ the cost is \$70,8 million.

In addition to the cost of the ship, the cost of the NH₃ tank has been considered, which according to the paper (Sophie & Ness, 2021) has a specific cost of \$720/m³, while the marine diesel tank has a specific cost of \$313/m³. The CAPEX is calculated by multiplying the cost of a

ship, obtained by adding the purchase/build cost of the ship and the tank costs, by the number of ships involved.

The paper (Kawakami et al., 2019) considers similar construction costs, in particular it assumes a cost of \$70 million for a ship of 55.000 tonnes capacity, and a cost of \$52 million for ships of 25.000 tonnes.

The same document considers the annual operating costs to be 14 % of the investment cost, they include crew costs, maintenance and repair, insurance and costs for furnishings and consumables. In this paper the operating costs have been assumed to be 8 % of the CAPEX. The cost of pilot fuel has been calculated separately, referring to the market price of marine diesel, which is \$400/tonne of HFO.

The LCOA of transport refers to the total amount of NH₃ carried during the lifetime of the project. The table 3.13 shows the results of the economic analysis for the three different vessel types considered. The CAPEX, OPEX and fuel cost results shown in the table have been calculated using the formulas described and are used as input data in the equation to calculate LCOH.

<i>Option</i>	<i>Scenario 1</i>		
	Small Vessel	Medium Vessel	Big Vessel
<i>Vessel Capacity [m³]</i>	24.000	60.000	84.000
<i>Vessel Cost [\$]</i>	42.000.000	63.020.000	70.800.000
<i>NH₃ Fuel Tank Capacity [m³]</i>	2.421	4.460	5.582
<i>NH₃ Fuel Tank Cost [\$]</i>	1.743.338	3.211.256	4.018.774
<i>Number of Vessel Required</i>	9	5	4
<i>CAPEX [\$]</i>	393.828.192	331.297.655	299.416.638
<i>OPEX [\$]</i>	31.506.255	26.503.812	23.953.331
<i>Cost of Pilot Fuel [\$]</i>	1.320.869	1.094.878	1.027.651
<i>LCOA [\$/kgNH₃]</i>	0,0547	0,0467	0,0425

Table 3.13: Maritime transportation economic analysis, scenario 1 (NH₃ supply chain)

The use of small ships results in a higher LCOA, as the number of ships involved is almost twice as high as in the case of medium or large ships. This leads to a higher investment cost, even though the cost of a small ship is almost half that of a large ship. The adoption of more vessels also results in higher maintenance and repair costs, as well as a higher cost of pilot fuel, which is consumed in greater quantities. LCOA for large ships is \$0,0425/kgNH₃ and increases to

\$0,0547/kgNH₃ for small ships. In scenario 2, the LCOA of NH₃ transport is slightly lowered. For small ships LCOH is \$0,0492/kgNH₃, for medium-sized ships it is \$0,0304/kgNH₃, and for large ships it is \$0,0304/kgNH₃.

Transport costs agree with values reported in the literature, (Fúnez Guerra et al., 2020) adopts a transport cost of \$50/tonNH₃ from Chile to Japan in its study. The paper (Kawakami et al., 2019), which studied the logistics chain of ocean transport of ammonia, also calculated a transport cost of \$41,3/tonNH₃ and an average logistics cost of \$65,7/tonNH₃ in 2030, which decreases to a transport cost of \$40,4/tonNH₃ and an average logistics cost of \$62,9/tonNH₃. These values confirm the validity of the results obtained in this work.

Also from the economic perspective, as well as for logistical and environmental reasons, the use of large ships is cost-effective compared to small or medium-sized ships.

When considering the levelized cost of final hydrogen produced for steel industry, LCOH related to ammonia transport for large ships is \$0,372/kgH₂ in scenario 1 and \$0,263/kgH₂ in second scenario.

3.2.12 *Liquid ammonia storage and unloading terminal facility*

The unloading terminal at the port of arrival is very similar to the loading terminal at the port of departure, the facilities are the same, the unloading of the liquid ammonia involves the use of a pumping system that transports the NH₃ from the ship to the land tanks. Insulated tanks maintain the cryogenic conditions, and a refrigeration system liquefies the evaporated ammonia by Boil-Off.

The levelized cost of the unloading terminal depends on the investment cost for the construction of the cryogenic storage facility and the infrastructure required for the terminal's unloading operations, the operating and management costs, and the cost of electricity necessary for port operations. Electricity related to liquefaction is not very relevant since it is only used to liquefy evaporated NH₃.

The specific cost of the storage facility is \$1,060/kgNH₃, that of the port infrastructure is \$5,036/kgNH₃ in scenario 1 and \$4,532/kgNH₃ in scenario 2, due to the scale factor considered. Operation and maintenance costs are 3 % of the CAPEX. For the electricity calculation, the current grid electricity price in Italy has been used, which is \$0,224/kWh according to TERNA's

data, an order of magnitude higher than the cost of electricity in Argentina. In scenario 1, two tanks of 58.660 m³ of NH₃ are used, while in scenario 2, 4 tanks of 73.325 m³ are employed. LCOH of the unloading terminal refers to the total amount hydrogen delivered to steel industry over the 20-year life of the project. The following table shows the economic calculations carried out to find the levelized cost of hydrogen. The CAPEX, OPEX and energy cost results shown in the table 3.14 have been calculated using the formulas described and are used as input data in the equation to calculate LCOH.

<i>Option</i>	<i>Scenario 1</i>	<i>Scenario 2</i>
<i>Storage Capacity [ton]</i>	80.000	200.000
<i>Storage Plant CAPEX [\$]</i>	84.800.000	212.000.000
<i>Port Infrastructure CAPEX [\$]</i>	428.800.000	906.400.000
<i>OPEX Terminal [\$]</i>	15.408.000	33.552.000
<i>Refrigeration Electricity Cost [\$]</i>	55.746	129.375
<i>Loading Terminal Electricity Cost [\$]</i>	10.230.725	25.422.504

Table 3.14: Unloading storage ammonia terminal plant economic analysis, scenarios 1 and 2

The levelized cost at the unloading terminal is higher than at the departure terminal, because of the cost of electricity, which in Italy is \$224/MWh, while in Argentina it is \$50/MWh. The cost of electricity for ammonia liquefaction is not relevant, since the ammonia already arrives in liquid form, and the refrigeration plant only works with the NH₃ evaporated in the storage tanks per Boil-Off. The largest contribution to the LCOH is made by the terminal's CAPEX, which accounts for 54,6 % in scenario 1, where LCOH is \$0,518/kgH₂, and 52 % of the LCOH in scenario 2, where the levelized cost of hydrogen is \$0,463/kgH₂.

3.2.13 Ammonia cracking and hydrogen purification plant

The final product required by the steel industry is pure hydrogen, which is obtained through the decomposition of ammonia into hydrogen and nitrogen in a cracking plant, and the subsequent purification of the hydrogen to a percentage of over 99,99 % in the PSA plant, for its use as synthesis gas and as green fuel in the Direct Iron Reduction plant. The conversion and purification process is explained in section 2.4.4.

According to the document (Ishimoto et al., 2020) the total efficiency of the cracker and the hydrogen purifier is 69,5 % by weight. This is due to the efficiency of the PSA purifier is 75 %,

and in addition, part of the Off-Gas produced, which contains hydrogen and nitrogen, is used as fuel for the cracker. For this reason, the levelized cost of hydrogen is not dependent on thermal energy. LCOH is calculated by considering the installation cost of the plant, fixed operating costs and the cost of the electricity needed especially in the PSA purification plant. To calculate the investment cost, the work carried out by (Makhloufi & Kezibri, 2021) has been considered, where a detailed cost analysis of the cracking and purification process has been carried out, in which direct costs, indirect costs and working capital are considered in addition to the cost of the components. Formula 3.5 has been used to calculate the CAPEX, where C_0 and S_0 are \$286.169.979 and 1.910 tons NH_3 /day, the exponent cost considered is 0,6. The parameters I_0 and I_1 refer to the years 2019 and January 2022, and are 607,5 and 797,6, respectively. Also, in accordance with the study mentioned above, the total CAPEX is divided into 55,22 % for the Cracking, NH_3 Recovery, Cooling, and Utilities plant, and 44,78 % for the Hydrogen Purification Plant. The annual operation and maintenance cost is 4,5 % of the CAPEX, while the electricity cost is calculated using the grid price of \$224/MWh. The specific CAPEX calculated for scenario 1 are \$87.226/ton NH_3 /day for cracking plant and \$70.735/ton NH_3 /day input for purification plant.

Using data from the paper (Ishimoto et al., 2020), which described the costs of a 2880 ton NH_3 /day plant with an investment cost of \$430.000.000, and using formula 3.5, a slightly higher CAPEX has been obtained than in the paper described above, that has been used as reference in this thesis work.

The calculation of the LCOH of the cracking plant refers to the total amount of NH_3 decomposed during the lifetime of the project, while LCOH for the hydrogen purification plant refers to the H_2 purified during the same period. The CAPEX, OPEX and energy cost results shown in the table 3.15 have been calculated using the formulas described and are used as input data in the equation to calculate LCOH.

<i>Option</i>	<i>Scenario 1</i>	<i>Scenario 2</i>
	Cracking Plant	
<i>Annual NH₃ Decomposed [ton]</i>	1.160.355	2.883.387
<i>Cracking Plant Capacity [tonNH₃/d]</i>	3.306	8.215
<i>Cracking Plant CAPEX [\$]</i>	288.355.936	497.870.086
<i>Cracking Plant OPEX [\$]</i>	12.913.008	22.295.363
<i>Cracking Plant Electricity Cost [\$]</i>	519.839	1.291.757
	Purification Plant	
<i>Annual H₂ Purified [ton]</i>	205.963	511.801
<i>Purification Plant Capacity [tonH₂/d]</i>	587	1.458
<i>Purification Plant CAPEX [\$]</i>	233.838.805	403.741.804
<i>Purification Plant OPEX [\$]</i>	10.471.650	18.080.159
<i>Purification Plant Electricity Cost [\$]</i>	180.201.562	447.785.932

Table 3.15: Ammonia cracking and hydrogen purification plant economic analysis, scenarios 1 and 2

The LCOH of the cracker is calculated considering the final hydrogen produced over the whole lifetime of the project, it is \$0,284/kgH₂ in scenario 1, while it decreases slightly in scenario 2 to \$0,198/kgH₂. CAPEX amounts to more than 65 % in the final cost of the cracking process, while the cost of electricity is very low, it accounts for only 2 %, since the electricity consumed by the plant is negligible, the cracking plant has an electricity consumption of 0,02 kWh/kgNH₃. Hydrogen purification, on the other hand, is characterised by very high electricity costs, as it is an energy-intensive process, and the cost of electricity in Italy is very expensive. The total cost of electricity exceeds 80 % in LCOH. The CAPEX of the PSA is very similar to that of the cracking plant, slightly lower. The levelized hydrogen cost for the PSA plant is \$1,486/kgH₂ in scenario 1 and \$1,417/kgH₂ in scenario 2.

3.2.14 *Civil works and other costs*

For the composition of the LCOH, the costs for civil works have been also considered. According to the document (Tractebel Engineerin, 2017), the costs of civil works are the costs of construction work. This includes foundations, industrial buildings, lighting, water supply, fencing, security. The costs of civil works are determined by the size of the structure. The cost function developed to estimate costs based on these factors is as follows.

$$CAPEX_{Civil\ Works} = (A + B) * (S_{adjust} * Area_{equipments}) \quad (3.7)$$

Index A represents the base cost, while B represents the additional cost for the land. S_{adjust} takes into account a correction factor for the construction area. $A_{equipments}$ represents the total area of built infrastructure. The following areas relating to the ammonia production process have been considered, while the costs for the transport and purification of hydrogen have been not accounted, as the civil works were already present within CAPEX.

<i>Option</i>	<i>Value</i>
<i>A [\$ /m²]</i>	950
<i>B [\$ /m²]</i>	150
<i>Sadjust [%]</i>	150%
<i>A equipment [m²/kW]</i>	0,10
<i>A H₂ Storage [m²/kgH₂]</i>	0,09
<i>A H₂ Compressor [m²/unit]</i>	11
<i>A ASU and N₂ Compressor [m²/kg]</i>	0,51
<i>A Desalinator [m²/m³/day]</i>	1,5
<i>A Ammonia Synthesis Plant [m²/tonNH₃/d]</i>	0,73

Table 3.16: Specific area for NH₃ process plants, base and additional cost indexes

The first six values are taken from the paper (Tractebel Engineering, 2017), the specific area of the ammonia synthesis plant is taken from the paper (Barrup Fertilisers, 2001), and the specific area of the desalinator is taken from (IAEA, 2006). The area of the equipment is 0,1 in the case of the alkaline electrolyser, and 0,05 for the PEM electrolyser. The area of the liquid ammonia tanks has been calculated by multiplying the base area of the tanks by a factor of 1,5 to consider also the area required for the refrigeration plant.

Still following (Tractebel Engineering, 2017), '*Other Costs*', that include non-equipment and additional costs, have been calculated and assumed to be 2 % of the electrolyser CAPEX.

The levelized cost of hydrogen related to civil works refers to the ammonia produced over the lifetime of the project. The table 3.17 shows the results obtained.

Data	Scenario 1	
	CF 54 %	CF 100 %
A equipment (Alkaline) [m ²]	252.880	136.555
A H ₂ Storage [m ²]	99.167	0
A H ₂ Compressor [m ²]	10.979	5.928
A ASU and N ₂ Compressor [m ²]	50.873	27.471
A Desalinator [m ²]	28.603	15.446
A Ammonia Synthesis Plant [m ²]	2.598	2.598
A NH ₃ Storage Loading Terminal [m ²]	4.003	4.003
A NH ₃ Storage unloading terminal [m ²]	3.449	3.449
Total Area [m ²]	452.552	195.451
CAPEX Civil Works [\$]	746.710.679	322.494.042
CAPEX Other Costs [\$]	45.518.478	24.579.978

Table 3.17: Areas of the plants involved in the NH₃ production process, CAPEX civil works and other costs, LCOH for scenario 1 (NH₃ supply chain)

The area of the electrolyser, the desalinator, the compressor and the intermediate compressed hydrogen tank are influenced by the electricity capacity factor, while the areas of the other plants remain constant by varying this factor. By switching from the wind configuration to the mix configuration, the construction surfaces of the above-mentioned plants decrease by half, which significantly lowers the civil costs. In scenario 1, LCOH for the wind configuration is \$0,522/kgH₂, while switching to the mix configuration the levelized cost of ammonia decreases to \$0,229/kgH₂.

With the use of the PEM electrolyser LCOH decreases slightly, in the case of wind energy it is \$0,396/kgH₂, while with the energy mix configuration LCOH takes on a value of \$0,160/kgH₂, this is due to the area occupied by the PEM being half the area required by the alkaline electrolyser. In scenario 2 the LCOH remains almost constant for all configurations evaluated.

3.3 Levelized cost of ammonia carrier supply chain

The final cost of the hydrogen sent to the direct reduction iron plant is the sum of the costs of producing ammonia with the costs of storing, transporting, and decomposing NH₃ to obtain H₂, and its subsequent purification. The graph 3.6 shows the contributions of the various phases in the supply chain, both for scenarios 1 and 2.

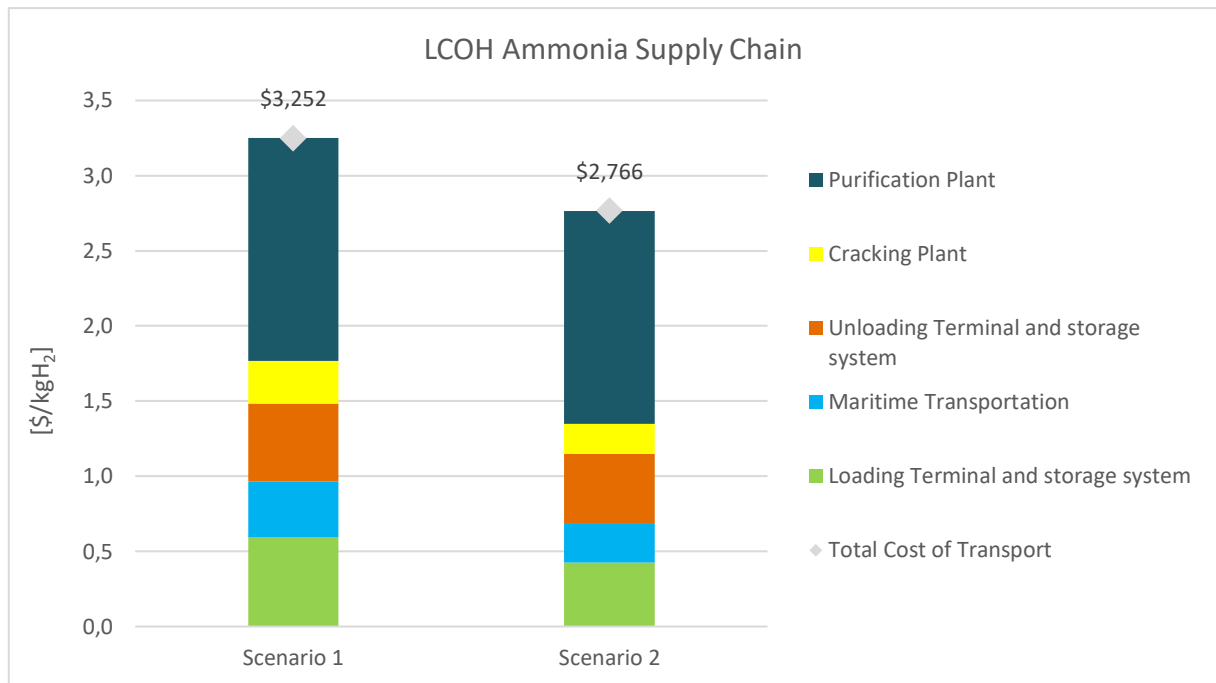


Figure 3.6: Levelized cost of ammonia supply chain, scenario 1 and 2

The costs related to ammonia storage, transport and re-transformation into hydrogen are independent from the type of electrolyser adopted, and from the capacity factor selected, hence the levelized cost of hydrogen related to these processes is constant for all four configurations evaluated.

The most expensive process is the hydrogen purification because it is energy intensive, and the price of Italian grid is more than four times higher than the price of Argentinian electricity grid. LCOH related to hydrogen purification is \$1,486/kgH₂ in scenario 1 and \$1,417/kgH₂ in scenario 2. The LCOH related to the loading and unloading terminals are \$0,592/kgH₂ and \$0,518/kgH₂ in scenario 1, while they slightly decrease to \$0,425/kg and \$0,463/kg in scenario 2. The cost related to the transport phase is the most economic, accounting for \$0,372/kg in scenario 1 and falling to \$0,263/kg in second scenario.

Without considering the H₂ reconversion, the total cost of ammonia storage and transport is \$1482/tonH₂ in scenario 1 and \$1150/tonH₂ in scenario 2.

The final cost of hydrogen considering all the phases investigated is reported in the graph 3.7.

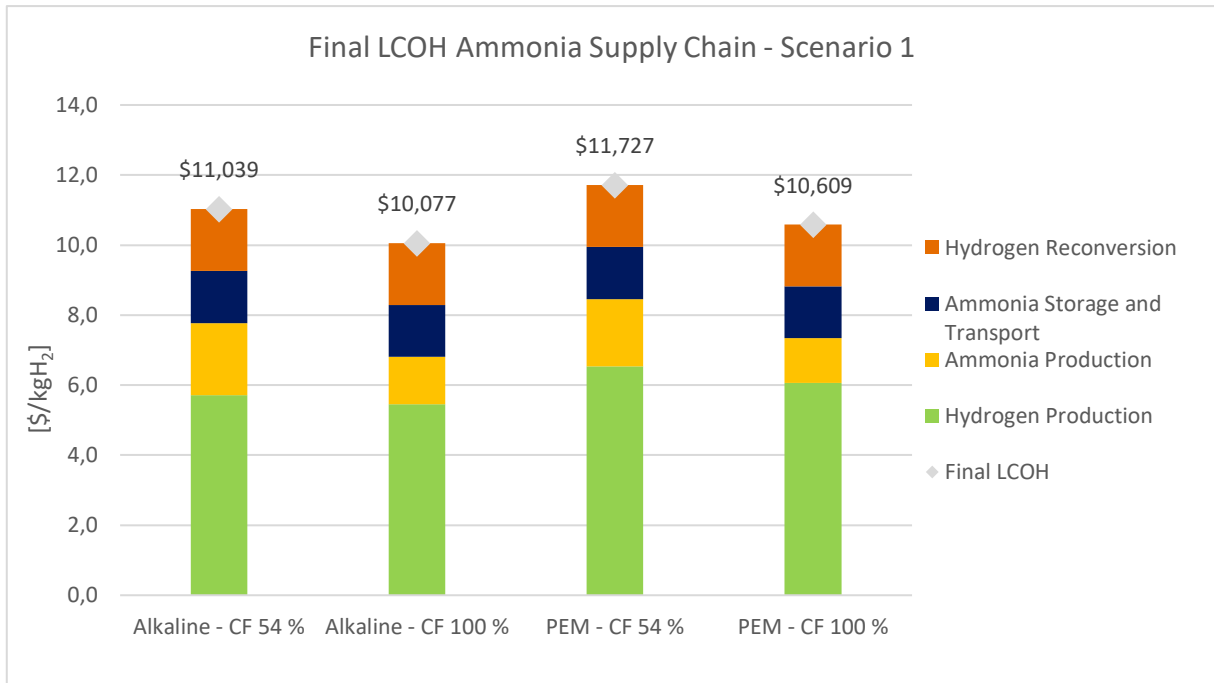


Figure 3.7: Final levelized cost of hydrogen, scenario 1 (NH₃ supply chain)

Hydrogen production accounts for most of the final cost of hydrogen, followed by the ammonia production process and the cracking and purification phase. Ammonia storage and ocean transport have the lower impact on the final cost, proving to be the strong point of this energy carrier. The most economic configuration continues to be the one adopting alkaline electrolyser and wind-grid electricity mix, the final cost of the hydrogen is \$10,077/kgH₂. The most expensive configuration involves PEM and wind energy, which guarantees a CF of 54 %, the final LCOH is \$11,714/kgH₂ (Appendix A1 reports the LCOH contributions of all processes involved in NH₃ transport chain).

The graph 3.8 shows the final cost of hydrogen for the different configurations in scenario 2.

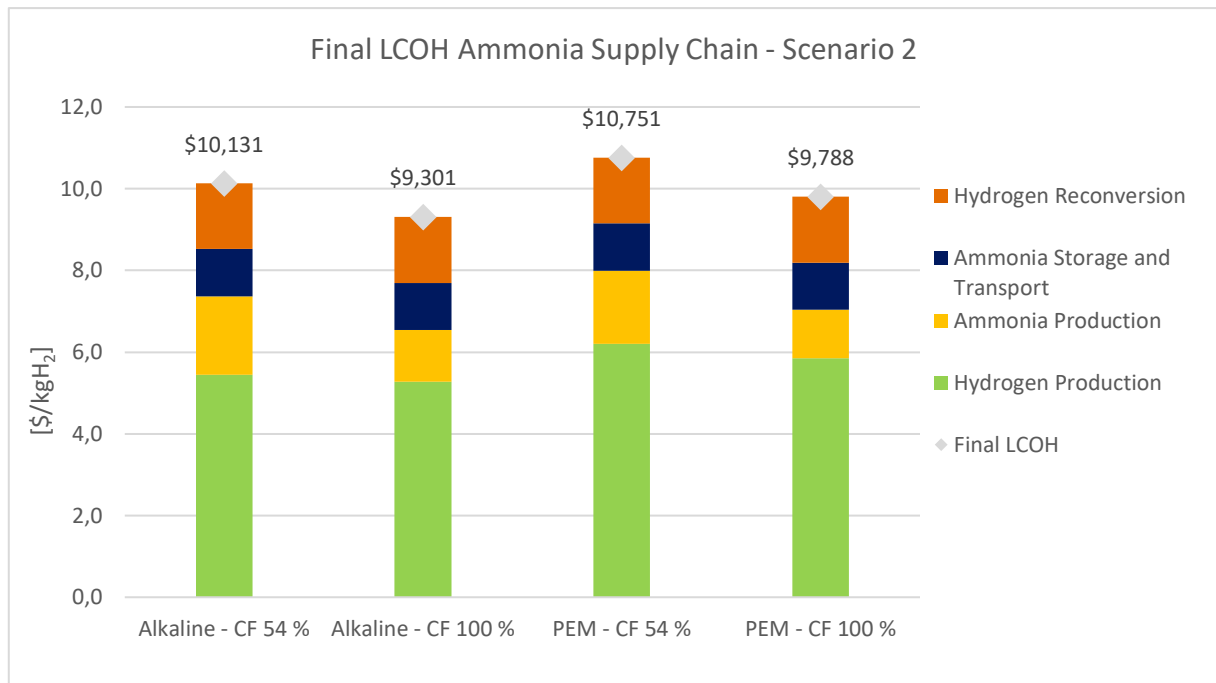


Figure 3.8: Final levelized cost of hydrogen, scenario 2 (NH₃ supply chain)

Scenario 2 follows the same cost trend as scenario 1. Final LCOH of hydrogen diminishes of \$0,892/kgH₂ in first configuration, \$0,755/kgH₂ in the cheapest case, \$0,952/kgH₂ in the most expensive configuration, and in the last configuration it decreases of \$0,789/kgH₂. This is due to the scale effect considered for the majority of the plant involved in the process of ammonia production and storage (Appendix A2 reports all the contributions to the final hydrogen LCOH for the ammonia supply chain in scenario 2).

The final cost of green hydrogen calculated in the different case studies is by far higher than green hydrogen market prices. According to (CEPCONSULT, 2019), the cost of hydrogen obtained through electrolysis in Europe in 2019 ranged between 3,5 and 5 \$/kgH₂. The same paper states that the price will drop in 2030, varying between 1 and 1,5 \$/kgH₂. The company's website 'sgh2energy' reports average values of green hydrogen in the range between 10 and 13 \$/kgH₂. The site 'Fuel Cell and Hydrogen' reports a price range of green hydrogen between 6 and 8 \$/kgH₂. The site 'Statista.com' reports the cost of producing green hydrogen in the Netherlands in 2021 in the SeaH2Land plant at \$5750/tonH₂, considering a price of wind energy equal to 2 \$/kWh, while the hydrogen cost of an electrolysis plant in Chile is \$3,180/kgH₂, in line with the production cost calculated in this paper.

Final hydrogen cost of the liquid ammonia supply chain is not competitive with the current costs of hydrogen produced in the world, which furthermore are set to decrease in the next future becoming more competitive with grey and blue hydrogen prices.

3.4 LCOA evaluation considering ammonia as final product

The final cost of hydrogen produced via the liquid ammonia chain does not guarantee favourable economic results, the main drawback has been identified to be the inefficiency of the cracking and purification plant and the elevated cost of this process. The ammonia production and transport phase, on the other hand, are characterised by competitive costs. For this reason, the Authors have decided to study LCOA, considering ammonia stored in the arrival terminal as the final product, eliminating the reconversion phase into hydrogen. The NH_3 stored annually is 1.160.355 tonnes in scenario 1 and 2.883.387 tonnes in scenario 2. The graph below shows LCOA of the final ammonia stored at the port of arrival for the four main configurations.

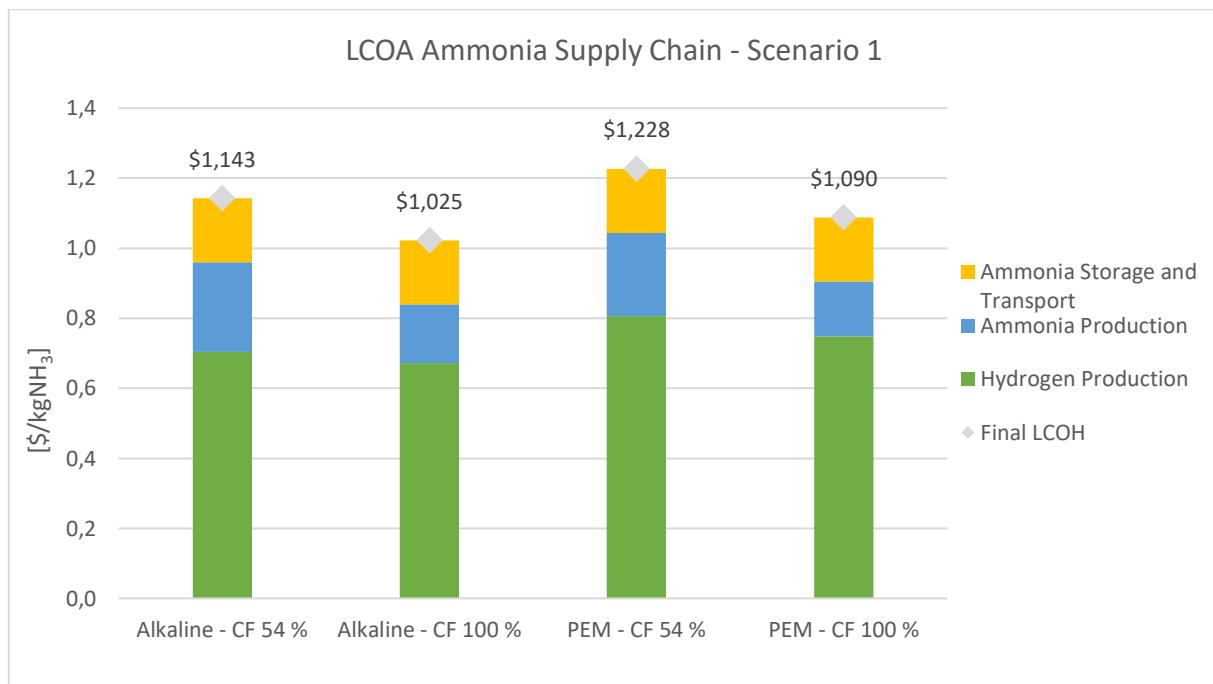


Figure 3.9: Final levelized cost of ammonia, scenario 1

The levelized cost of ammonia is much lower than the cost of hydrogen, although the absolute expenditures are the same. The main reason is the amount of the final product, which is about 10 times larger, and the avoiding of costs and losses related to the cracking and purification plant.

The cheapest scenario involves alkaline electrolyser and 100 % CF, giving an LCOA of \$1,025/kgNH₃. The most expensive scenario involves PEM and 54 % CF, in which case LCOA is \$1,228/kgNH₃. The most impactful process is hydrogen production, which contributes \$0,673/kgNH₃ to the LCOA in the second case and \$0,806/kgNH₃ in the third. LCOA related to ammonia production is \$0,255/kgNH₃ in the cheapest case and \$0,238/kgNH₃ in the most

expensive case. The cost related to storage and transport is the same for all configurations and is \$0,183/kgNH₃ (Appendix A5 reports all the contributions to the final ammonia LCOA for the ammonia supply chain in scenario 1). The graph 3.10 shows LCOA for scenario 2.

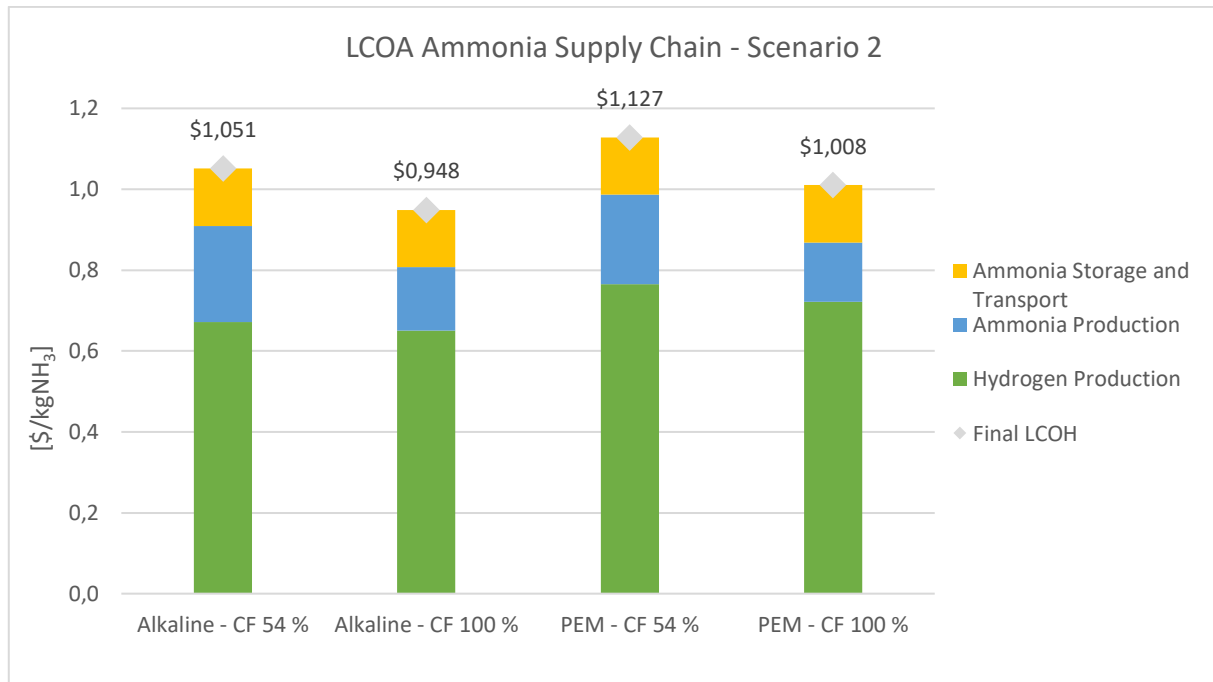


Figure 3.10: Final levelized cost of ammonia, scenario 2

LCOA in scenario 2 is slightly lowered due to the scale factor included. The cheapest and most expensive configurations are the same, and the considerations remain the same as for scenario 1. LCOA diminishes of \$74/tonNH₃ in cheapest configuration and \$98/tonNH₃ in the most expensive configuration (Appendix A6 reports all the contributions to the final ammonia LCOA for the ammonia supply chain in scenario 2).

The calculated LCOA is slightly higher, but in line with current green ammonia levelized costs. The paper (Ye et al. 2017) predicts LCOA for a grid-connected production plant ranging between \$713/kgNH₃ and \$1178/kgNH₃. (Arnaiz del Pozo & Cloete, 2022) have calculated an ammonia production cost of €381/tonNH₃, but using an electricity cost of \$60/MWh, which is far lower than the current electricity cost in Europe. (Trevor Brown, 2020) describes an LCOA of \$650/tonNH₃ using an electricity cost of \$50/MWh.

The results obtained for ammonia are promising, and suggest a further exploration, given the sharp increase in the cost of electricity and natural gas in Europe, which is expected to rise in the coming years due to the energetic crisis.

3.5 *Liquid hydrogen supply chain*

The final levelized cost of H₂ for the liquid hydrogen chain is found by adding up the costs of production, liquefaction, storage, and transport. The liquefied hydrogen production chain, unlike the ammonia production chain, involves the possibility of feeding all processes only with wind energy.

The economic analysis considers the same parameters selected for ammonia production. The cost of electricity produced by the wind power plant is \$42/MWh, the cost of grid electricity in Argentina is \$60/MWh, and the cost of grid electricity in Italy is \$224/MWh. The electricity cost of the energy mix is calculated using formula 3.3.

The project life is 20 years, the discount rate has been considered equal to 7 %. The investment cost is associated with year 0, the year in which there is no hydrogen production, while the operating costs are considered from year 1 to year 20, the project's operating period.

The final hydrogen cost depends on the type of fuel chosen for the maritime transportation, that can be hydrogen or ammonia. The following economic analysis has been developed only considering the hydrogen as fuel.

3.5.1 *Electrolyser*

The economic parameters of investment and operating costs chosen for the electrolyser are the same as those shown in table 3.1. The levelized cost for hydrogen production considers the investment cost of stacks and auxiliaries, operating costs and the cost of electricity used for the electrolysis process. The life of the stacks is shorter than the total life of the project, so the investment cost to replace the stacks will occur several times.

Production-related LCOH refers to the final hydrogen produced for steel plant during the life of the project. The hydrogen yearly delivered is 143.144.352 kg in scenario 1, and 355.701.840 kg in scenario 2.

The table 3.18 shows the economic results for the electrolysis process. The costs of CAPEX, OPEX and Electricity in the table below represent the input values in equation 3.1 which allows LCOH to be calculated.

Option	Scenario 1			
	CF 54 %		CF 100 %	
	Alkaline	PEM	Alkaline	PEM
<i>Annual H₂ Production [kg]</i>	155.972.073	155.972.073	155.972.073	155.972.073
<i>Electrolyser Power [GW]</i>	1,71	1,78	0,92	0,96
<i>CAPEX Stack [\$]</i>	616.232.081	784.554.733	332.765.324	423.659.556
<i>CAPEX Auxiliaries [\$]</i>	924.348.122	1.176.832.100	499.147.986	635.489.334
<i>OPEX System [\$]</i>	61.623.208	78.455.473	33.276.532	42.365.956
<i>Electricity Price [\$/MWh]</i>	42	42	50	50
<i>Annual Electricity Cost [\$]</i>	327.041.760	340.668.500	391.515.707	407.828.862

Table 3.18: Electrolyser cost analysis, scenario 1, (LH₂ supply chain)

Investment costs are strongly influenced by the capacity factor, and by the type of electrolyser chosen, increasing in the case of PEM and using a lower CF. The cost of electricity is higher in the case of PEM since this type of electrolyser has a higher specific consumption than the alkaline electrolyser. The cost of electricity is higher in the case of energy mix because the specific cost of energy is higher. The cost of electricity has the greatest impact on the LCOH of the electrolyser, higher than 60 % in all the configurations evaluated; decreasing it can significantly lower the cost of producing hydrogen. The investment cost for the system accounts for more than 20 % of the total LCOH, its reduction is also important for the LCOH abatement. The levelized cost of producing hydrogen from the electrolysers is equal to the cost calculated in chapter 3.2.1.

3.5.2 Desalinator

The cost of the water required for the electrolysis process is obtained from the LCOH related to the production of H₂O in the reverse osmosis desalination plant. The economic parameters of the electrolyser have been reported in section 3.2.2. The LCOW is calculated considering the investment cost, fixed operating costs and the cost of electricity used in the desalination process, and refers to the total amount of water produced during the life of the project. The amount of water produced annually depends on the electrolyser used. The costs of CAPEX, OPEX and Electricity in the table below represent the input values in equation that calculate the cost of water.

Option	Scenario 1			
	CF 54 %		CF 100 %	
	Alkaline	PEM	Alkaline	PEM
Annual Water Production [m^3]	2.479.053	2.231.147	2.479.053	2.231.147
Plant Capacity [m^3/day]	13.102	11.792	7.075	6.367
Plant Power [kW]	1.365	1.228	737	663
CAPEX [\$]	22.272.902	20.045.612	12.027.367	10.824.630
OPEX [\$]	890.916	801.824	481.095	432.985
Cost of Electricity [\$]	260.301	234.270	311.617	280.455
Cost of Water [$$/m^3$]	1,312	1,312	0,778	0,778

Table 3.19: Desalinator cost analysis, scenario 1, (LH₂ supply chain)

The levelized cost of water depends only on the capacity factor used, decreasing from a value of \$1,312/m³ in the case of a plant powered only by wind energy, to \$0,778/m³ with wind-grid feeding configuration. The cost increase depends on the increase of the CAPEX and OPEX, which depend on the capacity of the plant, that is directly related to the capacity factor. The cost of electricity increases in the case of 100 % CF due to the increase in the cost of electricity. The LCOW is strongly influenced by CAPEX, while the cost of electricity and operating costs have a lower weight. The cost of water remains the same in the second scenario.

3.5.3 Hydrogen liquefaction plant

The hydrogen produced by the electrolysis process is sent to the liquefaction plant, the operation of which is described in section 2.6.4, which brings the hydrogen to cryogenic conditions for storage and transport in liquid form. The economic analysis of the liquefaction plant includes the investment cost, the operating costs, which also involve the cost of the refrigerant, and the cost of the electricity used in the process by the compressor, the chiller, the Joule Brayton refrigeration cycle, and the expansion turbine.

The following papers have been considered for the economic study, (Connelly et al., 2019) reported in its economic study an investment cost for the hydrogen liquefaction plant of \$104 million for a plant with a capacity of 27 tonLH₂/day. The paper (Kan & Shibata, 2018) consider an investment cost of \$128 million for a liquefier that has a capacity of 50.000 kgLH₂/day.

Plant costs have been calculated from the work of (Stolzenburg et al., 2013), which describes a plant similar to the one proposed in this thesis, with a capacity of 50 tonLH₂/day calculated an investment cost of \$105 million. The CAPEX has been obtained using formula 3.6, where the indices I_0 and I_1 are 567,3 and 797,6 and refer to the years 2013 and January 2022. The exponent n has been taken as 0,6 because the capacity difference between the two plants considered is big. The S_1 capacity of the plant depends on the case study considered. The same study adopts operating costs equal to 4 % of the CAPEX. The paper (UMAS, 2020) reports the operational costs equal to the 5 % of the CAPEX. The electricity cost is calculated by multiplying the specific electricity cost by the annual amount of kWh consumed.

LCOH is calculated considering all the amount of H₂ delivered to steel plant over the lifetime of the project. The table 3.20 shows the economic results obtained. The costs of CAPEX, OPEX and electricity in the table represent the input values in equation that calculate the Levelized Cost Of Hydrogen.

Option	Scenario 1		Scenario 2	
	CF 54 %	CF 100 %	CF 54 %	CF 100 %
Hydrogen Liquefied [kg]	155.196.093	155.196.093	380.851.733	380.851.733
Plant Capacity [tonH ₂ /day]	862	466	2.116	1.143
Plant Power [MW]	423	229	1.038	561
CAPEX [\$]	814.975.635	563.093.976	1.396.592.537	964.952.583
OPEX [\$]	32.599.025	22.523.759	55.863.701	38.598.103
Cost of Electricity [\$]	76.812.320	91.955.321	188.282.790	225.401.397

Table 3.20: Economic calculations hydrogen liquefaction plant, scenarios 1 and 2

The process of liquefaction is characterised by relevant costs, mainly due to the cost of electricity, and the investment cost of the plant. LCOH is influenced by the capacity factor that determines the capacity of the plant, which is linked to CAPEX through formula 3.5. In scenario 1, the wind configuration LCOH is equal to \$1,302/kgH₂ and decreases to \$1,171/kgH₂ in the wind-grid mix configuration, as the plant capacity decreases from 862 tonH₂/day to 466 tonH₂/day, this is balanced in part from the higher annual expenditure for electricity in the CF 100 % configuration.

In scenario 2 LCOH is lower, this is due to the scale factor. LCOH decreases from \$1,057/kg in the wind configuration to \$0,998/kg in the wind-grid mix configuration.

3.5.4 Liquid hydrogen storage and loading terminal

Liquid hydrogen is stored in insulated tanks that are able to maintain cryogenic conditions inside, preventing heat exchange with the external environment. The tanks are located in the terminal at the port of departure, which also includes the port facilities required for loading the hydrogen from the land-based tanks to the ship. The loading terminal components and operation are explained in section 2.6.5 and 2.6.6. The economic analysis of the storage facility and terminal infrastructure have been carried out together, and include the investment cost, operating and maintenance costs, and the cost of electricity required for hydrogen transfer and loading operations. The loading terminal, unlike the other elements in the hydrogen production chain, is continuously powered by electricity, which is supplied by the grid-wind mix. The cost of electricity is \$50/MWh.

The CAPEX has been calculated from the data provided by the paper (Ishimoto et al., 2020), which used an investment cost of the loading terminal and storage facility of \$1295 million for an S_0 storage capacity of 200.000 m³. To find the CAPEX for the project, formula 3.6 has been used, where I_0 and I_1 are 603,1 and 797,6, and refer to the years 2018 and January 2022. The exponent n is equal to 0,6. The storage capacity S_1 is 150.000 m³ in scenario 1 and 350.000 m³ in scenario 2. The paper (UMAS, 2020) reports annual operating costs of 3 % of CAPEX. The specific CAPEX of the storage and loading terminal is \$9608/m³ in scenario 1 and \$8647/m³ in scenario 2.

LCOH refers to the total amount of liquid hydrogen provided to the steel industry during the lifetime of the project. The table 3.21 shows the economic results for the storage facility and the storage terminal. The costs of CAPEX, OPEX and Electricity in the table represent the input values in equation that calculate the Levelized Cost Of Hydrogen.

<i>Option</i>	<i>Scenario 1</i>	<i>Scenario 2</i>
<i>Annual Hydrogen Stored [kg]</i>	153.655.694	377.071.591
<i>Storage Capacity [m³]</i>	150.000	350.000
<i>CAPEX [\$]</i>	1.441.125.000	3.026.380.000
<i>OPEX [\$]</i>	43.233.750	90.791.400
<i>Cost of Electricity [\$]</i>	1.529.710	3.753.914

Table 3.21: Economic calculation LH₂ storage tank and loading terminal infrastructures, scenarios 1 and 2

The hydrogen storage cost is independent of the electrolyser used and of the capacity factor, which is fixed 100 %. The final cost of the loading terminal is mainly due to the investment cost, which accounts for about 75 % of the LCOH. The investment cost is very high due to the limited development of this technology, that is not available on large scale, and currently in an advanced research phase. LCOH related to hydrogen storage and loading terminal operations decreases from \$1,263/tonLH₂ to \$1,069/tonLH₂ from scenario 1 to scenario 2, due to the scale factor. The cost of electricity is secondary, as the loading terminal has no major energy consumption.

3.5.5 Maritime transport

The ocean transport of liquid hydrogen is done by specialised vessels that are able to keep the hydrogen in cryogenic conditions, isolating it from the external environment. The total capacity of a ship is 160.000 m³, according to (Johnston et al., 2022), and the charging capacity is 150.400 m³.

The calculation of the levelized cost of hydrogen is computed by the investment cost to buy or build the ships, the operating and maintenance costs, and the cost of the fuel used for ship propulsion. The CAPEX is calculated by multiplying the investment cost for the construction/purchase of a ship by the number of ships required to provide the shipping service. According to the paper (Johnston et al., 2022), the cost of a hydrogen transport ship of the size of 160.000 m³ is \$216 million. The paper (Kan & Shibata, 2018) utilizes a cost per ship of \$413 million for a vessel of 160.000 m³ cargo capacity.

For this thesis work, data from (Al-Breiki & Bicer, 2020) has been used, which proposes a specific cost of the ship of 1355 \$/m³. The specific tank cost is \$1400/m³ for hydrogen and \$313/m³ of HFO. The formula 3.8 is applied to calculate the cost of a ship is as follows.

$$Vessel\ Cost\ [\$] = (SC_{ShipTanker} * Vessel\ Capacity + SC_{FuelTank} * Tank\ Capacity) \quad (3.8)$$

Operating and maintenance costs are evaluated 4 % of CAPEX from (Johnston et al., 2022). For this work the operating costs are considered to be 8 % of the CAPEX. The specific pilot fuel cost is \$400/tonHFO, for which the current market price has been considered.

LCOH refers to the total amount of hydrogen delivered to steel plants during the lifetime of the project. The CAPEX, OPEX and fuel cost results shown in the table 3.22 have been calculated using the formulas described and are used as input data in the equation to calculate LCOH.

<i>Option</i>	<i>Scenario 1</i>	<i>Scenario 2</i>
<i>Annual LH₂ Transported [kg]</i>	153.655.694	377.071.591
<i>Vessel Cost [\$]</i>	225.036.788	225.036.788
<i>Number of Vessels Required</i>	3	5
<i>CAPEX [\$]</i>	675.110.365	1.125.183.942
<i>OPEX [\$]</i>	54.008.829	90.014.715
<i>Pilot Fuel Cost [\$]</i>	74.978	149.957

Table 3.22: Maritime transportation economic analysis, scenarios 1 and 2 (LH₂ supply chain)

LCOH related to the transport of liquefied hydrogen is strongly influenced by the investment cost, which accounts for about 55 % of the final cost, and the remaining 45 % of the cost is related to the operational costs of the transport, including crew costs, maintenance, and repair costs, as well as insurance and expenses. In scenario 1 LCOH of the oceanic transport is \$0,823/kgH₂ and decreases to \$0,552/kgH₂ in scenario 2.

The calculated LCOH is slightly lower than the value calculated by the paper (Heuser et al., 2019), which estimates a transport cost of €1,13/kgH₂, for a total distance of 21.400 km between Argentina and Japan, about twice the distance considered in this work. The paper (Johnston et al., 2022) estimates a transport cost of \$0,41/kgH₂ for ocean transport of liquid hydrogen from Australia to Japan, and a cost of \$1,002/kgH₂ for transport between Australia and the port of Rotterdam in the Netherlands.

3.5.6 Liquid hydrogen storage and unloading terminal

The last step in the liquefied hydrogen transport chain is the storage of the incoming hydrogen at the unloading terminal before it can be sent to the reduced iron production plant as a final product. The total storage capacity has been selected to ensure storage for more than 20 days,

to guarantee the supply of hydrogen despite possible delays due to transport or production problems.

The economic analysis of the port of arrival has been developed similarly to the port of departure. The investment and operating costs include both the storage facility and the port infrastructure required for the hydrogen unloading processes. The description of the unloading terminal is given in section 2.6.8.

LCOH includes the investment cost for the construction of the storage facility and port infrastructure, the operating costs and the cost of energy used for re-liquefying the evaporated gas during the storage period, and the hydrogen unloading and transfer to land storage tanks. CAPEX has been calculated using formula 3.6, starting from the investment cost used in the paper (Ishimoto et al., 2020), which for a total capacity facility S_0 of 350.000 m³ considers an investment cost C_0 of \$1473 million. The indices I_0 and I_1 for the years 2018 and 2022 are 603,1 and 797,6 respectively. The exponent n is 0,6. In first scenario the specific CAPEX of \$7811/m³ has been used, while in the second scenario the specific CAPEX selected is equal to \$7030/ m³ of hydrogen. Operating costs are 3 % of CAPEX, while the cost of energy used is obtained by multiplying the total kWh by the cost of grid electricity in Italy (the National Average Energy Price for the month of January 2022, prior to the conflict that caused large variations in the average energy price, has been adopted), which is \$0,224/kWh.

LCOH refers to the total amount of hydrogen provided to steel plants during the total life of the project. The CAPEX, OPEX and electricity cost results shown in the table have been calculated using the formulas described and are used as input data in the equation to calculate LCOH. The table 3.23 shows the economic results.

<i>Option</i>	<i>Scenario 1</i>	<i>Scenario 2</i>
<i>Annual Hydrogen stored [kg]</i>	143.860.074	357.480.349
<i>Storage Capacity [m³]</i>	150.000	300.000
<i>CAPEX [\$]</i>	1.171.689.000	2.109.039.000
<i>OPEX [\$]</i>	35.150.670	63.271.170
<i>Cost of Electricity [\$]</i>	16.239.937	35.573.878

Table 3.23: Economic calculation LH₂ storage tank and unloading terminal infrastructures, scenarios 1 and 2

LCOH related to the unloading terminal is attributed mainly to CAPEX, which accounts for about 70 % of the total cost. Although the price of electricity is very high, the energy cost does not have a great influence on the levelized cost of hydrogen, accounting for slightly more than 10

% of LCOH. In scenario 1 LCOH is \$1,132/kgH₂, while in scenario 2 LCOH drops to \$0,838/kgH₂ due to the scale factor.

3.5.7 Civil works and other costs

Costs related to civil works have been calculated, which, as explained in section 3.2.14, represent the costs of supporting infrastructures for the construction. The formula used is 3.7, and the parameters of the formula are shown in table 3.16. The specific areas considered are the electrolyser which is 0,1 m²/kW for alkaline and 0,05 m²/kW for PEM, the desalinator has a specific area of 1,5 m²/m³/day, that have been taken from (Tractebel Engineering, 2017). In addition, the area of the liquefaction plant, equal to 0,05 m²/kg/day, and the areas of the liquid hydrogen storage facilities at the loading and unloading terminals are considered. The area of the port terminal is calculated by considering the area of the storage facility, multiplied by a factor of 3, to consider all the storage area.

In addition to civil works, '*other costs*', that represent unforeseen additional costs, have been calculated and amount to 2 % of equipment's cost. The table 3.24 illustrates the surface area and costs of civil works. LCOH of civil works refers to the total amount of hydrogen produced during the lifetime of the project.

Option	Scenario 1	
	CF 54 %	CF 100 %
<i>A equipment (Alkaline) [m²]</i>	171.176	92.435
<i>A H₂ Liquefaction Plant [m²]</i>	43.110	23.279
<i>A Desalinator [m²]</i>	19.653	10.612
<i>A LH₂ Storage Loading Terminal [m²]</i>	14.768	14.768
<i>A LH₂ Storage Unloading terminal [m²]</i>	14.768	14.768
<i>Total Area [m²]</i>	263.474	155.862
<i>CAPEX Civil Works [\$]</i>	434.731.432	257.172.365
<i>CAPEX Other Costs [\$]</i>	11.571.469	6.248.593

Table 3.24: Areas of the plants involved in the NH₃ production process, CAPEX civil works and other costs, LCOH for scenario 1

The total area occupied by the production and storage process facilities is 155.862 m² in case of CF 100 % and increases to around 263.474 m² for CF 54 %, and the associated levelized cost increases from \$0,174/kgH₂ to \$0,294/kgH₂. If the PEM electrolyser is selected the LCOH is

\$0,205/kgH₂ in case of wind energy, and \$0,126/kgH₂ in energy mix configuration. The plant requiring the most area is the electrolyzers. LCOH of the civil costs in scenarios slightly decreases in scenario 2, but the results are very similar.

3.6 Final levelized cost of liquid hydrogen carrier supply chain

The final cost of the hydrogen sent to the direct iron reduction plant is the sum of the hydrogen production costs and the costs of liquefaction, storage and transport. The graph shows the contributions of the various steps in the supply chain.

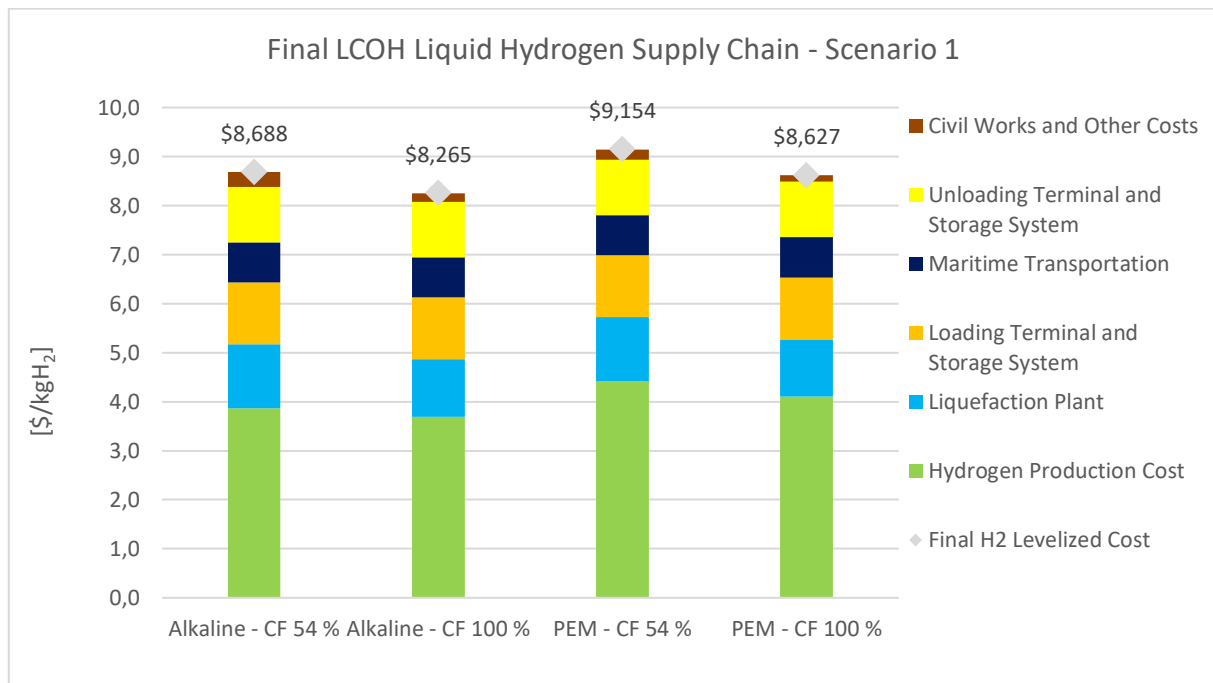


Figure 3.11: Levelized cost of hydrogen, liquid hydrogen supply chain, scenario 1

The graph reports the final LCOH values of hydrogen for the four main configurations. The cost to produce hydrogen gives the main contribution to the LCOH, accounting for roughly 45 % of the total cost in all the configurations. The cost of liquefaction is also important, accounting for roughly 15 % of the final cost, as well as the loading and unloading terminals cost. The maritime transportation is equal in all configurations, and it is the cheaper phase, accounting only for 9 % of the final cost.

Even if the storage and transport cost are higher for liquid hydrogen respect to ammonia, because LH₂ has not a worldwide existing supply chain, and this implies to higher expenditures for the lack of mature technologies, such as the LH₂ vessels and the terminal infrastructures, also the liquefaction process is characterised by expensive cost of investment and is energy-

intensive, the final cost of hydrogen is cheaper with respect to ammonia supply chain, mainly because there are not costs associated to hydrogen reconversion, and the losses in the supply chain are by far smaller.

The cheapest configuration, which involves the alkaline electrolyser and energy mix feeding, ensures hydrogen final cost of \$8,265/kgH₂. The hydrogen production cost is \$3,702/kgH₂, and the sum of liquefaction storage and transport costs is \$4,562/kgH₂. The most expensive configuration has a final hydrogen cost of \$9,154/kgH₂, involves a PEM electrolyser and wind power supply, the hydrogen production cost is \$4,429/kgH₂, and the sum of downstream costs is \$4,725/kgH₂ (Appendix A3 reports all the contributions to the final hydrogen LCOH for the liquid hydrogen supply chain in scenario 1).

The final cost in the cheapest configuration in the LH₂ supply chain case is \$1,808/kgH₂ lower than the cheapest configuration in the NH₃ supply chain case. In the most expensive configuration, the cost difference is \$2,569/kgH₂.

In scenario 2, storage and liquefaction costs decrease compared to scenario 1, due to the scale factor. The table 3.12 shows the LCOH for scenario 2.

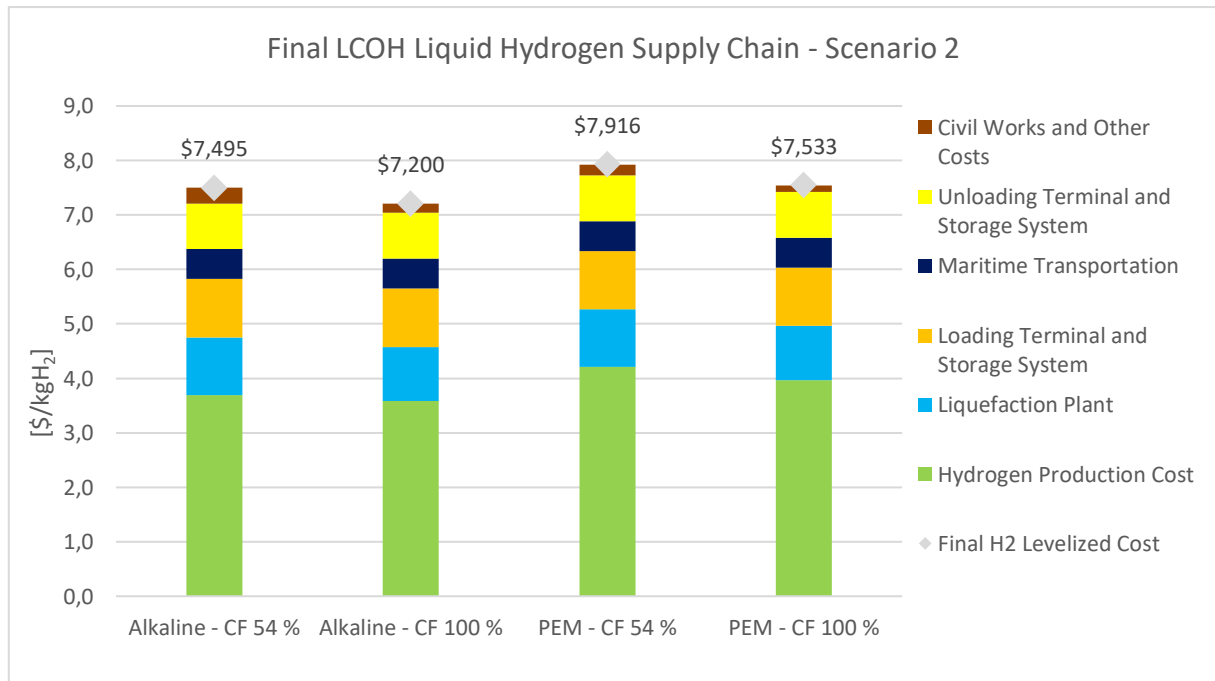


Figure 3.12: Levelized cost of hydrogen, liquid hydrogen supply chain, scenario 2

Increasing the size of liquefaction, storage and transport facilities causes a decrease in the levelized cost of hydrogen. The alkaline and CF 100 % configuration, that is the cheapest, receives a decrease in LCOH of \$1,050/tonH₂ compared to the same configuration in scenario 1. The cost of producing hydrogen is \$3,575/kgH₂, the subsequent costs in the chain are

\$3,625/kgH₂. The most expensive configuration is PEM and CF 54 %, in this case LCOH related to hydrogen production is \$4,202/kgH₂, and the post hydrogen production processes account for \$3,714/kgH₂ (Appendix A4 reports all the contributions to the final hydrogen LCOH for the liquid hydrogen supply chain in scenario 2). The difference in the most expensive configuration is \$1,221/kgH₂ between scenario 1 and 2.

The final LCOH of hydrogen has been evaluated also for the case in which green ammonia is used as fuel. The NH₃ cost has been assumed to be \$1200/tonH₂. The cheapest configuration in scenario 1 is characterised by a cost increase of \$0,126/kgH₂, and the most expensive configuration shows a cost increase of \$0,094/kgH₂. Also in scenario 2 the cost differences are negligible. It is possible to conclude that the maritime fuel is not an influence for the LCOH.

The final levelized cost of hydrogen is cheaper in the case of liquid hydrogen carrier than in the case of ammonia carrier. Neither option provides a competitive final cost in the market for different reasons. NH₃ despite having advantageous storage and transport costs, pays for the conversion back to hydrogen and large mass losses in the chain. Liquid hydrogen has the advantage of a simpler production process, as well as the fact that it does not have large losses in the chain. The disadvantage of liquid hydrogen is the high storage and transport costs due mainly to the non-maturity of this technology. In the following chapter, a sensitivity analysis is performed for both energy carriers to identify and adjust the most influential parameters in the final cost of hydrogen and to understand the possibilities for improvement in LCOH.

References Chapter 3

- Al-Breiki, M., & Bicer, Y. (2020). Comparative cost assessment of sustainable energy carriers produced from natural gas accounting for boil-off gas and social cost of carbon. *Energy Reports*, 6, 1897–1909. <https://doi.org/10.1016/j.egy.2020.07.013>
- Armijo, J., & Philibert, C. (2020). Flexible production of green hydrogen and ammonia from variable solar and wind energy: Case study of Chile and Argentina. *International Journal of Hydrogen Energy*, 45(3), 1541–1558. <https://doi.org/10.1016/j.ijhydene.2019.11.028>
- Arnaiz del Pozo, C., & Cloete, S. (2022). Techno-economic assessment of blue and green ammonia as energy carriers in a low-carbon future. In *Energy Conversion and Management* (Vol. 255). <https://doi.org/10.1016/j.enconman.2022.115312>
- Babarit, A., Gilloteaux, J. C., Clodic, G., Duchet, M., Simoneau, A., & Platzer, M. F. (2018). Techno-economic feasibility of fleets of far offshore hydrogen-producing wind energy converters. *International Journal of Hydrogen Energy*, 43(15), 7266–7289. <https://doi.org/10.1016/j.ijhydene.2018.02.144>
- CEPCONSULT. (2019). *The formation of a market for green hydrogen in the EU*. 4–9. <https://cepconsult.com/publications/the-formation-of-a-market-for-green-hydrogen-in-the-eu/>
- Cesaro, Z., Ives, M., Nayak-Luke, R., Mason, M., & Bañares-Alcántara, R. (2021). Ammonia to power: Forecasting the levelized cost of electricity from green ammonia in large-scale power plants. *Applied Energy*, 282(July 2020). <https://doi.org/10.1016/j.apenergy.2020.116009>
- CHEM.pdf. (n.d.).
- Connelly, E., Penev, M., Elgowainy, A., & Hunter, C. (2019). Current Status of Hydrogen Liquefaction Costs. *DOE Hydrogen and Fuel Cells Program Record*, 1–10.
- Correa, G., Volpe, F., Marocco, P., Muñoz, P., Falagüerra, T., & Santarelli, M. (2022). Evaluation of levelized cost of hydrogen produced by wind electrolysis: Argentine and Italian production scenarios. *Journal of Energy Storage*, 52, 105014. <https://doi.org/10.1016/J.EST.2022.105014>
- Curto, D., Franzitta, V., & Guercio, A. (2021). A review of the water desalination technologies. *Applied Sciences (Switzerland)*, 11(2), 1–36. <https://doi.org/10.3390/app11020670>
- Dinh, V. N., Leahy, P., McKeogh, E., Murphy, J., & Cummins, V. (2021). Development of a viability assessment model for hydrogen production from dedicated offshore wind farms. *International Journal of Hydrogen Energy*, 46(48), 24620–24631. <https://doi.org/10.1016/j.ijhydene.2020.04.232>
- Ebrahimi, A., Meratizaman, M., Reyhani, H. A., Pournali, O., & Amidpour, M. (2015). Energetic, exergetic and economic assessment of oxygen production from two columns cryogenic air separation unit. *Energy*, 90, 1298–1316. <https://doi.org/10.1016/j.energy.2015.06.083>

- Fertilisers, B. (2001). *Ammonia Plant , Burrup Peninsula. December.*
- Fúnez Guerra, C., Reyes-Bozo, L., Vyhmeister, E., Jaén Caparrós, M., Salazar, J. L., & Clemente-Jul, C. (2020). Technical-economic analysis for a green ammonia production plant in Chile and its subsequent transport to Japan. *Renewable Energy*, *157*, 404–414. <https://doi.org/10.1016/j.renene.2020.05.041>
- Heuser, P. M., Ryberg, D. S., Grube, T., Robinius, M., & Stolten, D. (2019). Techno-economic analysis of a potential energy trading link between Patagonia and Japan based on CO₂ free hydrogen. *International Journal of Hydrogen Energy*, *44*(25), 12733–12747. <https://doi.org/10.1016/j.ijhydene.2018.12.156>
- Hou, P., Enevoldsen, P., Eichman, J., Hu, W., Jacobson, M. Z., & Chen, Z. (2017). Optimizing investments in coupled offshore wind -electrolytic hydrogen storage systems in Denmark. *Journal of Power Sources*, *359*, 186–197. <https://doi.org/10.1016/j.jpowsour.2017.05.048>
- IAEA. (2006). Economics of Nuclear Desalination: New Developments and Site Specific Studies. *International Atomic Energy Agency*, July, 222.
- Ikäheimo, J., Kiviluoma, J., Weiss, R., & Holttinen, H. (2018). Power-to-ammonia in future North European 100 % renewable power and heat system. *International Journal of Hydrogen Energy*, *43*(36), 17295–17308. <https://doi.org/10.1016/j.ijhydene.2018.06.121>
- International Renewable Energy Agency, T. (2020). *GREEN HYDROGEN COST REDUCTION SCALING UP ELECTROLYSERS TO MEET THE 1.5°C CLIMATE GOAL H 2 O 2*. www.irena.org/publications
- Ishimoto, Y., Voldsund, M., Nekså, P., Roussanaly, S., Berstad, D., & Gardarsdottir, S. O. (2020). Large-scale production and transport of hydrogen from Norway to Europe and Japan: Value chain analysis and comparison of liquid hydrogen and ammonia as energy carriers. *International Journal of Hydrogen Energy*, *45*(58), 32865–32883. <https://doi.org/10.1016/j.ijhydene.2020.09.017>
- Johnston, C., Ali Khan, M. H., Amal, R., Daiyan, R., & MacGill, I. (2022). Shipping the sunshine: An open-source model for costing renewable hydrogen transport from Australia. *International Journal of Hydrogen Energy*, *47*(47), 20362–20377. <https://doi.org/10.1016/j.ijhydene.2022.04.156>
- Kan, S., & Shibata, Y. (2018). Evaluation of the Economics of Renewable Hydrogen Supply in the APEC Region. *The Institute of Energy Economics*, 1–5. <https://eneken.ieej.or.jp/data/7944.pdf>
- Kawakami, Y., Endo, S., & Hirai, H. (2019). *A Feasibility Study on the Supply Chain of CO₂-Free Ammonia with CCS and EOR*. April, 27.
- Lazard. (2021). *Levelized Cost of Hydrogen Analysis — Executive Summary*. June.
- Makhloufi, C., & Kezibri, N. (2021). Large-scale decomposition of green ammonia for pure hydrogen production. *International Journal of Hydrogen Energy*, *46*(70), 34777–34787. <https://doi.org/10.1016/j.ijhydene.2021.07.188>

- Mongird, K., Viswanathan, V., Alam, J., Vartanian, C., Sprenkle, V., & Baxter, R. (2020). 2020 Grid Energy Storage Technology Cost and Performance Assessment. *Energy Storage Grand Challenge Cost and Performance Assessment 2020, December*, 1–20. https://www.pnnl.gov/sites/default/files/media/file/PSH_Methodology_0.pdf
- Morgan, E. R. (2013). Techno-economic feasibility study of ammonia plants powered by offshore wind. *University of Massachusetts - Amherst, PhD Dissertations*, 432. http://scholarworks.umass.edu/open_access_dissertations/697
- Nagasawa, K., Davidson, F. T., Lloyd, A. C., & Webber, M. E. (2019). Impacts of renewable hydrogen production from wind energy in electricity markets on potential hydrogen demand for light-duty vehicles. *Applied Energy*, 235(June 2018), 1001–1016. <https://doi.org/10.1016/j.apenergy.2018.10.067>
- Nayak-Luke, R. M., Forbes, C., Cesaro, Z., Bañares-Alcántara, R., & Rouwenhorst, K. H. R. (2021). Techno-Economic Aspects of Production, Storage and Distribution of Ammonia. In *Techno-Economic Challenges of Green Ammonia as an Energy Vector*. Elsevier Inc. <https://doi.org/10.1016/b978-0-12-820560-0.00008-4>
- Parks, G., Boyd, R., Cornish, J., & Remick, R. (2014). Hydrogen Station Compression, Storage, and Dispensing Technical Status and Costs: Systems Integration. *Related Information: Independent Review Published for the U.S. Department of Energy Hydrogen and Fuel Cells Program, May*, Medium: ED; Size: 74 pp. <http://www.osti.gov/scitech//servlets/purl/1130621/>
- Products, A., Group, M., Industrial, S., Berhad, G., Sanso, T. N., Cryo, G., Gases, M., Products, B. G., Gases, U. I., & Brothers, W. (2022). *EU Nitrogen Market Report : Production , Exports , Imports , and Forecast to 2030 – IndexBox*. 1–6.
- Purchasing.com. (2015). *Air Compressor Purchasing Guide Introduction to the Air Compressor Buying Process*. 888, 1–15. <http://www.purchasing.com/construction-equipment/air-compressors/purchasing-guide/>
- Seo, Y., & Han, S. (2021). Economic evaluation of an ammonia-fueled ammonia carrier depending on methods of ammonia fuel storage. *Energies*, 14(24). <https://doi.org/10.3390/en14248326>
- Sonavane, P. B., Chirathadam, T. A., & Simmons, H. R. (2015). *3 rd Middle East Turbomachinery Symposium (METS III) 15-18 February 2015 | Doha , Qatar | mets . tamu . edu REMAINING LIFE ASSESSMENT AND PERFORMANCE CHARACTERIZATION OF CENTRIFUGAL COMPRESSORS IN LNG TRAINS*. February, 15–18.
- Sophie, A., & Ness, S. (2021). *Conceptual Design of Ammonia- fueled Vessels for Deep-sea Shipping*. June.
- Stolzenburg, K., Berstad, D., Decker, L., Elliott, A., Haberstroh, C., Hatto, C., Klaus, M., Mortimer, N. D., Mubbala, R., Mwabonje, O., Nekså, P., Quack, H., Rix, J. H. R., Seemann, I., & Walnum, H. T. (2013). Efficient Liquefaction of Hydrogen: Results of the IDEALHY Project. *Proceedings of the Energie – Symposium, Stralsund/Germany, November, November*, 1–8. https://www.idealhy.eu/uploads/documents/IDEALHY_XX_Energie-

Symposium_2013_web.pdf

Takeaways, K. E. Y. (2011). Discount Rate. *SpringerReference*, 1–14.
https://doi.org/10.1007/springerreference_1293

Technical assistant facility, sustainable energy for all, W. and central A. (2016). *Sustainable Energy Handbook. Simplified Financial Models. 6.1*, 1–14. https://europa.eu/european-union/index_es

Techno-economic assessment of. (2020). *March*.

Teknik, E. I. (2021). *An Industrial Perspective on Ultrapure Water Production for Electrolysis*.

Toth, A. J. (2020). Modelling and optimisation of multi-stage flash distillation and reverse osmosis for desalination of saline process wastewater sources. *Membranes*, 10(10), 1–18. <https://doi.org/10.3390/membranes10100265>

Tractebel Engineering, & Inicio. (2017). *Early business cases for H2 in energy storage and more broadly power to H2 applications*. *June*.

Trevor Brown. (2020). Industry report sees multi-billion ton market for green ammonia. *Ammonia Energy Association*, 1–7.

Tzimas, E., Filiou, C., Peteves, S. D., & Veyret, J. (2003). Hydrogen Storage : State-of-the-Art and Future Perspective. In *European Commission* (Issue January 2003).

Young, A. F., Villardi, H. G. D., Araujo, L. S., Raptopoulos, L. S. C., & Dutra, M. S. (2021). Detailed Design and Economic Evaluation of a Cryogenic Air Separation Unit with Recent Literature Solutions. *Industrial and Engineering Chemistry Research*, 60(41), 14830–14844. <https://doi.org/10.1021/acs.iecr.1c02818>

Chapter 4

Sensitivity analysis

The results achieved in the previous chapter have been obtained by considering specific operational and economic parameters, which may also vary significantly, especially for the cost of hydrogen production. In this chapter, the variation of the hydrogen production cost and the final cost of hydrogen will be studied based on the variation of certain parameters such as the capacity factor and the cost of wind energy, the CAPEX and the energy consumption of the electrolyser. The starting data are the following.

- Wind Capacity Factor: 54 %;
- Wind energy cost: \$42/MWh;
- Alkaline CAPEX: \$900/kW;
- PEM CAPEX: \$1100/kW;
- Alkaline power consumption: 48 kWh/kgH₂;
- PEM power consumption: 50 kWh/kgH₂;

The first analysis carried out concerns the maximum possible integration of the electricity grid for green hydrogen production.

4.1 Permitted use of the electricity grid for hydrogen production

Various configurations have been considered in the previous study, some of which involved maximum integration of the electricity grid for hydrogen production and subsequent conversion to ammonia or hydrogen liquefaction. The aim of this section is to understand the limit of electricity grid utilisation for hydrogen production via electrolysis. This is due to the fact that the electricity grid is responsible for indirect carbon dioxide emissions due to the energy production mix of a given country. In case of Argentina the CO₂ grid related emissions are 344 g/kWh.

Over the past few years, the restrictions concerning the CO₂ emissions allowed for green hydrogen production have been constantly increased. The document (Barth, 2016) published by the European Union gives a definition of green hydrogen based on the maximum GHG emissions, which for low-carbon hydrogen must be 60 % lower than emissions from fossil-based

hydrogen production. In particular, CO₂ emissions must decrease from a level of 91 gCO₂/MJH₂ to a level of 36,4 gCO₂/MJH₂, which considering a Low Heating Value of hydrogen equal to 120 MJ/kgH₂, is equal to 4,368 kgCO₂/kgH₂. The paper (Bloomberg, 2022) reports that Europe has set an emission threshold of 3,38 kgCO₂/kgH₂. The paper (Oyarzabal et al., 2022) of January 2022 explains the legislative package enacted by the European Union that defines low-carbon hydrogen as hydrogen with an energy content that is derived from non-renewable sources, and that meets a GHG emission reduction threshold of 70 % compared to fossil-based hydrogen, which results in an emission threshold of 27,3 gCO₂/kgH₂, this means that the maximum specific consumption allowed is 3,276 kgCO₂/kgH₂.

(McKenzie et al., 2021) reports in its document that for the Draft Delegated Act of the Taxonomy regulation the emission limit is 2,256 kgCO₂/kgH₂. Finally (Green Hydrogen Organization, 2022) in its document published in May 2022 imposes an even stricter limitation than the previous ones, the standard requires that green hydrogen projects operate with an emission rate less than or equal to 1 kg CO₂ per kg H₂, taken as an average over a 12-month period.

For this reason, the maximum permitted grid integration threshold has been evaluated to deal with the various restrictions described, in order to understand the possible limits of operation for hydrogen production in Patagonia.

To calculate the specific carbon dioxide emissions [kgCO₂/kgH₂], the first step has been related to the evaluation of the specific emissions for the wind-grid electricity mix. The wind emissions are considered to be zero as only the energy production phase is considered, while the grid emissions are 344 gCO₂/kWh. Using formula 2.38, the specific emissions related to the energy mix are calculated [gCO₂/kWh]. Multiplying the specific emissions by the total amount of electricity consumed annually by the electrolyser it is possible to calculate the total kgCO₂ emitted annually. Finally, the specific emissions of the electrolyser are found by dividing the total quantity of CO₂ by the total amount of H₂ produced annually.

The graph 4.1 shows the CO₂ emission's trend in relation to the percentage of grid integrated in the energy mix, compared to the different threshold levels described above.

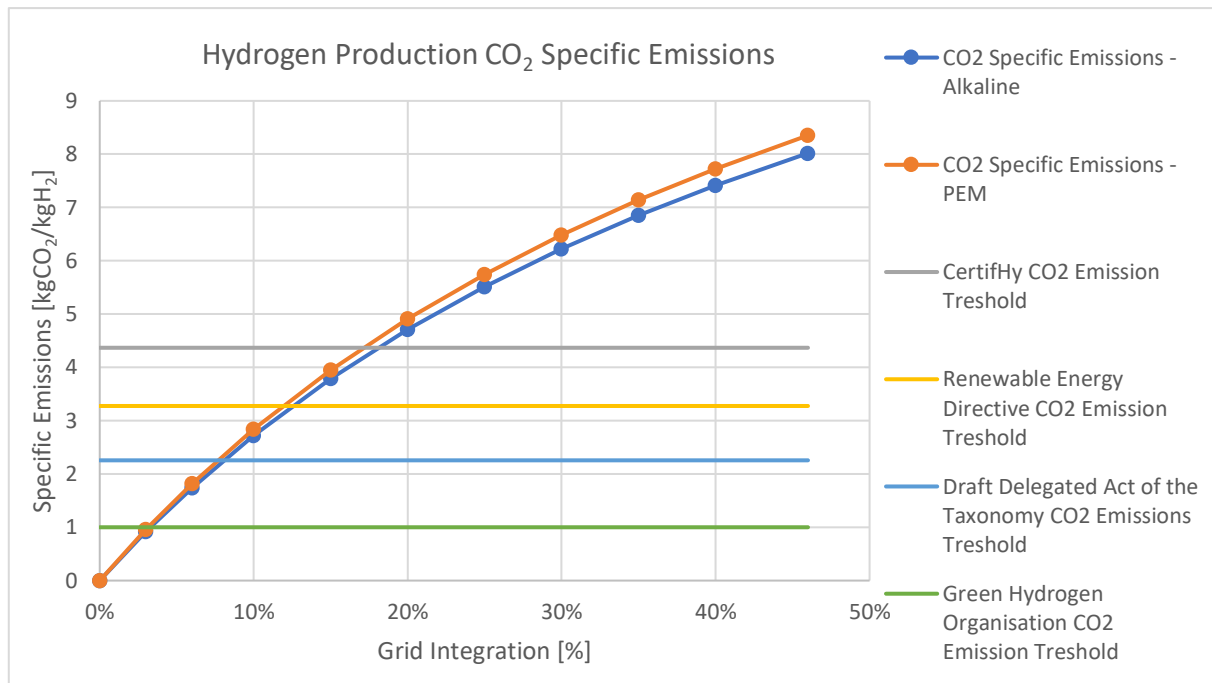


Figure 4.1: Specific emissions of hydrogen production trend for alkaline and PEM electrolyzers

The specific emissions of alkaline and PEM electrolyzers are slightly different, this is due to the fact that a bit higher energy consumption has been considered for PEM, but in any case, the end result is very similar. Considering the most permissive emission threshold, it is possible to have a maximum grid integration of 18 %, resulting in a total capacity factor of 72 %. If, on the other hand, the most restrictive and current regulations are considered, the maximum allowed grid integration is 3 %. The table 4.1 shows the maximum grid integration percentages for the different limits considered.

<i>CO₂ Emissions Limit</i>	<i>Alkaline</i>	<i>PEM</i>
<i>Maximum Grid Integration - CertifHY Restrictions (4,368kgCO₂/kgH₂)</i>	18,14%	17,19%
<i>Maximum Grid Integration - Renewable Energy Directive Restrictions (3,276 kgCO₂/kgH₂)</i>	12,59%	11,98%
<i>Maximum Grid Integration - Draft Delegated Act of the Taxonomy Restrictions (2,256 kgCO₂/kgH₂)</i>	8,09%	7,72%
<i>Maximum Grid Integration - Green Hydrogen Organisation Restriction (1 kgCO₂/kgH₂)</i>	3,30%	3,15%

Table 4.1: Grid integration limits related to CO₂ emissions thresholds, for alkaline and PEM electrolyzers

In this work, it has been decided to comply with the most stringent and current regulations, published by the Green Hydrogen Organisation in May 2022, which stipulate an emission limit

of 1 kgCO₂/kgH₂ on an annual average. The maximum grid integration possible under these conditions is 3,30 % for the alkaline electrolyser and 3,15 % for the PEM electrolyser, negligible values to ensure technological and economic advantages. For this reason, in the following sensitivity analysis, only hydrogen production powered by wind power has been considered, with a capacity factor of 54 %.

The graph 4.2 shows the development of specific CO₂ emissions related to the electricity grid required to ensure maximum grid integration in the electrolysis process (46 %) and, at the same time, to guarantee specific emissions production below the imposed limits.

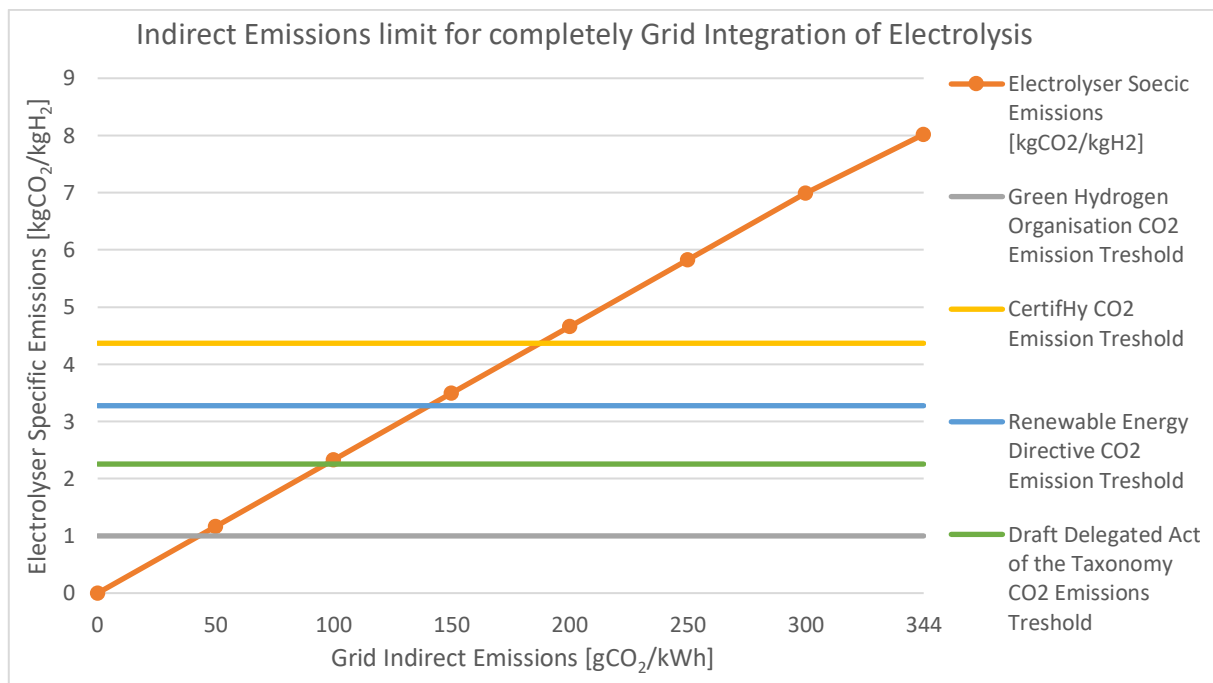


Figure 4.2: Indirect emissions limit for completely grid integration in electrolysis process

The maximum indirect emissions associated with the electricity grid, which are necessary to ensure the complete integration of the grid into the electrolysis process, are 187 gCO₂/kWh in the case of permitted specific emissions of 4,37 kgCO₂/kgH₂. In the most restrictive case, which allows a maximum emission threshold of 1 kgCO₂/kgH₂, the indirect emissions of the electricity grid would have to be less than 43 gCO₂/kWh, which would be ensured by a national electricity generation mix strongly driven by renewable technologies, an ideal situation far from the current scenario.

The following sensitivity analysis is developed considering feeding the electrolysers only with wind power, without grid integration.

4.2 Sensitivity analysis considering only one variable

In this section, the sensitivity analysis is carried out calculating the levelized cost of hydrogen production (related to the H₂ produced by the electrolyser), and final LCOH of hydrogen sent to the steel plants for both energy carriers, NH₃ and LH₂. These results are obtained by varying only one operating parameter.

4.2.1 Wind capacity factor

The sensitivity analysis concerning the capacity factor of the wind plant has been performed because this parameter is very influential on the final cost of the hydrogen produced. According to a study conducted by 'Hychico', which indicates an average capacity factor of 54,9 % in Patagonia, there are places in this region where the CF can exceed 70 %. For this reason, the CF wind value has been varied in the range of 20 - 70 %.

- Levelized cost of hydrogen production

The levelized cost of hydrogen production refers to the hydrogen produced by the electrolyser during the lifetime of the project.

Scenario 1 – Alkaline

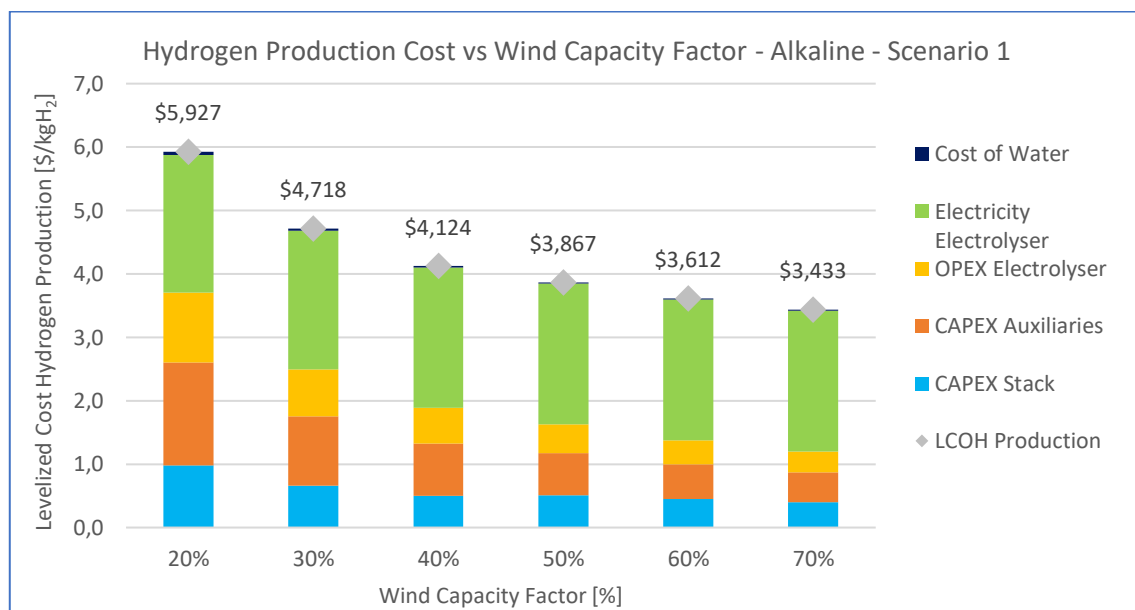


Figure 4.3: Hydrogen cost production trend respect wind capacity factor, alkaline – scenario 1

The most affected costs by the capacity factor are the CAPEX of the stacks and auxiliaries, and consequently the operating costs, which decrease abruptly. The cost of electricity undergoes

almost negligible variations, as does the cost of water. The reduction in costs is non-linear, it is very pronounced for low capacity factor values up to 40 %, after which its variation smooths out.

Scenario 1 – PEM

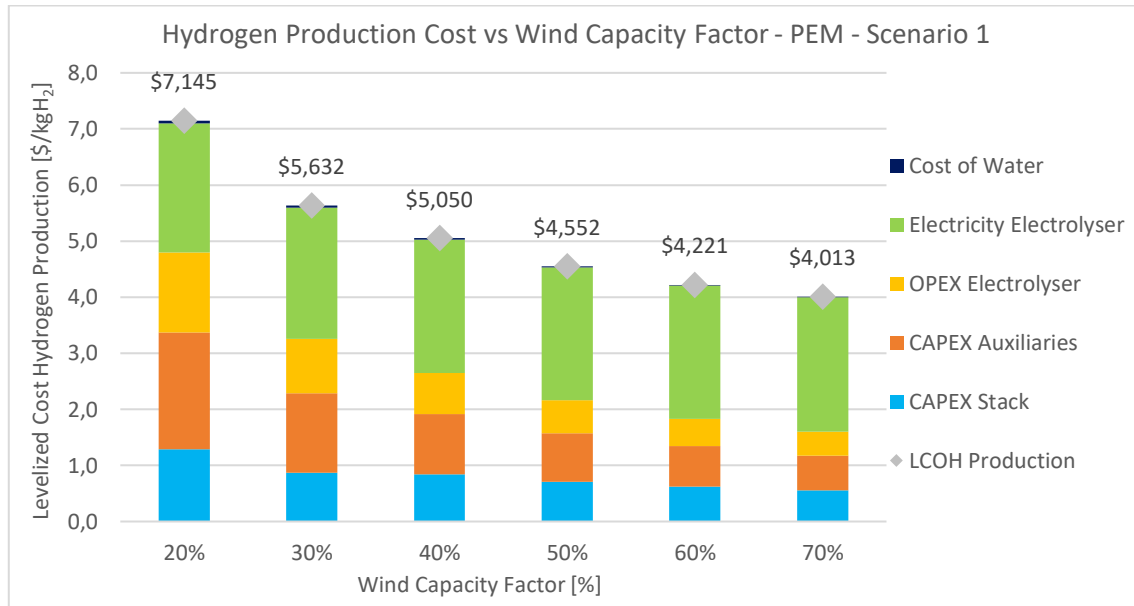


Figure 4.4: Hydrogen cost production trend respect wind capacity factor, PEM – scenario 1

The same considerations done for the alkaline electrolyser can also be extended to the PEM. In this case, the costs are higher, and the cost difference is also more pronounced. LCOH between PEM and alkaline differs by \$1,219/kgH₂ for CF equal to 20 %, and decreases to \$0,580/kgH₂ for CF 70 %.

Scenario 2 – Alkaline

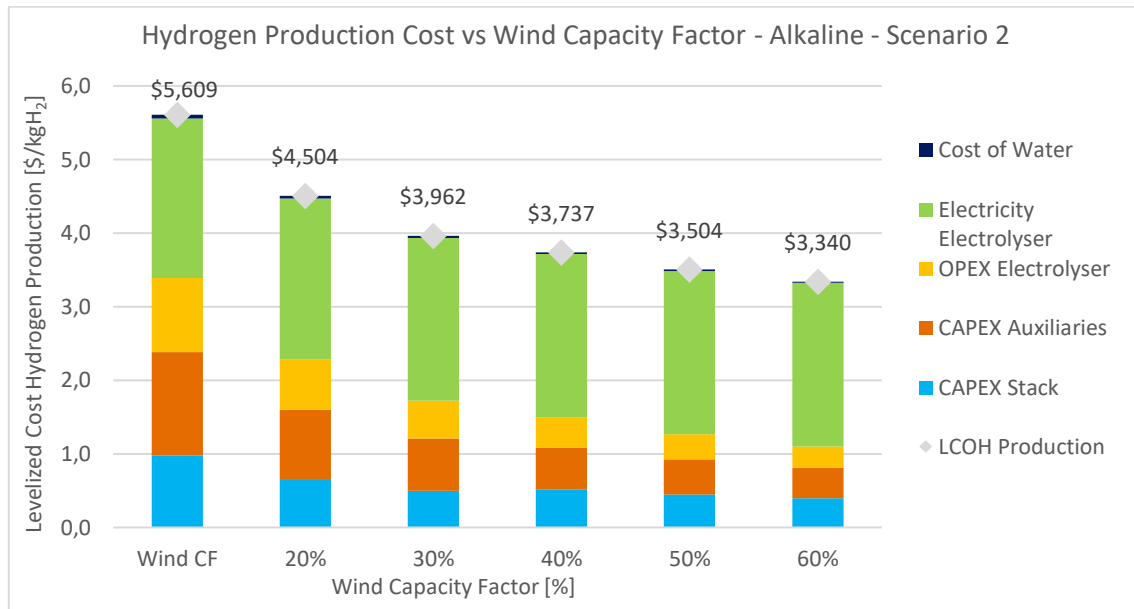


Figure 4.5: Hydrogen cost production trend respect wind capacity factor, alkaline – scenario 2

In scenario 2, costs are slightly lower than in scenario 1 because the scale effect is considered. The CAPEX of alkaline is \$823/kW.

Scenario 2 – PEM

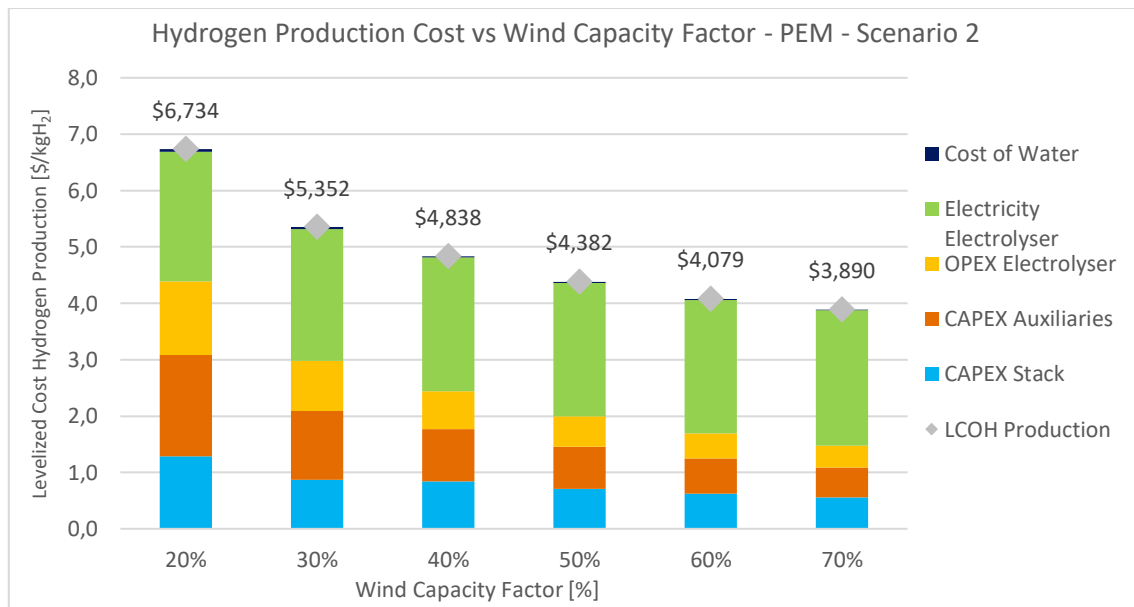


Figure 4.6: Hydrogen cost production trend respect wind capacity factor, PEM – scenario 2

The CAPEX of PEM is \$1006/kW. In scenario 2 the cost difference between alkaline and PEM passes from \$1,125/kgH₂ when CF is 70 %, to \$0,550/kgH₂ for CF 20 %.

- Levelized cost of final hydrogen

The development of the final LCOH of the hydrogen sent to the steel plant has been evaluated in the case of both NH_3 and LH_2 , and the cases of alkaline and PEM have been also distinguished.

Scenario 1

The table 4.2 shows the total LCOH values for the four cases considered.

Wind CF	NH_3 Alkaline	LH_2 Alkaline	NH_3 PEM	LH_2 PEM
20%	\$17,243	\$12,132	\$18,604	\$13,048
30%	\$13,875	\$10,276	\$14,827	\$10,918
40%	\$12,184	\$9,324	\$13,186	\$10,002
50%	\$11,333	\$8,856	\$12,056	\$9,346
60%	\$10,653	\$8,464	\$11,297	\$8,900
70%	\$10,158	\$8,175	\$10,724	\$8,560

Table 4.2: Final LCOH with respect wind capacity factor variation, scenario 1

The variation of the final LCOH when the carrier is NH_3 is strongly dependent on the capacity factor, the difference between CF 20 % and CF 70 % in the case of the alkaline electrolyser is \$7,085/kg H_2 , and for the PEM it rises to \$7,879/kg H_2 . In the case of the LH_2 carrier, the difference is less, \$3,957/kg H_2 for the alkaline and \$4,488/kg H_2 for the PEM.

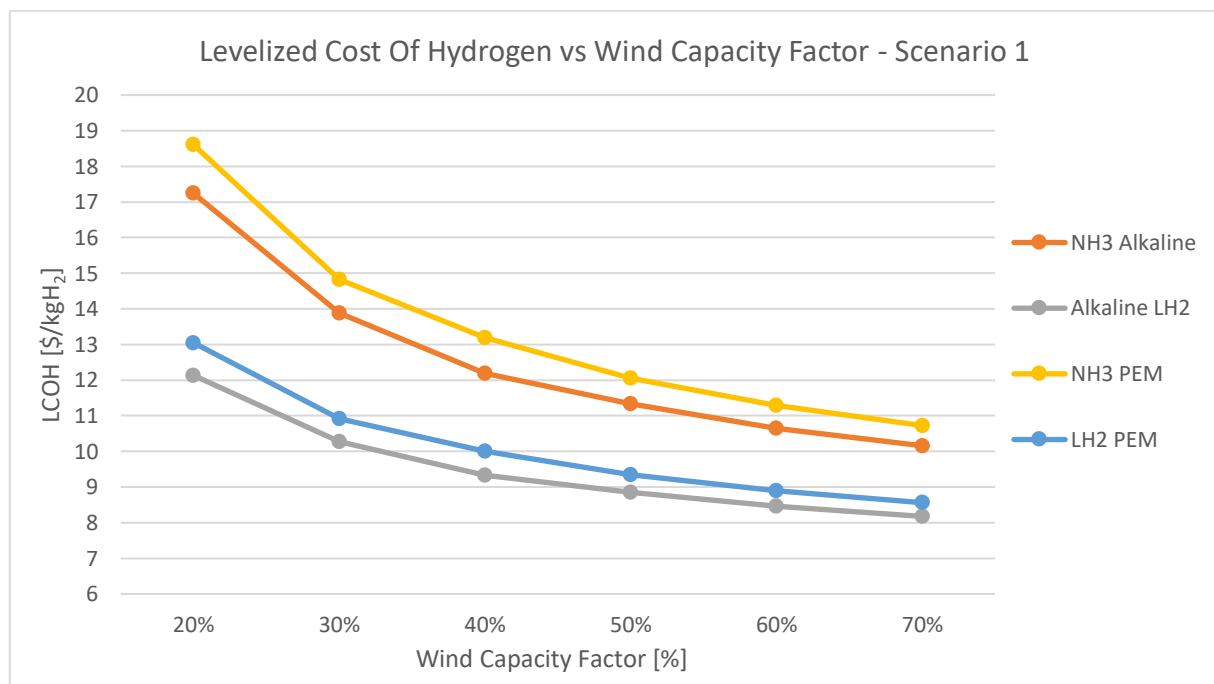


Figure 4.7: Final LCOH with respect wind capacity factor variation, scenario 1

The capacity factor influences more LCOH in the NH_3 chain than in the LH_2 chain, which has a flatter trend, this is due to the fact that in the former case also the compressor and the

hydrogen buffer (whose capacity is strongly influenced by the CF) are affected by the capacity factor variation, whereas in the latter case only the liquefaction plant is affected.

Scenario 2

Wind CF	NH ₃ Alkaline	LH ₂ Alkaline	NH ₃ PEM	LH ₂ PEM
20%	\$15,808	\$10,514	\$17,014	\$11,327
30%	\$12,728	\$8,879	\$13,576	\$9,453
40%	\$11,181	\$8,047	\$12,102	\$8,671
50%	\$10,415	\$7,652	\$11,074	\$8,099
60%	\$9,793	\$7,311	\$10,383	\$7,712
70%	\$9,340	\$7,061	\$9,860	\$7,415

Table 4.3: Final LCOH with respect wind capacity factor variation, scenario 2

In scenario 2, the final costs are lower, because of the scale factor considered for the most important equipment in the production process. When considering the ammonia carrier, the LCOH difference from CF 20 % to 70 % is \$6,469/kgH₂ per alkaline electrolyser and increases to \$7,155/kgH₂ using the PEM electrolyser. In the case of liquid hydrogen, the cost difference is \$3,453/kgH₂ for alkaline and \$3,913/kgH₂ for PEM.

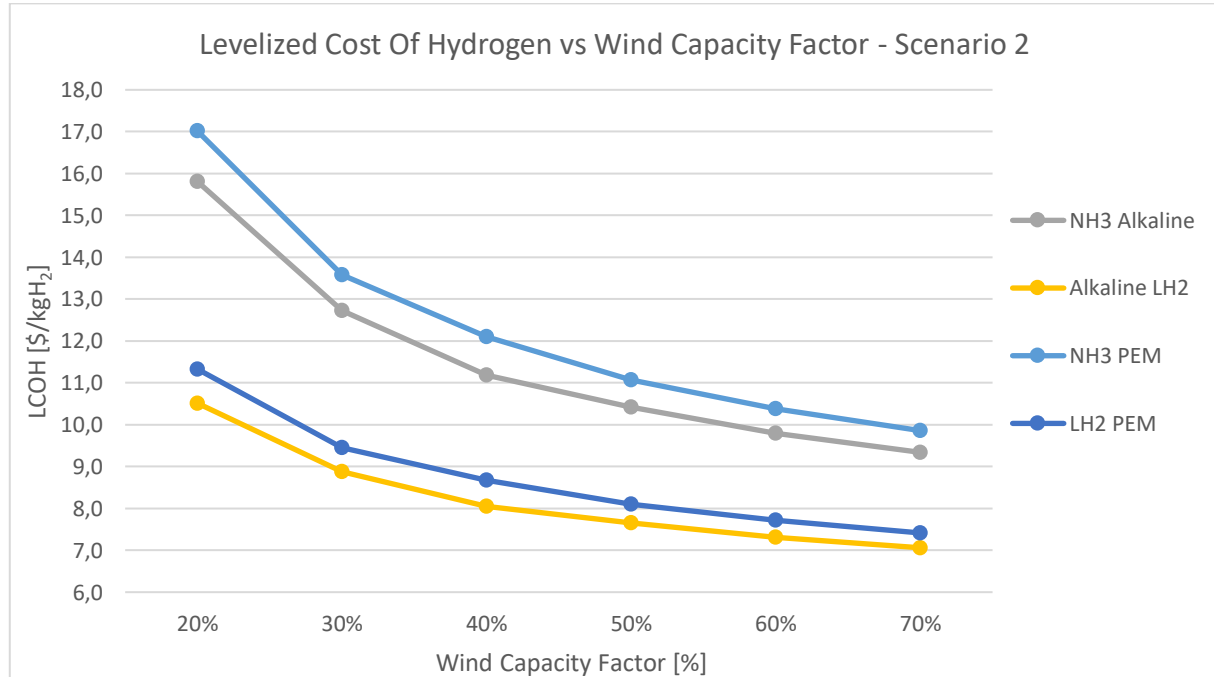


Figure 4.8: Final LCOH with respect wind capacity factor variation, scenario 2

4.2.2 Electrolyser consumption

Another parameter considered for the sensitivity analysis is the power consumption of the electrolyser, which is related to the energy cost for hydrogen production, that is the highest cost in the final LCOH in the case of both NH_3 and LH_2 . According to the paper (International Renewable Energy Agency, 2020) in 2020, the consumption range of the alkaline electrolyser is 50-78 kWh/kgH_2 , while that of the PEM electrolyser is 50 - 83 kWh/kgH_2 . The same paper estimates an improvement in efficiency and for both technologies predicts a power consumption of less than 45 kWh/kgH_2 in 2050. The paper (Tractebel Engineering & Inicio, 2017) reports a consumption range for the alkaline electrolyser between 58 and 49 kWh/kgH_2 , while for the PEM the consumption range is between 63 and 52 kWh/kgH_2 . In this sensitivity analysis, the consumption of both electrolysers has been varied in the range between 60 and 42 kWh/kgH_2 .

- Levelized cost of hydrogen production

The levelized cost of hydrogen production refers to the hydrogen produced by the electrolyser during the lifetime of the project. The other parameters are kept constant to the values highlighted at the beginning of the chapter.

Scenario 1 – Alkaline

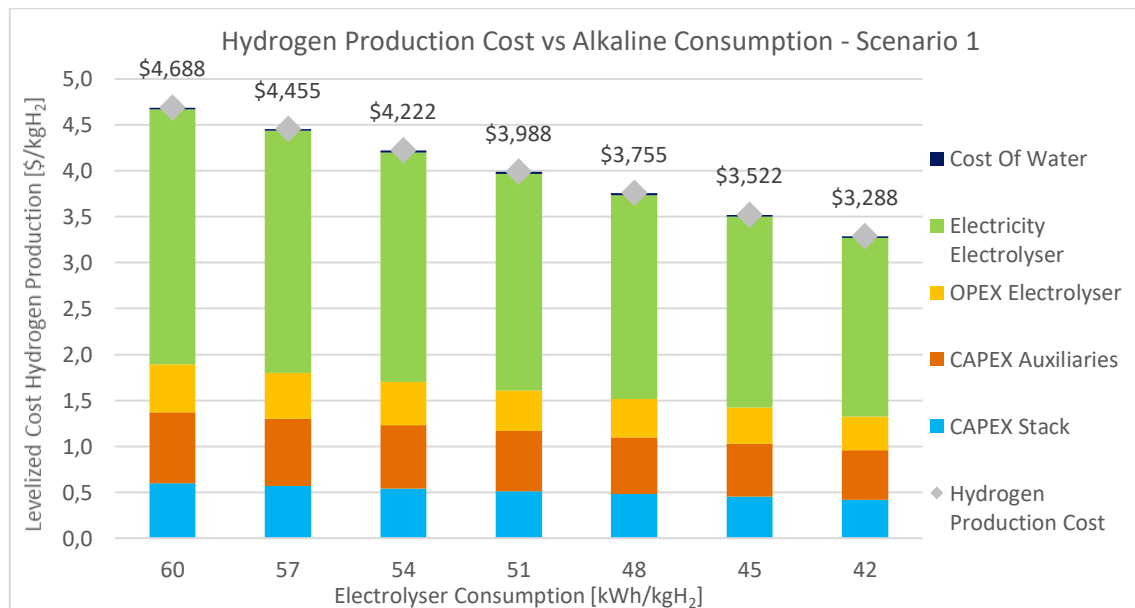


Figure 4.9: Hydrogen cost production trend respect electrolyser consumption, alkaline – scenario 1

The item most affected by this parameter is the cost of the electricity consumed by the electrolyser, which decreases linearly as the specific consumption of the electrolyser decreases.

The CAPEX also varies, although less than the cost of energy. This is due to the fact that energy consumption is linked to the power of the electrolyser, which in turn is a figure used to calculate the system's CAPEX.

Scenario 1 - PEM

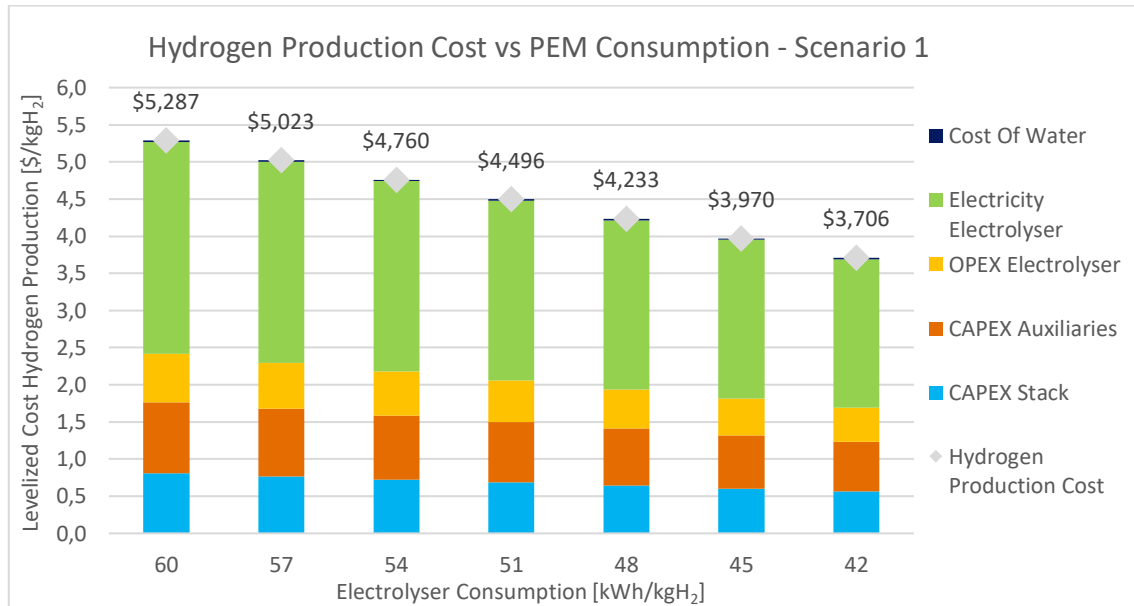


Figure 4.10: Hydrogen cost production trend respect electrolyser consumption, PEM – scenario 1

The same considerations done for the alkaline electrolyser can also be extended to the PEM. In this case, the costs are higher, but the cost difference remains almost constant. LCOH between PEM and alkaline differs by \$0,598/kgH₂ for power consumption equal to 60 kWh/kgH₂ and decreases to \$0,418/kgH₂ for electrolyser consumption of 42 kWh/kgH₂.

In scenario 2, hydrogen production costs are slightly lowered due to the scale factor considered. The production cost trend remains the same.

- Levelized cost of final hydrogen

The development of the final LCOH of the hydrogen sent to the steel plant has been evaluated in the case of both NH_3 and LH_2 , and the cases of alkaline and PEM have been also distinguished.

Scenario 1

The table 4.4 shows the total LCOH values for the four cases considered.

<i>Power Consumption</i>	<i>NH₃ Alkaline</i>	<i>LH₂ Alkaline</i>	<i>NH₃ PEM</i>	<i>LH₂ PEM</i>
60	12,524	9,690	13,051	10,047
57	12,150	9,438	12,650	9,776
54	11,776	9,185	12,249	9,506
51	11,402	8,933	11,848	9,236
48	11,028	8,680	11,447	8,965
45	10,654	8,428	11,046	8,695
42	10,280	8,176	10,645	8,424

Table 4.4: Final LCOH with respect electrolyser consumption variation, scenario 1

The variation of the final hydrogen LCOH is not significantly affected by the variation of the power consumption of the electrolyser, this is due to the costs of the other production processes that are independent from this parameter. The range of results of the final LCOH is just under \$2,500/kgH₂ in the case of NH_3 carrier, and just over \$1,500/kgH₂ in the case of LH_2 carrier. The graph 4.11 illustrates the cost trend reported in the table above.

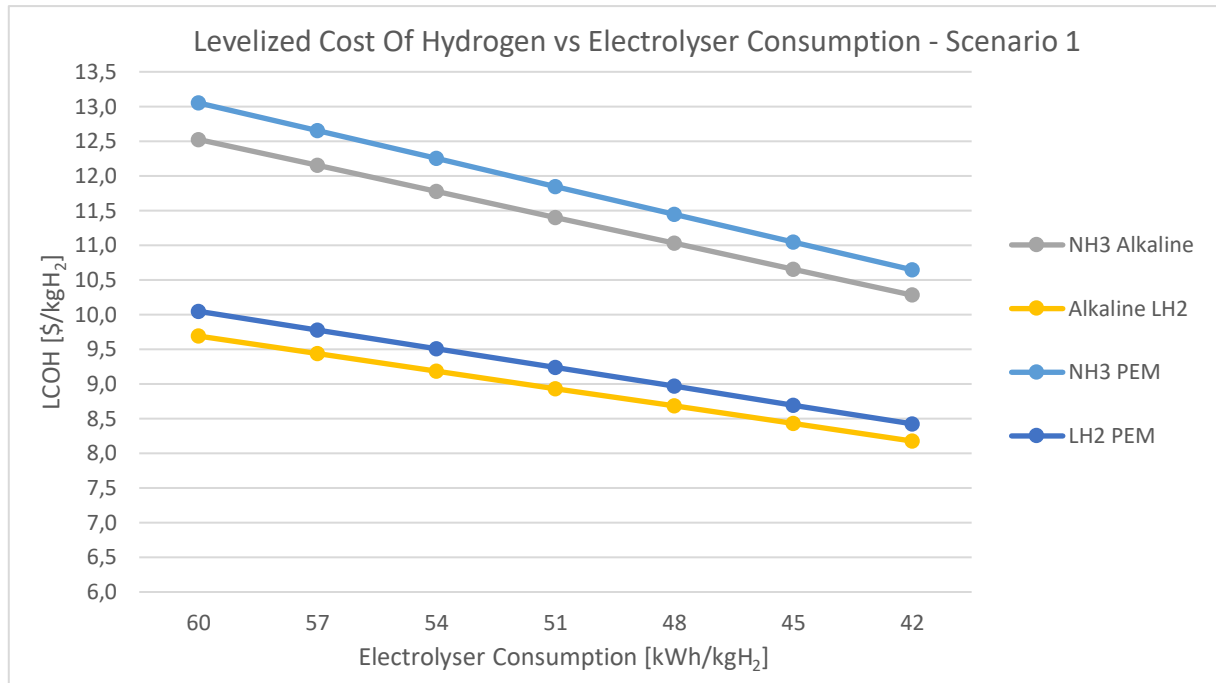


Figure 4.11: Final LCOH with respect electrolyser consumption variation, scenario 1

The decrease in LCOH follows a linear trend in all cases considered. The minimum value achieved for NH₃ supply chain is \$10,280/kgH₂, while for LH₂ supply chain it falls to \$8,176/kgH₂.

Scenario 2

Electrolyser Consumption	NH ₃ Alkaline	LH ₂ Alkaline	NH ₃ PEM	LH ₂ PEM
60	11,564	8,465	12,033	8,783
57	11,207	8,223	11,652	8,526
54	10,850	7,982	11,270	8,268
51	10,493	7,740	10,889	8,010
48	10,136	7,499	10,508	7,753
45	9,779	7,257	10,127	7,495
42	9,422	7,015	9,746	7,237

Table 4.5: Final LCOH with respect electrolyser consumption variation, scenario 2

The final LCOH in scenario 2 slightly decrease because of the scale factor considered. The final cost trend has the same path as in scenario 1.

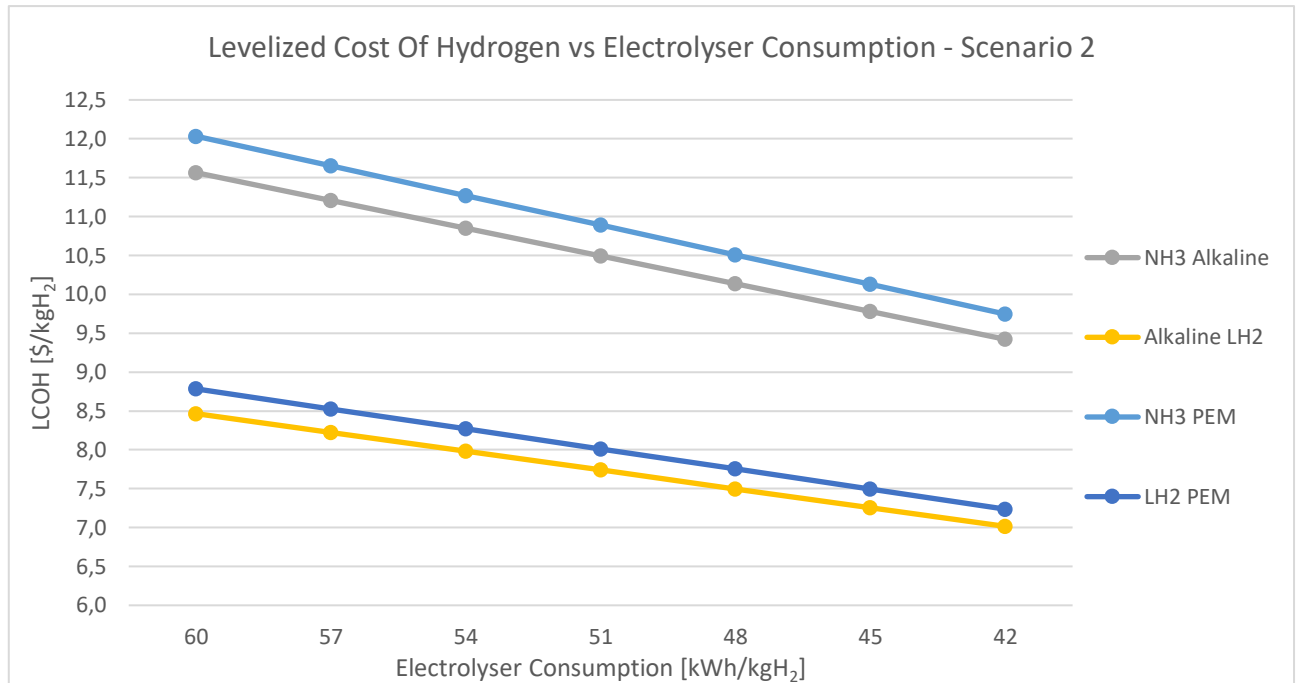


Figure 4.12: Final LCOH with respect electrolyser consumption variation, scenario 2

4.2.3 Electrolyser CAPEX

The third parameter considered for the sensitivity analysis is the installation cost of electrolyzers, which represents the second most important cost for hydrogen production, following the cost of the electricity for the electrolysis. The paper (International Renewable Energy Agency, 2020) reports CAPEX values for the year 2020 in the range of 500-1000 \$/kW for alkaline electrolyzers, and 700-1400 \$/kW for PEM electrolyzers. The same paper estimates a decrease in costs in the future to below \$200/kW due to the greater technological maturity of these technologies and the expansion of markets globally, which will bring benefits for production and installation costs. In this paper, the cost range has been assumed to vary between 1200 and 200 \$/kW, to consider both the current and possible future scenarios.

- Levelized cost of hydrogen production

The levelized cost of hydrogen production refers to the hydrogen produced by the electrolyser during the lifetime of the project. The other parameters are kept constant to the values highlighted at the beginning of the chapter. For this analysis there is no difference between scenario 1 and 2 because the cost of electricity and the cost of water are not influenced by the scale factor, and the CAPEX is the parameter chosen for the analysis.

Alkaline

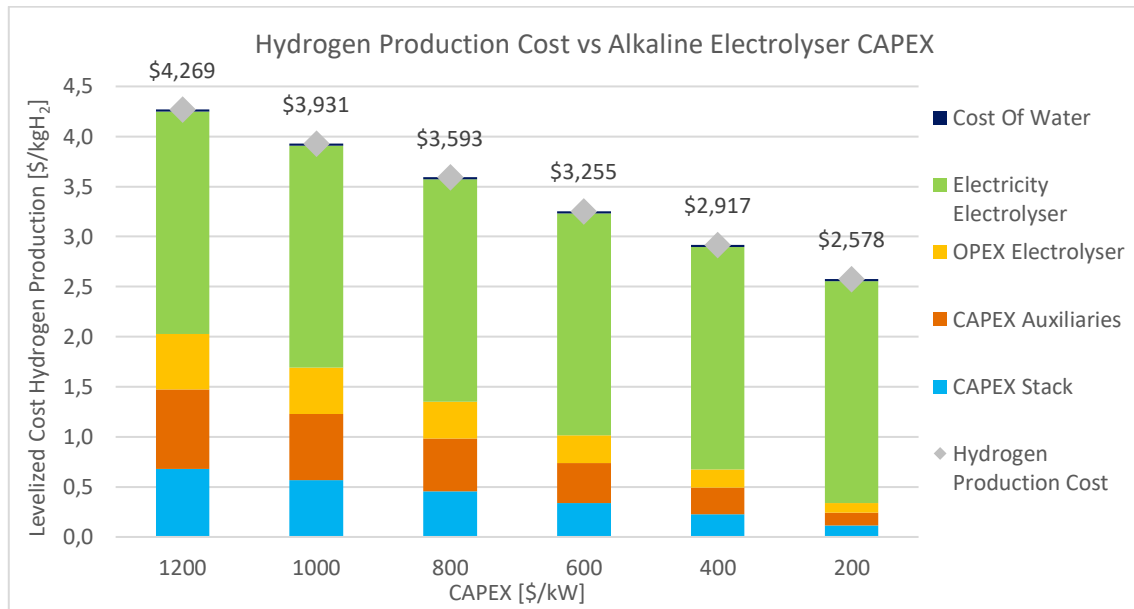


Figure 4.13: Hydrogen cost production trend respect electrolyser CAPEX, alkaline

The levelized cost of hydrogen production decreases linearly due to decreasing installation and operating costs. The cost of electricity and the cost of water are constant. For a specific installation cost of \$400/kW the LCOH reaches interesting value, lower than \$3.000/tonH₂.

PEM

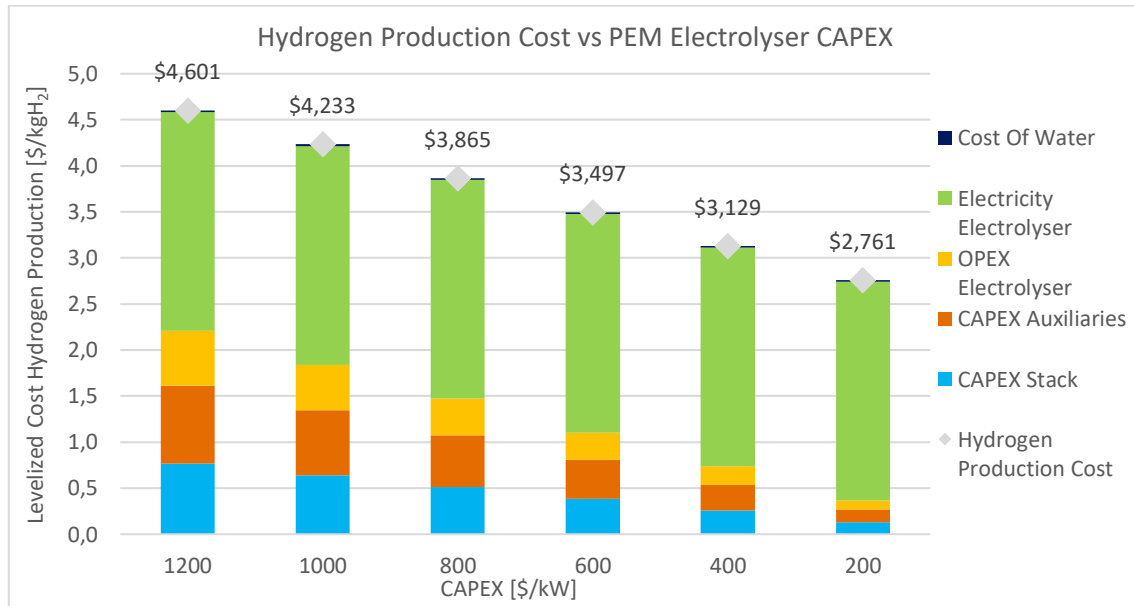


Figure 4.14: Hydrogen cost production trend respect electrolyser CAPEX, PEM

The LCOH related to PEM is slightly higher because of the higher power consumption. Also in this case the cost trend is linearly decreasing. In this case the threshold of \$3.000/tonH₂ is achieved for specific installation costs lower than \$400/kW.

- Levelized cost of final hydrogen

The development of the final LCOH of the product sent to the steel plant has been evaluated in the case of both NH_3 and LH_2 , and the cases of alkaline and PEM have been also distinguished. Only the scenario 1 has been considered. The table 4.6 shows the results for the main four cases evaluated.

<i>Electrolyser CAPEX</i>	<i>NH₃ Alkaline</i>	<i>LH₂ Alkaline</i>	<i>NH₃ PEM</i>	<i>LH₂ PEM</i>
1200	11,820	9,213	12,003	9,340
1000	11,299	8,863	11,451	8,969
800	10,778	8,513	10,899	8,598
600	10,257	8,163	10,347	8,227
400	9,736	7,813	9,795	7,857
200	9,215	7,463	9,243	7,486

Table 4.6: Final LCOH with respect electrolyser CAPEX

There is not a big difference in the final LCOH because the electrolyser CAPEX only affects the hydrogen production cost, while all the other processes of NH_3 or LH_2 production are not influenced by it. The cost difference in NH_3 supply chain between the most expensive and the cheapest configuration is \$2,605/kgH₂ considering alkaline electrolyser, and slightly increases to \$2,760/kgH₂ for PEM electrolyser. If LH_2 supply chain is considered, the LCOH difference is \$1,750/kgH₂ using alkaline, and \$1,854/kgH₂ adopting PEM. The graph 4.15 shows the final levelized cost trend.

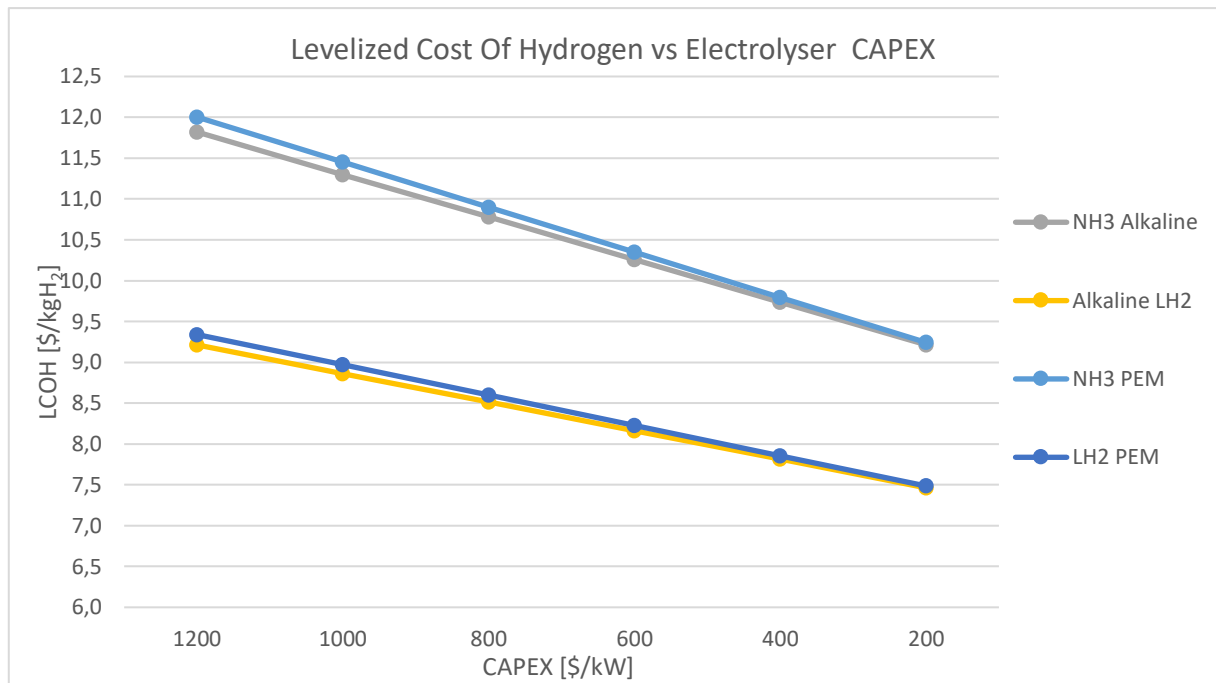


Figure 4.15: Final LCOH with respect electrolyser CAPEX

As it shown in the graph the difference of cost between alkaline and PEM is almost negligible, and it further decreases by diminishing the specific cost of installation of the electrolyser. For CAPEX of \$200/kW the final LCOH is the same for alkaline and PEM, both in NH₃ supply chain and in LH₂ supply chain, being respectively \$9,200/kgH₂ and \$7,500/kgH₂.

4.2.4 Wind electricity cost

The last parameter evaluated is the cost of wind energy, that in the region of Chubut in Patagonia it varies between \$66/MWh and \$38,9/MWh. For this analysis a range variation between 20 and 60 \$/MWh has been considered.

- Levelized cost of hydrogen production

The levelized cost of hydrogen production is related to the total amount of hydrogen produced by the electrolyzers during the whole lifetime of the project, that is 20 years. In this cost are considered the costs related to the electrolysis process and the cost of desalination.

Scenario 1 – Alkaline

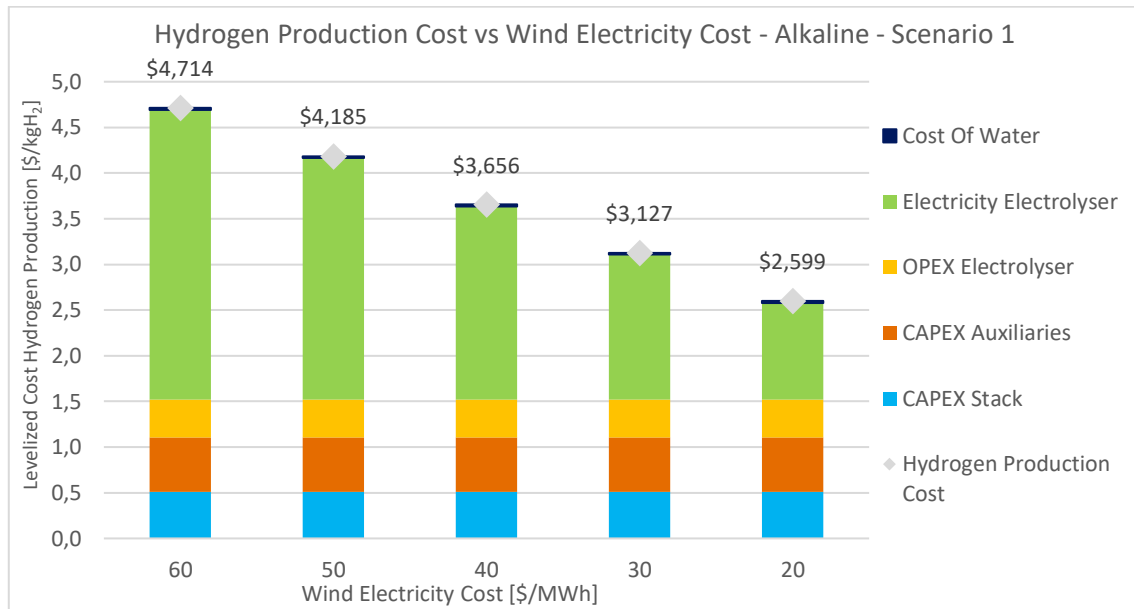


Figure 4.16: Hydrogen cost production trend respect wind energy cost, alkaline, scenario 1

The production cost of hydrogen is strongly influenced by the cost of electricity, going from an LCOH of \$4,714/kgH₂ for a cost of \$60/MWh to a production cost of \$2,599/kgH₂ for \$20/MWh. The cost of CAPEX and OPEX are kept constant because they are not affected by the cost of electricity. The cost of water is influenced by the cost of electricity, but its weight in the LCOH is negligible.

Scenario 1 – PEM

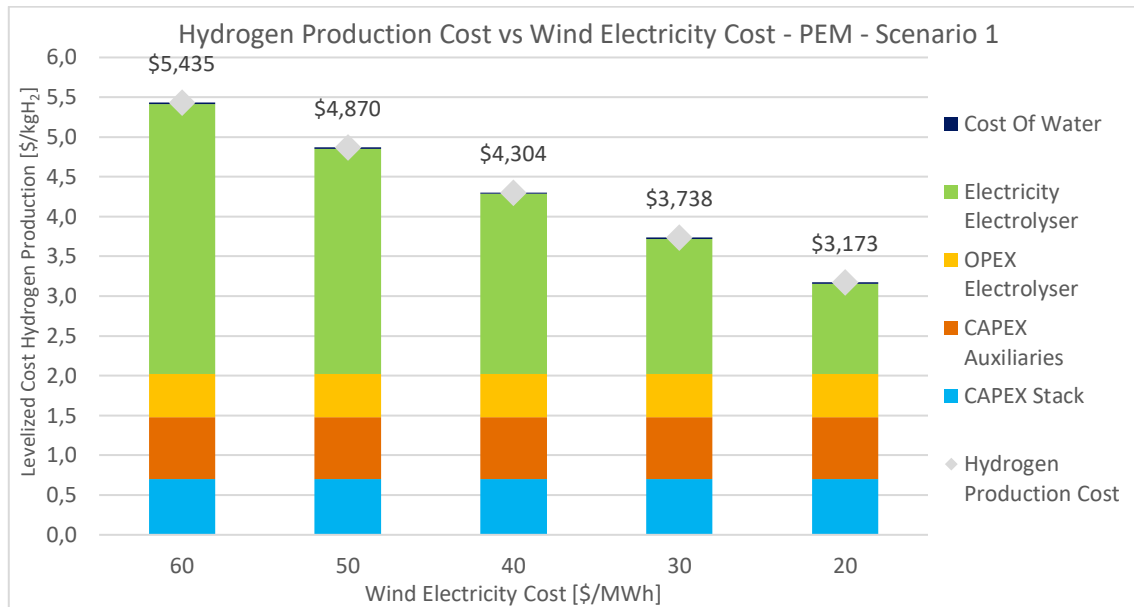


Figure 4.17: Hydrogen cost production trend respect wind energy cost, PEM, scenario 1

Again, CAPEX and OPEX remain constant as the cost of electricity changes, and the trend in LCOH is the same as described for alkaline. The final cost is slightly higher due to the higher power consumption that characterises PEM. The cost of water remains negligible.

In the second scenario, the costs are slightly lower for both PEM and alkaline because the scale effect is considered. The cheapest configuration, related to wind energy cost of \$20/MWh determines a LCOH equal to \$2,468/kgH₂ for alkaline and \$2,999/kgH₂ for PEM.

- Levelized cost of final hydrogen

The development of the final LCOH of the product sent to the steel plant has been evaluated in the case of both NH₃ and LH₂, and the cases of alkaline and PEM have been also distinguished. The table 4.7 shows the results for the main four cases for scenario 1.

Scenario 1

Wind Electricity Cost [\$/MWh]	NH ₃ Alkaline	LH ₂ Alkaline	NH ₃ PEM	LH ₂ PEM
60	12,580	9,900	13,326	10,407
50	11,724	9,227	12,438	9,711
40	10,868	8,554	11,549	9,015
30	10,011	7,880	10,661	8,319
20	9,155	7,207	9,773	7,623
15	8,727	6,870	9,329	7,275

Table 4.7: Final LCOH with respect wind electricity cost, scenario 1

The cost of wind energy, unlike in the previous cases, also greatly influences the processes downstream of electrolysis, such as liquefaction plants, nitrogen production plant and ammonia synthesis. In the NH₃ alkaline configuration, the difference between the highest and lowest cost is \$3,424/kgH₂, rising to \$3,553/kgH₂ taking PEM. In the case of the LH₂ configuration, the cost difference is \$2,693/kgH₂ for alkaline and \$2,784/kgH₂ for PEM. The graph 4.18 shows the trend in final hydrogen level costs.

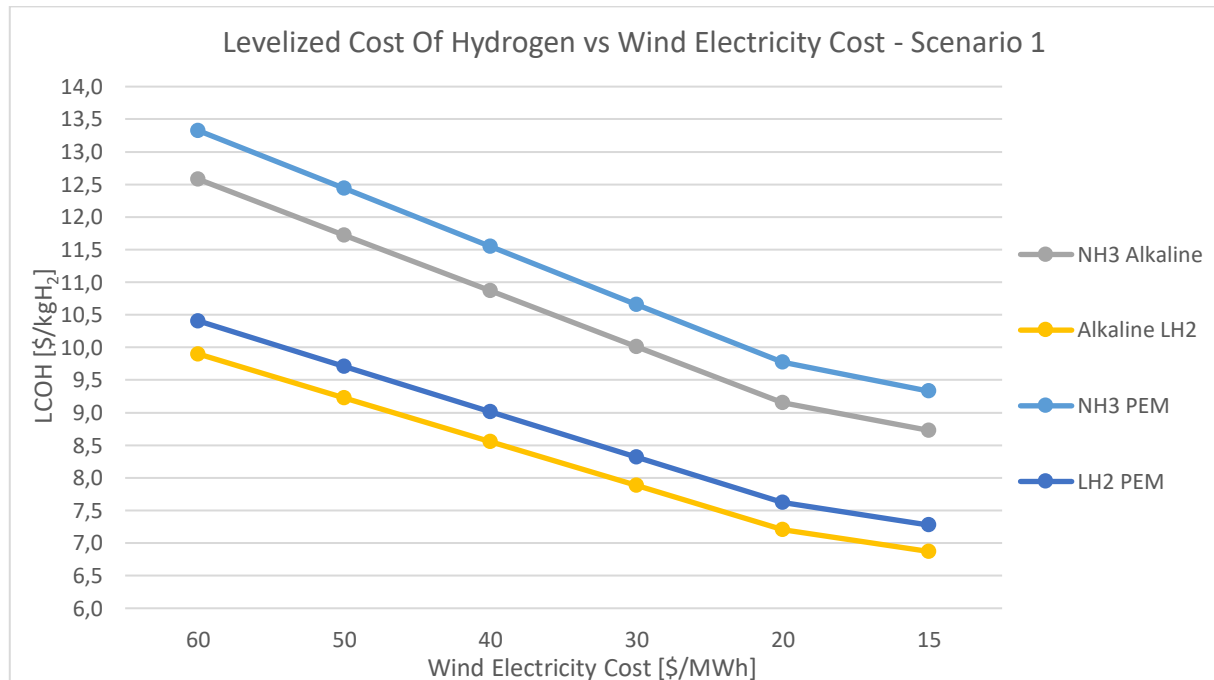


Figure 4.18: Final LCOH with respect wind electricity cost, scenario 1

The final hydrogen cost has a linear trend for both NH₃ and LH₂. In the best-case scenario, the final LCOH could fall below \$9.000/tonH₂ in the case of NH₃, and fall below \$7.000/tonH₂ in the case of LH₂.

Scenario 2

Wind Electricity Cost [\$/MWh]	NH ₃ Alkaline	LH ₂ Alkaline	NH ₃ PEM	LH ₂ PEM
60	11,650	8,692	12,327	9,153
50	10,806	8,027	11,452	8,466
40	9,963	7,362	10,576	7,779
30	9,119	6,698	9,701	7,092
20	8,275	6,033	8,826	6,405
15	7,854	5,700	8,388	6,061

Table 4.8: Final LCOH with respect wind electricity cost, scenario 2

In the second scenario, costs are lowered even further due to the scale factor. For an electricity cost of \$20/MWh, the levelized cost of hydrogen reaches \$8,275/kgH₂ in the case of alkaline NH₃, \$8,826/kgH₂ in the case of PEM. For the LH₂ chain, the final hydrogen cost is \$6,003/kgH₂ considering alkaline electrolyser and \$6,405/kgH₂ in the case of PEM.

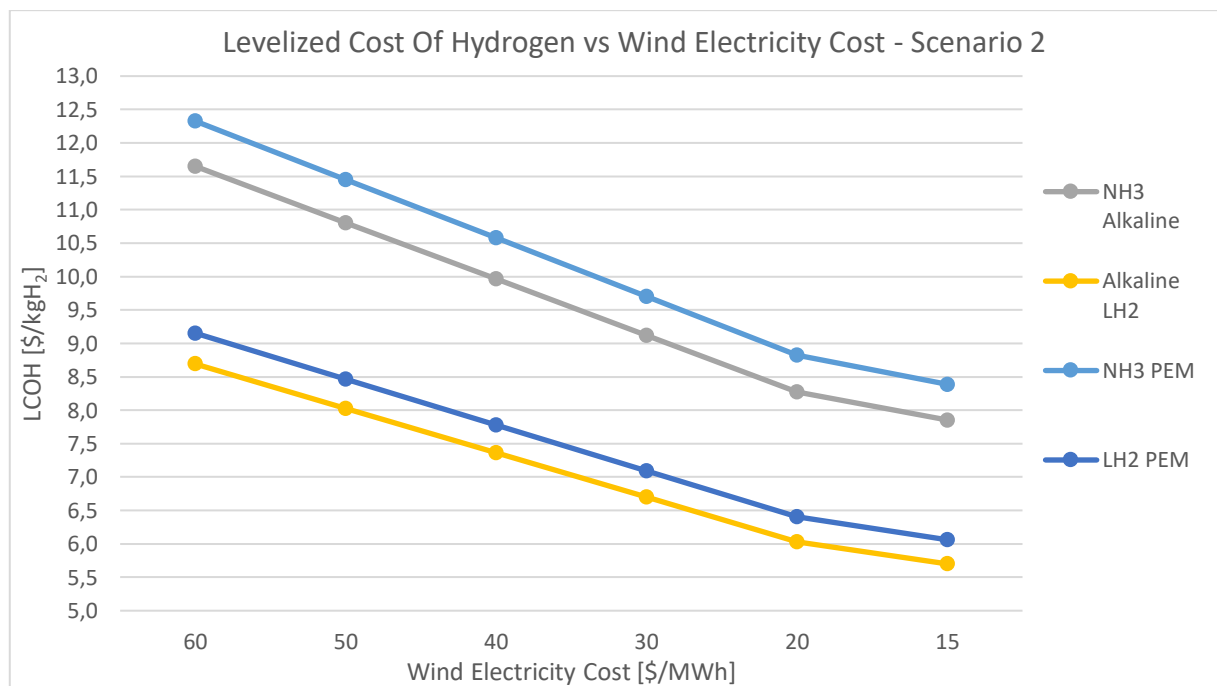


Figure 4.19: Final LCOH with respect wind electricity cost, scenario 2

4.3 Sensitivity analysis considering two variables

In this section, the sensitivity analysis is carried out calculating the levelized cost of hydrogen production (related to the H₂ produced by the electrolyser), and final LCOH of hydrogen sent to the steel plants for both energy carriers, NH₃ and LH₂. These results are obtained by varying contemporary two operating parameters, to deeply understand the effects of the combination of more parameters on the final LCOH. The analysis with two parameters is carried out only for alkaline electrolyser and for scenario 1, because the cost related to PEM electrolyser are similar, and also the costs in second scenario do not vary significantly, as is demonstrated by the studies of the previous sections.

4.3.1 Capacity factor and electrolyser consumption

The capacity factor varies between 20 and 70 %, and the electrolyser consumption goes from 42 to 57 kWh/kg. The other parameters remain constant at the base case values:

- Wind electricity cost: \$42/MWh
- CAPEX alkaline: \$900/kW
- Levelized cost of hydrogen production

The levelized cost of hydrogen production is related to the total amount of hydrogen produced by the electrolyzers during the whole lifetime of the project, that is 20 years.

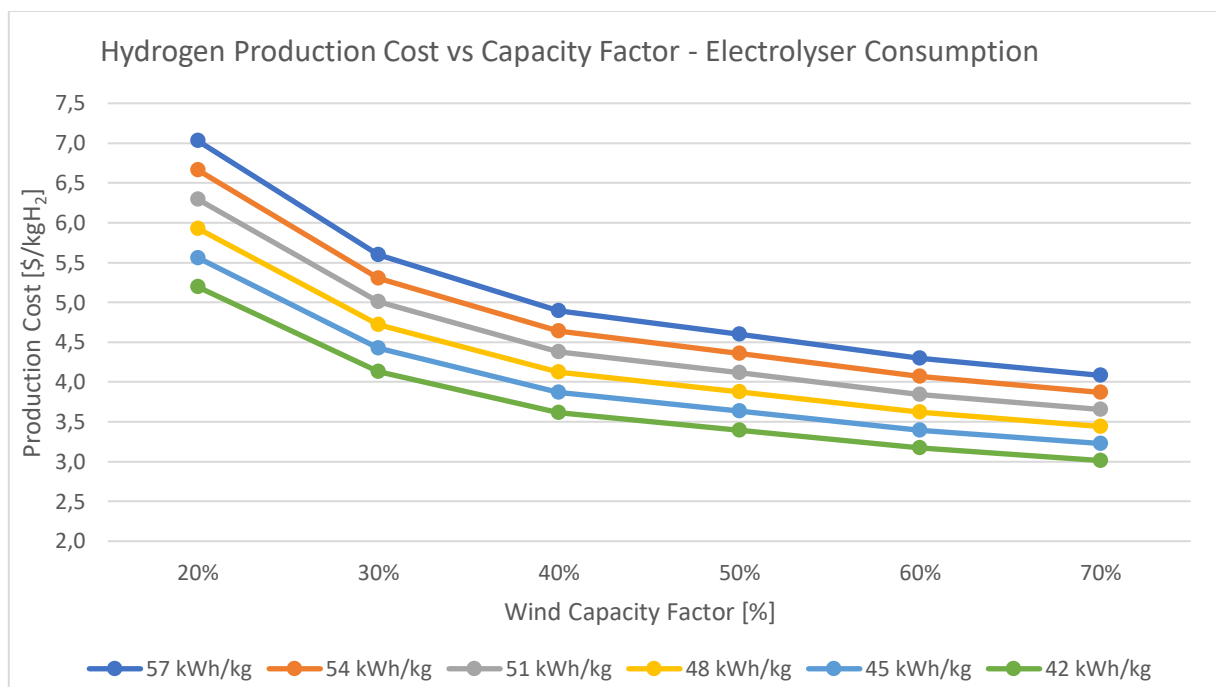


Figure 4.20: Levelized cost of hydrogen production with respect capacity factor and electrolyser consumption

The cost of hydrogen production varies non-linearly with respect to capacity factor, tending to flatten out for high CF values, while decreasing linearly with respect to the power required for electrolysis. With this combination, it is not possible to fall below the \$3.000/tonH₂ threshold.

- Levelized cost of final hydrogen

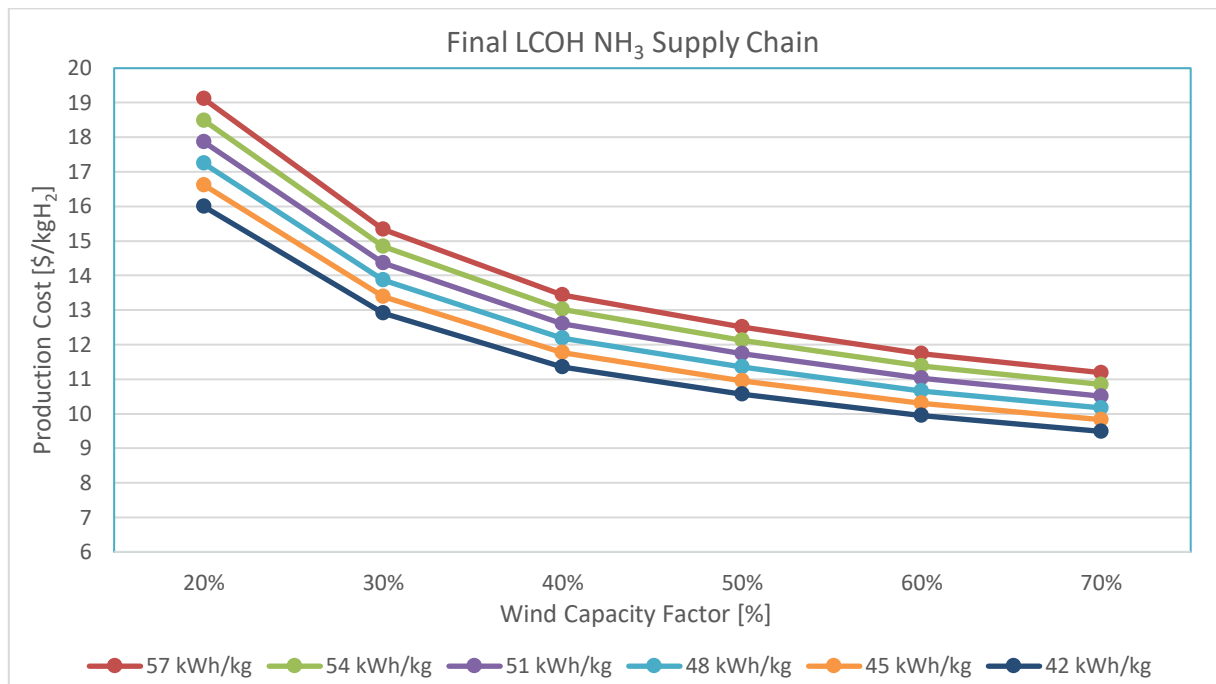


Figure 4.21: Final levelized cost of hydrogen for NH₃ supply chain with respect capacity factor and electrolyser consumption

There is a big gap between the 20 % CF configuration and the 70 % CF configuration. For an optimistic but feasible combination, i.e. CF 60 % and consumption of 45 kWh/kgH₂, the final LCOH of hydrogen is \$10,304/kgH₂.

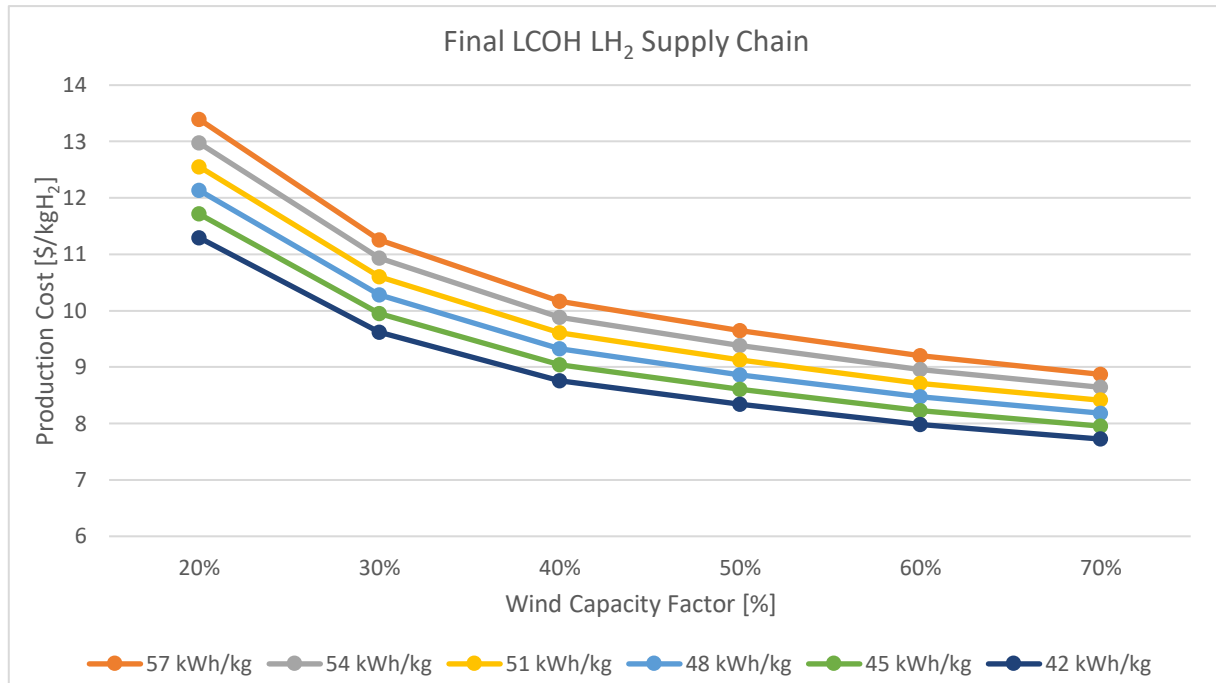


Figure 4.22: Final levelized cost of hydrogen for LH₂ supply chain with respect capacity factor and electrolyser consumption

The curve pattern is the same as in the previous case, but the results are significantly lower. Considering the same optimistic case with CF 60 % and electricity consumption 45 kWh/kg, the final LCOH of hydrogen in this case is \$8,229/kgH₂.

4.3.2 Capacity factor and wind energy cost

The capacity factor varies between 20 and 70 %, and the wind energy cost goes from 20 to 60 \$/kWh. The other parameters remain constant at the base case values:

- Electrolyser consumption: 48 kWh/kgH₂
- CAPEX alkaline: \$900/kW
- Levelized cost of hydrogen production

The levelized cost of hydrogen production is related to the total amount of hydrogen produced by the electrolyzers during the whole lifetime of the project, that is 20 years.

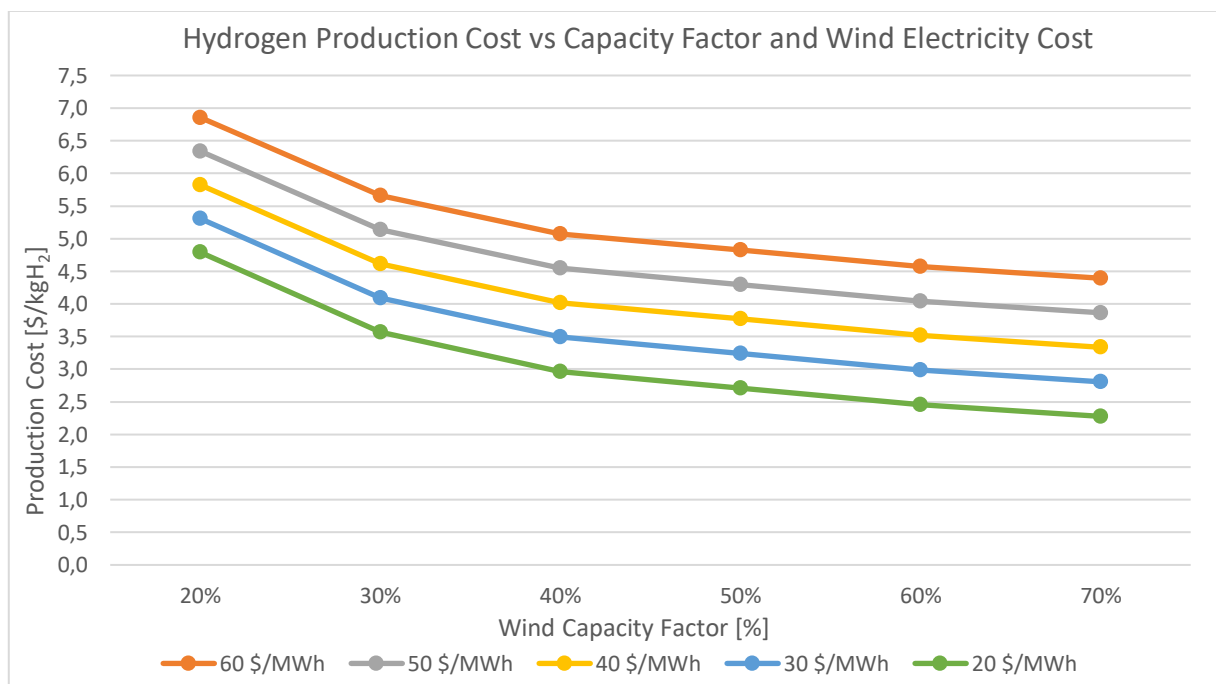


Figure 4.23: Levelized cost of hydrogen production with respect capacity factor and wind electricity cost

The curve trend is non-linear, and the cost difference between the considered configurations remains almost constant. Considering the feasible combination of CF 60 % and wind energy cost \$30/MWh, the levelized cost of hydrogen production is \$2,986/kgH₂, and further decreases to \$2,457/kgH₂ when considering the energy cost of \$20/MWh.

- Levelized cost of final hydrogen

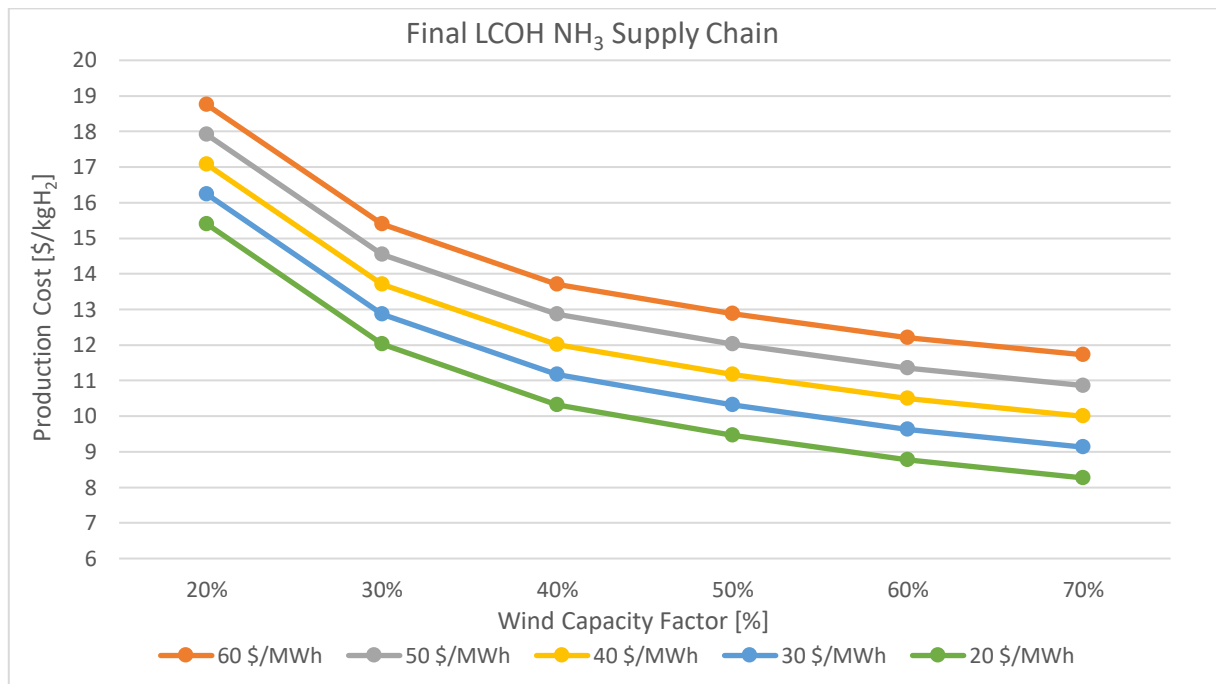


Figure 4.24: Final levelized cost of hydrogen for NH₃ supply chain with respect capacity factor and wind energy cost

The capacity factor, as in the previous cases, has a very high impact on the final hydrogen cost when the carrier is ammonia. Considering the optimistic case of 60 % CF and electricity cost \$30/MWh, the final LCOH assumes a value of \$9,633/kgH₂, while decreasing the wind power cost further down to \$8,773/kgH₂. The last configuration is less feasible in the short run.

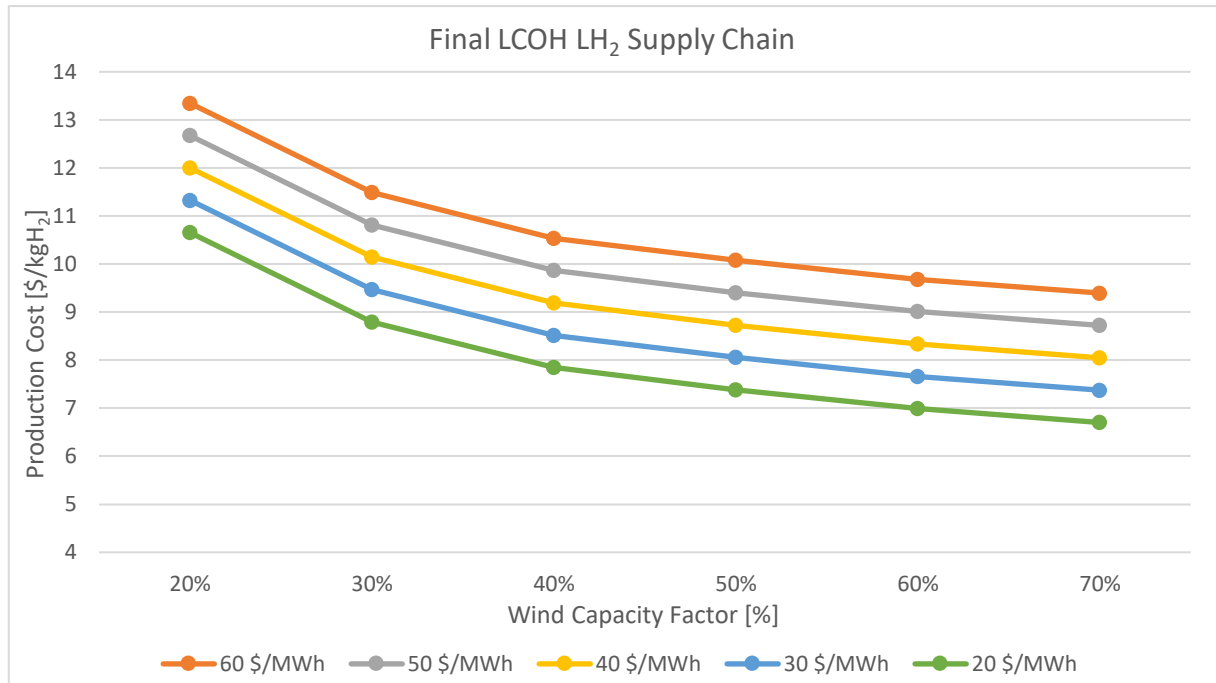


Figure 4.25: Final levelized cost of hydrogen for LH₂ supply chain with respect capacity factor and wind energy cost

The difference in costs relative to capacity factor is less pronounced than in the previous case. Final LCOH in the case of LH₂ are lower than for NH₃. Considering CF 60 % and wind cost \$30/MWh the final hydrogen cost is \$7,664/kgH₂, while decreasing electricity cost the hydrogen cost drops to \$6,990/kgH₂.

4.3.3 Capacity factor and electrolyser CAPEX

The capacity factor varies between 20 and 70 %, and the electrolyser CAPEX goes from 1200 to 200 \$/kW. The other parameters remain constant at the base case values:

- Electrolyser consumption: 48 kWh/kgH₂
- Wind electricity cost: \$42/MWh
- Levelized cost of hydrogen production

The levelized cost of hydrogen production is related to the total amount of hydrogen produced by the electrolyzers during the whole lifetime of the project, that is 20 years.

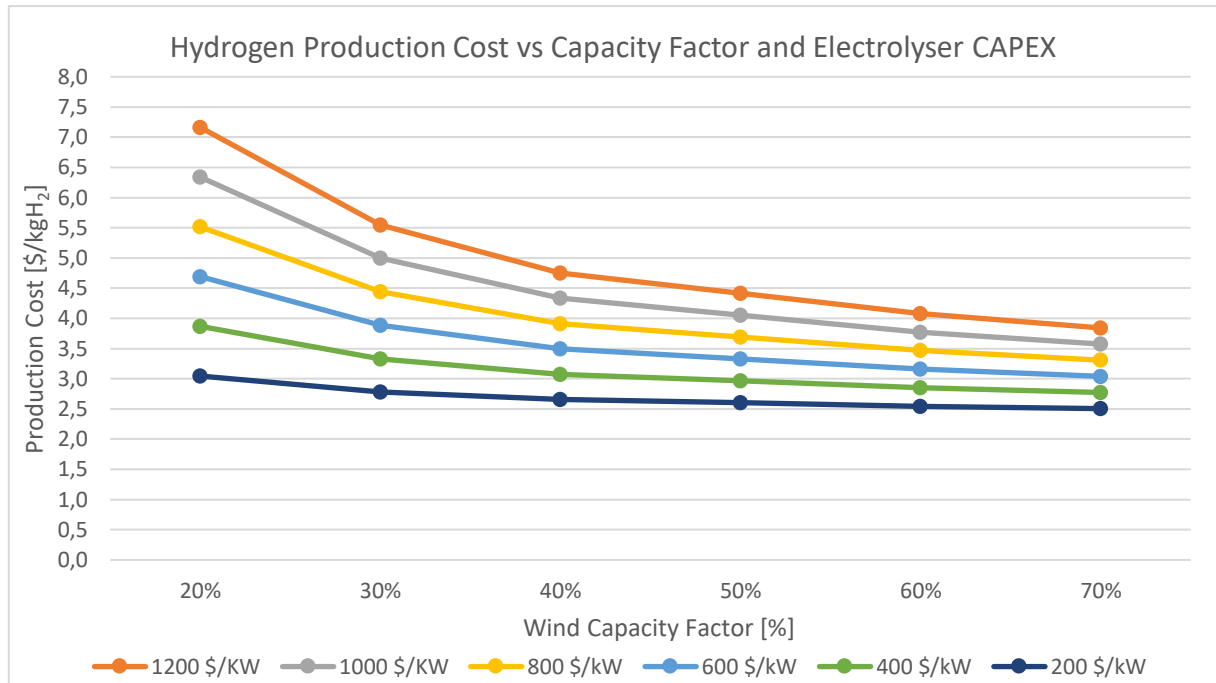


Figure 4.26: Levelized cost of hydrogen production with respect capacity factor and electrolyser CAPEX

The slope of the curves with respect to the capacity factor softens as the CAPEX of the electrolyser decreases. In the case of CAPEX equal to \$400/kW and CF 60 %, the levelized cost of hydrogen produced is \$2,851/kgH₂, and drops further the specific installation cost, LCOH reaches \$2,544/kgH₂.

- Levelized cost of final hydrogen

The final hydrogen cost refers to the total hydrogen sent to the direct reduced iron plant during the 20-year life of the project.

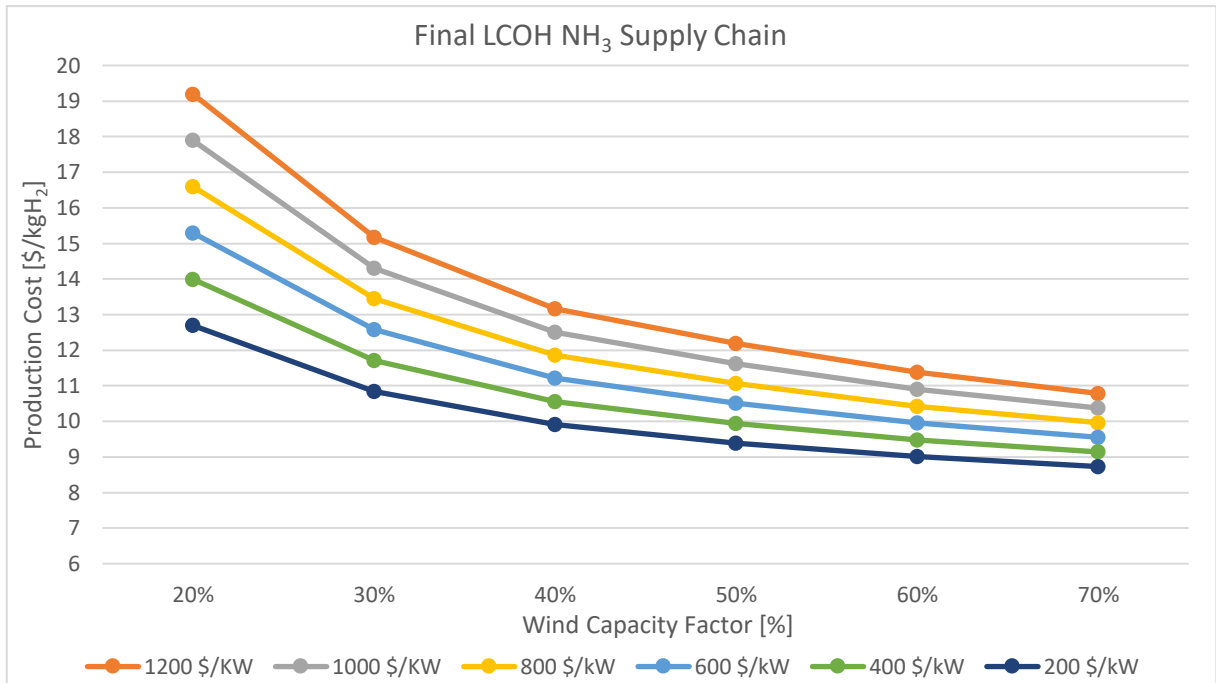


Figure 4.27: Final levelized cost of hydrogen for NH₃ supply chain with respect capacity factor and electrolyser CAPEX

The curves decrease with a non-linear trend, tending to flatten out for capacity factor values greater than 50 %. Considering an optimistic CAPEX of \$400/kW, the final hydrogen cost drops below \$10.000/tonH₂ for 50 % CF, and decreases further to \$9,479/kgH₂ for 60 % CF. In the more challenging case of increasing CF to 70 %, final LCOH would drop to \$9,141/kgH₂.

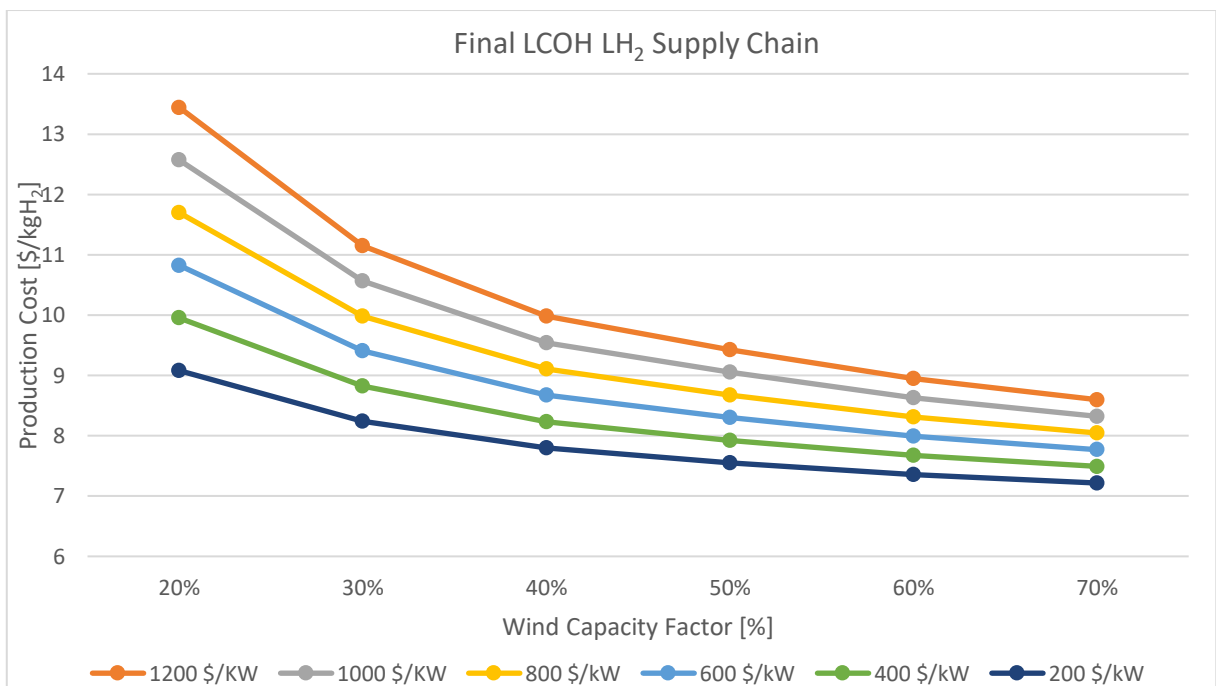


Figure 4.28: Final levelized cost of hydrogen for LH₂ supply chain with respect capacity factor and electrolyser CAPEX

Final LCOH adopting the LH₂ carrier are much lower than the NH₃ vector, especially for low-capacity factors. Considering the optimistic case of CAPEX \$400/kW breaks the \$8.000/tonH₂

threshold with a 50 % CF, and results in a final LCOH of \$7,676/kgH₂ for a 60 % CF. Considering an even higher CF of 70 %, LCOH drops to \$7,357/kgH₂.

4.3.4 Electrolyser CAPEX and wind energy cost

The wind electricity cost varies between 20 and 60 \$/MWh, and the electrolyser CAPEX goes from 1200 to 200 \$/kW. The other parameters remain constant at the base case values:

- Electrolyser consumption: 48 kWh/kgH₂
- Wind capacity factor: 54 %

- Levelized cost of hydrogen production

The levelized cost of hydrogen production is related to the total amount of hydrogen produced by the electrolyzers during the whole lifetime of the project, that is 20 years.

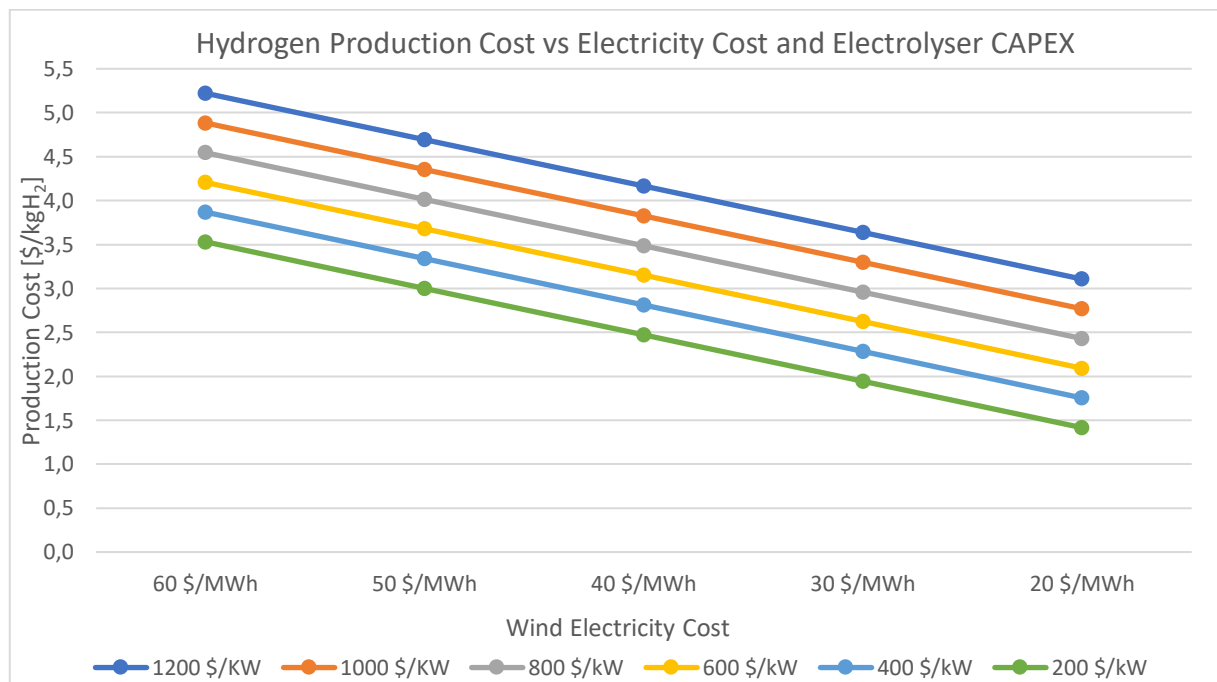


Figure 4.29: Levelized cost of hydrogen production with respect wind electricity cost and electrolyser CAPEX

The curves have a linear downward trend and the difference between them remains constant throughout the range of values considered. Considering an installation cost of \$600/kW, hydrogen can be produced at a very competitive value using a wind power cost of \$30/MWh, LCOH is \$2,620/kgH₂. If a CAPEX of \$400/kgH₂ is assumed, the levelized cost of \$2,811/kgH₂ for energy cost of \$40MWh is obtained, and it drops to \$2,282/kgH₂ at \$30/MWh. In the most

extreme case of electricity cost of \$20/MWh, LCOH would fall to \$1,753/kgH₂, a highly competitive value.

- Levelized cost of final hydrogen

The final hydrogen cost refers to the total hydrogen sent to the direct reduced iron plant during the 20-year life of the project.

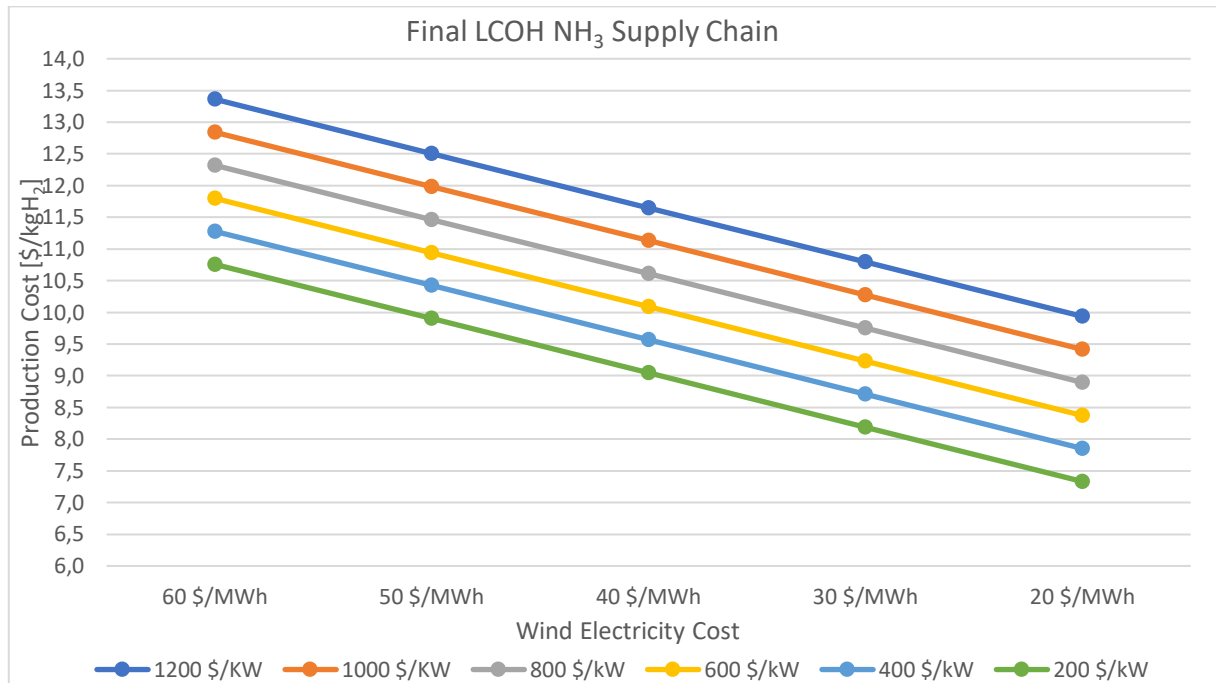


Figure 4.30: Final levelized cost of hydrogen for NH₃ supply chain with respect wind electricity cost and electrolyser CAPEX

The final hydrogen costs that can be achieved by combining the effects of electricity cost and electrolyser installation cost are very interesting. Considering an installation cost of \$600/kW yields an LCOH of \$9,230/kgH₂ for an energy cost of \$30MWh. Decreasing the CAPEX to \$400/kW LCOH drops to \$8,709/kgH₂ for the same energy cost, and further reduces to \$7,853/kgH₂ for a wind energy cost of \$20/MWh.

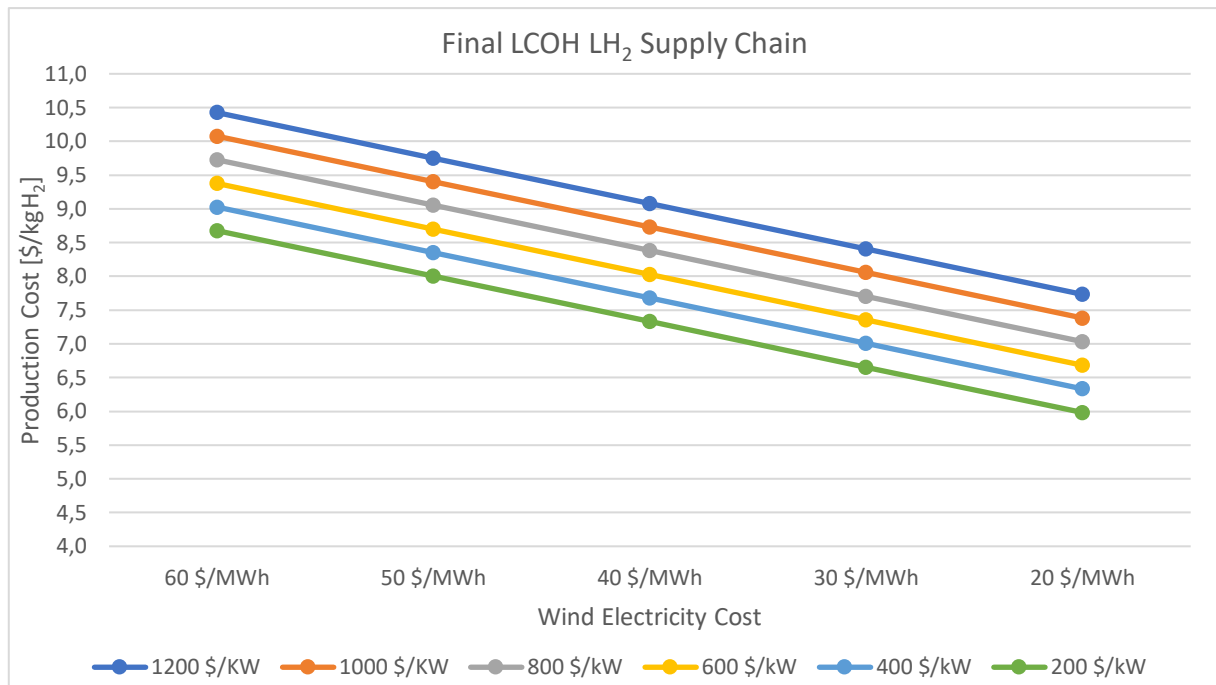


Figure 4.31: Final levelized cost of hydrogen for LH₂ supply chain with respect wind electricity cost and electrolyser CAPEX

LCOH in the case of using liquid hydrogen as H₂ carrier is lower than in the case of ammonia. Considering a CAPEX of \$600/kW and an energy cost of \$40/MWh LCOH is \$8,029/kgH₂, and decreases to \$7,355/kgH₂ in the case of \$30/MWh. On the other hand, if CAPEX of \$400/kW is selected with an electricity cost of \$30/MWh, LCOH is \$7,005/kgH₂, and decreases to \$6,332/kgH₂ for energy cost of \$20/MWh.

4.3.5 Electrolyser CAPEX and electrolyser consumption

The electrolyser consumption varies between 42 and 57 kWh/kg, and the electrolyser CAPEX goes from 1200 to 200 \$/kW. The other parameters remain constant at the base case values:

- Wind Electricity Cost: 42 \$/MWh
- Wind Capacity Factor: 54 %
- Levelized cost of hydrogen production

The levelized cost of hydrogen production is related to the total amount of hydrogen produced by the electrolyzers during the whole lifetime of the project, that is 20 years.

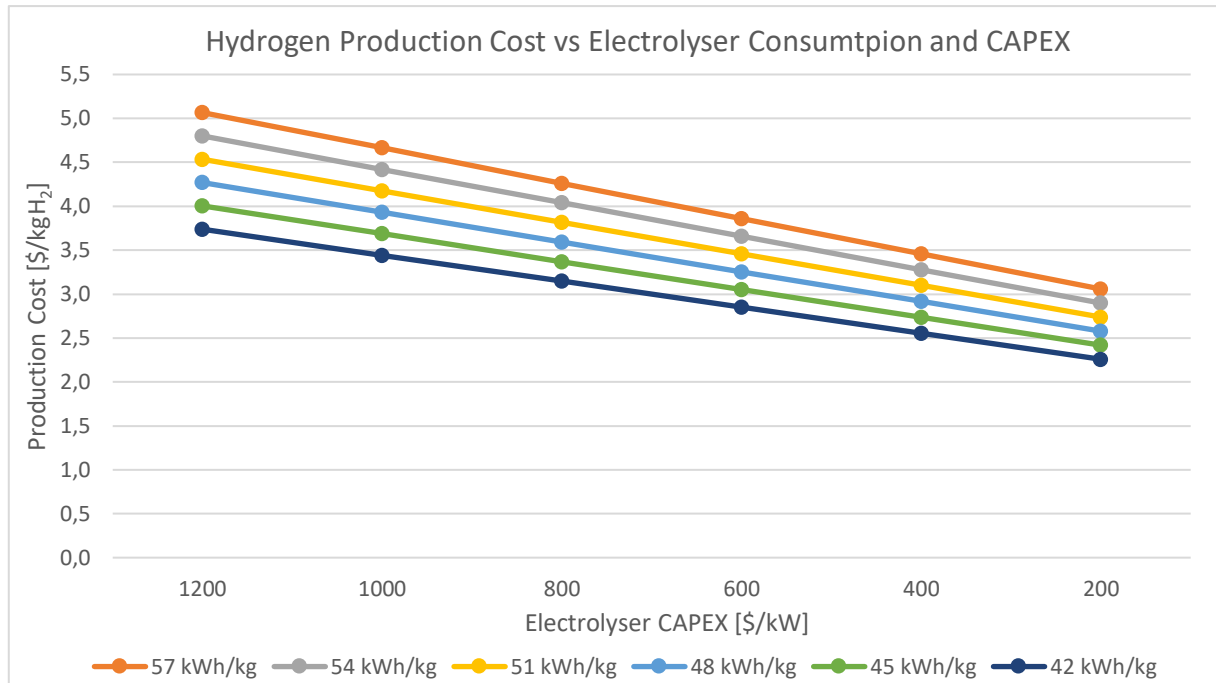


Figure 4.32: Levelized cost of hydrogen production with respect electrolyser power consumption and CAPEX

The curves obtained in the graph above have a decreasing linear trend and converge for diminishing CAPEX values. For a CAPEX of \$600/kW and a consumption of 45 kWh/kg results in a LCOH \$3,053/kgH₂. Using a CAPEX of \$400/kW yields a production cost of \$2,736/kgH₂, which decreases further to \$2,419/kgH₂ in the ideal case of power consumption of 42 kWh/kg.

- Levelized cost of final hydrogen

The final hydrogen cost refers to the total hydrogen sent to the direct reduced iron plant during the 20-year life of the project.

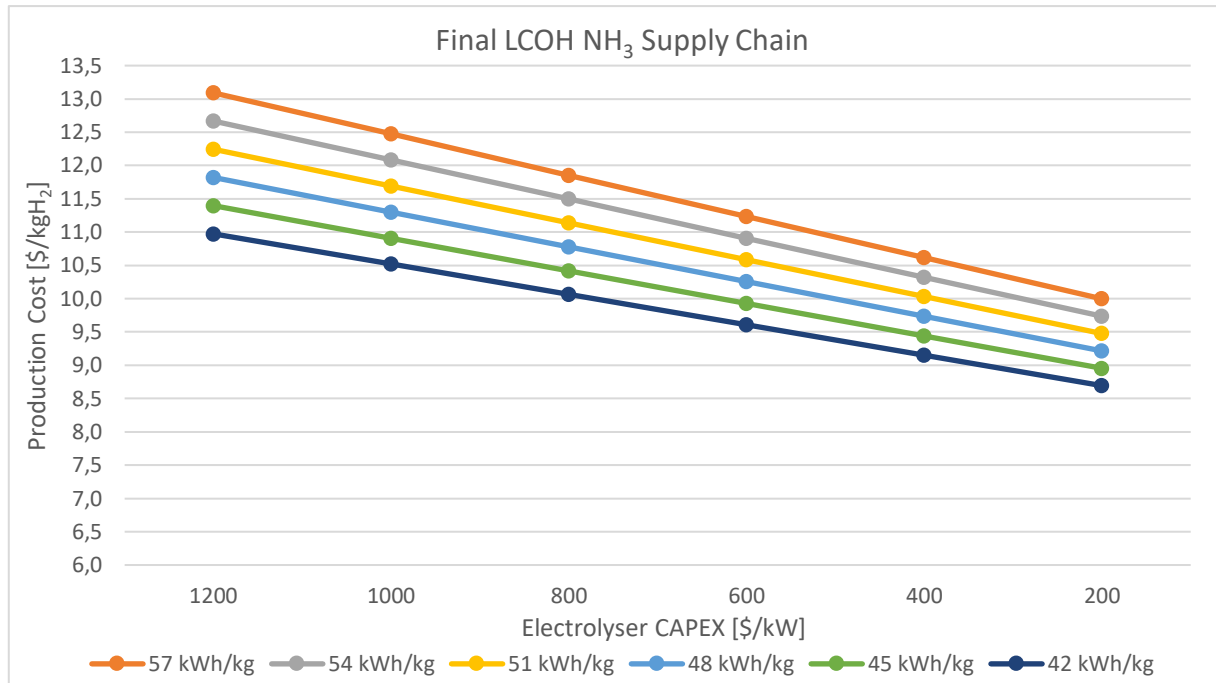


Figure 4.33: Final levelized cost of hydrogen for NH₃ supply chain with respect electrolyser power consumption and CAPEX

The two parameters considered in this analysis only affect the hydrogen production cost, while all the following processes are independent of it. The trend of the curves is the same as the trend of the hydrogen production cost curves. Considering the configuration with electricity consumption of 45 kWh/kg and CAPEX of \$400/kW gives a final hydrogen cost of \$9,443/kgH₂. This falls below the \$9.000/ton only when considering a specific installation cost of \$200/kW.

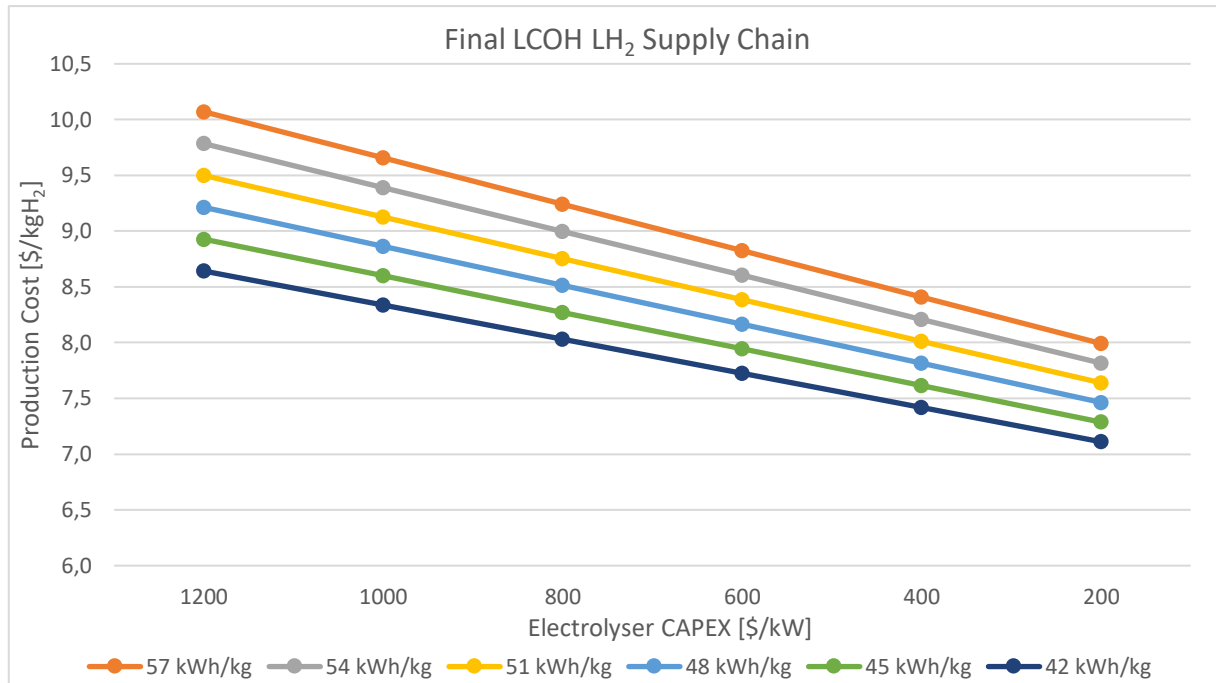


Figure 4.34: Final levelized cost of hydrogen for LH₂ supply chain with respect electrolyser power consumption and CAPEX

Considering CAPEX \$600/kW and 45 kWh/kg results in a final LCOH of \$7,493/kgH₂, which decreases by lowering CAPEX to \$400/kW to a final value of \$7,615/kgH₂. The most competitive value is achieved by considering a further lower investment cost of \$200/kW, for which the final hydrogen has a levelized cost of \$7,287/kgH₂.

4.3.6 Wind energy cost and electrolyser consumption

The electrolyser consumption varies between 42 and 57 kWh/kg, and the wind energy cost goes from 20 to 60 \$/MWh. The other parameters remain constant at the base case values:

- Electrolyser CAPEX: 900 \$/kW
- Wind capacity factor: 54 %
- Levelized cost of hydrogen production

The levelized cost of hydrogen production is related to the total amount of hydrogen produced by the electrolyzers during the whole lifetime of the project, that is 20 years.

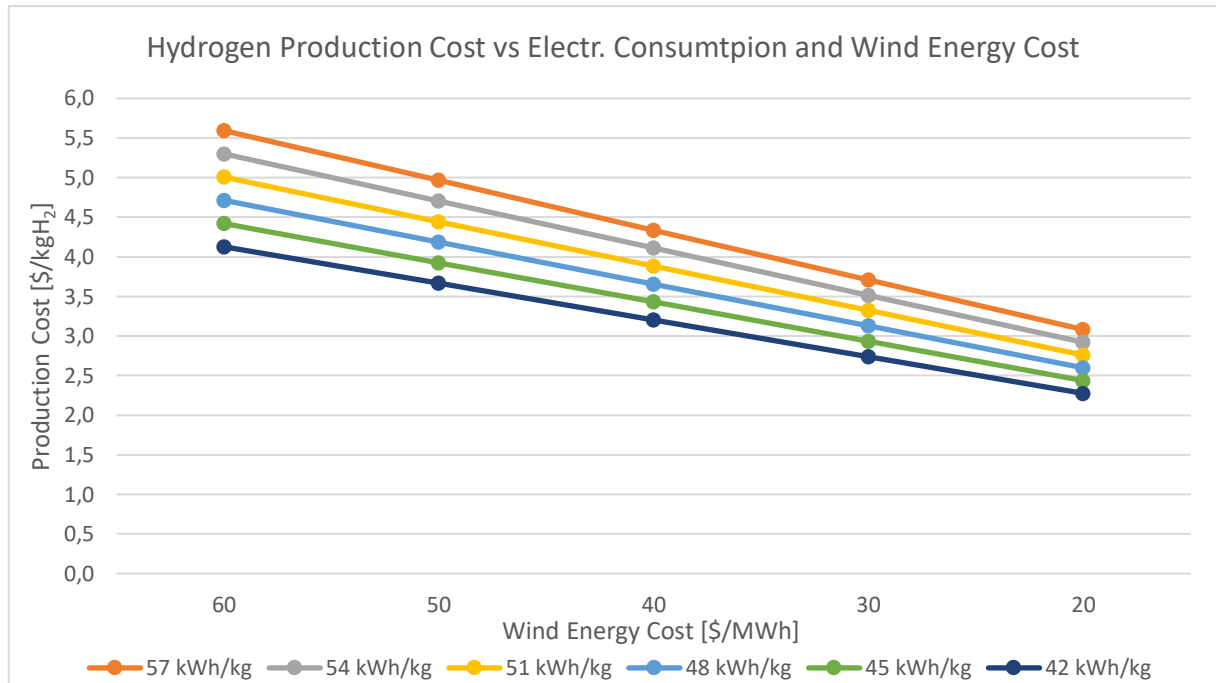


Figure 4.35: Levelized cost of hydrogen production with respect electrolyser power consumption and wind energy cost

The curves have a linear trend and tend to converge for low electricity costs. Power consumption does not determine a strong difference in the final cost of hydrogen.

Considering the optimistic case of 45 kWh/kg and a wind power cost of \$30/MWh results in a production cost of \$2,933/kgH₂, which further decreases to \$2,437/kgH₂ for power costs of \$20/MWh.

- Levelized cost of final hydrogen

The final hydrogen cost refers to the total hydrogen sent to the direct reduced iron plant during the 20-year life of the project.

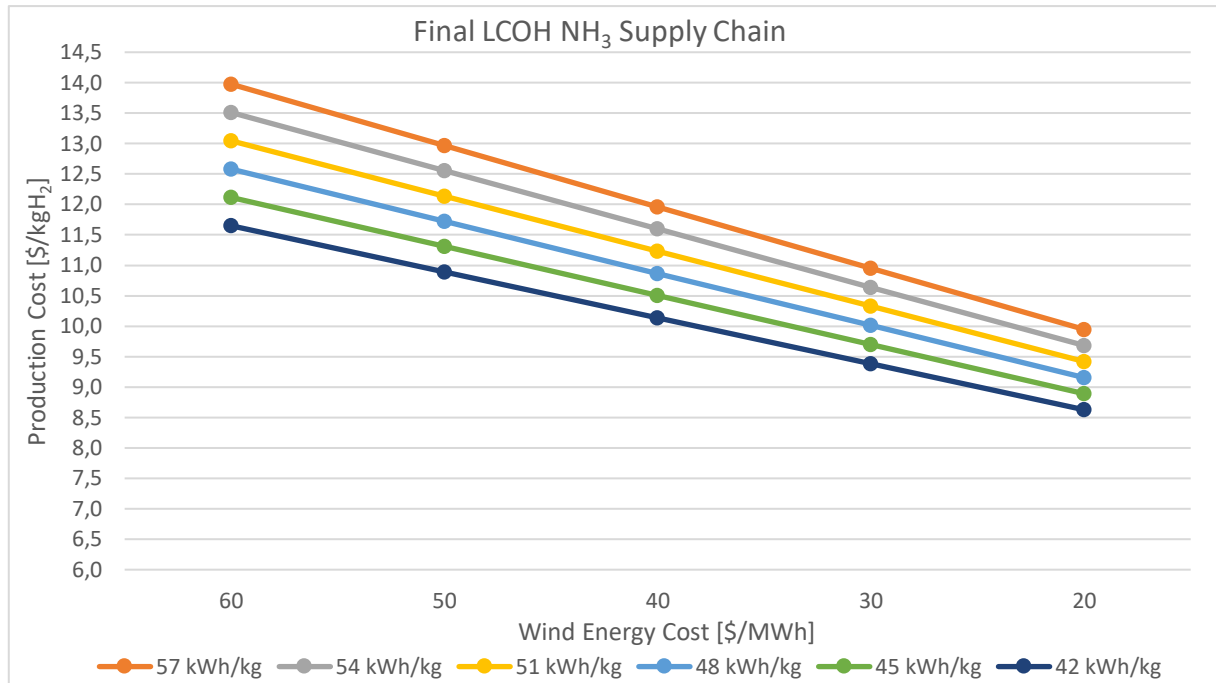


Figure 4.36: Final levelized cost of hydrogen for NH₃ supply chain respect electrolyser consumption and wind energy cost

The most attractive and feasible configuration involves a power consumption of 45 kWh/kg combined with a wind power cost of \$30/MWh, leading to a final hydrogen cost of \$9,697/kgH₂. The less probable option of an energy cost of \$20/MWh would bring the final hydrogen cost to \$8,891/kgH₂.

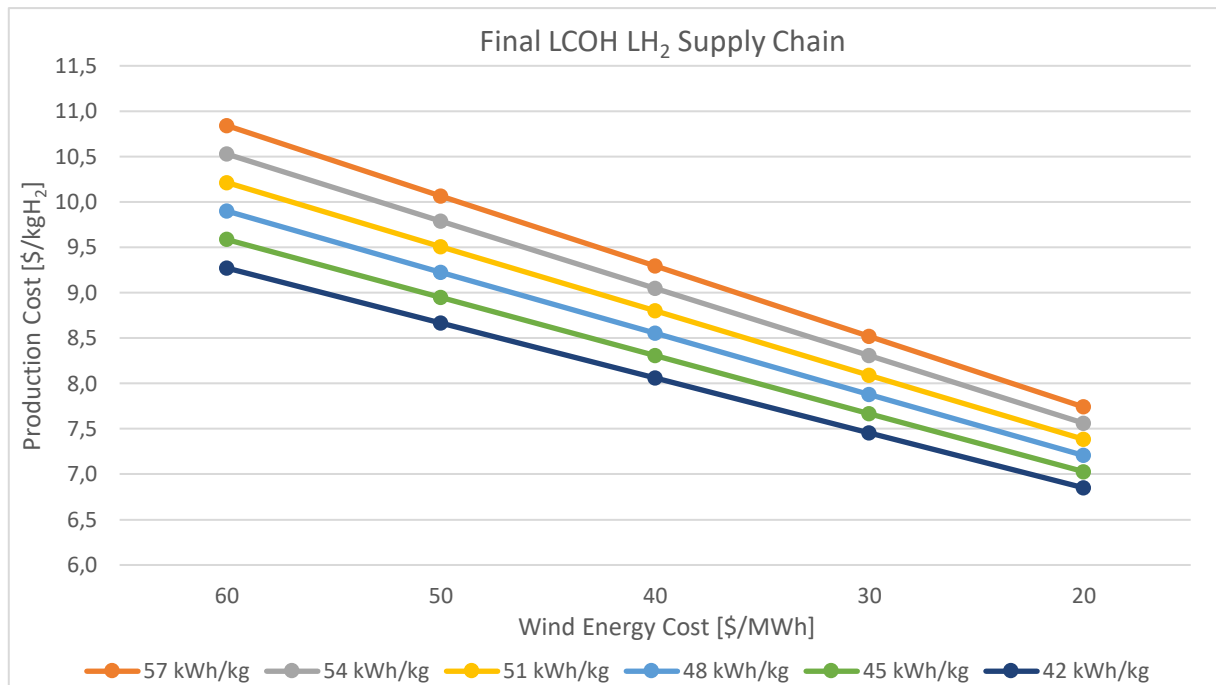


Figure 4.37: Final levelized cost of hydrogen for LH₂ supply chain respect electrolyser consumption and wind energy cost

Again, liquefied hydrogen is cheaper than ammonia. Considering the same case, with a power consumption of 45 kWh/kg and an energy cost of \$30/MWh, LCOH is \$7,668/kgH₂, and drops to \$7,029/kgH₂ for an energy cost of \$20/MWh.

4.4 Best feasible scenario by varying all parameters

In the previous sensitivity analyses, obtained by varying a maximum of two parameters, it has been possible to find values, for each parameter, that would yield attractive hydrogen levelized costs. In this section, the aim is to consider all the best parameters simultaneously in order to evaluate their total influence on the final hydrogen cost. The following values have been considered:

- Electrolyser CAPEX: 600 \$/kW
- Wind capacity factor: 60 %
- Electrolyser consumption: 45 kWh/kg
- Wind energy cost: \$30/MWh

These are the best practicable parameters, and the graph 4.38 shows the hydrogen levelized costs obtained.

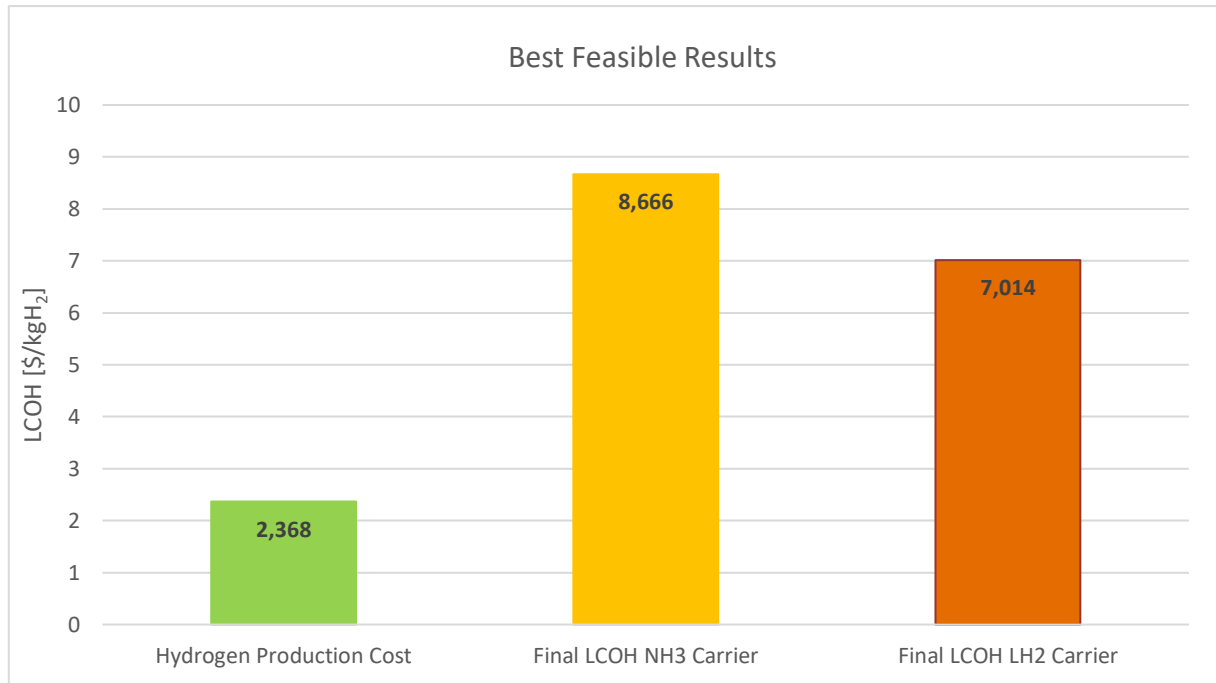


Figure 4.38: LCOH of hydrogen production and delivery both for NH₃ and LH₂ carriers, varying all the parameters

The best result is obtained for hydrogen production, since all the parameters used directly influence its value. There is also an improvement in the levelized costs of hydrogen sent to the direct reduced iron plant, both in the case of NH₃ and LH₂. The downstream costs in production, transport and storage are not greatly influenced by the parameters, except in part by the capacity factor and the cost of electricity. To achieve further reductions in final costs, work would also have to be done to decrease storage and transport costs, whose impact on the LCOH is significant.

4.5 Sensitivity analysis for ammonia as final product

In the chapter 'Economic Analysis', the levelized cost of ammonia has been studied, considering it as a final product. The main disadvantage of the NH₃ chain is the large losses and inefficiencies of the cracking and purification process, as well as the high cost of energy in Italy, which led to a sharp increase in the final cost of hydrogen. In contrast, the costs of synthesis, storage and transport of ammonia are attractive and cheaper than liquid hydrogen. For this reason, it has been considered interesting to evaluate the LCOA of ammonia arriving in Italy, and in this chapter a sensitivity analysis is carried out to understand the potential for decreasing its final cost.

The sensitivity analysis has been performed considering the same parameters selected for LCOH, considering the simultaneous effect of two of them, and considering only scenario 1. LCOA is referred to the total ammonia delivered to the Italian port during the whole lifetime of the project, that is 20 years. The annual NH_3 that arrives in Italy is 1.160.355.473 kg per year.

4.5.1 Capacity factor and electrolyser consumption

The capacity factor varies between 20 and 70 %, and the electrolyser consumption goes from 42 to 57 kWh/kg. The other parameters remain constant at the base case values:

- Wind electricity cost: \$42/MWh
- CAPEX alkaline: \$900/kW

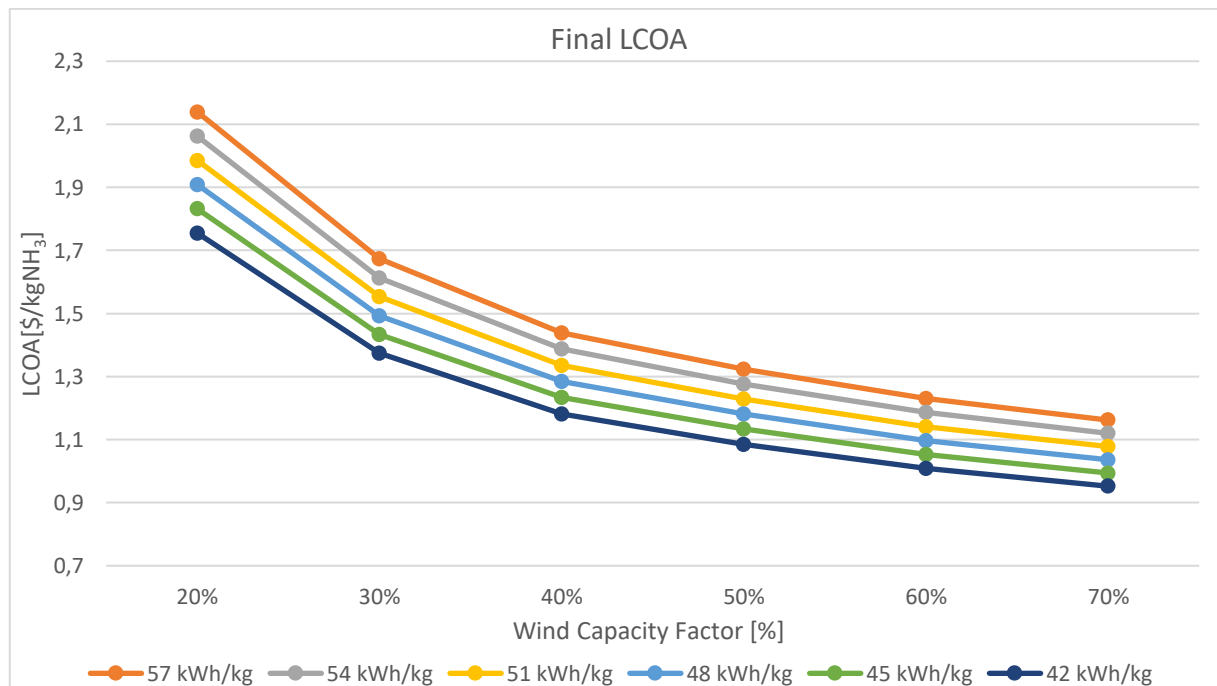


Figure 4.39: Final levelized cost of ammonia with respect electrolyser power consumption and capacity factor

The final cost of ammonia reaches \$1053/ton NH_3 considering a consumption of 45 kWh/kg and a CF of 60 %. Increasing the capacity factor further to 70 % gives an LCOA of \$0,994/kg NH_3 .

4.5.2 Capacity factor and wind energy cost

The capacity factor varies between 20 and 70 %, and the wind energy cost goes from 20 to 60 \$/MWh. The other parameters remain constant at the base case values:

- Electrolyser consumption: 48 kWh/kgH₂
- CAPEX alkaline: \$900/kW

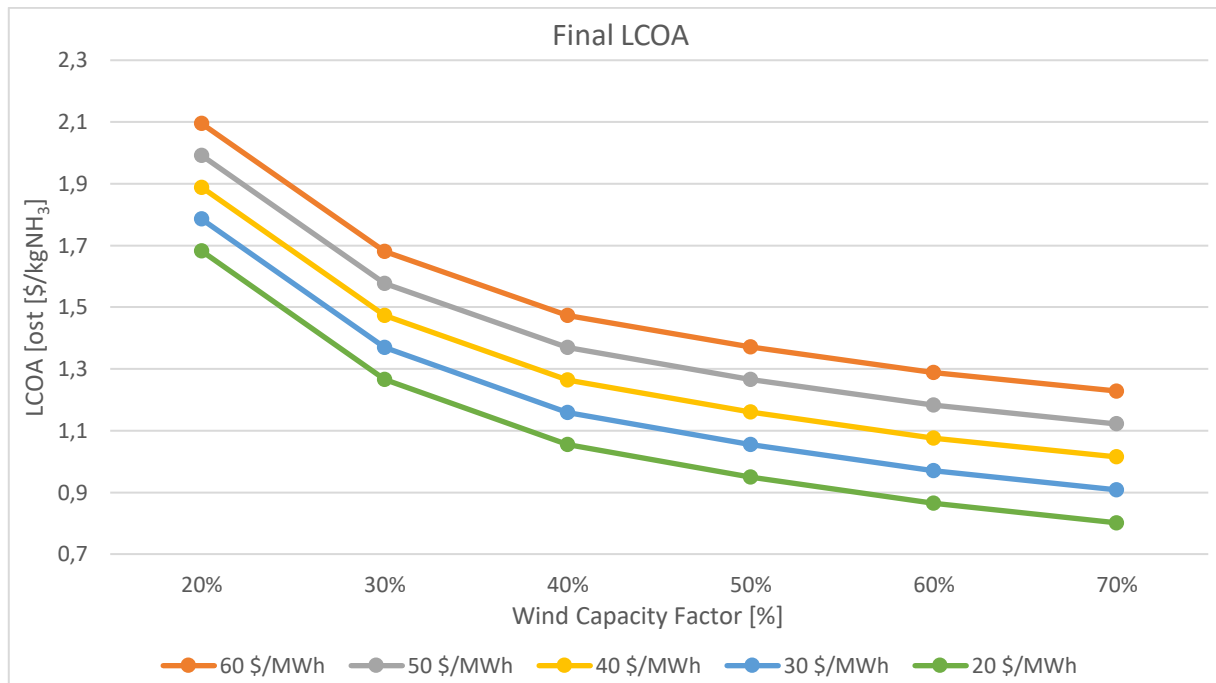


Figure 4.40: Final levelized cost of ammonia with respect wind electricity cost and capacity factor

Considering CF 60 % and wind energy cost of \$30/MWh, this gives an LCOA of \$0,970/kgNH₃, which decreases to \$0,864/kgNH₃ with an energy cost of \$20/MWh.

4.5.3 Capacity factor and electrolyser CAPEX

The capacity factor varies between 20 and 70 %, and the electrolyser CAPEX goes from 1200 to 200 \$/kW. The other parameters remain constant at the base case values:

- Electrolyser consumption: 48 kWh/kgH₂
- Wind electricity cost: \$42/MWh

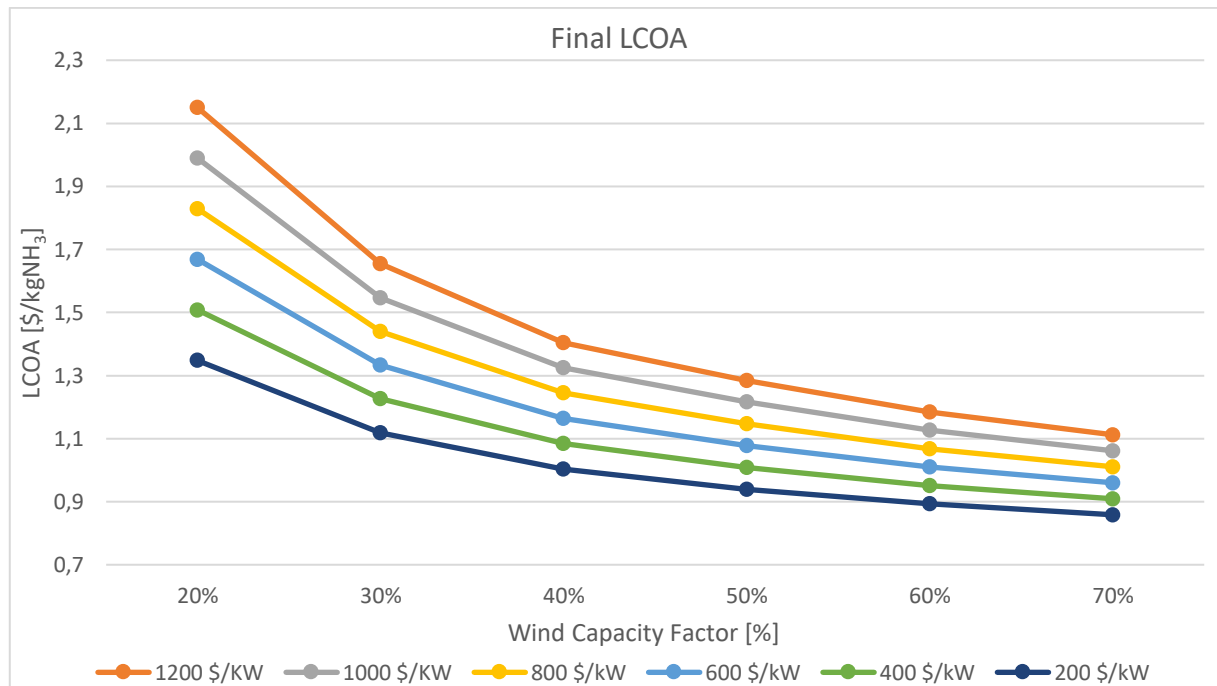


Figure 4.41: Final levelized cost of ammonia with respect electrolyser CAPEX and capacity factor

Considering CF 60 % and an electrolyser investment cost of \$600/kW gives an LCOA \$1,009/kgNH₃, which drops to \$0,951/kgNH₃ with a CAPEX of \$400/kW.

4.5.4 Wind energy cost and electrolyser CAPEX

The wind electricity cost varies between 20 and 60 \$/MWh, and the electrolyser CAPEX goes from 1200 to 200 \$/kW. The other parameters remain constant at the base case values:

- Electrolyser consumption: 48 kWh/kgH₂
- Wind capacity factor: 54 %

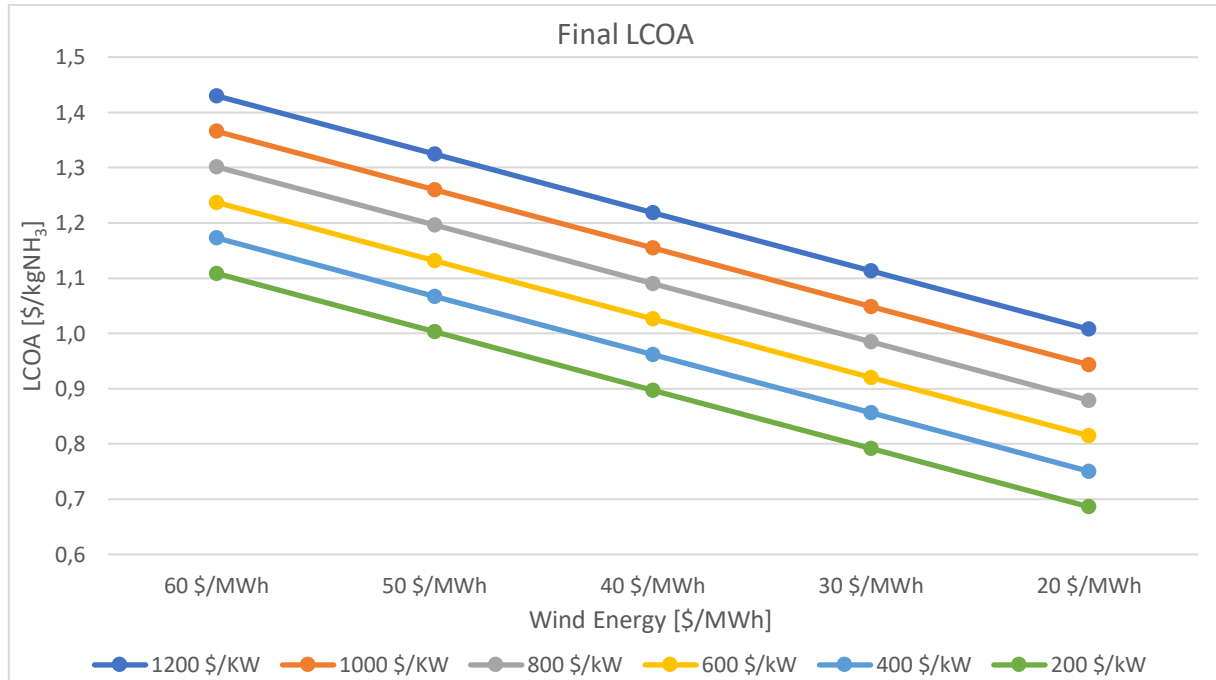


Figure 4.42: Final levelized cost of ammonia with respect electrolyser CAPEX and wind energy cost

Considering the optimistic energy cost of \$30/MWh, and an electrolyser installation cost of \$600/kW, it is obtain an LCOA of \$0,920/kgNH₃, which decreases to \$0,856/kgNH₃ for \$400/kW, and further improves to \$0,792/kgNH₃ considering CAPEX \$200/kW.

4.5.5 Electrolyser consumption and electrolyser CAPEX

The electrolyser consumption varies between 42 and 57 kWh/kg, and the electrolyser CAPEX goes from 1200 to 200 \$/kW. The other parameters remain constant at the base case values:

- Wind electricity cost: 42 \$/MWh
- Wind Capacity Factor: 54 %

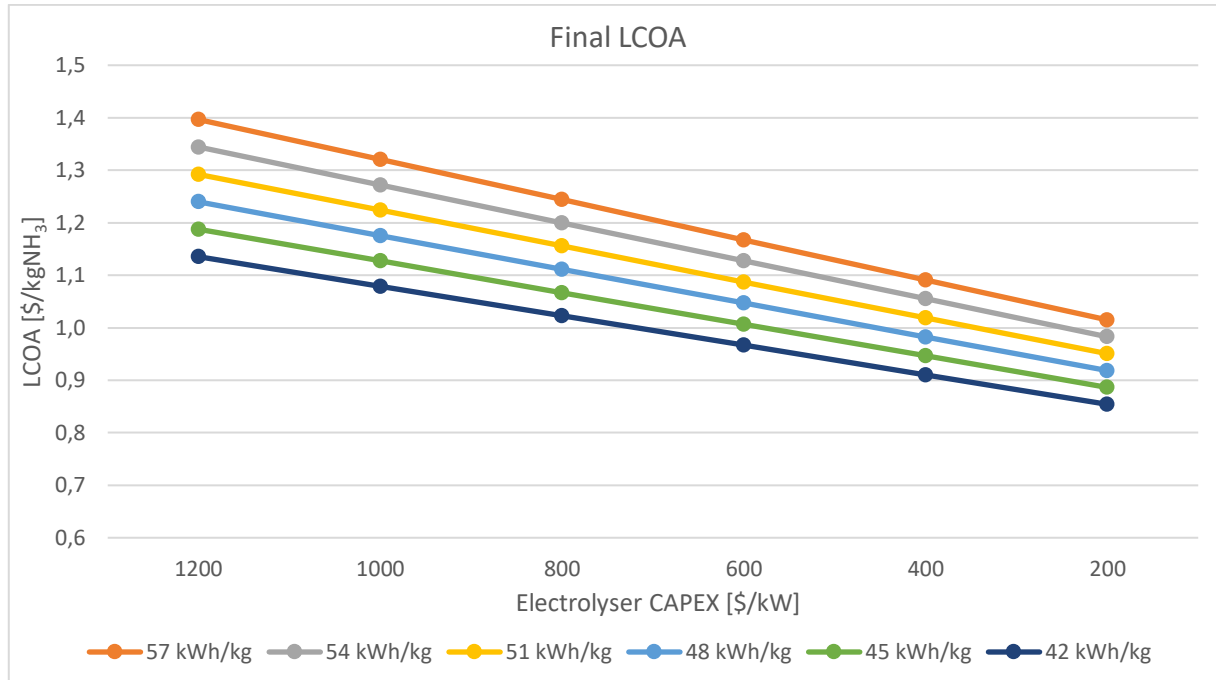


Figure 4.43: Final levelized cost of ammonia with respect electrolyser CAPEX and power consumption

For an electrolyser consumption of 45 kWh/kg and a CAPEX of \$600/kW, this results in a levelized cost of ammonia of \$1007/tonNH₃, which drops to \$967/tonNH₃ for CAPEX \$400/kW and \$886/tonNH₃ for \$200/kW.

4.5.6 Electrolyser consumption and wind energy cost

The electrolyser consumption varies between 42 and 57 kWh/kg, and the wind energy cost goes from 20 to 60 \$/MWh. The other parameters remain constant at the base case values:

- Electrolyser CAPEX: 900 \$/kW
- Wind capacity factor: 54 %

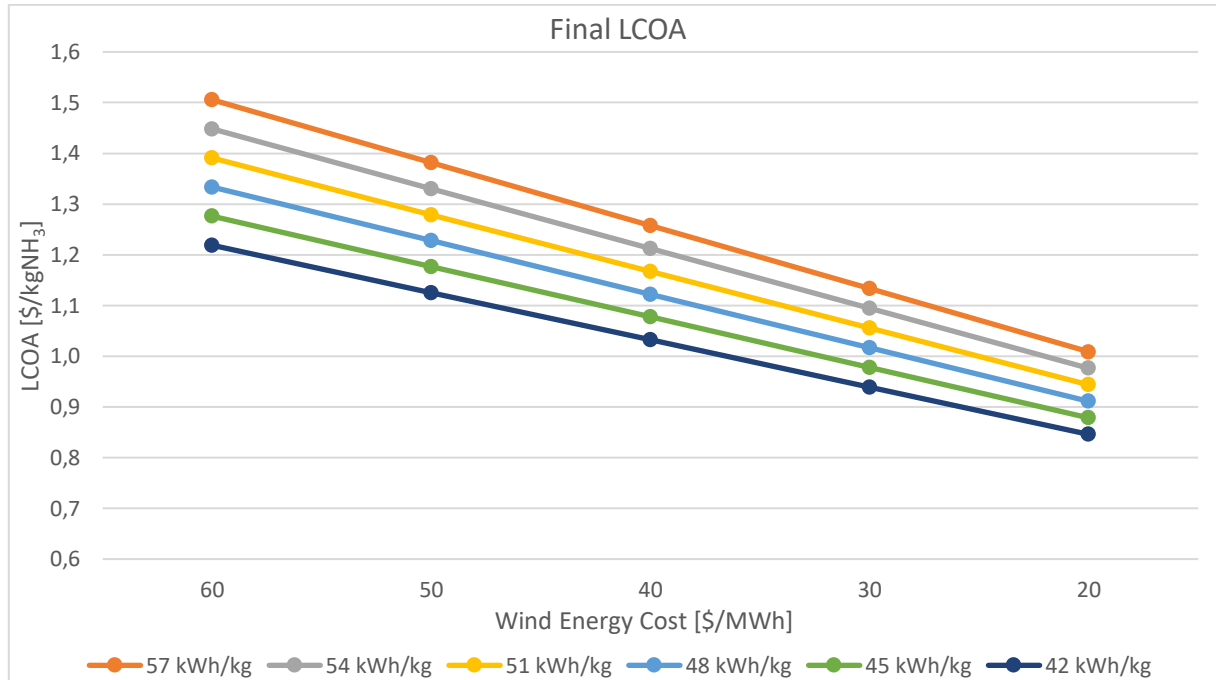


Figure 4.44: Final levelized cost of ammonia with respect electrolyser consumption and wind energy cost

For a consumption of 45 kWh/kgH₂ and a wind energy cost of \$30/MWh, this gives an LCOA of \$0,978/kgNH₃, and decreases to \$0,878/kgNH₃ corresponding to \$20/MWh.

4.6 Best feasible scenario by varying all parameters

Also in the case of ammonia as final product has been evaluated the LCOA varying all the parameters simultaneously. The following values have been considered:

- Electrolyser CAPEX: 600 \$/kW
- Wind capacity factor: 60 %
- Electrolyser consumption: 45 kWh/kg
- Wind energy cost: \$30/MWh

These are the best practicable parameters, and the graph 4.45 shows the hydrogen levelized costs obtained.

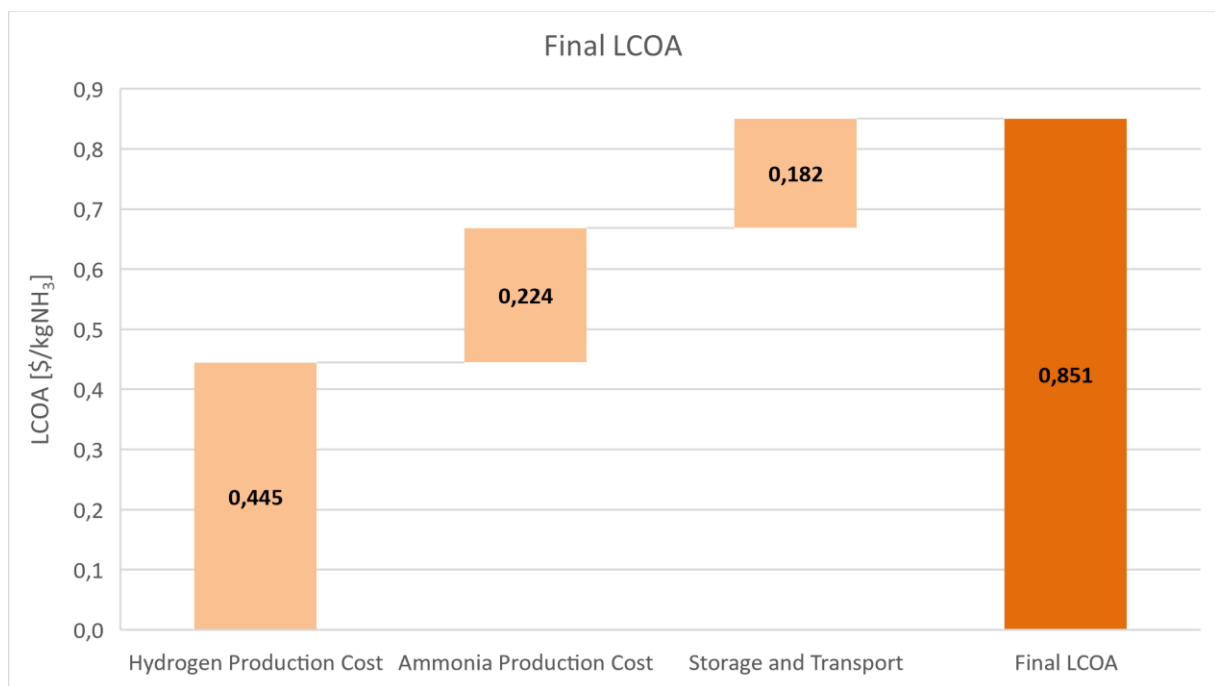


Figure 4.45: LCOA considering hydrogen production, ammonia synthesis, storage and transport

Picking all the most promising parameters at the same time yields a levelized cost of ammonia of \$0,851/kgNH₃, of which the largest cost, about 50 % of the total, is related to hydrogen production. The production of NH₃ has a total cost of only \$224/tonNH₃, while the storage and transport phase is the cheapest, costing only \$0,182/kgNH₃.

References Chapter 4

- Barth, F. (2016). *CertifHy — Developing a European guarantee of origin scheme for green hydrogen*.
https://certifhy.eu/images/media/files/CertifHy_Presentation_19_10_2016_final_Definition_of_Premium_Hydrogen.pdf
- Company, T., Terminal, B., Request, D., Login, B. A., & Support, C. (n.d.). *Europe 's Green Hydrogen Rules Raise Costs for*. 1–8.
- Does, W., Mean, E. U. T., Industry, H., & Mckenzie, B. (2021). *What Does the EU Taxonomy Mean for the Hydrogen Industry ? William-James Kettlewell*. May, 1–6.
- International Renewable Energy Agency, T. (2020). *GREEN HYDROGEN COST REDUCTION SCALING UP ELECTROLYSERS TO MEET THE 1.5°C CLIMATE GOAL H 2 O 2*.
www.irena.org/publications
- Oyarzabal, R., Mertenskötter, P., & Molyneux, C. G. (2022). New Definitions for Blue and Green Hydrogen: The European Commission's Package on Hydrogen and Decarbonized Gas Markets. *Covington - Inside Energy & Environment*, i, 1–8.
<https://www.insideenergyandenvironment.com/2022/01/new-definitions-for-blue-and-green-hydrogen-the-european-commissions-package-on-hydrogen-and-decarbonized-gas-markets/#:~:text=The expectation is that by,that remains to be seen.>
- Technical, H., & Panel, A. (1995). *the Green Hydrogen*. *Secretary*.
- Tractebel Engineering, & Inicio. (2017). *Early business cases for H2 in energy storage and more broadly power to H2 applications*. June.

Chapter 5

Conclusions

The aim of this thesis work is to calculate the levelized cost of hydrogen required for the decarbonisation of the Italian steel industry. Starting from the annual steel production and considering different hypotheses for the use of hydrogen as reducing agent and as heat source for the direct iron reduction plant, which is characterised by an annual production of 3.460.000 tonnes of reduced iron, two demand scenarios have been considered. The first scenario, in which only 30 % of the natural gas is replaced with pure hydrogen, results in the annual production of 143.144 tonnes of hydrogen. The second scenario involves the total replacement of natural gas with hydrogen, and the annual demand for H₂ is 355.702 tonnes.

To satisfy the demand of the steel plant, the hypothesis of producing hydrogen by electrolysis in Patagonia Argentina, where wind power plants are characterised by a high capacity factor, taken 54 %, has been considered; and maritime transport, for which two energy vectors, ammonia and liquid hydrogen, have been compared.

Four configurations have been considered during the elaboration of the results, which differs by type of electrolyser, alkaline or PEM, and by energy supply, either purely through wind power (CF 54 %), or considering full grid integration (CF 100 %), which is characterised by indirect carbon dioxide emissions.

In scenario 1, LCOH of hydrogen production is \$3,613/kgH₂ in the cheapest configuration, which considers the alkaline electrolyser and wind-grid mix power supply. The power of the electrolyser is 1,37 GW. LCOH of the most expensive configuration, involving off-grid PEM electrolyser, is \$4,417/kgH₂, and the power plant is 2,63 GW.

In scenario 2 LCOH is slightly lower due to the scaling factor considered. The cheapest configuration has an LCOH of \$3,533/kgH₂, and a power plant of 3,34 GW, while the most expensive configuration has a production cost of \$4,244/kgH₂ and an electrolyser of 6,43 GW. The majority of the cost of producing hydrogen is related to the electricity consumed for electrolysis, followed by the CAPEX of the electrolyser. Water, on the other hand, has a marginal cost.

The final cost of hydrogen sent to the steel plant is strongly influenced by the type of energy carrier chosen. In the case of ammonia, the final cost is the sum of the costs of ammonia

synthesis and storage, sea transport and reconversion into hydrogen at the port of arrival. Considering scenario 1, final LCOH is \$10,077/kgH₂ in the cheapest configuration and \$11,714/kgH₂ in the most expensive configuration. In the second scenario, LCOH values decrease and are \$9,301/kgH₂ and \$10,751/kgH₂, respectively.

Most of the cost is attributed to the production of hydrogen, due to the high cost of the electricity needed for electrolysis and the CAPEX of electrolyzers. The cracking and purification process is characterised by a high cost, amounting to \$1,486/kgH₂ in scenario 1 and \$1,417/kgH₂ in scenario 2, this is because the hydrogen purification process is energy intensive and the price of grid electricity in Italy is very high. The transport cost of ammonia is competitive, it is \$0,372/kgH₂ in scenario 1 and drops to \$0,263/kgH₂ in scenario 2.

The total levelized cost of ammonia storage, transport and conversion is \$3,252/kgH₂ in scenario 1 and \$2,766/kgH₂ in scenario 2.

Ammonia is not the right carrier for hydrogen because, although it has competitive synthesis, storage and transport costs, the decomposition phase is very costly and is characterised by huge losses and inefficiencies, which cause the production plant to be considerably oversized, which in scenario 1 has been calculated to be 58,6 % and in scenario 2 equal to 56,3 %.

The final LCOA of ammonia has been further analysed, considering NH₃ arriving in Italy as the final product, eliminating the reconversion phase. In scenario 1, LCOA in the cheapest configuration is \$1,023/kgNH₃, while in the most expensive configuration it rises to \$1,227/kgNH₃. In scenario 2, LCOA is lowered by the scaling factor and is equal to \$0,949/kgNH₃ and \$1,128/kgNH₃ in the cheapest and most expensive configurations. The results obtained show that ammonia is a very attractive and cost-competitive carrier, but is not suitable for applications requiring pure hydrogen.

The configuration choice is also important for carbon dioxide emissions. The off-grid plant configuration saves 4.330.146 tonnes of CO₂ annually in scenario 1 and 10.551.090 tonnes of CO₂ in scenario 2, compared to the case where all power is withdrawn from the grid. The on-grid plant configuration characterized by wind-grid mix energy supply is responsible for an increase in emissions, and the emissions saved annually compared to the case of supplying only from the grid is 2.461.240 tonnes CO₂ in scenario 1 and 5.974.578 tonnes CO₂ in scenario 2.

Considering liquid hydrogen as carrier, the final LCOH decreases because, despite its high liquefaction, storage and transport costs, the production process is very simple, and losses in

the chain are much lower than in the case of ammonia, in particular total losses amount to 9,0 % in scenario 1 and 7,6 % in scenario 2. LCOH for hydrogen production remains unchanged.

In Scenario 1, the final LCOH of hydrogen sent to direct iron reduction plants is \$8,265/kgH₂ in the cheapest configuration, which involves the alkaline electrolyser and the feeding of the wind-grid energy mix. The hydrogen production cost is \$3,702/kgH₂ and the sum of liquefaction, storage and transport costs is \$4,562/kgH₂. The most expensive configuration has a final hydrogen cost of \$9,154/kgH₂, involves a PEM electrolyser and wind power, the hydrogen production cost is \$4,429/kgH₂ and the sum of downstream costs is \$4,725/kgH₂.

The final cost of the cheapest configuration in the case of the LH₂ supply chain is \$1,808/kgH₂ lower than the cheapest configuration in the case of the NH₃ supply chain. In the most expensive configuration, the cost difference is \$2,569/kgH₂.

In scenario 2 the final LCOH is \$7,200/kgH₂ in the cheapest configuration and rises to \$7,916/kgH₂ in the most expensive configuration.

In the case of an off-grid plant, the saved annual carbon dioxide emissions compared to the hypothetical use of grid-sourced electricity alone is 3.403.208 tons CO₂ in scenario 1, and 8.280.500 tons CO₂ in scenario 2. Considering on-grid plant, the saved annual carbon dioxide emissions are 1.880.659 tons CO₂ in scenario 1, and 4.544.969 tons CO₂ in scenario 2.

In the case of liquid hydrogen, the final cost is lower than in the case of ammonia, but still high compared to the levelized costs of green hydrogen on the market today, and to the forecasts of cost reductions proposed in the literature.

In the last chapter of the thesis, sensitivity analysis has been proposed to study the trend of LCOH as function of certain parameters, both technological and economic, that greatly influence the costs of hydrogen production and the downstream processes involved. The parameters considered are the wind power capacity factor and cost, CAPEX and power consumption of the electrolyser. The analysis has been performed both by varying each parameter individually and by varying the parameters in pairs.

The sensitivity analysis has been carried out considering the off-grid production plant, due to the latest regulation concerning green hydrogen, which imposes an emission threshold of 1 kgCO₂/kgH₂. The maximum grid quantity allowed to comply with this regulation is 3,30 % in the case of alkaline electrolyser and 3,15 % in the case of PEM electrolyser.

If optimistic, but achievable values are considered, such as CAPEX of \$600/kW, wind CF of 60 %, electrolyser consumption 45 kWh/kg and wind energy cost of \$30/MWh, the LCOH of hydrogen production is \$2,368/kgH₂, while the final LCOH is \$8,666/kgH₂ in the case of ammonia carrier and \$7,014/kgH₂ in the case of liquid hydrogen carrier. Considering the same parameters with ammonia as the final product, LCOA is \$0,851/kgNH₃.

Appendix A

In this appendix A the Levelized Costs of Hydrogen composition is reported, considering all the processes required for the NH₃ and LH₂ supply chains.

A1

The following table shows all the LCOHs related to the final hydrogen sent to the steel plant in case of NH₃ supply chain, for all the configurations evaluated in scenario 1.

SCENARIO 1	Alkaline	Alkaline	PEM	PEM
INVESTMENT COSTS [\$/kgH ₂]	CF 54 %	CF 100 %	CF 54 %	CF 100 %
CAPEX Stack	\$0,778	\$0,579	\$1,041	\$0,793
CAPEX Auxiliaries	\$0,900	\$0,486	\$1,146	\$0,619
OPEX Electrolyser	\$0,636	\$0,343	\$0,810	\$0,437
Electricity Electrolyser	\$3,375	\$4,041	\$3,516	\$4,209
Cost Of Water	\$0,033	\$0,020	\$0,030	\$0,018
Hydrogen Production Cost	\$5,723	\$5,469	\$6,543	\$6,076
CAPEX Hydrogen Compressor	\$0,041	\$0,027	\$0,041	\$0,027
OPEX Hydrogen Compressor	\$0,011	\$0,008	\$0,011	\$0,008
Electricity Hydrogen Compressor	\$0,088	\$0,105	\$0,082	\$0,099
CAPEX Hydrogen Storage	\$0,341	\$0,000	\$0,341	\$0,000
OPEX Hydrogen Storage	\$0,072	\$0,000	\$0,072	\$0,000
Cost Of Nitrogen (ASU)	\$0,395	\$0,395	\$0,395	\$0,395
Cost of Nitrogen Compression	\$0,070	\$0,070	\$0,070	\$0,070
CAPEX NH ₃ Synthesis Plant	\$0,336	\$0,336	\$0,336	\$0,336
OPEX NH ₃ Synthesis Plant	\$0,145	\$0,145	\$0,145	\$0,145
Electricity NH ₃ Synthesis Plant	\$0,042	\$0,042	\$0,041	\$0,041
Ammonia Production Cost	\$7,264	\$6,596	\$8,079	\$7,197
Loading Terminal and NH ₃ Liquefied Storage	\$0,592	\$0,592	\$0,592	\$0,592
Maritime Transportation	\$0,372	\$0,372	\$0,372	\$0,372
Unloading Terminal and NH ₃ Liquefied Storage	\$0,518	\$0,518	\$0,518	\$0,518
Cracking Plant	\$0,284	\$0,284	\$0,284	\$0,284
Purification Plant	\$1,486	\$1,486	\$1,486	\$1,486
CAPEX Civil Works & Other Costs	\$0,522	\$0,229	\$0,396	\$0,160
Final H₂ Levelized Cost	\$11,039	\$10,077	\$11,727	\$10,609

Table A1: LCOH final hydrogen NH₃ supply chain, scenario 1

A2

The following table shows all the LCOHs related to the final hydrogen sent to the steel plant in case of NH₃ supply chain, for all the configurations evaluated in scenario 2.

SCENARIO 2	Alkaline	Alkaline	PEM	PEM
INVESTMENT COSTS [\$/kgH ₂]	CF 54 %	CF 100 %	CF 54 %	CF 100 %
CAPEX Stack	\$0,701	\$0,521	\$0,938	\$0,714
CAPEX Auxiliaries	\$0,811	\$0,438	\$1,033	\$0,558
OPEX Electrolyser	\$0,573	\$0,309	\$0,730	\$0,394
Electricity Electrolyser	\$3,326	\$3,982	\$3,465	\$4,148
Cost Of Water	\$0,033	\$0,019	\$0,029	\$0,017
Hydrogen Production Cost	\$5,444	\$5,270	\$6,195	\$5,831
CAPEX Hydrogen Compressor	\$0,030	\$0,020	\$0,030	\$0,020
OPEX Hydrogen Compressor	\$0,008	\$0,006	\$0,008	\$0,006
Electricity Hydrogen Compressor	\$0,086	\$0,103	\$0,081	\$0,097
CAPEX Hydrogen Storage	\$0,308	\$0,000	\$0,308	\$0,000
OPEX Hydrogen Storage	\$0,065	\$0,000	\$0,065	\$0,000
Cost Of Nitrogen (ASU)	\$0,368	\$0,368	\$0,368	\$0,368
Cost of Nitrogen Compression	\$0,069	\$0,069	\$0,069	\$0,069
CAPEX NH ₃ Synthesis Plant	\$0,303	\$0,303	\$0,303	\$0,303
OPEX NH ₃ Synthesis Plant	\$0,132	\$0,132	\$0,132	\$0,132
Electricity NH ₃ Synthesis Plant	\$0,041	\$0,041	\$0,041	\$0,041
Ammonia Production Cost	\$6,855	\$6,312	\$7,600	\$6,867
Loading Terminal and NH ₃ Liquefied Storage	\$0,425	\$0,425	\$0,425	\$0,425
Maritime Transportation	\$0,263	\$0,263	\$0,263	\$0,263
Unloading Terminal and NH ₃ Liquefied Storage	\$0,463	\$0,463	\$0,463	\$0,463
Cracking Plant	\$0,198	\$0,198	\$0,198	\$0,198
Purification Plant	\$1,417	\$1,417	\$1,417	\$1,417
CAPEX Civil Works & Other Costs	\$0,511	\$0,223	\$0,386	\$0,155
Final H₂ Levelized Cost	\$10,131	\$9,301	\$10,751	\$9,788

Table A2: LCOH final hydrogen NH₃ supply chain, scenario 2

A3

The following table shows all the LCOHs related to the final hydrogen sent to the steel plant in case of LH₂ supply chain, for all the configurations evaluated in scenario 1.

<i>SCENARIO 1</i>	<i>Alkaline</i>	<i>Alkaline</i>	<i>PEM</i>	<i>PEM</i>
<i>INVESTMENT COSTS [\$/kgH₂]</i>	<i>CF 54 %</i>	<i>CF 100 %</i>	<i>CF 54 %</i>	<i>CF 100 %</i>
<i>CAPEX Stack</i>	\$0,527	\$0,392	\$0,705	\$0,537
<i>CAPEX Auxiliaries</i>	\$0,610	\$0,329	\$0,776	\$0,419
<i>OPEX Electrolyser</i>	\$0,430	\$0,232	\$0,548	\$0,296
<i>Electricity Electrolyser</i>	\$2,285	\$2,735	\$2,380	\$2,849
<i>Cost of Water</i>	\$0,023	\$0,013	\$0,020	\$0,012
<i>Hydrogen Production Cost</i>	\$3,874	\$3,702	\$4,429	\$4,113
<i>CAPEX Liquefaction Plant</i>	\$0,537	\$0,371	\$0,537	\$0,371
<i>OPEX Liquefaction Plant</i>	\$0,228	\$0,157	\$0,228	\$0,157
<i>Electricity Liquefaction Plant</i>	\$0,537	\$0,642	\$0,537	\$0,642
<i>CAPEX Loading Storage Terminal</i>	\$0,950	\$0,950	\$0,950	\$0,950
<i>OPEX Loading Storage Terminal</i>	\$0,302	\$0,302	\$0,302	\$0,302
<i>Electricity Loading Storage Terminal</i>	\$0,011	\$0,011	\$0,011	\$0,011
<i>CAPEX Shipping</i>	\$0,445	\$0,445	\$0,445	\$0,445
<i>OPEX Shipping</i>	\$0,377	\$0,377	\$0,377	\$0,377
<i>Cost of Fuel</i>	\$0,001	\$0,001	\$0,001	\$0,001
<i>CAPEX Unloading Storage Terminal</i>	\$0,773	\$0,773	\$0,773	\$0,773
<i>OPEX Unloading Storage Terminal</i>	\$0,246	\$0,246	\$0,246	\$0,246
<i>Electricity Unloading Storage Terminal</i>	\$0,113	\$0,113	\$0,113	\$0,113
<i>CAPEX Civil Works & Other Costs</i>	\$0,295	\$0,174	\$0,206	\$0,126
<i>TOTAL EXPENDITURE</i>	\$8,688	\$8,265	\$9,154	\$8,627

Table A3: LCOH final hydrogen LH₂ supply chain, scenario 1

A4

The following table shows all the LCOHs related to the final hydrogen sent to the steel plant in case of LH₂ supply chain, for all the configurations evaluated in scenario 2.

<i>SCENARIO 2</i>	<i>Alkaline</i>	<i>Alkaline</i>	<i>PEM</i>	<i>PEM</i>
<i>INVESTMENT COSTS [\$/kgH₂]</i>	<i>CF 54 %</i>	<i>CF 100 %</i>	<i>CF 54 %</i>	<i>CF 100 %</i>
<i>CAPEX Stack</i>	\$0,475	\$0,354	\$0,636	\$0,484
<i>CAPEX Auxiliaries</i>	\$0,550	\$0,297	\$0,701	\$0,378
<i>OPEX Electrolyser</i>	\$0,389	\$0,210	\$0,495	\$0,267
<i>Electricity Electrolyser</i>	\$2,256	\$2,701	\$2,350	\$2,814
<i>Cost of Water</i>	\$0,022	\$0,013	\$0,020	\$0,012
<i>Hydrogen Production Cost</i>	\$3,693	\$3,575	\$4,202	\$3,956
<i>CAPEX Liquefaction Plant</i>	\$0,371	\$0,256	\$0,371	\$0,256
<i>OPEX Liquefaction Plant</i>	\$0,157	\$0,109	\$0,157	\$0,109
<i>Electricity Liquefaction Plant</i>	\$0,529	\$0,634	\$0,529	\$0,634
<i>CAPEX Loading Storage Terminal</i>	\$0,803	\$0,803	\$0,803	\$0,803
<i>OPEX Loading Storage Terminal</i>	\$0,255	\$0,255	\$0,255	\$0,255
<i>Electricity Loading Storage Terminal</i>	\$0,011	\$0,011	\$0,011	\$0,011
<i>CAPEX Shipping</i>	\$0,299	\$0,299	\$0,299	\$0,299
<i>OPEX Shipping</i>	\$0,253	\$0,253	\$0,253	\$0,253
<i>Cost of Fuel</i>	\$0,000	\$0,000	\$0,000	\$0,000
<i>CAPEX Unloading Storage Terminal</i>	\$0,560	\$0,560	\$0,560	\$0,560
<i>OPEX Unloading Storage Terminal</i>	\$0,178	\$0,178	\$0,178	\$0,178
<i>Electricity Unloading Storage Terminal</i>	\$0,100	\$0,100	\$0,100	\$0,100
<i>CAPEX Civile Works & Other Costs</i>	\$0,287	\$0,168	\$0,198	\$0,120
<i>TOTAL EXPENDITURE</i>	\$7,495	\$7,200	\$7,916	\$7,533

Table A4: LCOH final hydrogen LH₂ supply chain, scenario 2

A5

The following table shows all the LCOAs related to the final ammonia arriving in the Italian port in case of NH₃ supply chain, for all the configurations evaluated in scenario 1.

<i>SCENARIO 1</i>	<i>Alkaline</i>	<i>Alkaline</i>	<i>PEM</i>	<i>PEM</i>
<i>INVESTMENT COSTS [\$/kgH₂]</i>	<i>CF 54 %</i>	<i>CF 100 %</i>	<i>CF 54 %</i>	<i>CF 100 %</i>
<i>CAPEX Stack</i>	\$0,096	\$0,071	\$0,128	\$0,098
<i>CAPEX Auxiliaries</i>	\$0,111	\$0,060	\$0,141	\$0,076
<i>OPEX Electrolyser</i>	\$0,078	\$0,042	\$0,100	\$0,054
<i>Electricity Electrolyser</i>	\$0,416	\$0,498	\$0,434	\$0,519
<i>Cost Of Water</i>	\$0,004	\$0,002	\$0,004	\$0,002
<i>Hydrogen Production Cost</i>	\$0,706	\$0,675	\$0,807	\$0,750
<i>CAPEX Hydrogen Compressor</i>	\$0,005	\$0,003	\$0,005	\$0,003
<i>OPEX Hydrogen Compressor</i>	\$0,001	\$0,001	\$0,001	\$0,001
<i>Electricity Hydrogen Compressor</i>	\$0,011	\$0,013	\$0,010	\$0,012
<i>CAPEX Hydrogen Storage</i>	\$0,042	\$0,000	\$0,042	\$0,000
<i>OPEX Hydrogen Storage</i>	\$0,009	\$0,000	\$0,009	\$0,000
<i>Cost Of Nitrogen (ASU)</i>	\$0,049	\$0,049	\$0,049	\$0,049
<i>Cost of Nitrogen Compression</i>	\$0,009	\$0,009	\$0,009	\$0,009
<i>CAPEX NH₃ Synthesis Plant</i>	\$0,042	\$0,042	\$0,042	\$0,042
<i>OPEX NH₃ Synthesis Plant</i>	\$0,018	\$0,018	\$0,018	\$0,018
<i>Electricity NH₃ Synthesis Plant</i>	\$0,005	\$0,005	\$0,005	\$0,005
<i>Ammonia Production Cost</i>	\$0,896	\$0,814	\$0,997	\$0,888
<i>Loading Terminal and NH₃ Liquefied Storage</i>	\$0,073	\$0,073	\$0,073	\$0,073
<i>Maritime Transportation</i>	\$0,046	\$0,046	\$0,046	\$0,046
<i>Unloading Terminal and NH₃ Liquefied Storage</i>	\$0,064	\$0,064	\$0,064	\$0,064
<i>Cracking Plant</i>	\$0,000	\$0,000	\$0,000	\$0,000
<i>Purification Plant</i>	\$0,000	\$0,000	\$0,000	\$0,000
<i>CAPEX Civil Works & Other Costs</i>	\$0,064	\$0,028	\$0,049	\$0,020
<i>Final H₂ Levelized Cost</i>	\$1,143	\$1,025	\$1,228	\$1,090

Table A5: LCOA final ammonia NH₃ supply chain, scenario 1

A6

The following table shows all the LCOAs related to the final ammonia arriving in the Italian port in case of NH₃ supply chain, for all the configurations evaluated in scenario 2.

SCENARIO 2	Alkaline	Alkaline	PEM	PEM
INVESTMENT COSTS [\$/kgH ₂]	CF 54 %	CF 100 %	CF 54 %	CF 100 %
CAPEX Stack	\$0,086	\$0,064	\$0,116	\$0,088
CAPEX Auxiliaries	\$0,100	\$0,054	\$0,127	\$0,069
OPEX Electrolyser	\$0,071	\$0,038	\$0,090	\$0,049
Electricity Electrolyser	\$0,410	\$0,491	\$0,427	\$0,512
Cost Of Water	\$0,004	\$0,002	\$0,004	\$0,002
Hydrogen Production Cost	\$0,672	\$0,650	\$0,764	\$0,719
CAPEX Hydrogen Compressor	\$0,004	\$0,002	\$0,004	\$0,002
OPEX Hydrogen Compressor	\$0,001	\$0,001	\$0,001	\$0,001
Electricity Hydrogen Compressor	\$0,011	\$0,013	\$0,010	\$0,012
CAPEX Hydrogen Storage	\$0,038	\$0,000	\$0,038	\$0,000
OPEX Hydrogen Storage	\$0,008	\$0,000	\$0,008	\$0,000
Cost Of Nitrogen (ASU)	\$0,045	\$0,045	\$0,045	\$0,045
Cost of Nitrogen Compression	\$0,008	\$0,008	\$0,008	\$0,008
CAPEX NH ₃ Synthesis Plant	\$0,037	\$0,037	\$0,037	\$0,037
OPEX NH ₃ Synthesis Plant	\$0,016	\$0,016	\$0,016	\$0,016
Electricity NH ₃ Synthesis Plant	\$0,005	\$0,005	\$0,005	\$0,005
Ammonia Production Cost	\$0,846	\$0,779	\$0,938	\$0,847
Loading Terminal and NH ₃ Liquefied Storage	\$0,052	\$0,052	\$0,052	\$0,052
Maritime Transportation	\$0,032	\$0,032	\$0,032	\$0,032
Unloading Terminal and NH ₃ Liquefied Storage	\$0,057	\$0,057	\$0,057	\$0,057
Cracking Plant	\$0,000	\$0,000	\$0,000	\$0,000
Purification Plant	\$0,000	\$0,000	\$0,000	\$0,000
CAPEX Civil Works & Other Costs	\$0,063	\$0,028	\$0,048	\$0,019
Final H₂ Levelized Cost	\$1,051	\$0,948	\$1,127	\$1,008

Table A6: LCOA final ammonia NH₃ supply chain, scenario 2